Characterising Skin Immune Cells to Inform Development of Intradermal Vaccines and Therapeutics

A thesis submitted in accordance with the conditions governing candidates for the degree of Philosophiae Doctor in Cardiff University

by

Matthew Owen Ivory

August 2016

Cardiff School of Pharmacy and Pharmaceutical Science

Cardiff University

Acknowledgements

First and foremost, I would like to thank my supervisors: James Birchall, Vincent Piguet and Sion Coulman for the opportunity to complete my PhD at Cardiff University. Their guidance throughout my laboratory work has been invaluable. I would also like to thank them for their time correcting drafts of my Thesis, allowing me to produce this work. I am also grateful for the financial support they provided me to travel to international conferences, allowing me to present my work to leaders in the fields of immunology and drug delivery and giving me the chance to see exotic, foreign locations (like Edinburgh).

I would also like to thank my family- my parents Nicholas and Sarah and my siblings James and Rosie for their love and support during my postgraduate years, even if I did occasionally drop off the face of the Earth for weeks at a time during the busy lab weeks!

Thanks also go to Professor Sarah Hook at the University of Otago for inviting me to complete a month's work in Osaka, Japan where we were graciously hosted by Professor Masaru Ishii, Junichi Kikuta and Keita Aoi. It was an unforgettable experience and I've been heckled for talking about it too much ever since I returned. Thanks also go to David Price and Sian Llewellyn-Lacey for their provision of lots of lovely T-cell clones and to Kristin Ladell and Kelly Miners for their assistance with cell sorting experiments. I would also like to acknowledge my labmates through the years for all their help and friendship- Marc Pearton, Xin Zhao, Etta Gualeni, Paul Mitchell, Magda Czubala, Stephane Caucheteux and Zahra Ahmed. Particularly appreciated are those who spent their evenings (or entire nights) stuck in the lab, helping me to manually process skin samples- Maria Dul, Simona Pekáčová and Priscilla Porta.

Finally, a massive thank you to my friends: Andy Jenkins, Andrew and Harri Kings, Jess Arneil, Sean Dodington, Bethan Broad, Rhys Kerr, William Burke and the Eagles cricket team for their provision of a bad influence to ensure that there were plenty of fun times in between the most frustrating lab times.

Abstract

Epidermal Langerhans cells (LCs) and multiple subsets of dermal dendritic cells (dDCs) make skin a valuable route for vaccination, offering the potential for antigen-sparing immunisation. The interconnected immunological functions of dDC subsets and LCs are not fully understood however. This Thesis therefore aimed to explore the interactions of skin immune cells with viral pathogens and vaccines to inform the development of future therapeutics and intradermal vaccines.

LCs and dDCs were isolated from ex vivo human skin tissue using a walkout protocol which allowed the enrichment of the migratory cells from the tissue. LCs and dDCs were infected with a lentiviral vector encoding GFP, allowing study of post-entry HIV viral restriction. The study uncovered the existence of a SAMHD-1-independent antiviral factor unique to LCs.

LCs and dDCs from ex vivo skin were used to examine the cross-presentation of an inactivated influenza virus-derived matrix peptide to CD8+ T-cells. Two CD11c+ subsets of dDCs were found to potently cross present the antigen. Delivery of VLPs, which lack genetic material, markedly reduced cross-presentation, suggesting that viral genetic material is vital for dDCs to activate cross-presentation pathways. Future work is required to determine if this is true of other influenza peptides or pathogens.

Vaccine delivery studies performed using murine and human models found that dDCs were responsible for the greatest uptake of ovalbumin peptide antigen and LCs did not migrate out of the epidermis in the first 4 hours after inactivated influenza virus vaccine delivery respectively.

Collectively, this work highlighted the importance of dDCs in antigen uptake and cross-presentation to prime cytotoxic T-cell responses. Innovative delivery methods such as microneedles offer a means of accessing the dermal compartment in a pain-free manner, though further work is required to determine the optimal combination of vaccine formulation and delivery method to harness the immunostimulatory abilities of dDCs.

Table of Contents

ACKNOWLEDGEMENTS ..... **II**

ABSTRACT ..... **III**

LIST OF ABBREVIATIONS ..... **IX**

CHAPTER 1 - GENERAL INTRODUCTION **1**

1.1 THE HUMAN IMMUNE SYSTEM 1

1.1.1 Innate Immunity *1*

1.1.2 Adaptive Immunity *2*

1.2 SKIN STRUCTURE 5

1.2.1 Epidermis *6*

1.2.2 Dermis *8*

1.3 SKIN IMMUNE CELLS 9

1.3.1 Dermal Dendritic Cells (dDCs) *9*

1.3.2 Langerhans Cells (LCs) *11*

1.3.3 Dendritic Cells in Human and Mouse Skin *12*

1.3.4 Skin-Resident T-cells *12*

1.3.5 Macrophages *14*

1.3.6 Inflammatory Response Cells *14*

1.4 VACCINATION 15

1.5 INTRADERMAL DELIVERY OF VACCINES 16

1.6 INTRADERMAL DELIVERY TECHNOLOGIES 18

1.6.1 Negation of the Stratum Corneum Barrier *19*

1.6.2 Jet Injectors *20*

1.6.3 Gene Gun Technology *20*

1.6.4 Microneedle (MN) Technology *21*

1.6.4.1 Solid Microneedles 21

1.6.4.2 Hollow Microneedles 22

1.6.4.3 Dissolvable Microneedles 23

1.6.5 Intrafollicular Delivery *24*

1.6.6 Cellular Targeting of Skin Immune Cells *24*

1.7 PROJECT RATIONALE 25

1.8 THESIS AIM AND OBJECTIVES 26

1.9 BIBLIOGRAPHY 27

CHAPTER 2: THE EX VIVO HUMAN SKIN MODEL **41**

2.1 INTRODUCTION 41

2.1.1 Vaccine Technologies *41*
2.1.2 Vaccine Research *42*
2.1.3 The Ex Vivo Human Skin Model *43*
2.1.4 Histological Analysis of Human Skin *44*
2.1.4.1 Sectioning of Tissue 44
2.1.4.2 Immunohistochemistry and Immunofluorescence 45
2.1.5 Influenza *46*
2.1.6 Influenza Vaccines *47*
2.1.7 Changes in Human Skin Following Intradermal Influenza Vaccination *48*
2.2 AIMS AND OBJECTIVES 49
2.3 MATERIALS AND METHODS 50
2.3.1 Microneedle Arrays *50*
2.3.2 Fluorescent Protein Formulation *50*
2.3.3 Fluorescent Nanoparticle Formulation *51*
2.3.4 Insertion of Microneedles into Ex Vivo Human Skin *52*
2.3.5 Microneedle Skin Penetration and Formulation Release in Skin *52*
2.3.6 Changes in Langerhans Cell Numbers After Intradermal Vaccination *53*
2.4 RESULTS AND DISCUSSION 55
2.4.1 Formulation Coating onto Solid Microneedles *55*
2.4.2 Insertion of Microneedles into Ex Vivo Human Skin *56*
2.4.3 Microneedle Skin Penetration and Formulation Deposition in Skin *57*
2.4.4 Changes in Langerhans Cell Numbers After Intradermal Vaccination *59*
2.5 GENERAL DISCUSSION 60
2.6 POTENTIAL FOR PUBLICATION 64
2.7 CONCLUSION 64
2.8 BIBLIOGRAPHY 65

CHAPTER 3 - THE EX VIVO HUMAN SKIN IMMUNE CELL MODEL 71

3.1 INTRODUCTION 71
3.1.1 Limitations of the Human Ex Vivo Skin Model *71*
3.1.2 Methods of Obtaining Cells from Skin *72*
3.1.3 The Skin Cell Walkout Method *73*
3.1.4 Assessing Dendritic Cell Responsiveness *73*
3.1.5 Human Immunodeficiency Virus (HIV) *74*
3.1.6 Pseudotyped Virus Models *76*
3.1.6.1 Vesicular Stomatitis Virus (VSV) 76
3.1.6.2 GFP-Encoding VSV-G-Pseudotyped HIV 77
3.1.7 SAM and HD Domain-Containing Protein 1 (SAMHD1) *77*
3.1.7.1 Simian Immunodeficiency Virus and Vpx Protein 77

3.1.8 Flow Cytometry ... *78*
3.1.8.1 Compensation Controls ... 79
3.1.8.2 Isotype Control Antibodies ... 80
3.1.8.3 Live/Dead Cell Staining ... 80
3.1.8.4 Fluorescence-Activated Cell Sorting ... 81
3.2 Aims and Objectives ... 81
3.3 Materials and Methods ... 82
3.3.1 Isolation of Dermal and Epidermal Walkout Cells from Skin ... *82*
3.3.2 Characterisation of LCs and dDCs ... *82*
3.3.3 Characterisation of Dermal T-cells ... *84*
3.3.4 Walkout Cell Viability Staining ... *84*
3.3.5 Stimulation of Skin LCs and dDCs with TLR Agonists ... *85*
3.3.6 Functional Testing of Skin Walkout Cells ... *86*
3.3.6.1 Production of Lentiviral Vectors ... 86
3.3.6.2 Knockdown of SAMHD1 in LCs/dDCs ... 88
3.3.7 Infection of LCs/dDCs with VSV-G-HIV-GFP ... *89*
3.3.8 Sorting of LCs and dDCs from Skin ... *90*
3.4 Results and Discussion ... 91
3.4.1 Isolation of epidermal LCs and dDCs from skin ... *91*
3.4.2 Characterisation of dermal T-cells ... *95*
3.4.3 Stimulation of Skin LCs and dDCs with TLR Agonists ... *97*
3.4.4 Knockdown of SAMHD1 in LCs/dDCs ... *97*
3.4.5 Infection of LCs/dDCs with VSV-G-HIV-GFP ... *98*
3.4.6 Sorting of LCs and dDCs from Skin ... *100*
3.5 General Discussion ... 103
3.6 Potential for Publication ... 107
3.7 Conclusion ... 107
3.7 Bibliography ... 108

CHAPTER 4 - CROSS-PRESENTATION OF INFLUENZA VACCINE ANTIGEN ... 116

4.1 Introduction ... 116
4.1.1 Monocyte-Derived Dendritic Cell Models ... *116*
4.1.2 T-cells ... *117*
4.1.3 Cross-Presentation ... *118*
4.1.4 T-Cell Response Testing ... *119*
4.1.4.1 T-Cell Clones ... 120
4.2 Aims and Objectives ... 121
4.3 Materials and Methods ... 121
4.3.1 Derivation of Monocyte-Derived Cell Models ... *121*

4.3.1.1 Isolation of CD14+ Monocytes 121
4.3.1.2 Monocyte-Derived Dendritic Cells 122
4.3.1.3 Monocyte-Derived CD141 Dendritic Cells (CD141 mdDCs) 122
4.3.1.4 Monocyte-Derived Langerhans Cells (mdLCs) 122
4.3.2 Responsiveness of Monocyte Models to LPS Stimulation 123
4.3.3 ALF3 T-Cell clones 124
4.3.3.1 Validation of ALF-3 Peptide Specificity 125
4.3.4 Cross-Presentation by Monocyte-Derived DCs/LCs 125
4.3.5 Cross-Presentation by Skin-Derived DCs/LCs 126
4.3.6 Sorted Skin Cell Subset Cross-Presentation Investigation 126
4.4 Results and Discussion 128
4.4.1 Derivation of Monocyte-Derived Cell Models 128
4.4.2 Responsiveness of Monocyte Models to LPS Stimulation 129
4.4.3 Validation of ALF-3 T-Cell Clones 131
4.4.4 Cross-Presentation by Monocyte-Derived DCs/LCs 132
4.4.5 Cross-Presentation by Skin-Derived DCs/LCs 133
4.4.6 Sorted Skin Cell Subset Cross-Presentation Investigation 135
4.5 General Discussion 137
4.6 Potential for Publication 141
4.7 Conclusion 141
4.7 Bibliography 143

CHAPTER 5 - DELIVERY OF PEPTIDE ANTIGEN INTO SKIN UTILISING CUBOSOMES 150

5.1 Introduction 150
5.1.1 Colloidal Formulations for Intradermal Vaccine Delivery 150
5.1.1.1 Cubosomes 152
5.1.2 Formulation Characterisation 153
5.1.2.1 Transmission Electron Microscopy 154
5.1.2.2 Malvern Zetasizer Nano 154
5.1.3 Intravital Two-Photon Microscopy 156
5.1.4 Mouse Skin Model 157
5.2 Aim and Objectives 158
5.3 Materials and Methods 159
5.3.1 Synthesis of Cubosomes 159
5.3.2 Physical Characterisation of Cubosomes 160
5.3.2.1 Zeta Potential and Particle Size Analysis 160
5.3.2.2 Transmission Electron Microscopy (TEM) 161
5.3.3 Protein Entrapment in Cubosomes 161
5.3.4 Stability Testing of Formulations 163

5.3.5 Effects of Hollow Microneedle Delivery on Cubosome Formulations 163
5.3.6 Coating of Cubosome Formulation onto Stainless Steel Microneedles 164
5.3.7 Protein Delivery into the Skin by Injection of Cubosome Formulation 165
5.3.8 Antigen Uptake by Skin APCs 165
5.3.8.1 Cubosome Formulations 166
5.3.8.2 Transgenic Mice 166
5.3.8.3 Treatment with SIINFEKL-TAMRA Formulation 167
5.3.8.4 Two-Photon Microscopy 168
5.3.8.5 Antigen Uptake Analysis by Flow Cytometry 169
5.4 RESULTS AND DISCUSSION 170
5.4.1 Characterisation of Cubosomes 170
5.4.1.1 Zeta Potential and Particle Size Analysis 170
5.4.1.2 Transmission Electron Microscopy (TEM) 171
5.4.2 Protein Insertion into Cubosomes 172
5.4.3 Stability Testing of Formulations 173
5.4.4 Effects of Hollow Microneedle Delivery on Cubosome Formulations 174
5.4.5 Coating of Cubosome Formulation onto Stainless Steel Microneedles 176
5.4.6 Protein Delivery into the Skin by Injection of Cubosome Formulation 177
5.4.7 Two-Photon Microscopy 179
5.4.7.1 Structure of Skin 179
5.4.7.2 Microneedle Channel Healing 180
5.4.7.3 Antigen Retention at the Site of Injection 182
5.4.7.4 Changes in LC Density Following Antigen Delivery 185
5.4.8 Antigen Uptake Analysis by Flow Cytometry 186
5.4.9 Visualising Cubosome Lipid Phase Distribution 188
5.5 GENERAL DISCUSSION 189
5.6 POTENTIAL FOR PUBLICATION 195
5.7 CONCLUSION 195
5.7 BIBLIOGRAPHY 197

CHAPTER 6: GENERAL DISCUSSION 204

6.1 BRIEF OVERVIEW 204
6.2 DERMAL DENDRITIC CELLS 204
6.3 EPIDERMAL LANGERHANS CELLS 210
6.4 INTRADERMAL VACCINE DELIVERY 214
6.5 FUTURE WORK 217
6.6 CONCLUDING REMARKS 219
6.7 BIBLIOGRAPHY 221

List of Abbreviations

-- dDC	CD11c-/CD141- dermal dendritic cell
+- dDC	CD11c+/CD141- dermal dendritic cell
++ dDC	CD11c+/CD141+ dermal dendritic cell
2PM	Two-photon microscopy
AIDS	Acquired immunodeficiency syndrome
ANOVA	Analysis of variance
APC	Allophycocyanin
APC	Antigen presenting cell
APC-Cy7	Allophycocyanin-cyanine 7
APOBEC3G	Apolipoprotein B mRNA editing enzyme, catalytic polypeptide-like 3G
AqPQM	Aqueous formulation of SIINFEKL-TAMRA peptide, Quil-A and MPL-A
BCR	B-cell receptor
BSA	Bovine serum albumin
CCR	C-C motif chemokine receptor
CD	Cluster of differentiation
CD207	Langerin
CFSE	Carboxyfluorescein succinimidyl ester
CR	Complement receptor
Cu0	Cubosome formulation without fluorescent OVA protein
CuFL	Cubosome formulation with fluorescent OVA protein
CuNQM	Cubosome formulation with Nile red, Quil-A and MPL-A
CuPQM	Cubosome formulation with SIINFEKL-TAMRA peptide, Quil-A and MPL-A
DAB	3,3'-Diaminobenzidine
DAMP	Damage-associated molecular pattern
DC-RPMI	RPMI supplemented with 10% human AB serum and 1% Pen/Strep/Fungizone solution

dDC	Dermal dendritic cell
ddH_2O	Double-distilled water
DLS	Dynamic light scattering
DMEM	Dulbecco's Modified Eagle's Medium
DNA	Deoxyribonucleic acid
Dnase	Deoxyribonuclease
dNTP	Deoxynucleoside triphosphate
dsRNA	Double-stranded ribonucleic acid
EDM	Electrical discharge machining
EDTA	Ethylenediaminetetraacetic acid
eYFP	Enhanced yellow fluorescent protein
FACS	Fluorescence-activated cell sorting
Fc	Fragment, crystallisable region
FITC	Fluorescein isothiocyanate
Fl-NP	Fluorescent nanoparticle
Fl-OVA	Fluorescently-conjugated ovalbumin protein
FSC	Forward-scattered light
Gag	Group-specific antigen
GFP	Green fluorescent protein
GM-CSF	Granulocyte macrophage colony-stimulating factor
H&E	Haematoxylin and eosin stain
HBS	HEPES-buffered saline
HEK293T	Human embryonic kidney 293 cells expressing the simian vacuolating virus 40 large tumour antigen
HEPES	2-[4-(2-Hydroxyethyl)piperazin-1-yl]ethanesulfonic acid
HiB	Haemophilus influenzae type b
HIV	Human immunodeficiency virus
HLA	Human leukocyte antigen

HRP	Horseradish peroxidase
ICC	Intracellular cytokine
ID	Intradermal
IF	Immunofluorescence
IFN	Interferon
Ig	Immunoglobulin
IHC	Immunohistochemistry
IL	Interleukin
IM	Intramuscular
IMDM	Iscove's Modified Dulbecco's Medium
ITGAX	Integrin Subunit Alpha X
IV	Inactivated virus
LC	Langerhans cell
LDL	Low-density lipoprotein
LogP	Logarithm of octanol/water partition coefficient
LPS	Lipopolysaccharide
mAb	Monoclonal antibody
MACS	Magnetic-activated cell sorting
mdDC	Monocyte-derived dendritic cell model
mdLC	Monocyte-derived Langerhans cell
MFI	Median fluorescence intensity
MHC	Major histocompatibility complex
MN	Microneedle
MNPT	Microneedle poke-through
moDC	Monocyte-derived dendritic cell
MPL-A	Monophosphoryl Lipid A
mRNA	Messenger RNA

n	Sample size (number of samples)
Nef	Negative regulatory factor
NP	Nanoparticle
OCT	Optimal cutting temperature
OVA	Ovalbumin protein
p	Statistical p-value
PAMP	Pathogen-associated molecular pattern
PBMC	Peripheral blood mononuclear cell
PBS	Phosphate-buffered saline
PDI	Polydispersity index
PE	Phycoerythrin
PE-Cy7	Phycoerythrin-cyanine 7
PerCP	Peridinin chlorophyll
Pol	DNA polymerase
Poly(I:C)	Polyinosinic:polycytidylic acid
PRR	Pattern recognition receptor
Rev	Regulator of expression of virion proteins
RNA	Ribonucleic acid
RPMI	Roswell Park Memorial Institute medium
SAMHD1	Sterile alpha motif and histidine-aspartate domain-containing protein 1
SD	Standard deviation
SHG	Second-harmonic generation
SIINFEKL-TAMRA	5(6)-Tetramethylcarboxy rhodamine labelled peptide from ovalbumin residues 257–264
SIV	Simian immunodeficiency virus
SSC	Side-scattered light
ssRNA	Single-stranded ribonucleic acid
TAMRA	Carboxytetramethylrhodamine

Tat	Trans-activator of transcription
TCR	T-cell receptor
TEM	Transmission electron microscopy
TGF	Transforming growth factor
TLR	Toll-like receptor
TNF	Tumor necrosis factor
UT	Untreated
Vif	Viral infectivity factor
VLP	Virus-like particle
Vp(x,r,u)	Viral protein (x, r or u)
VSV-G-HIV-GFP	HIV-1 lentiviral vector encoding GFP pseudotyped with VSV envelope G protein
β-2M	β-mercaptoethanol

Chapter 1- General Introduction

1.1 The Human Immune System

During normal interactions with its external environment, the human body is under constant threat from invading pathogens. These may be bacterial, viral or fungal, exploiting different pathways to lead to diseases (Murphy et al., 2012). For this reason, the human body has evolved multiple, often overlapping, systems which can allow it to resist invasion by pathogens. The subtleties of the immune system are important in allowing the body to differentiate between 'self' and 'foreign' cells and molecules in order to stop the growth of invading pathogens without adversely affecting host cells or systems (Dempsey et al., 2003). The components of the immune system are categorised into two structures- the innate immune system and the adaptive immune system.

1.1.1 Innate Immunity

The innate immune system is also known as the non-specific immune system as its components develop from birth and are not guided by exposure to specific pathogens as is the case for the adaptive immune system (Medzhitov and Janeway, 2000). Innate immunity can be considered a more primitive protective system than adaptive immunity, recognising and responding to a range of pathogens in a broadly similar manner (Kumar et al., 2011). The first line of innate immunity provides a physical barrier to pathogen entry, with the hydrophobic stratum corneum preventing ingress of pathogens into the skin (which represents the vast majority of the body's surface which is exposed to the external environment) (Elias, 2007). There are also transit systems such as mucociliary clearance (Antunes and Cohen, 2007) and gastrointestinal peristalsis (Hao and Lee, 2004) that act to physically limit contact time of pathogens with bodily surfaces and thus reduce the chances of their entry into the body .

Occasionally, a pathogen is able to overcome the external barriers and colonise the body, perhaps due to an injury which negates the barrier properties of the skin such as a burn or incision wound. The innate immune system possesses several mechanisms to neutralise such pathogens. Leukocytes such as neutrophils, macrophages and dendritic cells (DCs) are able to recognise pathogens based on shared structural

molecules known as pathogen-associated molecular patterns (PAMPs) via pattern recognition receptors (PRRs) on their surface (Kumar et al., 2011). These cells may then phagocytose the pathogen, degrading it via the lysosomal pathway or via a respiratory burst within the cell (Murphy et al., 2012). The triggering of PRRs on these cells also leads to the release of substances such as histamine, leukotrienes and prostaglandins which trigger inflammation in the local area (Medzhitov, 2008). Inflammation increases blood flow to the site of infection and increases the permeability of blood vessels, allowing entry of circulating immune cells such as granulocytes into the tissue (Takeuchi and Akira, 2010). If the pathogen entry is the result of local trauma, damaged cells will release substances that possess damage-associated molecular patterns (DAMPs) that are also recognised by leukocytes and trigger activation of inflammatory pathways (Bianchi, 2007). The innate immune system also includes the complement system, an array of small proteins that circulate in the blood and bind pathogens to indicate their presence to immune cells (known as opsonisation) or to initiate lysis of the pathogen by creating pores in the pathogen's cell membrane (Murphy et al., 2012).

Whilst many potentially harmful pathogens are recognised and stopped by the innate immune system, there are cases where the pathogen has evolved evasive strategies to allow it to circumvent the innate immune system. HIV-1 is a good example, circumventing early defences to propagate in the host (Piguet et al., 2014). In these cases, the adaptive immune system allows the body to recognise the pathogens and to mount an immune response against them and limit or prevent disease development depending on the pathogen.

1.1.2 Adaptive Immunity

The second arm of the immune system provides 'acquired immunity'- creating an immunological memory to pathogens that it has encountered to allow more effective responses to be effected upon subsequent exposure to identical pathogens. It varies from the innate immune system in that the response which is raised against a pathogen is tailored to best combat that pathogen rather than the 'one-size-fits-all' approach of the innate immune system (Medzhitov and Janeway, 2000). The two main effector cell types of the adaptive immune system are T-cells and B-cells, collectively known as

lymphocytes (Rajewsky and von Boehmer, 2008). Unlike the cellular response that forms part of the innate immune response, each lymphocyte can only recognise a single PAMP in the form of an antigenic epitope (Dempsey et al., 2003). Antigen may be large structural components of pathogens such as polysaccharides (Weintraub, 2003) or small molecules such as the hapten urushiol (Kalish et al., 1994). This diversity of antigen detection allows the adaptive immune system to distinguish and counteract pathogens which have evolved means of evading innate immune system detection- for example bacteria with membranous envelopes which protect their bacterial cell wall from PRR recognition (Hornef et al., 2002).

The initiation of an adaptive immune response that has not been encountered previously is dependent on antigen presenting cells (APCs) within the body. These fall into two categories: 'professional' APCs whose major function is the presentation of antigen and all other nucleated cells which may act in an APC capacity during intracellular infection (Murphy et al., 2012). Professional APCs include macrophages (Unanue, 1984) and DCs (Guermonprez et al., 2002) which are able to recognise pathogens via PRRs on their surface and uptake them. Following processing which lyses the pathogen into its antigenic components, the APCs present the antigen on their surface on major histocompatibility (MHC) molecules; the interaction with the antigen:MHC complex then activates lymphocytes (Heath and Carbone, 2001).

B-cells are responsible for the humoral immune response, releasing antibodies which bind to specific epitopes on the pathogen. Antibodies, also known as immunoglobulin (Ig) molecules, are soluble proteins which possess antigen-binding regions which are specific to a single antigenic epitope (Schroeder and Cavacini, 2010). The simplest monomeric Ig molecule possesses two identical antigen binding sites, though they can form polymers of 2-5 monomers which can bind multiple copies of the epitope (Woof and Russell, 2011, Martin, 1969). Antibody binding may negate the threat of pathogens if they bind to cell surface proteins on the pathogen which allow it to mediate its effects such as cell entry (Forthal, 2014). The presence of more than one binding site on an Ig molecule means that they can also aggregate pathogens, rendering them ineffective and encouraging their phagocytosis (Thomas et al., 1986). Antibodies may also bind soluble bacterial toxins, forming insoluble precipitates and preventing their negative effects (Forthal, 2014). Antibody binding can also signal the initiation of

complement binding to the pathogen where it can mediate its chemoattractant and cytotoxic effects (Ochsenbein and Zinkernagel, 2000). Finally, antibodies can opsonise pathogens in a manner similar to complement, attracting cells which will engulf the pathogen (Dunkelberger and Song, 2010). Antibodies may also be linked to the surface of B-cells as part of the B-cell receptor (BCR), allowing the B-cell to recognise antigen and become activated (Murphy et al., 2012).

T-cells possess T-cell receptors (TCRs) on their surface which, like Ig and the BCR, are specific to a single antigenic epitope. Unlike antibodies, the TCR requires antigen to be bound within a MHC molecule to be recognised (Davis et al., 1998). T-cells are able to perform one of a range of functions depending on which subtype of T-cell is activated (Broere et al., 2011). Cytotoxic T-cells are responsible for killing virally-infected or tumour cells to prevent the propagation of infection or the tumour respectively (Andersen et al., 2006). Helper T-cells direct other cells of the immune system- notably B-cells, cytotoxic T-cells and macrophages- to facilitate the humoral and cellular aspects of the adaptive immune response (Kaech et al., 2002). Regulatory T-cells have a tolerogenic role within the immune system, ensuring that immune responses do not go unchecked and cause damage to the host (Belkaid and Rouse, 2005). There are a further two minor subsets of human T-cells, γδ T-cells and natural killer T-cells, which are able to recognise antigen outside of MHC molecules and act in a manner that bridges both innate and adaptive immunity (Holtmeier and Kabelitz, 2005, Brennan et al., 2013).

Whereas the cells of the innate immune system are able to recognise an array of PAMPs via a number of PRRs, the lymphocytes of the adaptive immune system are each only able to recognise a single antigenic epitope (Rajewsky and von Boehmer, 2008). Also, whereas PRRs and antibodies are able to bind epitopes on a range of antigen types, the TCR is only able to recognise peptide antigen (Ni and O'Neill, 1997).

The raising of an adaptive immune response, particularly upon initial exposure to a pathogen, is a much lengthier process than an innate immune response. Whereas the cellular and complement innate responses are active within hours of exposure, a first adaptive immune response can take up to 5 days to be fully deployed (Murphy et al., 2012). Most of the lymphocytes that proliferate to implement the first adaptive immune response against a pathogen will die after the removal of the pathogen (Jiang

et al., 2012). A minority are instead differentiated into memory T- and B-cells (Kurosaki et al., 2015, Lalvani et al., 1997). These cells are able to respond upon subsequent exposure, producing a quicker and stronger immune response (Kaech et al., 2002).

This 'immunological memory' is the goal of vaccination. Exposing a person to a weakened or dead form of a pathogen (which does not pose a threat of causing disease), can allow the adaptive immune response to produce an antigen-specific response mimicking that of initial exposure to the actual pathogen (Siegrist, 2013). After this, the quicker and more effective immune response can be launched against the pathogen and ideally prevent the pathogen from being able to replicate to a great enough level to produce the disease state in the patient (Murphy et al., 2012).

1.2 Skin Structure

Human skin is the interface between the external environment and the body's internal microenvironment, which is prone to infection by an array of pathogens. For this reason, the complex structure of the skin is designed to act both as an impassive physical barrier and also as an active organ that can distinguish foreign antigen from innocuous substances and self-antigen (Elias, 2007, Pasparakis et al., 2014). The outermost skin layer is the epidermis and below it is the dermis (Figure 1.1), each of which is made up of multiple sub-layers.

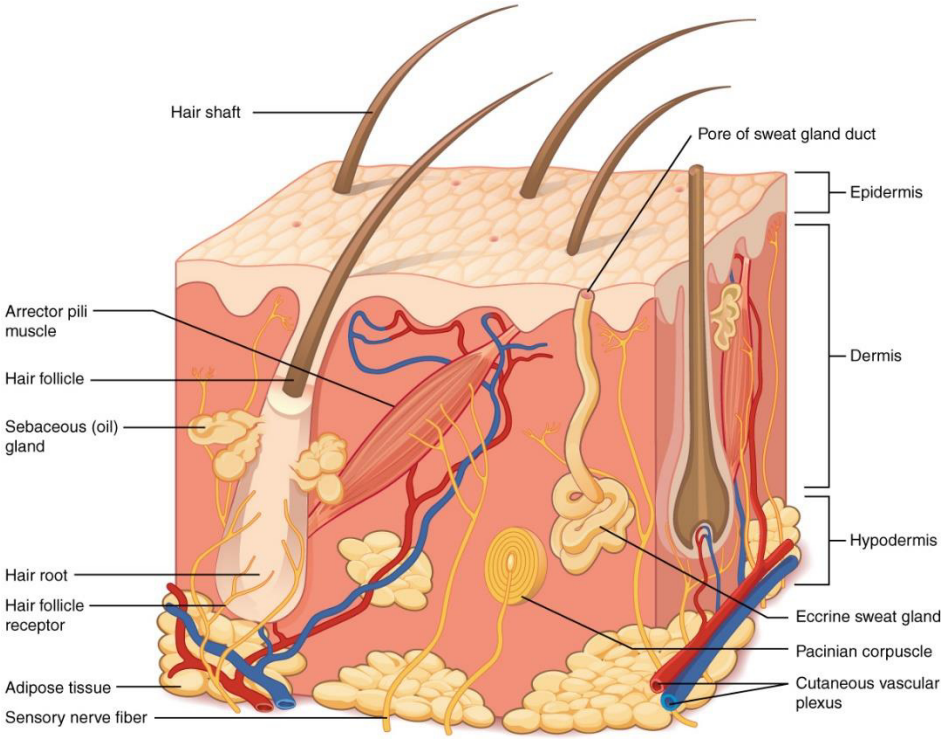

Figure 1.1: The structure of human skin (adapted from: http://philschatz.com/anatomy-book/resources/501_Structure_of_the_skin.jpg)

1.2.1 Epidermis

The outermost layers of the epidermis, the stratum corneum and stratum lucidum (Figure 1.2), are non-viable, lipophilic layers which act as a physical barrier to hydrophilic substances in the external environment (Elias, 2005). The stratum corneum is made up of layers of keratinocytes which have terminally differentiated into corneocytes- dead cells embedded in a matrix of keratin, fatty acids, cholesterol, and ceramides (Yamamoto et al., 1991, Norlén, 2006). The thickness of the stratum corneum varies by body site, with increased thickness on the palms of the hand and soles of the feet (Fore, 2006). Beneath this lies the viable stratum granulosum, stratum spinosum and stratum basale. The stratum basale contains basal keratinocyte stem cells which proliferate asymmetrically to maintain the population of stem cells and also to produce new keratinocytes (Lechler and Fuchs, 2005). These keratinocytes are pushed upwards by the proliferation of cells beneath them- moving them into the stratum spinosum (Fore, 2006). As keratinocytes move outwards, they begin to accumulate the lipid and protein deposits characteristic of the cells in the stratum corneum. After the stratum spinosum, they transition through the stratum granulosum where they lose their nuclei and begin to release lipids which will fill the intracellular space in the stratum corneum (Eckert and Rorke, 1989). The vast majority of cells in the viable layers are keratinocytes,

though the stratum spinosum and stratum basale also contain other cell types, including immunological Langerhans cells (LCs) (Berger et al., 2006), melanocytes (that confer skin pigmentation) (Fore, 2006), Merkel cells (touch receptors) (Maksimovic et al., 2014) and skin-resident T-cells (Clark, 2010). The basal lamina- or basement membrane- forms the junction between the epidermis and the dermis below it (Briggaman et al., 1971).

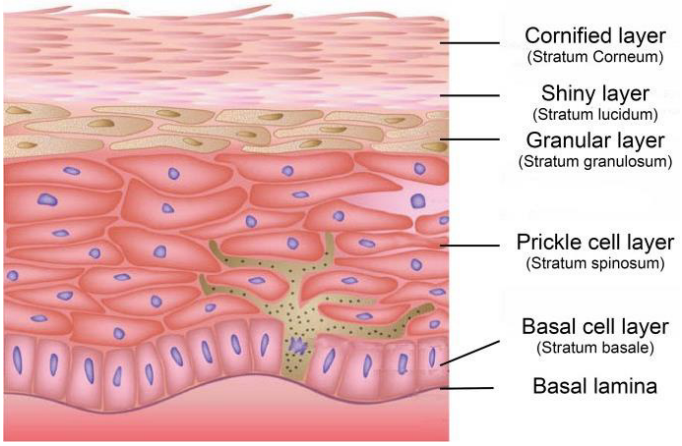

Figure 1.2: Structure of human epidermis (adapted from: http://www.molcare-consulting.com/wp-content/uploads/Hautengl600dpib.jpg)

The stratum corneum acts as both a passive and active barrier. The hydrophobic nature of the stratum corneum prevents water-soluble substances from entering the skin. The barrier function also limits the amount of trans-epidermal water loss, preventing dehydration over the large body surface area (Kalia et al., 2000). The 'brick and mortar' structure of the stratum corneum means it can only be penetrated by small molecules (ca. 500Da or less) and the diffusion path is tortuous, increasing diffusion time (Brown et al., 2006). Molecules can diffuse through the stratum corneum by one of two routes. The first is transcellular absorption, where the molecule crosses the plasma membrane of corneocytes into the cytoplasm and then out of the cell through the plasma membrane on the distal side. While this is the shortest route, it is less common as it requires the delivered molecule to possess lipophilic and hydrophilic characteristics to allow it to pass into the plasma membrane and corneocyte cytoplasm respectively (Barbero and Frasch, 2006). The most common route is the paracellular route, with the molecule passing between corneocytes without crossing the cells. This greatly increases the length of the diffusion path, increasing delivery time into the skin (Aungst, 2012). The properties of the stratum corneum mean that most pathogens are unable to permeate through intact skin. The constant turnover of skin cells and shedding of layers

from the stratum corneum (known as desquamation) also reduces pathogen residence time on the skin and lowers the risk of entry into the skin (Milstone, 2004). As well as protection from physical insults, melanin which is produced by melanocytes and transferred into keratinocytes via melanosomes, also protects lower skin layers from the mutagenic effects of UV radiation in sunlight (Brenner and Hearing, 2008). The epidermis can respond to UV exposure, producing further melanin to allow greater protection. The epidermis also possesses resident immune cells, which are discussed in more detail later in this chapter.

1.2.2 Dermis

The dermis comprises two layers- the uppermost of which is the papillary dermis (stratum papillare) which possesses protuberances that project towards the epidermis housing blood capillaries and nerve endings (Figure 1.3). The protuberances allow a greater surface area of the blood capillaries to exchange oxygen and nutrients with the epidermis, which does not possess a blood supply of its own (Fore, 2006). Below this is the reticular dermis (stratum reticulare), a thicker layer containing large amounts of

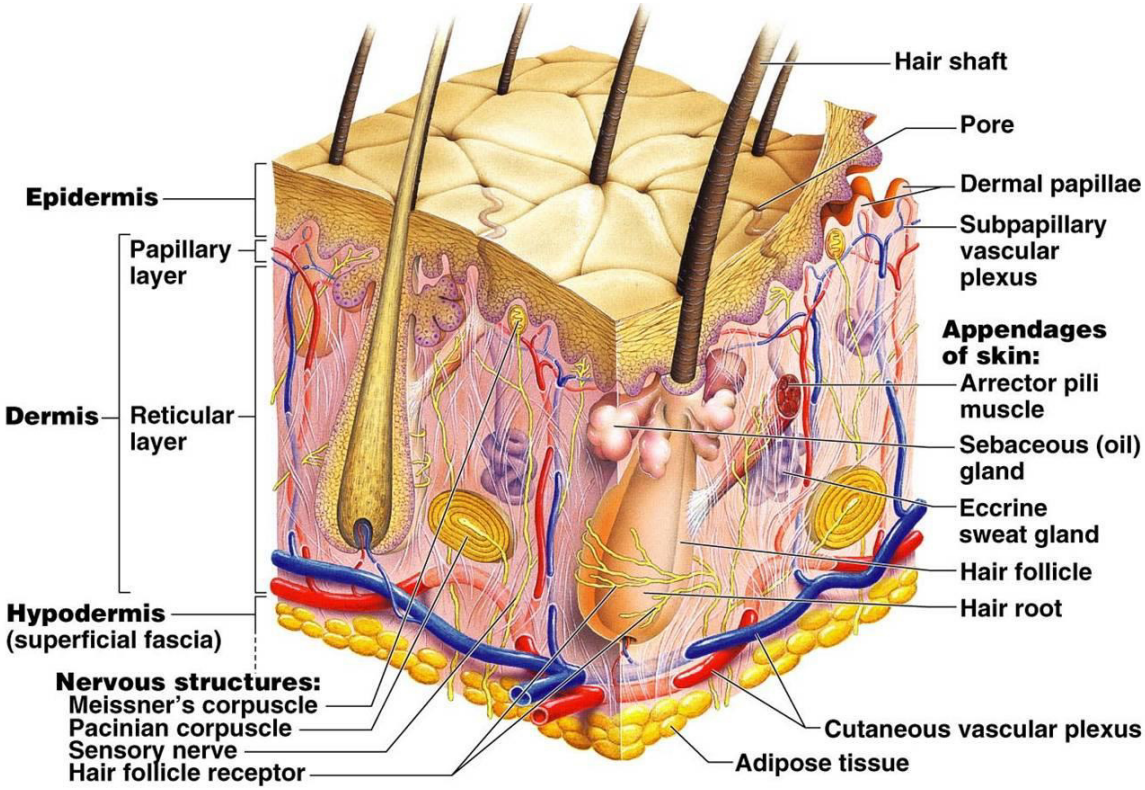

Figure 1.3: Structure of human dermis (adapted from: http://www.austincc.edu/apreview/NursingPics/IntegumentPics/Picture2.jpg)

connective tissue, blood vessels and glands. The main components of the reticular dermis are fibroblasts, collagen and elastin fibrils and ground substance which acts to support the tissue (Holbrook et al., 1982). The various dermal components allow the skin to perform many of its regulatory functions. Sebaceous glands release a mixture of lipids at the surface of the skin, ensuring it remains hydrated and its barrier intact (Fluhr et al., 2003). Sweat glands and the arrector pilli muscles attached to hair follicles are important in thermoregulation during hot and cold conditions respectively (Romanovsky, 2014).

The two dermal layers are home to a multitude of immunological cells- both resident and transiently-present cells. Under homeostatic conditions, resident DCs and macrophages patrol the dermis in search of pathogenic antigen (Haniffa et al., 2009, Malissen et al., 2014). Tissue-resident dermal T-cells are also present and able to elicit an adaptive immune response (Clark, 2010). The dermis also contains lymph vessels which are utilised to transport antigen and immune cells from the skin to lymph nodes where they can initiate adaptive immune responses (Lukas et al., 1996). Under inflammatory conditions, blood flow to the capillaries of the dermis is increased and the vessel wall permeability increases, allowing the migration of leukocytes and immunological proteins into the tissue to assist in removing pathogens (Pasparakis et al., 2014).

1.3 Skin Immune cells

To allow it to perform its complex role as an active barrier against pathogenic ingress into the body, the skin possesses an assortment of immune cells that combine to effect innate and adaptive immune functions.

1.3.1 Dermal Dendritic Cells (dDCs)

DCs are broadly divided into myeloid and plasmacytoid DCs- the former is of interest to this project due to their residence in tissues (e.g. skin), whereas plasmacytoid DCs are found in the blood and lymphoid organs of humans (Banchereau and Steinman, 1998, Dudziak et al., 2007). Myeloid dDCs express human leukocyte antigen type DR

(HLA-DR; part of the MHC-II complex), allowing them to present antigen to CD4+ T-cells (Janeway, 1991). They also express cluster of differentiation 45 (CD45)- also known as the common leukocyte antigen- on their surface, due to their leukocyte lineage (Merad et al., 2013). The DCs of the dermis are a heterogeneous population with several subsets existing. Early work utilising dDCs in homeostatic human skin classified them into CD1a+ and CD14+ subsets (Haniffa et al., 2009, Nestle et al., 1993), though gating strategies varied between groups. One method involves gating human skin dDCs on CD14 expression, then subdivide the CD14- dDCs (which are referred to collectively as CD1a+ dDCs) into CD141+ and CD141- dDC subsets (Artyomov et al., 2015, Klechevsky et al., 2008b). Another method gates human skin dDCs on CD14 initially but subsequently divides the CD14- dDCs into CD11c+ and CD141+ subsets (Carpentier et al., 2016, Haniffa et al., 2012). The CD14+ dDCs have been classified as monocyte-derived cells (thus not from the same precursors as myeloid DCs) (Carpentier et al., 2016, Haniffa et al., 2012), though CD14 has also been found to be co-expressed by human CD141+ dDCs (Chu et al., 2012). Recent work has classified dDCs into CD141+ and CD1c+ subsets (Chu et al., 2012, Haniffa et al., 2012), though overlap of markers (such as CD14 and CD11c) between the two subsets means classification is still not straightforward (Carpentier et al., 2016). The divisions in function between the dDC subsets are not currently fully understood (Carpentier et al., 2016).

Immature human dDCs develop from CD34+ hematopoietic bone marrow progenitor cells and enter the dermis via its capillary beds (Nguyen et al., 2002). At steady state, dDCs are motile and patrol the dermis in search of antigen. Their dendritic morphology increases their surface area and allows them to interact with a greater area of their external environment (Steinman, 1991). They uptake antigen by endocytosis following binding of antigen to cell-surface receptors (Engering et al., 1997), macropinocytosis of the external liquid phase containing soluble antigen (Sallusto et al., 1995) or phagocytosis of large particulate antigen or whole pathogens (Inaba et al., 1998, Guermonprez et al., 2002). Encounters with foreign antigen signals maturation in human dDCs which leads to a reduction in antigen uptake ability (Sallusto and Lanzavecchia, 1994) alongside upregulation of MHC-I and MHC-II molecules to improve antigen presentation (Hackstein and Thomson, 2004). Mature human dDCs express the maturation markers CD80, CD83 and CD86 (Hackstein and Thomson, 2004, Aerts-

Toegaert et al., 2007). CD80 and CD86 are important co-stimulatory molecules that determine the T-cell response that will be raised in the lymph node (Hubo et al., 2013). Mature dDCs upregulate CCR7 which facilitates their migration to the lymph node in both mice (Forster et al., 2008) and humans (Bruckner et al., 2012). Upon entering the lymph node, dDCs present the antigen to T-cells to initiate an adaptive immune response if the antigen is deemed to be pathogenic.

1.3.2 Langerhans Cells (LCs)

Found exclusively in the epidermis, LCs are immature myeloid-derived cells with multiple dendritic processes that extend between keratinocytes (Berger et al., 2006). LCs precursors are found in the epidermis prior to the development of haematopoiesis in human embryos, suggesting that they are formed from yolk sac and foetal liver precursors as is the case in mice (Hoeffel et al., 2012). Under steady state, human LCs can divide by mitosis to maintain cell numbers (Czernielewski and Demarchez, 1987, Kanitakis et al., 1993). LC precursors are also produced in the bone marrow and migrate towards the skin in blood vessels. Upon exiting the blood vessels, they migrate towards the epidermis where they take up residence. LC migration into and continued residence in the epidermis in mice has been shown to be controlled by transforming growth factor beta (TGF-β) which is activated from its precursor by keratinocytes (Mohammed et al., 2016).

LC dendrites allow them to uptake antigen from a relatively large area of the epidermis without the constant movement employed by dDCs (Merad et al., 2008). They are spatially arranged within the epidermis to create a close-knit network which reduces the chances of pathogens evading their detection (Romani et al., 2010). When LCs uptake antigen in human skin, they become mature (expressing maturation markers and co-stimulatory molecules on their surface) and withdraw their dendrites, taking on a more rounded morphology (Pearton et al., 2010b). They then extend towards the basement membrane and enter the dermis where they enter lymph vessels. Following migration to lymph nodes, LCs present antigen to T-cells, initiating an adaptive immune response (Stoitzner et al., 2006, Hunger et al., 2004). At rest, there is a constant turnover of LCs with cells spontaneously migrating towards the lymph node (Merad et al., 2002).

At steady state, mitosis is sufficient to maintain adequate LC numbers (Czernielewski and Demarchez, 1987, Kanitakis et al., 1993). In cases of mouse model inflammation or tissue insult where LC numbers are greatly reduced they are replaced by precursors recruited from the blood (Merad et al., 2002).

Unlike dDCs, LCs are a homogeneous population with no subsets. Human LCs express CD45 and HLA-DR owing to their leukocyte lineage and role as professional APCs respectively (Merad et al., 2008) along with high levels of CD1a which is involved in presentation of lipid and glycolipid antigen to T-cells (Hunger et al., 2004). They are however distinguishable from other skin DCs by their expression of Langerin (CD207) within Birbeck granules and on the cell surface in mice and humans (Romani et al., 2010, Merad et al., 2008). CD207 is a C-type lectin receptor with specificity for mannose, allowing LCs to efficiently bind and uptake glycosylated antigen (Ng et al., 2016, Engering et al., 1997). CD207 is also implicated in viral uptake by LCs in viruses such as influenza A (Ng et al., 2016) and HIV (Ahmed et al., 2015).

1.3.3 Dendritic Cells in Human and Mouse Skin

Immunological studies are often carried out using murine models due to the similarities between murine and human immune systems. It is important, therefore, that correct alignment of immune cell subsets across the two species is made if results in the animal model can inform human immunology. Table 1 contains LC and dDC populations which have been aligned based on recent reviews of the literature.

1.3.4 Skin-Resident T-cells

As discussed in Section 1.1.2, cytotoxic and helper T-cells are integral in the implementation of adaptive immune responses against a pathogen. The skin is home to roughly 20 billion T-cells, the largest reservoir of any organ and twice the number in the systemic circulation (Clark, 2010). Only about 5% of these T-cells are naïve, indicating a limited scope for raising an initial immune response purely within the skin (Bos et al., 1989). The vast majority of T-cells present (95%) are memory T-cells, which allows the

Table 1.1: Alignment of dendritic cell subsets in mouse and human skin

DC Subset	Human Phenotype	Mouse Phenotype	Major Function(s)	References
Langerhans cells	CD1a+ CD207+ HLA-DR+ CD205+ CD11c+ CD11b+	CD1a+ CD207+ HLA-DR+ CD205+ CD11c+ CD11b+	Conflicting evidence suggesting antigen presentation/ cross-presentation or tolerising/self-recognition roles	(Artyomov et al., 2015, Carpentier et al., 2016, Ginhoux and Merad, 2010, Hunger et al., 2004, Klechevsky et al., 2008b, Malissen et al., 2014, Merad et al., 2008, Mutyambizi et al., 2009, Romani et al., 1989, Romani et al., 2012, Shklovskaya et al., 2011, Stoitzner et al., 2006, Stoitzner, 2010, van der Aar et al., 2013, van der Vlist et al., 2011)
'Cross-presenting' dermal dendritic cells	XCR1+ CD11c+ HLA-DR+ CLEC9A+ CD141+ CD103+	CD11b- CD207+ XCR1+ CD11c+ HLA-DR+ CLEC9A+ CD103+	Cross-presentation of pathogen and dead tumour cell-associated antigens to CD8+ naïve T-cells	(Artyomov et al., 2015, Bachem et al., 2010, Bigley et al., 2015, Chu et al., 2012, Haniffa et al., 2012, Jongbloed et al., 2010, Poulin et al., 2010, Lauterbach et al., 2010)
Conventional dermal dendritic cells	CD1c+ CD11b+ CD11c+ HLA-DR+ CD16+ CLEC7A+ CLEC6A+	CD11b+ CD207- CD172a+ HLA-DR+ CX_3CR1+	Antigen presentation to naïve CD4+ T-cells. Produce IL-12 and TNF-α upon activation	(Dutertre et al., 2014, Wollenberg et al., 2002, Carpentier et al., 2016, Harman et al., 2013, Lundberg et al., 2013, Malissen et al., 2014, Merad et al., 2013, Satpathy et al., 2012, Ganguly et al., 2013)
XCR1-/CD11c-double-negative dermal dendritic cells	Not yet reliably characterised in human skin	XCR1- CD207- CD11b-/low	Function unknown	(Mollah et al., Tamoutounour et al., 2013, Henri et al., 2010, Malissen et al., 2014)

rapid initiation of a response to a previously-encountered pathogen (Nomura et al., 2014). The initiation of an immune response against a previously unencountered pathogen leads to the seeding of distal sites with memory T-cells, thus creating widespread systemic immunity (Clark, 2010). The distribution of T-cells is not even, with CD8+ cytotoxic T-cells preferentially locating in the epidermis- mostly in the acrosyringial epithelium of eccrine sweat ducts (Challier et al., 2013). Conversely, dermal-resident T-cells are mostly CD4+ helper cells and located in the area immediately surrounding the dermal vasculature (Nomura et al., 2014).

1.3.5 Macrophages

As one of the cellular mediators of innate and adaptive immunity, macrophages patrol the tissues of the body in search of pathogens. Within the skin, macrophages are found in the dermis but not the epidermis (Malissen et al., 2014). If they encounter pathogens they are able to uptake them and process their antigen for presentation to T-cells (Unanue, 1984). They are also able to release a number of cytokines which can activate the other skin immune cells and lead to recruitment of further immune cells from the blood (Murphy et al., 2012). Macrophages are derived from circulating CD14+ monocytes within the blood and become tissue-resident macrophages upon exit from the vasculature into the dermal environment (McGovern et al., 2014).

1.3.6 Inflammatory Response Cells

Under homeostatic conditions, the immune cells of the skin exist in a state of preparedness for the ingress of pathogens into the body. If a pathogen or some other immunogenic stimuli is encountered, the skin undergoes a number of changes to assist in combating the threat. Mast cells in the dermis are able to detect pathogens via Fc receptors, PAMPs or DAMPs on their surface and this triggers degranulation of the cells, releasing histamine and other inflammatory mediators into the local environment (Sangiuliano et al., 2014, Theoharides et al., 2012). This leads to an increase in local blood flow and increased permeability of the vasculature walls, causing the redness and swelling associated with inflammation (Medzhitov, 2008). The leakage of plasma into the tissue carries with it complement proteins and antibodies which can help to

counteract the pathogen (Murphy et al., 2012). The permeability of the vasculature walls allows entry of leukocytes into the tissue (Pasparakis et al., 2014). Monocytes are in particular recruited and can become macrophages (Malissen et al., 2014) or a further type of DC- the monocyte-derived dendritic cell (moDC) (Leon et al., 2005). Following antigen presentation in the lymph node and T-cell proliferation, the effector T-cells that will implement the adaptive immune response will also enter the tissue via the permeable vasculature (Clark, 2010).

1.4 Vaccination

Since its invention by Edward Jenner in 1796, vaccination has been established as one of the most effective tools in the battle against human disease (Morgan and Parker, 2007). It involves administering dose(s) of antigen representative of a pathogen, allowing the body's adaptive immune system to be primed in the way it would do if the actual pathogen was encountered (Murphy et al., 2012). The antigen used in place of the pathogen may be a component of the pathogen, one of its products or a whole killed or inactivated pathogen (Siegrist, 2013). This eschews the need for exposure to the pathogen to create an initial adaptive response. In many cases the long lag time for an initial adaptive response to be mounted after exposure to a pathogen will provide the pathogen with enough time to cause serious morbidity or mortality in the patient (Duclos and Bentsi-Enchill, 1993). If the immunised person should subsequently encounter the actual pathogen, an effective adaptive immune response can be raised thereby preventing potential harmful infection (Siegrist, 2013). The benefits of vaccination also extend beyond the vaccinated individual via a phenomenon termed 'herd immunity', whereby if enough people are immunised then it is impossible for a pathogen to create a 'chain of infection', thus passively protecting unimmunised individuals (Fox et al., 1971).

Given that the antigen must be encountered by the systemic immune system and the oral route would lead to degradation of the vast majority of antigen (Russell-Jones, 2000), vaccine delivery is normally via the parenteral route. Although the very first 'vaccine' involved variolation of a patient's skin, historically nearly all subsequent vaccines have been delivered by the intramuscular (IM) route (Hickling et al., 2011). This

involves the delivery of a small volume of liquid formulation through a hypodermic needle inserted through the skin to the muscle tissue below. The muscle tissue receives relatively high blood supply, allowing blood-resident APCs (including DCs) to access the antigen which they can then present in the lymph nodes or spleen to initiate adaptive immunity (Zuckerman, 2000). Some common IM vaccines include vaccines against diphtheria, tetanus, pertussis, haemophilus influenzae type b, hepatitis A/B, human papillomavirus and influenza (IAC, 2015). Although IM injection has proved to be an effective delivery route- drastically reducing the number of cases of diseases that used to be common (e.g. polio (Bhaumik, 2012) or measles (Levin et al., 2011)) - it also possesses a number of disadvantages. The injection is painful, as the muscle tissue is well innervated and not suited to receiving volumes of liquid (Jin et al., 2015). The variable blood flow in muscle tissue can affect antigen kinetics (Parthasarathi et al., 2004). It is also does not have scope to provide site-specific immunisation at the site of infection for most vaccines (Leenaars and Hendriksen, 1998). IM vaccines also create disposal issues relating to the production of contaminated sharps associated with the use of hypodermic needles (Beltrami et al., 2000). Finally, although it is well supplied with blood, the muscle is not a particularly potent immune target- meaning that large or repeated doses of antigen are often required to elicit immunity (Hickling et al., 2011). For this reason, there has been a large amount of research in recent years into vaccine delivery into skin which may prove advantageous for a number of reasons.

1.5 Intradermal Delivery of Vaccines

The accessibility of skin and its large population of immune cells make it a suitable route for immunisation. Classically, intradermal (ID) injection has been utilised to take advantage of the skin's immunological properties. This is normally achieved by the Mantoux technique- a short, small bore needle is inserted into the dermis at an angle almost parallel to the skin surface then withdrawn slightly before the liquid formulation is injected into the dermal tissue (Norman et al., 2014). The elastic nature of the dermis allows it to expand slightly to accommodate the liquid, forming the characteristic 'bleb' associated with ID injection (Figure 1.4). The injection technique demands a higher level of skill than IM injection and high variability in delivery depth can occur between healthcare professionals (Kim and Prausnitz, 2011, Suh et al., 2014a). Where it is used

Figure 1.4: Intradermal injection by the Mantoux technique
(adapted from: http://www.novosanis.com/sites/default/files/application/field_image/Mantoux_tuberculin_skin_test.jpg)

correctly, it allows the delivery of liquid formulation into the dermis where it can be accessed by dDCs. The fibrous nature of the dermis means that the formulation will also be able to permeate towards the basement membrane, where it will be encountered by LCs (Liard et al., 2012). Finally, the high level of hydrostatic pressure associated with ID injection forces some of the formulation into the lymph vessels of the dermis (Tozuka et al., 2016). In the case of vaccines, this will allow the transport of antigen to the lymph nodes where it can be processed by resident APCs resulting in adaptive immune response (Murphy et al., 2012).

At present only the Bacille Calmette-Guérin (BCG) vaccine against tuberculosis and rabies vaccine are preferentially delivered into skin (Hickling et al., 2011). The BCG vaccine is delivered intradermally to reduce the risk of neurovascular injury if the live bacillus within the vaccine is delivered to deeper tissues (WHO, 2012b). The rabies vaccine is delivered intradermally mostly in developing countries due to the reduced cost (a 60-80% reduction) and increased coverage with a limited supply of vaccine that is achieved by the antigen-sparing achieved by this delivery route (WHO, 2010). Research into a number of other intradermal vaccines is ongoing (Kenney et al., 2004, Soonawala et al., 2013, van den Berg et al., 2009, Caucheteux et al., 2016). An ID influenza vaccine was first made available during the 2011-12 influenza season and possesses advantages over the established intramuscular (IM) injection in antigen sparing (using only 60% of the antigen of an IM dose) and patient acceptability (due to a smaller hypodermic needle being used) (Reygrobellet et al., 2010). As discussed in Section 1.3.3, the induction of an immune response via skin-draining lymph nodes leads

to the population of other tissues with pathogen-specific CD8+ T-cells. In the case of influenza, an intradermal injection of antigen leads to the population of lung mucosa with influenza-specific CD8+ T-cells which have been shown to be vital in viral clearance from the lung (Helft et al., 2012).

Though there is currently no HIV vaccine available for delivery by any route, the intradermal route is a logical choice for testing new vaccine candidates. When HIV is transmitted via mucous membranes (e.g. during sexual activity) (de Witte et al., 2007), the DCs present within the membranes have been shown to uptake the virus and transport it to lymph nodes, where it is transmitted to T-cells (which it remains able to infect) (Ahmed et al., 2015). Therefore, the DCs of the skin may be a useful target for vaccination if they can be conditioned to recognise and destroy HIV rather than transmitting it to T-cells. Thus effective systemic immunity may be best created using vaccine antigen delivered intradermally (Johnston and Fauci, 2008, Caucheteux et al., 2016).

1.6 Intradermal Delivery Technologies

There are established methods for delivering low molecular weight drugs (typically only up to a few hundred Daltons such as opioid analgesics, local anaesthetics and hormonal contraceptives) into the skin (Prausnitz and Langer, 2008). Transdermal patches (Isaac and Holvey, 2012) and topical semisolid formulations (Touitou, 2002) can facilitate the delivery of small molecules of appropriate molecular properties into the skin without the need for compromising the stratum corneum. Vaccine antigens are macromolecular in nature however, therefore these delivery technologies are not viable for vaccination- the size and hydrophilicity of the antigen prevents entry into the skin through an intact stratum corneum (Kim and Prausnitz, 2011). Instead, some physical disruption of the hydrophobic stratum corneum must occur to allow delivery of vaccines into the skin.

The variable nature of intradermal injections via Mantoux technique and the high level of skill required have led to research into a number of alternative delivery methods into the skin that look to take advantage of its immunological properties. As

well as delivery of liquid vaccine formulation via a smaller hypodermic needle (as in the Fluzone™ vaccine), a number of technologies have been explored to deliver vaccine to skin immune cells. All of them aim to overcome the hydrophobic physical barrier of the stratum corneum to deliver to the cellular epidermal and dermal compartments below.

1.6.1 Negation of the Stratum Corneum Barrier

In order for large and/or hydrophilic vaccine antigen to be delivered to skin-resident immune cells, the stratum corneum must somehow be bypassed. One strategy to achieve this goal is temporary chemical permeabilisation of the barrier by application of formulation applied to the surface of the skin (Andrews et al., 2013, Benson and Namjoshi, 2008). A study utilising combinations of permeation enhancers used commonly in topical formulations increased the delivery of macromolecules such as luteinising hormone-releasing hormone and heparin into porcine skin by 50- to 100- fold without skin irritation (Karande et al., 2004). The study was not able to deliver either substance at therapeutic concentrations however. Vaccination, which requires much lower levels of macromolecule delivery was shown to be effective using penetration enhancers to both deliver and increase the antigenicity of ovalbumin in murine skin (Karande et al., 2009). This strategy will preferentially deliver to the epidermal compartment given the application to the skin's surface.

It is also possible to physically negate the stratum corneum barrier using tape-stripping, where multiple applications of adhesive tape pull off successive layers of the hydrophobic barrier (Bashir et al., 2001). Tape-stripping prior to application of whole inactivated influenza virus has been shown to induce both cellular and humoral immune responses especially when delivered to mice along with cholera toxin or the penetration enhancers oleic acid and retinoic acid (Skountzou et al., 2006). Another study found that tape-stripping murine skin enhanced T-helper cell responses against both protein and DNA vaccines (Vandermeulen et al., 2009).

Alternative methods of ablating the stratum corneum include the use of laser (Jacques et al., 1987, Nelson et al., 1991) or electrical energy (Chen et al., 1998, Fukushima et al., 2001). As well as helping to breach the stratum corneum, laser treatment of murine skin has been shown to improve cellular and humoral responses

against intradermally-delivered ovalbumin or influenza vaccine (Chen et al., 2010). It has been noted that laser enhancement of delivery into the skin provides only a moderate benefit and skin healing after treatment is slow (Lee et al., 2010). Electroporation has been shown to induce a peptide-specific cytotoxic T-cell immune response against the ovalbumin peptide SIINFEKL equivalent to an intradermal injection control in mice (Zhao et al., 2006). Electroporation is often used in combination with DNA vaccines, showing promising results for vaccination against influenza in rhesus macaque (Laddy et al., 2009) as well as therapeutic vaccination against hepatitis C in human patients (Weiland et al., 2013).

1.6.2 Jet Injectors

Alternatively, transient physical disruption of the stratum corneum barrier can be achieved using a jet injector device (Williams et al., 2000, Soonawala et al., 2013) which uses high pressure air to mechanically breach the stratum corneum and deliver a liquid formulation into the skin (Zehrung, 2009). The stream characteristics (such as shape and width) along with the velocity of liquid delivered can be tailored in order to deliver to a specific depth within the skin (Schramm-Baxter et al., 2004). Jet injectors have shown promising results in non-inferiority human clinical trials versus intramuscular injection of trivalent influenza vaccine (McAllister et al., 2014). As a result, the FDA approved the use of the PharmaJet Stratis 0.5ml Needle-free Jet Injector for delivery of AFLURIA® by bioCSL Inc. for patients 18-64 years old in 2014 (Hogan et al., 2015). Jet injectors have also been used clinically to immunise against tuberculosis (Parker, 1984), measles (Kok et al., 1983) and hepatitis A (Williams et al., 2000).

1.6.3 Gene Gun Technology

Particle bombardment can also be used for the delivery of solid particles into the skin, though the technology is associated with higher frequencies of local skin reaction (Levine, 2003) and delivery depth varies with differing skin sites (Schramm and Mitragotri, 2002). Studies utilising DNA vaccines formulated onto particles for delivery via gene gun have shown consistent immunisation in mice against ovalbumin compared to an intramuscular control (Yoshida et al., 2000) and promising results in a small cohort

of patients immunised against *Plasmodium*, the causative agent of malaria (Bergmann-Leitner and Leitner, 2015).

1.6.4 Microneedle (MN) Technology

MN arrays are a promising technology based on their ability to deliver antigen efficiently to the immune cell-rich uppermost skin layers for potent immunisation (Van Damme et al., 2009). Their reduction of post-injection pain and bleeding (Gill et al., 2008) and the avoidance of hypodermic needles maximise patient acceptability. Some MN approaches may offer avoidance of cold-chain requirements for vaccine transport, which can help to improve vaccine coverage in developing countries (Zehrung, 2009). The broad definition of a MN is a needle less than 1mm in length and the devices are generally classified as solid MNs, hollow MNs and dissolvable MNs.

1.6.4.1 Solid Microneedles

Solid MNs can be manufactured from a variety of inert materials- most commonly silicon (Kim et al., 2006, McGrath et al., 2011) or stainless steel (Torrisi et al., 2013, Gill and Prausnitz, 2007a). MNs are often manufactured in arrays containing tens or hundreds of needles in an evenly-spaced array (Zehrung, 2009). Care must be taken to ensure appropriate sharpness and spacing of needles to ensure effective skin penetration and avoid the 'bed of nails' effect (Cheung et al., 2014). These arrays can then be used in a number of ways. The arrays may be pre-applied into the skin, creating a number of small channels in the stratum corneum. After the array is removed, a topical liquid or semi-solid formulation (Pearton et al., 2008) or transdermal patch (Prausnitz, 2004) can be applied to the treated area where drug will be able to permeate into the skin more freely through the breaches in the stratum corneum. This is a straightforward, albeit two-step, approach, allowing conventional liquid and topical formulations to be used in combination with the new technology. The arrays might have a relatively straightforward route to regulatory approval as a single array type could be used in combination with many formulations. It does not, however, offer any potential for cold chain avoidance as existing formulations will be used. Also, in the absence of topical vaccine formulations, new formulations would have to be developed. Finally, it would

likely be an inefficient delivery method and difficult to guarantee that a therapeutic/protective dose had been delivered.

It is also possible to coat liquid formulation onto the surface of the needles, allowing it to dry and solidify (Gill and Prausnitz, 2007a). The coating ideally does not negate the needle array's ability to penetrate the stratum corneum (Pearton et al., 2010c). Following insertion, the interstitial fluid of the skin rehydrates the formulation and dissolves it from the array- leaving it deposited in the skin when the array is removed (Bariya et al., 2012). Microneedles coated with a reduced dose of influenza vaccine have been shown to provide protective immunity comparable to the intramuscular injection in mice (Kim et al., 2010). Another study in mice showed priming of CD8+ T-cells following administration of a DNA vaccine against hepatitis C coated onto microneedles (Gill et al., 2010).

This represents an efficient method of delivery as theoretically all of the formulation can be delivered into skin, though this may vary with both skin insertion success and formulation release. It may also be possible to colour the formulation so that its deposition in skin can be assessed visually by the health care professional or patient. Importantly for improving vaccine coverage in developing countries, a dry formulation would be the most likely to eschew the need for cold chain storage (Zehrung, 2009). The straightforward application process (provided device design is robust) could allow for self-application of vaccines, also reducing the burden on healthcare professionals (Donnelly et al., 2014). Regulatory approval of coated MNs represents a major barrier to these products though, given that they will likely involve novel formulation components and manufacturing processes (Ita, 2015).

1.6.4.2 Hollow Microneedles

Similar in concept to a smaller hypodermic needle, hollow MNs can allow the delivery of liquid formulation into the upper layers of the skin (Norman et al., 2013, Kim et al., 2012b). The hydrostatic pressure generated by passing liquid through a small-bore channel and the limited liquid capacity of a given area of dermis means that hollow MN are also often used in arrays (Wang et al., 2006) to distribute the hydrostatic pressure across multiple channels. The use of arrays also acts as a failsafe if one needle channel

becomes blocked during injection. The number of hollow needles in arrays are often lower than their solid counterparts. It is possible to design arrays that can be attached to a syringe for ease of use (Levin et al., 2015). The close analogy to conventional hypodermic needle injections means that liquid formulations may not need to be redesigned to be used with these MNs, and regulatory approval may be more straightforward. Studies in rats using the commercial poliovirus vaccine showed equivalency at a reduced dose compared to intramuscular vaccination (Kouiavskaia et al., 2015). Studies in human patients have shown superiority to intradermal vaccination against influenza by the Mantoux technique (Levin et al., 2014). Care must be taken in MN design as incomplete insertion of an array will lead to formulation following the path of least resistance and being lost outside of the skin. Their use does generate contaminated sharps with the associated health risks and cost of disposal, though shallow insertion depths should lower the risk of blood-borne pathogens contaminating the arrays.

1.6.4.3 Dissolvable Microneedles

A third MN approach is to design arrays where the therapeutic cargo is incorporated into dissolvable hydrophilic polymers or sugars (Lee et al., 2008). The MNs remain solid at room temperature, allowing them to be inserted into the skin (Hirobe et al., 2015). They are then able to uptake interstitial fluid in a manner similar to coated MN formulations leading to their dissolution in the skin (Moga et al., 2013). This will allow for quick visual confirmation of delivery success and will also avoid the generation of contaminated sharps. For vaccines, it is possible to disperse the antigen in the needle polymer so it can be delivered into skin. A study delivering influenza vaccine dispersed in polymer microneedles showed improved viral clearance from the lungs compared to intramuscular vaccination (Sullivan et al., 2010). Again, a non-liquid formulation may be able to reduce or avoid the need for cold chain transport. It will be important to design packaging that avoids atmospheric humidity from being absorbed by the needles which could soften them and prevent proper skin penetration (Chu et al., 2016). As this approach uses novel formulations and manufacturing processes there will be a need to overcome a raft of regulatory obstacles for clinical translation of the technology.

1.6.5 Intrafollicular Delivery

Hair follicles present on skin represent a potential delivery route into the skin. They are well-populated with immune cells, making them ideal targets for vaccination (Fan et al., 1999). Antigen-conjugated nanoparticle vaccines have shown particular suitability for this route where they can penetrate deeper into the follicles of porcine skin than a solution of peptide (Mittal et al., 2013). Another study using ovalbumin-conjugated nanoparticles in mice found that adjuvant is necessary within the formulation to ensure cellular and humoral immune responses are generated (Mittal et al., 2015). Intrafollicular application to murine skin of a DNA vaccine encoding hepatitis B surface antigen has been shown to provide an equivalent immune response to the commercially available intramuscular polypeptide vaccine (Fan et al., 1999).

1.6.6 Cellular Targeting of Skin Immune Cells

As well as the methods mentioned above, many of which can be tailored to target a particular region or depth within the skin, it is also possible to design vaccines to have an affinity for a specific immune cell population. For example, conjugating ovalbumin to monovalent monoclonal antibodies against the C-type lectin receptor CD205 has been shown to improve CD8+ T-cell responses in mice (Bonifaz et al., 2002, Bonifaz et al., 2004). One caveat of these promising results is that if DC-targeted vaccines are delivered in the absence of DC activating substances (such as adjuvant), then DCs will induce a state of tolerance against the antigen rather than immunity (Hawiger et al., 2001). The ability to target specific subsets of DCs can allow for the desired immune response to be tailored- for example delivery of identical antigen conjugated to antibodies either specific for CD205 or the dendritic cell inhibitory receptor-2 (DCIR2) to murine skin showed preferential CD8+ or CD4+ T-cell responses respectively (Dudziak et al., 2007). It is important that the full phenotype and functions of the various DC subsets are well understood before this method of vaccination can be implemented successfully.

1.7 Project Rationale

The intradermal delivery of vaccines represents a potentially beneficial healthcare approach. Intradermal delivery has been described in a PATH report as having the potential to reduce the cost of vaccination whilst improving compliance, immunisation success rates and geographical coverage (Zehrung, 2009). The high cost and regulatory obstacles associated with developing novel intradermal vaccines suggest that it may not be commercially attractive to replace vaccines which are currently delivered effectively via the IM route. Perhaps the best candidates would be novel vaccines against pathogens where no vaccine currently exist and will benefit from early stage research to optimise intradermal delivery. Influenza vaccines, where new vaccines must be delivered annually to immunise against the currently prevalent strains may also be a candidate for a new delivery approach (Kenney et al., 2004). The commercial success of FluMist® quadrivalent intranasal and Fluzone™ Fluzone quadrivalent intradermal vaccines show that new delivery approaches are marketable and it may be possible that technological development can further improve vaccine efficiency. This may become important in pandemic situations, where a limited supply of antigen is available at short notice and as many people need to be vaccinated as possible.

Given that intradermal vaccination may become an important route for emerging vaccines, it is vital that the characteristics of the skin tissue and the behaviours of the immune cells that reside there are fully understood. Whilst LCs were first described in 1868, it was over 100 years until they were recognised for their role in the immune system (Jolles, 2002). Dermal DCs were described later, with Ralph Steinman being recognised for his work in the field during the latter half of the 20th century with the 2011 Nobel Prize in Physiology or Medicine (Moberg, 2011). Subsequent work has uncovered the complexities that exist within the subsets of dDCs and the heterogeneity of function between these cells and LCs. Our understanding of the adaptive immune system and virology are concurrently expanding, allowing us to better comprehend and thereby treat or prevent pathogenic disease.

This project has the aim of improving the knowledge of human skin immune cells in the context of host interactions and intradermal vaccination. Specifically, their interactions with viral pathogens and vaccines against viral pathogens will be explored.

This will be combined with research into novel delivery technologies with the hope of informing intradermal vaccine research in the future.

1.8 Thesis Aim and Objectives

The aim of this Thesis is to further the understanding of human skin immune cells in order to inform how best to deliver vaccines into the skin for effective immunisation. The objectives are:

- Characterise the coating of peptide, protein and particulate vaccines onto solid MN arrays
- Assess the delivery of peptide, protein and particulate vaccines into the skin by MNs and to assess the response of skin cells
- Optimise a protocol to obtain migratory immune cells from skin for use in downstream cellular experiments
- Use the skin cell model to measure the immunostimulatory properties of vaccine candidates
- Utilise the skin cell model to study the infection pathways of the HIV virus
- Attempt to differentiate the vaccine antigen presentation properties of LCs and the subsets of dDCs in skin
- Assess whether novel formulation technologies can assist in the delivery of vaccines into the skin

1.9 Bibliography

AHMED, Z., KAWAMURA, T., SHIMADA, S. & PIGUET, V. 2015. The role of human dendritic cells in HIV-1 infection. *J Invest Dermatol,* 135**,** 1225-33.

ANDERSEN, M. H., SCHRAMA, D., THOR STRATEN, P. & BECKER, J. C. 2006. Cytotoxic T cells. *J Invest Dermatol,* 126**,** 32-41.

ANDREWS, S. N., JEONG, E. & PRAUSNITZ, M. R. 2013. Transdermal delivery of molecules is limited by full epidermis, not just stratum corneum. *Pharm Res,* 30**,** 1099-109.

ANTUNES, M. B. & COHEN, N. A. 2007. Mucociliary clearance--a critical upper airway host defense mechanism and methods of assessment. *Curr Opin Allergy Clin Immunol,* 7**,** 5-10.

ARTYOMOV, M. N., MUNK, A., GORVEL, L., KORENFELD, D., CELLA, M., TUNG, T. & KLECHEVSKY, E. 2015. Modular expression analysis reveals functional conservation between human Langerhans cells and mouse cross-priming dendritic cells. *J Exp Med,* 212**,** 743-57.

AUNGST, B. J. 2012. Absorption Enhancers: Applications and Advances. *The AAPS Journal,* 14**,** 10-18.

BANCHEREAU, J. & STEINMAN, R. M. 1998. Dendritic cells and the control of immunity. *Nature,* 392**,** 245-252.

BARBERO, A. M. & FRASCH, H. F. 2006. Transcellular route of diffusion through stratum corneum: results from finite element models. *J Pharm Sci,* 95**,** 2186-94.

BARIYA, S. H., GOHEL, M. C., MEHTA, T. A. & SHARMA, O. P. 2012. Microneedles: an emerging transdermal drug delivery system. *J Pharm Pharmacol,* 64**,** 11-29.

BELKAID, Y. & ROUSE, B. T. 2005. Natural regulatory T cells in infectious disease. *Nat Immunol,* 6**,** 353-60.

BELTRAMI, E. M., WILLIAMS, I. T., SHAPIRO, C. N. & CHAMBERLAND, M. E. 2000. Risk and Management of Blood-Borne Infections in Health Care Workers. *Clinical Microbiology Reviews,* 13**,** 385-407.

BENSON, H. A. E. & NAMJOSHI, S. 2008. Proteins and Peptides: Strategies for Delivery to and Across the Skin. *Journal of Pharmaceutical Sciences,* 97**,** 3591-3610.

BERGER, C. L., VASQUEZ, J. G., SHOFNER, J., MARIWALLA, K. & EDELSON, R. L. 2006. Langerhans cells: Mediators of immunity and tolerance. *The International Journal of Biochemistry & Cell Biology,* 38**,** 1632-1636.

BHAUMIK, S. 2012. Polio eradication: Current status and challenges. *Journal of Family Medicine and Primary Care,* 1**,** 84-85.

BIANCHI, M. E. 2007. DAMPs, PAMPs and alarmins: all we need to know about danger. *J Leukoc Biol,* 81**,** 1-5.

BOS, J. D., HAGENAARS, C., DAS, P. K., KRIEG, S. R., VOORN, W. J. & KAPSENBERG, M. L. 1989. Predominance of "memory" T cells (CD4+, CDw29+) over "naive" T cells (CD4+, CD45R+) in both normal and diseased human skin. *Arch Dermatol Res,* 281**,** 24-30.

BRENNAN, P. J., BRIGL, M. & BRENNER, M. B. 2013. Invariant natural killer T cells: an innate activation scheme linked to diverse effector functions. *Nat Rev Immunol,* 13**,** 101-117.

BRENNER, M. & HEARING, V. J. 2008. The Protective Role of Melanin Against UV Damage in Human Skin. *Photochemistry and photobiology,* 84**,** 539-549.

BRIGGAMAN, R. A., DALLDORF, F. G. & WHEELER, C. E., JR. 1971. Formation and origin of basal lamina and anchoring fibrils in adult human skin. *J Cell Biol,* 51**,** 384-95.

BROERE, F., APASOV, S. G., SITKOVSKY, M. V. & VAN EDEN, W. 2011. A2 T cell subsets and T cell-mediated immunity. *In:* NIJKAMP, F. P. & PARNHAM, J. M. (eds.) *Principles of Immunopharmacology: 3rd revised and extended edition.* Basel: Birkhäuser Basel.

BROWN, M. B., MARTIN, G. P., JONES, S. A. & AKOMEAH, F. K. 2006. Dermal and transdermal drug delivery systems: current and future prospects. *Drug Deliv,* 13**,** 175-87.

CARPENTIER, S., VU MANH, T.-P., CHELBI, R., HENRI, S., MALISSEN, B., HANIFFA, M., GINHOUX, F. & DALOD, M. 2016a. Comparative genomics analysis of mononuclear phagocyte subsets confirms homology between lymphoid tissue-resident and dermal XCR1+ DCs in mouse and human and distinguishes them from Langerhans cells. *J Immunol Methods,* 432**,** 35-49.

CARPENTIER, S., VU MANH, T.-P., CHELBI, R., HENRI, S., MALISSEN, B., HANIFFA, M., GINHOUX, F. & DALOD, M. 2016b. Comparative genomics analysis of mononuclear phagocyte subsets confirms homology between lymphoid tissue-resident and dermal XCR1+ DCs in mouse and human and distinguishes them from Langerhans cells. *Journal of Immunological Methods,* 432**,** 35-49.

CAUCHETEUX, S. M., MITCHELL, J. P., IVORY, M. O., HIROSUE, S., HAKOBYAN, S., DOLTON, G., LADELL, K., MINERS, K., PRICE, D. A., KAN-MITCHELL, J., SEWELL, A. K., NESTLE, F., MORIS, A., KAROO, R. O., BIRCHALL, J. C., SWARTZ, M. A., HUBBEL, J. A., BLANCHET, F. P. & PIGUET, V. 2016. Polypropylene Sulfide Nanoparticle p24 Vaccine Promotes Dendritic Cell-Mediated Specific Immune Responses against HIV-1. *J Invest Dermatol,* 136**,** 1172-81.

CHALLIER, J., BRUNIQUEL, D., SEWELL, A. K. & LAUGEL, B. 2013. Adenosine and cAMP signalling skew human dendritic cell differentiation towards a tolerogenic phenotype with defective CD8(+) T-cell priming capacity. *Immunology,* 138**,** 402-10.

CHEUNG, K., HAN, T. & DAS, D. B. 2014. Effect of Force of Microneedle Insertion on the Permeability of Insulin in Skin. *Journal of Diabetes Science and Technology,* 8**,** 444-452.

CHU, C. C., ALI, N., KARAGIANNIS, P., DI MEGLIO, P., SKOWERA, A., NAPOLITANO, L., BARINAGA, G., GRYS, K., SHARIF-PAGHALEH, E., KARAGIANNIS, S. N., PEAKMAN, M., LOMBARDI, G. & NESTLE, F. O. 2012. Resident CD141 (BDCA3)+ dendritic cells in human skin produce IL-10 and induce regulatory T cells that suppress skin inflammation. *J Exp Med,* 209**,** 935-45.

CHU, L. Y., YE, L., DONG, K., COMPANS, R. W., YANG, C. & PRAUSNITZ, M. R. 2016. Enhanced Stability of Inactivated Influenza Vaccine Encapsulated in Dissolving Microneedle Patches. *Pharm Res,* 33**,** 868-78.

CLARK, R. A. 2010. Skin resident T cells: the ups and downs of on site immunity. *The Journal of investigative dermatology,* 130**,** 362-370.

CZERNIELEWSKI, J. M. & DEMARCHEZ, M. 1987. Further evidence for the self-reproducing capacity of Langerhans cells in human skin. *J Invest Dermatol,* 88**,** 17-20.

DAVIS, M. M., BONIFACE, J. J., REICH, Z., LYONS, D., HAMPL, J., ARDEN, B. & CHIEN, Y. 1998. Ligand recognition by alpha beta T cell receptors. *Annu Rev Immunol,* 16**,** 523-44.

DE WITTE, L., NABATOV, A., PION, M., FLUITSMA, D., DE JONG, M. A., DE GRUIJL, T., PIGUET, V., VAN KOOYK, Y. & GEIJTENBEEK, T. B. 2007. Langerin is a natural barrier to HIV-1 transmission by Langerhans cells. *Nat Med,* 13**,** 367-71.

DEMPSEY, P. W., VAIDYA, S. A. & CHENG, G. 2003. The art of war: Innate and adaptive immune responses. *Cell Mol Life Sci,* 60**,** 2604-21.

DONNELLY, R. F., MOFFATT, K., ALKILANI, A. Z., VICENTE-PEREZ, E. M., BARRY, J., MCCRUDDEN, M. T. & WOOLFSON, A. D. 2014. Hydrogel-forming

microneedle arrays can be effectively inserted in skin by self-application: a pilot study centred on pharmacist intervention and a patient information leaflet. *Pharm Res,* 31**,** 1989-99.

DUCLOS, P. & BENTSI-ENCHILL, A. 1993. Current thoughts on the risks and benefits of immunisation. *Drug Saf,* 8**,** 404-13.

DUDZIAK, D., KAMPHORST, A. O., HEIDKAMP, G. F., BUCHHOLZ, V. R., TRUMPFHELLER, C., YAMAZAKI, S., CHEONG, C., LIU, K., LEE, H.-W. & PARK, C. G. 2007. Differential antigen processing by dendritic cell subsets in vivo. *Science,* 315**,** 107-111.

DUNKELBERGER, J. R. & SONG, W. C. 2010. Complement and its role in innate and adaptive immune responses. *Cell Res,* 20**,** 34-50.

ECKERT, R. L. & RORKE, E. A. 1989. Molecular biology of keratinocyte differentiation. *Environmental Health Perspectives,* 80**,** 109-116.

ELIAS, P. M. 2005. Stratum corneum defensive functions: an integrated view. *J Invest Dermatol,* 125**,** 183-200.

ELIAS, P. M. 2007. The skin barrier as an innate immune element. *Seminars in Immunopathology,* 29**,** 3-14.

ENGERING, A. J., CELLA, M., FLUITSMA, D. M., HOEFSMIT, E. C., LANZAVECCHIA, A. & PIETERS, J. 1997. Mannose receptor mediated antigen uptake and presentation in human dendritic cells. *Adv Exp Med Biol,* 417**,** 183-7.

FLUHR, J. W., MAO-QIANG, M., BROWN, B. E., WERTZ, P. W., CRUMRINE, D., SUNDBERG, J. P., FEINGOLD, K. R. & ELIAS, P. M. 2003. Glycerol regulates stratum corneum hydration in sebaceous gland deficient (asebia) mice. *J Invest Dermatol,* 120**,** 728-37.

FORE, J. 2006. A review of skin and the effects of aging on skin structure and function. *Ostomy Wound Manage,* 52**,** 24-35; quiz 36-7.

FORSTER, R., DAVALOS-MISSLITZ, A. C. & ROT, A. 2008. CCR7 and its ligands: balancing immunity and tolerance. *Nat Rev Immunol,* 8**,** 362-71.

FORTHAL, D. N. 2014. Functions of Antibodies. *Microbiology spectrum,* 2**,** 1-17.

FOX, J. P., ELVEBACK, L., SCOTT, W., GATEWOOD, L. & ACKERMAN, E. 1971. Herd Immunity: Basic Concept and Relevance to Public Health and Immunization Practices. *American Journal of Epidemiology,* 94**,** 179-189.

GILL, H. S., DENSON, D. D., BURRIS, B. A. & PRAUSNITZ, M. R. 2008. Effect of microneedle design on pain in human volunteers. *Clin J Pain,* 24**,** 585-94.

GILL, H. S. & PRAUSNITZ, M. R. 2007. Coated microneedles for transdermal delivery. *J Control Release,* 117**,** 227-37.

GRANUCCI, F., FERRERO, E., FOTI, M., AGGUJARO, D., VETTORETTO, K. & RICCIARDI-CASTAGNOLI, P. 1999. Early events in dendritic cell maturation induced by LPS. *Microbes and Infection,* 1**,** 1079-1084.

GUERMONPREZ, P., VALLADEAU, J., ZITVOGEL, L., THERY, C. & AMIGORENA, S. 2002. Antigen presentation and T cell stimulation by dendritic cells. *Annu Rev Immunol,* 20**,** 621-67.

HACKSTEIN, H. & THOMSON, A. W. 2004. Dendritic cells: emerging pharmacological targets of immunosuppressive drugs. *Nat Rev Immunol,* 4**,** 24-34.

HANIFFA, M., GINHOUX, F., WANG, X. N., BIGLEY, V., ABEL, M., DIMMICK, I., BULLOCK, S., GRISOTTO, M., BOOTH, T., TAUB, P., HILKENS, C., MERAD, M. & COLLIN, M. 2009. Differential rates of replacement of human dermal dendritic cells and macrophages during hematopoietic stem cell transplantation. *J Exp Med,* 206**,** 371-85.

HANIFFA, M., SHIN, A., BIGLEY, V., MCGOVERN, N., TEO, P., SEE, P., WASAN, P. S., WANG, X. N., MALINARICH, F., MALLERET, B., LARBI, A., TAN, P., ZHAO, H., POIDINGER, M., PAGAN, S., COOKSON, S., DICKINSON, R., DIMMICK, I., JARRETT, R. F., RENIA, L., TAM, J., SONG, C., CONNOLLY, J., CHAN, J. K., GEHRING, A., BERTOLETTI, A., COLLIN, M. & GINHOUX, F. 2012. Human tissues contain CD141hi cross-presenting dendritic cells with functional homology to mouse CD103+ nonlymphoid dendritic cells. *Immunity,* 37**,** 60-73.

HAO, W. L. & LEE, Y. K. 2004. Microflora of the gastrointestinal tract: a review. *Methods Mol Biol,* 268**,** 491-502.

HEATH, W. R. & CARBONE, F. R. 2001. Cross-presentation, dendritic cells, tolerance and immunity. *Annu Rev Immunol,* 19**,** 47-64.

HELFT, J., MANICASSAMY, B., GUERMONPREZ, P., HASHIMOTO, D., SILVIN, A., AGUDO, J., BROWN, B. D., SCHMOLKE, M., MILLER, J. C., LEBOEUF, M., MURPHY, K. M., GARCIA-SASTRE, A. & MERAD, M. 2012. Cross-presenting CD103+ dendritic cells are protected from influenza virus infection. *J Clin Invest,* 122**,** 4037-47.

HICKLING, J. K., JONES, K. R., FRIEDE, M., ZEHRUNG, D., CHEN, D. & KRISTENSEN, D. 2011. Intradermal delivery of vaccines: potential benefits and current challenges. *Bulletin of the World Health Organization,* 89**,** 221-226.

HIROBE, S., AZUKIZAWA, H., HANAFUSA, T., MATSUO, K., QUAN, Y.-S., KAMIYAMA, F., KATAYAMA, I., OKADA, N. & NAKAGAWA, S. 2015. Clinical study and

stability assessment of a novel transcutaneous influenza vaccination using a dissolving microneedle patch. *Biomaterials,* 57**,** 50-58.

HOEFFEL, G., WANG, Y., GRETER, M., SEE, P., TEO, P., MALLERET, B., LEBOEUF, M., LOW, D., OLLER, G., ALMEIDA, F., CHOY, S. H. Y., GRISOTTO, M., RENIA, L., CONWAY, S. J., STANLEY, E. R., CHAN, J. K. Y., NG, L. G., SAMOKHVALOV, I. M., MERAD, M. & GINHOUX, F. 2012. Adult Langerhans cells derive predominantly from embryonic fetal liver monocytes with a minor contribution of yolk sac–derived macrophages. *J Exp Med,* 209**,** 1167-1181.

HOLBROOK, K. A., BYERS, P. H. & PINNELL, S. R. 1982. The structure and function of dermal connective tissue in normal individuals and patients with inherited connective tissue disorders. *Scan Electron Microsc***,** 1731-44.

HOLTMEIER, W. & KABELITZ, D. 2005. gammadelta T cells link innate and adaptive immune responses. *Chem Immunol Allergy,* 86**,** 151-83.

HORNEF, M. W., WICK, M. J., RHEN, M. & NORMARK, S. 2002. Bacterial strategies for overcoming host innate and adaptive immune responses. *Nat Immunol,* 3**,** 1033-40.

HUBO, M., TRINSCHEK, B., KRYCZANOWSKY, F., TÜTTENBERG, A., STEINBRINK, K. & JONULEIT, H. 2013. Costimulatory molecules on immunogenic versus tolerogenic human dendritic cells. *Frontiers in Immunology,* 4.

HUNGER, R. E., SIELING, P. A., OCHOA, M. T., SUGAYA, M., BURDICK, A. E., REA, T. H., BRENNAN, P. J., BELISLE, J. T., BLAUVELT, A., PORCELLI, S. A. & MODLIN, R. L. 2004. Langerhans cells utilize CD1a and langerin to efficiently present nonpeptide antigens to T cells. *Journal of Clinical Investigation,* 113**,** 701-708.

IAC. 2015. *How to Administer Intramuscular and Subcutaneous Vaccine Injections* [Online]. Minnesota: Centers for Disease Control and Prevention. Available: http://www.immunize.org/catg.d/p2020.pdf [Accessed 30 June 2016].

INABA, K., TURLEY, S., YAMAIDE, F., IYODA, T., MAHNKE, K., INABA, M., PACK, M., SUBKLEWE, M., SAUTER, B., SHEFF, D., ALBERT, M., BHARDWAJ, N., MELLMAN, I. & STEINMAN, R. M. 1998. Efficient presentation of phagocytosed cellular fragments on the major histocompatibility complex class II products of dendritic cells. *J Exp Med,* 188**,** 2163-73.

ISAAC, M. & HOLVEY, C. 2012. Transdermal patches: the emerging mode of drug delivery system in psychiatry. *Therapeutic Advances in Psychopharmacology,* 2**,** 255-263.

ITA, K. 2015. Transdermal Delivery of Drugs with Microneedles-Potential and Challenges. *Pharmaceutics,* 7**,** 90-105.

JANEWAY, C. A., JR. 1991. The co-receptor function of CD4. *Semin Immunol,* 3**,** 153-60.

JIANG, X., CLARK, R. A., LIU, L., WAGERS, A. J., FUHLBRIGGE, R. C. & KUPPER, T. S. 2012. Skin infection generates non-migratory memory CD8+ TRM cells providing global skin immunity. *Nature,* 483**,** 227-231.

JIN, J.-F., ZHU, L.-L., CHEN, M., XU, H.-M., WANG, H.-F., FENG, X.-Q., ZHU, X.-P. & ZHOU, Q. 2015. The optimal choice of medication administration route regarding intravenous, intramuscular, and subcutaneous injection. *Patient preference and adherence,* 9**,** 923-942.

JOHNSTON, M. I. & FAUCI, A. S. 2008. An HIV vaccine--challenges and prospects. *N Engl J Med,* 359**,** 888-90.

JOLLES, S. 2002. Paul Langerhans. *Journal of Clinical Pathology,* 55**,** 243-243.

KAECH, S. M., WHERRY, E. J. & AHMED, R. 2002. Effector and memory T-cell differentiation: implications for vaccine development. *Nat Rev Immunol,* 2**,** 251-262.

KALIA, Y. N., ALBERTI, I., SEKKAT, N., CURDY, C., NAIK, A. & GUY, R. H. 2000. Normalization of Stratum Corneum Barrier Function and Transepidermal Water Loss In Vivo. *Pharmaceutical Research,* 17**,** 1148-1150.

KALISH, R. S., WOOD, J. A. & LAPORTE, A. 1994. Processing of urushiol (poison ivy) hapten by both endogenous and exogenous pathways for presentation to T cells in vitro. *Journal of Clinical Investigation,* 93**,** 2039-2047.

KANITAKIS, J., HOYO, E., PERRIN, C. & SCHMITT, D. 1993. Electron-microscopic observation of a human epidermal Langerhans cell in mitosis. *J Dermatol,* 20**,** 35-9.

KENNEY, R. T., FRECH, S. A., MUENZ, L. R., VILLAR, C. P. & GLENN, G. M. 2004. Dose sparing with intradermal injection of influenza vaccine. *N Engl J Med,* 351**,** 2295-301.

KIM, S., SHETTY, S., PRICE, D. & BHANSALI, S. 2006. Skin penetration of silicon dioxide microneedle arrays. *Conf Proc IEEE Eng Med Biol Soc,* 1**,** 4088-91.

KIM, Y.-C., PARK, J.-H. & PRAUSNITZ, M. R. 2012. Microneedles for drug and vaccine delivery. *Advanced drug delivery reviews,* 64**,** 1547-1568.

KIM, Y.-C. & PRAUSNITZ, M. R. 2011. Enabling skin vaccination using new delivery technologies. *Drug Delivery and Translational Research,* 1**,** 7-12.

KLECHEVSKY, E., MORITA, R., LIU, M., CAO, Y., COQUERY, S., THOMPSON-SNIPES, L. A., BRIERE, F., CHAUSSABEL, D., ZURAWSKI, G., PALUCKA, A. K., REITER, Y., BANCHEREAU, J. & UENO, H. 2008. Functional Specializations of Human

Epidermal Langerhans Cells and CD14(+) Dermal Dendritic Cells. *Immunity,* 29**,** 497-510.

KUMAR, H., KAWAI, T. & AKIRA, S. 2011. Pathogen recognition by the innate immune system. *Int Rev Immunol,* 30**,** 16-34.

KUROSAKI, T., KOMETANI, K. & ISE, W. 2015. Memory B cells. *Nat Rev Immunol,* 15**,** 149-159.

LALVANI, A., BROOKES, R., HAMBLETON, S., BRITTON, W. J., HILL, A. V. & MCMICHAEL, A. J. 1997. Rapid effector function in CD8+ memory T cells. *J Exp Med,* 186**,** 859-65.

LECHLER, T. & FUCHS, E. 2005. Asymmetric cell divisions promote stratification and differentiation of mammalian skin. *Nature,* 437**,** 275-280.

LEE, J. W., PARK, J.-H. & PRAUSNITZ, M. R. 2008. Dissolving microneedles for transdermal drug delivery. *Biomaterials,* 29**,** 2113-2124.

LEENAARS, M. & HENDRIKSEN, C. F. 1998. Influence of Route of Injection on Efficacy and Side Effects of Immunisation. *Altex,* 15**,** 87.

LEON, B., LOPEZ-BRAVO, M. & ARDAVIN, C. 2005. Monocyte-derived dendritic cells. *Semin Immunol,* 17**,** 313-8.

LEVIN, A., BURGESS, C., GARRISON, L. P., JR., BAUCH, C., BABIGUMIRA, J., SIMONS, E. & DABBAGH, A. 2011. Global eradication of measles: an epidemiologic and economic evaluation. *J Infect Dis,* 204 Suppl 1**,** S98-106.

LEVIN, Y., KOCHBA, E., HUNG, I. & KENNEY, R. 2015. Intradermal vaccination using the novel microneedle device MicronJet600: Past, present, and future. *Hum Vaccin Immunother,* 11**,** 991-7.

LEVINE, M. M. 2003. Can needle-free administration of vaccines become the norm in global immunization? *Nat Med,* 9**,** 99-103.

LIARD, C., MUNIER, S., JOULIN-GIET, A., BONDUELLE, O., HADAM, S., DUFFY, D., VOGT, A., VERRIER, B. & COMBADIERE, B. 2012. Intradermal immunization triggers epidermal Langerhans cell mobilization required for CD8 T-cell immune responses. *J Invest Dermatol,* 132**,** 615-25.

LUKAS, M., STOSSEL, H., HEFEL, L., IMAMURA, S., FRITSCH, P., SEPP, N. T., SCHULER, G. & ROMANI, N. 1996. Human cutaneous dendritic cells migrate through dermal lymphatic vessels in a skin organ culture model. *J Invest Dermatol,* 106**,** 1293-9.

MAKSIMOVIC, S., NAKATANI, M., BABA, Y., NELSON, A. M., MARSHALL, K. L., WELLNITZ, S. A., FIROZI, P., WOO, S.-H., RANADE, S., PATAPOUTIAN, A. &

LUMPKIN, E. A. 2014. Epidermal Merkel cells are mechanosensory cells that tune mammalian touch receptors. *Nature,* 509**,** 617-621.

MALISSEN, B., TAMOUTOUNOUR, S. & HENRI, S. 2014. The origins and functions of dendritic cells and macrophages in the skin. *Nat Rev Immunol,* 14**,** 417-28.

MARTIN, N. H. 1969. The immunoglobulins: a review. *Journal of Clinical Pathology,* 22**,** 117-131.

MCGOVERN, N., SCHLITZER, A., GUNAWAN, M., JARDINE, L., SHIN, A., POYNER, E., GREEN, K., DICKINSON, R., WANG, X.-N., LOW, D., BEST, K., COVINS, S., MILNE, P., PAGAN, S., ALJEFRI, K., WINDEBANK, M., SAAVEDRA, DIEGO M., LARBI, A., WASAN, PAVANDIP S., DUAN, K., POIDINGER, M., BIGLEY, V., GINHOUX, F., COLLIN, M. & HANIFFA, M. 2014. Human Dermal CD14(+) Cells Are a Transient Population of Monocyte-Derived Macrophages. *Immunity,* 41**,** 465-477.

MCGRATH, M. G., VRDOLJAK, A., O'MAHONY, C., OLIVEIRA, J. C., MOORE, A. C. & CREAN, A. M. 2011. Determination of parameters for successful spray coating of silicon microneedle arrays. *International Journal of Pharmaceutics,* 415**,** 140-149.

MEDZHITOV, R. 2008. Origin and physiological roles of inflammation. *Nature,* 454**,** 428-435.

MEDZHITOV, R. & JANEWAY, C. 2000. Innate Immunity. *N Engl J Med,* 343**,** 338-344.

MERAD, M., GINHOUX, F. & COLLIN, M. 2008. Origin, homeostasis and function of Langerhans cells and other langerin-expressing dendritic cells. *Nat Rev Immunol,* 8**,** 935-947.

MERAD, M., MANZ, M. G., KARSUNKY, H., WAGERS, A., PETERS, W., CHARO, I., WEISSMAN, I. L., CYSTER, J. G. & ENGLEMAN, E. G. 2002. Langerhans cells renew in the skin throughout life under steady-state conditions. *Nat Immunol,* 3**,** 1135-41.

MERAD, M., SATHE, P., HELFT, J., MILLER, J. & MORTHA, A. 2013. The Dendritic Cell Lineage: Ontogeny and Function of Dendritic Cells and Their Subsets in the Steady State and the Inflamed Setting. *Annual review of immunology,* 31**,** 10.1146/annurev-immunol-020711-074950.

MILSTONE, L. M. 2004. Epidermal desquamation. *J Dermatol Sci,* 36**,** 131-40.

MOBERG, C. L. 2011. An appreciation of Ralph Marvin Steinman (1943–2011). *The Journal of Experimental Medicine,* 208**,** 2337-2342.

MOGA, K. A., BICKFORD, L. R., GEIL, R. D., DUNN, S. S., PANDYA, A. A., WANG, Y., FAIN, J. H., ARCHULETA, C. F., O'NEILL, A. T. & DESIMONE, J. M. 2013. Rapidly-dissolvable microneedle patches via a highly scalable and reproducible soft lithography approach. *Adv Mater,* 25**,** 5060-6.

MOHAMMED, J., BEURA, L. K., BOBR, A., ASTRY, B., CHICOINE, B., KASHEM, S. W., WELTY, N. E., IGYARTO, B. Z., WIJEYESINGHE, S., THOMPSON, E. A., MATTE, C., BARTHOLIN, L., KAPLAN, A., SHEPPARD, D., BRIDGES, A. G., SHLOMCHIK, W. D., MASOPUST, D. & KAPLAN, D. H. 2016. Stromal cells control the epithelial residence of DCs and memory T cells by regulated activation of TGF-beta. *Nat Immunol,* 17**,** 414-21.

MORGAN, A. J. & PARKER, S. 2007. Translational Mini-Review Series on Vaccines: The Edward Jenner Museum and the history of vaccination. *Clinical and Experimental Immunology,* 147**,** 389-394.

MURPHY, K., TRAVERS, P., WALPORT, M. & JANEWAY, C. 2012. *Janeway's Immunobiology (8th ed.),* New York, Garland Science.

NESTLE, F. O., ZHENG, X. G., THOMPSON, C. B., TURKA, L. A. & NICKOLOFF, B. J. 1993. Characterization of dermal dendritic cells obtained from normal human skin reveals phenotypic and functionally distinctive subsets. *J Immunol,* 151**,** 6535-45.

NG, W. C., LONDRIGAN, S. L., NASR, N., CUNNINGHAM, A. L., TURVILLE, S., BROOKS, A. G. & READING, P. C. 2016. The C-type Lectin Langerin Functions as a Receptor for Attachment and Infectious Entry of Influenza A Virus. *J Virol,* 90**,** 206-21.

NI, K. & O'NEILL, H. C. 1997. The role of dendritic cells in T cell activation. *Immunol Cell Biol,* 75**,** 223-30.

NOMURA, T., KABASHIMA, K. & MIYACHI, Y. 2014. The panoply of αβT cells in the skin. *Journal of Dermatological Science,* 76**,** 3-9.

NORLÉN, L. 2006. Stratum corneum keratin structure, function and formation – a comprehensive review. *International Journal of Cosmetic Science,* 28**,** 397-425.

NORMAN, J. J., CHOI, S. O., TONG, N. T., AIYAR, A. R., PATEL, S. R., PRAUSNITZ, M. R. & ALLEN, M. G. 2013. Hollow microneedles for intradermal injection fabricated by sacrificial micromolding and selective electrodeposition. *Biomed Microdevices,* 15**,** 203-10.

NORMAN, J. J., GUPTA, J., PATEL, S. R., PARK, S., JARRAHIAN, C., ZEHRUNG, D. & PRAUSNITZ, M. R. 2014. Reliability and accuracy of intradermal injection by Mantoux technique, hypodermic needle adapter, and hollow microneedle in pigs. *Drug Deliv Transl Res,* 4**,** 126-30.

OCHSENBEIN, A. F. & ZINKERNAGEL, R. M. 2000. Natural antibodies and complement link innate and acquired immunity. *Immunol Today,* 21**,** 624-30.

PARTHASARATHI, G., NYFORT-HANSEN, K. & NAHATA, M. C. 2004. *A text book of clinical pharmacy practice : essential concepts and skills,* Hyderabad ; Great Britain, Orient Longman Ltd.

PASPARAKIS, M., HAASE, I. & NESTLE, F. O. 2014. Mechanisms regulating skin immunity and inflammation. *Nature Reviews Immunology,* 14**,** 289-301.

PEARTON, M., ALLENDER, C., BRAIN, K., ANSTEY, A., GATELEY, C., WILKE, N., MORRISSEY, A. & BIRCHALL, J. 2008. Gene Delivery to the Epidermal Cells of Human Skin Explants Using Microfabricated Microneedles and Hydrogel Formulations. *Pharmaceutical Research,* 25**,** 407-416.

PEARTON, M., KANG, S.-M., SONG, J.-M., ANSTEY, A. V., IVORY, M., COMPANS, R. W. & BIRCHALL, J. C. 2010a. Changes in Human Langerhans Cells Following Intradermal Injection of Influenza Virus-Like Particle Vaccines. *PLoS ONE,* 5**,** e12410.

PEARTON, M., KANG, S.-M., SONG, J.-M., KIM, Y.-C., QUAN, F.-S., ANSTEY, A., IVORY, M., PRAUSNITZ, M. R., COMPANS, R. W. & BIRCHALL, J. C. 2010b. Influenza Virus-Like Particles coated onto microneedles can elicit stimulatory effects on Langerhans cells in human skin. *Vaccine,* 28**,** 6104-6113.

PIGUET, V., CAUCHETEUX, S. M., IANNETTA, M. & HOSMALIN, A. 2014. Altered antigen-presenting cells during HIV-1 infection. *Curr Opin HIV AIDS,* 9**,** 478-84.

PRAUSNITZ, M. R. 2004. Microneedles for transdermal drug delivery. *Advanced Drug Delivery Reviews,* 56**,** 581-587.

PRAUSNITZ, M. R. & LANGER, R. 2008. Transdermal drug delivery. *Nature biotechnology,* 26**,** 1261-1268.

PRAZMA, C. M. & TEDDER, T. F. 2008. Dendritic cell CD83: A therapeutic target or innocent bystander? *Immunology Letters,* 115**,** 1-8.

RAJEWSKY, K. & VON BOEHMER, H. 2008. Lymphocyte development. Overview. *Curr Opin Immunol,* 20**,** 127-130.

REYGROBELLET, C., VIALA-DANTEN, M., MEUNIER, J., WEBER, F. & NGUYEN, V. H. 2010. Perception and acceptance of intradermal influenza vaccination: Patient reported outcomes from phase 3 clinical trials. *Hum Vaccin,* 6**,** 336-45.

ROMANI, N., CLAUSEN, B. E. & STOITZNER, P. 2010. Langerhans cells and more: langerin-expressing dendritic cell subsets in the skin. *Immunological reviews,* 234**,** 120-141.

ROMANOVSKY, A. A. 2014. Skin temperature: its role in thermoregulation. *Acta physiologica (Oxford, England),* 210**,** 498-507.

RUSSELL-JONES, G. J. 2000. Oral vaccine delivery. *Journal of Controlled Release,* 65**,** 49-54.

SALLUSTO, F., CELLA, M., DANIELI, C. & LANZAVECCHIA, A. 1995. Dendritic cells use macropinocytosis and the mannose receptor to concentrate macromolecules in the major histocompatibility complex class II compartment: downregulation by cytokines and bacterial products. *J Exp Med,* 182**,** 389-400.

SANGIULIANO, B., PEREZ, N. M., MOREIRA, D. F. & BELIZARIO, J. E. 2014. Cell death-associated molecular-pattern molecules: inflammatory signaling and control. *Mediators Inflamm,* 2014**,** 821043.

SCHRAMM, J. & MITRAGOTRI, S. 2002. Transdermal drug delivery by jet injectors: energetics of jet formation and penetration. *Pharm Res,* 19**,** 1673-9.

SCHROEDER, H. W. & CAVACINI, L. 2010. Structure and Function of Immunoglobulins. *The Journal of allergy and clinical immunology,* 125**,** S41-S52.

SIEGRIST, C.-A. 2013. 2 - Vaccine immunology. *In:* OFFIT, S. A. P. A. O. A. (ed.) *Vaccines (Sixth Edition).* London: W.B. Saunders.

SOONAWALA, D., VERDIJK, P., WIJMENGA-MONSUUR, A. J., BOOG, C. J., KOEDAM, P., VISSER, L. G. & ROTS, N. Y. 2013. Intradermal fractional booster dose of inactivated poliomyelitis vaccine with a jet injector in healthy adults. *Vaccine,* 31**,** 3688-3694.

STEINMAN, R. M. 1991. The dendritic cell system and its role in immunogenicity. *Annu Rev Immunol,* 9**,** 271-96.

STOITZNER, P., TRIPP, C. H., EBERHART, A., PRICE, K. M., JUNG, J. Y., BURSCH, L., RONCHESE, F. & ROMANI, N. 2006. Langerhans cells cross-present antigen derived from skin. *Proc Natl Acad Sci U S A,* 103**,** 7783-8.

SUH, H., SHIN, J. & KIM, Y.-C. 2014. Microneedle patches for vaccine delivery. *Clinical and Experimental Vaccine Research,* 3**,** 42-49.

SULLIVAN, S. P., KOUTSONANOS, D. G., DEL PILAR MARTIN, M., LEE, J. W., ZARNITSYN, V., CHOI, S.-O., MURTHY, N., COMPANS, R. W., SKOUNTZOU, I.

& PRAUSNITZ, M. R. 2010. Dissolving polymer microneedle patches for influenza vaccination. *Nat Med,* 16**,** 915-920.

TAKEUCHI, O. & AKIRA, S. 2010. Pattern recognition receptors and inflammation. *Cell,* 140**,** 805-20.

THEOHARIDES, T. C., ALYSANDRATOS, K.-D., ANGELIDOU, A., DELIVANIS, D.-A., SISMANOPOULOS, N., ZHANG, B., ASADI, S., VASIADI, M., WENG, Z., MINIATI, A. & KALOGEROMITROS, D. 2012. Mast cells and inflammation. *Biochimica et Biophysica Acta (BBA) - Molecular Basis of Disease,* 1822**,** 21-33.

THOMAS, A. A., VRIJSEN, R. & BOEYE, A. 1986. Relationship between poliovirus neutralization and aggregation. *J Virol,* 59**,** 479-85.

TORRISI, B. M., ZARNITSYN, V., PRAUSNITZ, M. R., ANSTEY, A., GATELEY, C., BIRCHALL, J. C. & COULMAN, S. A. 2013. Pocketed microneedles for rapid delivery of a liquid-state botulinum toxin A formulation into human skin. *J Control Release,* 165**,** 146-52.

TOUITOU, E. 2002. Drug delivery across the skin. *Expert Opin Biol Ther,* 2**,** 723-33.

TOZUKA, M., OKA, T., JOUNAI, N., EGAWA, G., ISHII, K. J., KABASHIMA, K. & TAKESHITA, F. 2016. Efficient antigen delivery to the draining lymph nodes is a key component in the immunogenic pathway of the intradermal vaccine. *Journal of Dermatological Science,* 82**,** 38-45.

UNANUE, E. R. 1984. Antigen-presenting function of the macrophage. *Annu Rev Immunol,* 2**,** 395-428.

VAN DAMME, P., OOSTERHUIS-KAFEJA, F., VAN DER WIELEN, M., ALMAGOR, Y., SHARON, O. & LEVIN, Y. 2009. Safety and efficacy of a novel microneedle device for dose sparing intradermal influenza vaccination in healthy adults. *Vaccine,* 27**,** 454-9.

VAN DEN BERG, J. H., NUJIEN, B., BEIJNEN, J. H., VINCENT, A., VAN TINTEREN, H., KLUGE, J., WOERDEMAN, L. A., HENNINK, W. E., STORM, G., SCHUMACHER, T. N. & HAANEN, J. B. 2009. Optimization of intradermal vaccination by DNA tattooing in human skin. *Hum Gene Ther,* 20**,** 181-9.

WANG, P. M., CORNWELL, M., HILL, J. & PRAUSNITZ, M. R. 2006. Precise Microinjection into Skin Using Hollow Microneedles. *Journal of Investigative Dermatology,* 126**,** 1080-1087.

WEINTRAUB, A. 2003. Immunology of bacterial polysaccharide antigens. *Carbohydr Res,* 338**,** 2539-47.

WHO 2010. Rabies vaccines: WHO position paper. *Weekly Epidemiological Record,* 32**,** 309-320.

WHO. 2012. *Module 2- Types of Vaccine and Adverse Reactions* [Online]. Available: http://vaccine-safety-training.org/route-of-administration.html [Accessed July 11th 2016].

WILLIAMS, J., FOX-LEYVA, L., CHRISTENSEN, C., FISHER, D., SCHLICTING, E., SNOWBALL, M., NEGUS, S., MAYERS, J., KOLLER, R. & STOUT, R. 2000. Hepatitis A vaccine administration: comparison between jet-injector and needle injection. *Vaccine,* 18**,** 1939-1943.

WOOF, J. M. & RUSSELL, M. W. 2011. Structure and function relationships in IgA. *Mucosal Immunol,* 4**,** 590-7.

YAMAMOTO, A., SERIZAWA, S., ITO, M. & SATO, Y. 1991. Stratum corneum lipid abnormalities in atopic dermatitis. *Archives of Dermatological Research,* 283**,** 219-223.

ZEHRUNG, D. 2009. Intradermal Delivery of Vaccines: A review of the literature and the potential for development for use in low- and middle income countries. *In:* KRISTENSEN, D. (ed.). Program for Appropriate Technology in Health (PATH).

ZUCKERMAN, J. N. 2000. The importance of injecting vaccines into muscle : Different patients need different needle sizes. *BMJ : British Medical Journal,* 321**,** 1237-1238.

Chapter 2: The *Ex Vivo* Human Skin Model

2.1 Introduction

This chapter will explore an *ex vivo* human skin model as a useful tool for assessing intradermal vaccine delivery. It will assess the delivery of two different vaccine types into skin. It will also examine the response of skin immune cells to intradermally delivered vaccine.

2.1.1 Vaccine Technologies

Vaccine technologies have developed markedly since their inception. Early vaccines were often inactivated forms of the pathogen, with heat or formaldehyde being used to neutralise the virulence of the pathogen whilst maintaining its antigenicity (Stern and Markel, 2005). Inactivated vaccines possess advantages in that antigen is presented in its natural state and so will be processed, and immunity raised, via similar pathways to those that will counteract infection on subsequent exposure (Sanders et al., 2015). It is also possible to deliver live pathogen which has been attenuated to reduce its pathogenicity, termed an attenuated vaccine. Attenuated vaccines do not undergo heat or chemical treatment to facilitate inactivation and therefore damage to antigenic structures is minimised (Galinski et al., 2015). Both inactivated and attenuated vaccines possess an associated risk of infection following vaccination if pathogens escape complete inactivation or revert to the wild unattenuated state (Hanley, 2011, Sanders et al., 2015).

One strategy to avoid the risk of infection from vaccine reversion to the wild type pathogen is to only deliver part of the target pathogen, referred to as a subunit vaccine. For example, delivering envelope proteins from a virus can condition the immune system against the virion, whose particles contain that particular envelope protein (Khan et al., 2012). The antigen may be isolated from the wild type pathogen or produced in recombinant vectors, such as yeast (Bill, 2015). It is also possible, in diseases where a toxic substance released from a bacterium is the main cause of morbidity, to deliver inactivated toxin as a vaccine. These are termed toxoid vaccines, such as the diphtheria vaccine (Tiwari and Wharton, 2013). These vaccines are often less potently antigenic

than killed or attenuated vaccines so must be delivered with one or more immunostimulatory adjuvants to ensure an immune response is actualised (Coffman et al., 2010). The reduced potency is due to a subset of the total antigen from the pathogen being represented and that in isolation, the antigen may not exist in the same conformation as it does within the pathogen (Steimer and Haigwood, 1991)- both of which reduce the likelihood of a full immune response being raised against the pathogen. An adjuvant may be a separate chemical substance (e.g. alum) (Coffman et al., 2010) that is co-delivered with the antigen or, in the case of conjugate vaccines, covalently linked to the poorly antigenic molecule e.g. tetanus toxoid conjugated to haemophilus influenzae type B (HiB) polysaccharide to increase the latter's antigenicity in the HiB vaccine (Ravenscroft et al., 2015).

Nanoparticle technology may also be utilised in vaccines. Peptide conjugated to nanoparticles (solid particles under 1µm in diameter) offers improved stability and immunogenicity, versus free peptide (Wang et al., 2008, Caucheteux et al., 2016). Another vaccine technology that avoids the use of an attenuated or inactivated form of the wild-type virus is the virus-like particle (VLP) vaccine. VLP vaccines involve the manufacture of viral nucleocapsid and envelope structures without the inclusion of the pathogen's genetic material (Sitrin et al., 2015). This way the antigenic structures are maintained without the risk of viral replication and reversion to wild type. Finally, it is possible to use genetic vaccines, where DNA or RNA that encode antigenic peptides are delivered to cells. The successful delivery and expression of these vaccines leads to in situ production of antigenic peptides in a manner similar to the viral replication cycle following infection. This allows for the possibility of presenting antigen on MHC-I molecules and generating cellular immunity to a pathogen mediated by cytotoxic CD8+ T-cells (Srivastava and Liu, 2003).

2.1.2 Vaccine Research

When designing a novel vaccine, it is vital that the antigenic epitopes and their native conformations involved in an adaptive immune response are understood. An appropriate vaccine technology (inactivated virus, subunit, nanoparticle, etc.) can then selected and a vaccine formulation designed. The risk of an ineffective vaccine leaving a patient vulnerable to infection by a pathogen mean that thorough pre-clinical testing of vaccines is required. There is also a risk of local reactions (Cody et al., 1981) at the

delivery site or triggering autoimmune disease if the vaccine should elicit a cross-reactive response against self-antigen (Wraith et al., 2003). The intricacies of immunisation mean that complex models must be used- normally these are *in vivo* animal models. However, there are marked differences, both physical and immunological, between the commonly used animal models and human skin (Mestas and Hughes, 2004, Bronaugh et al., 1982, van der Worp et al., 2010, Netzlaff et al., 2006) which has led to the development of human skin models.

2.1.3 The *Ex Vivo* Human Skin Model

The *ex vivo* human skin model provides a useful laboratory tool to bridge the gap between animal models and the clinical scenario (Ng et al., 2009, van den Berg et al., 2009, Wu et al., 2000). This model utilises excised skin typically obtained from routine surgical procedures such as mastectomy/breast reduction (Pearton et al., 2010c), infant circumcision (Berton et al., 2000) or abdominoplasty (Chu et al., 2012). Skin is collected from patients and, with proper handling and culture conditions, can be maintained viable for at least 72 hours (Ng et al., 2009). The model has been used for a number of study types including wound repair (Danso et al., 2015, Xu et al., 2012), transdermal drug delivery (Swarbrick et al., 1982, Schmalfuß et al., 1997) and immunological studies (Wu et al., 2000, Chu et al., 2012).

Within Cardiff University, *ex vivo* human skin has been utilised to study intradermal delivery deposition and localised kinetics (Coulman et al., 2009, Torrisi et al., 2013), the delivery of genetic material (Chong et al., 2013) and transfection within the tissue (Ng et al., 2009, Pearton et al., 2012). The *ex vivo* skin model has also been used for immunological studies, showing changes in gene expression to vaccine delivery via microarray analysis (Pearton et al., 2013) as well as changes in LCs following the delivery of vaccine into the skin, showing their morphological changes and migration out of the epidermis (Pearton et al., 2010b, Pearton et al., 2010c).

Ex vivo human skin holds advantages over animal models in that it is human tissue and so represents the *in vivo* situation more closely. The use of tissue also allows for the complex interactions between the diverse skin cell populations to be studied. The model is, however, limited by a short window of viability following removal from

the patient which limits the range of experiments which it can be used for. It also possesses limitations in that it exists in isolation of the full human immune system. This means that cellular and chemical signalling which is delivered to skin via the circulatory system *in vivo* is not present in *ex vivo* human skin. The isolated nature of the tissue also means that cells which migrate through tissue are liable to migrate out into culture media from which they are unlikely to return into the skin tissue. The lack of a full immune system means that immune cell precursors cannot be recruited from the blood and so the overall immune cell population within the *ex vivo* skin tissue will decrease with increased culture time. Finally, the irregularity of surgical procedures means that tissue is not frequently available and sample size can vary greatly between patients depending on the nature of the surgery.

2.1.4 Histological Analysis of Human Skin

Given that changes in the *ex vivo* human skin model following treatment with a vaccine will largely occur at the cellular level, histological processes are commonly employed to allow their visualisation. The nature of full-thickness skin samples means that conventional microscopy cannot be used to analyse the sample, as light will not pass through the sample to the objective lens for visualisation (Murphy and Davidson, 2012). To allow the use of light or fluorescence microscopy, tissue is normally cut into thin sections which allow the transmission of light through the sample.

2.1.4.1 Sectioning of Tissue

There are two commonly used processes for sectioning of tissues- microtome sectioning or cryosectioning. Both are similar in concept- the sample is passed over a blade, removing a thin slice from the outside of the sample. The section is attached to a microscope slide, where it can undergo staining and imaging. The equipment then moves the sample forward by the desired section thickness and the process repeated, generating further sections. The two methods vary in how the sample is preserved and supported for sectioning. In both cases, tissue is fixed to halt cellular processes and maintain the integrity of the tissue structure (Zeller, 2001). Microtome sectioning involves the dehydration of tissue before embedding it in paraffin to allow it to be

sectioned. Cryosectioning of tissue involved the embedding of tissue in specially-designed media before freezing. The frozen tissue can then be sectioned in a cryotome, a microtome contained within a cooled housing that ensures the tissue remains frozen.

While both techniques for tissue sectioning have similar capabilities in terms of the tissue types that can be sectioned and the thickness of sections that can be produced, there are marked differences in the processing times of the tissue for the two processes (Winsor, 1994). The paraffin-embedding of tissue can be quite time-consuming, with tissue being moved through a water-ethanol gradient of increasing ethanol concentrations to remove water from the sample before infiltration with chloroform and finally molten paraffin. Following sectioning, paraffin must be removed from the sections which requires the use of organic solvent such as xylene. The tissue must then be rehydrated through an ethanol-gradient before it can be stained and imaged. In the case of cryosectioning, tissue can be snap frozen immediately after treatment and can be sectioned once it is completely frozen. As the embedding media protects the tissue from dehydration during freezing (Jones et al., 1986), sections can be stained following a PBS wash.

Tissue sections may be imaged without further treatment but in many cases, the subtleties of tissue structure and cellular behaviours cannot be seen without staining the tissue in some way (Kanitakis, 2002). For gross tissue structure, haematoxylin and eosin (H&E) staining is often used. Haematoxylin is used to stain the nuclei within the tissue blue. Eosin is then added which stains cytoplasm orange, collagen in pink and erythrocytes red. Other cellular structures are stained in shades of orange, red and pink. Specific cells will show characteristic H&E staining, allowing their identification in tissue (Fischer et al., 2008). For some investigations however, H&E staining does not provide adequate distinction between cell types and so more complex staining techniques must be used.

2.1.4.2 Immunohistochemistry and Immunofluorescence

Both immunohistochemistry (IHC) and immunofluorescence (IF) involve the use of antibodies to identify areas of interest within a tissue sample. The specificity of antibodies (as discussed in Section 1.1.2) means that they will bind to a single epitope.

Antibodies raised in animals to human epitopes can allow cells to be identified within tissue (Vandesande, 1979). For example, an antibody raised to an epitope within the CD207 receptor can be added to tissue where it will bind to LCs (Stoitzner et al., 2003). Where IHC and IF differ is how the antibody-stained areas within the tissue are visualised. IHC utilises enzyme-conjugated antibodies whereas IF uses fluorescently-conjugated antibodies. The conjugated antibody may be the primary antibody (specific to the target epitope) or a secondary antibody which binds to the primary antibody. The use of conjugated secondary antibodies can increase signal strength if multiple secondary antibodies can bind a single primary antibody (Buchwalow et al., 2011).

Following IHC antibody staining, a chemical substrate is added to the tissue which undergoes a colour change in the presence of the enzyme-linked antibody and stains the tissue. An example substrate is 3,3'-diaminobenzidine (DAB) which reacts in the presence of horseradish peroxidase-conjugated antibody to produce a dark brown colour which can be distinguished amongst H&E-stained tissue (Hobot and Newman, 1996). It is possible to stain a tissue with more than one enzyme-linked antibody, provided the coloured products of the substrates of the two enzymes are distinct from one another (Vandesande, 1979).

The antibodies used in IF are conjugated to a fluorophore that emits light at a given wavelength following excitation with a laser (Rani and Hussain, 2003). This allows IF-stained tissue to be visualised on a fluorescence microscope. It is possible to combine multiple fluorescent antibodies or stains (such as the nuclear stain Hoechst 33342) to distinguish between multiple cell types in a tissue section. It is important that the excitation/emission wavelengths of the fluorophores used do not overlap as this can provide false positive staining which will affect the reliability of data (Vandesande, 1979).

2.1.5 Influenza

Seasonal influenza is responsible for 3-5 million cases of serious illness and 250-500,000 deaths worldwide per year (WHO, 2014). Influenza represents a group of three genera: Influenzavirus A, Influenzavirus B and Influenzavirus C. Influenza A and B are most commonly associated with the seasonal epidemics in humans. Genetically, the

influenza virus is a negative-sense single-stranded RNA (ssRNA) virus- it contains single-stranded RNA which must be translated by RNA polymerase to produce the corresponding positive-sense mRNA to elicit viral production in the host cell (Samji, 2009). The ssRNA is contained within a protein 'core' which is in turn enveloped by a lipid bilayer (from the host cell in which it was produced) which contains two glycoproteins (Figure 2.1): haemagglutinin and neuraminidase- the subtypes of which are used to classify viral strains (e.g. H5N1, H1N1, etc.) (Samji, 2009). Infection by the virus causes respiratory symptoms (rhinorrhoea, cough and sore throat) as well as fever, myalgia, headache, malaise and (normally only in high-risk patients such as the elderly) death (Taubenberger and Morens, 2008). The virus undergoes constant antigenic shift, producing the various subtypes. Each emerging strain is able to evade immune responses against previous strains, rendering adaptive immune responses ineffective season to season (Taubenberger and Kash, 2010).

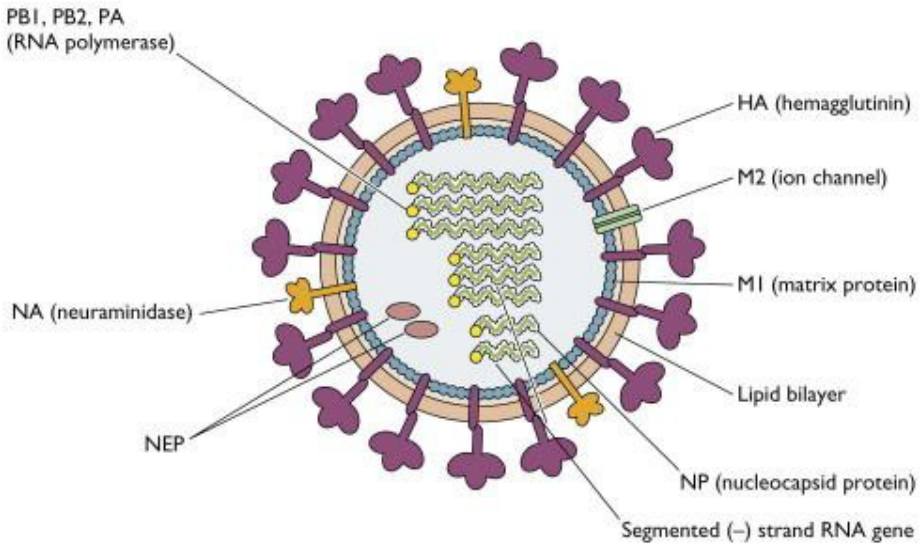

Figure 2.1: Structure of the influenza virus (adapted from: http://www.virology.ws/2009/04/30/structure-of-influenza-virus/)

2.1.6 Influenza Vaccines

Multivalent (i.e. containing antigen representative of multiple strains) inactivated virus vaccines for influenza have been available since 1942 (Hannoun, 2013). These have proven to be useful for protection against the strains of virus which they contain. However, influenza's constant antigenic shift amongst strains means that new vaccines must be under constant development. The ongoing development of vaccines has led to research into methods of improving vaccination. The potential for antigen sparing by intradermal immunisation has been recognised as potentially useful,

especially in pandemic situations where a limited amount of vaccine antigen will be available at short notice to immunise as many people as possible (Kenney et al., 2004, Van Damme et al., 2009).

2.1.7 Changes in Human Skin Following Intradermal Influenza Vaccination

Intradermal delivery of influenza vaccines has been studied previously, both in exploring the development of novel vaccines (Kang et al., 2009) and in studying the alternative delivery of existing intramuscular vaccines (Kenney et al., 2004). Work in animal models or human subjects provide useful systemic immune response data but possess disadvantages in terms of cost and ethical considerations. Clinical studies are also limited in their use of novel vaccines due to the need for extensive preclinical data to show suitability for delivery into human subjects. Some work has been done using *ex vivo* skin to provide this necessary preclinical data but this tended to be in suction blisters (Dearman et al., 2004). In previous work utilising the *ex vivo* human skin model, we have shown the response of Langerhans cells to both inactivated virus and novel virus-like particle vaccines (Pearton et al., 2010a, Pearton et al., 2010c). At 24 and 48 hours' post-vaccination there was a marked reduction in the number of Langerhans cells in the epidermis (Figure 2.2). There was also a change in the morphology of Langerhans cells, withdrawing their lateral dendrites before extending towards the basement membrane, suggesting migration towards the lymph vessels of the dermis. The data provided evidence for the use of virus-like particles as well as helping to characterise the early response seen in skin following intradermal vaccination.

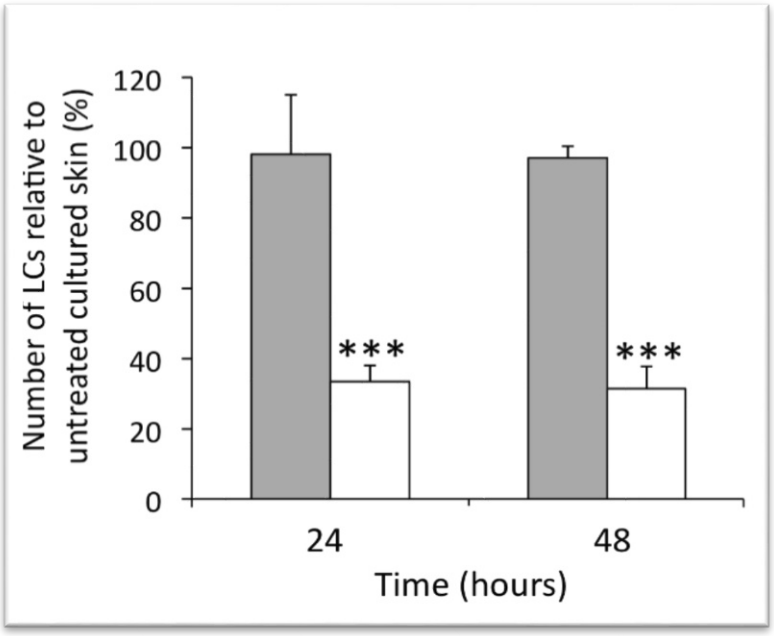

*Figure 2.2: LC numbers in epidermal sheets following PBS ID injection (grey bars) or H1 virus-like particles (white bars) [***p<0.001] taken from (Pearton et al., 2010c)*

2.2 Aims and Objectives

This chapter aims to use *ex vivo* human skin to visualise the intradermal delivery of protein or nanoparticle vaccines. It also aims to investigate the effects of influenza vaccine on Langerhans cells at early time points after delivery. The specific practical objectives are:

1. Formulate a model protein and a nanoparticle vaccine to enable coating onto solid stainless steel microneedles. Utilise fluorescence microscopy to visualise the coating of formulation on the needles' surface.
2. Insert formulation-coated microneedles into *ex vivo* human skin then, following their removal from skin, re-image the arrays to determine if formulation release was successful.
3. Utilise cryosectioning and histological staining of coated microneedle-treated skin to image deposition of formulation into the skin
4. Formulate inactivated influenza virus vaccine for coating onto solid stainless steel microneedles.
5. Utilise the previously described *ex vivo* human skin culture protocol and immunohistochemistry to characterise the migration of LCs out of the epidermis at 2 and 4 hours after vaccine delivery.

2.3 Materials and Methods

[All reagents were obtained from Fisher Scientific, UK unless otherwise stated]

2.3.1 Microneedle Arrays

Microneedle arrays, consisting of 10 needles in plane, were fabricated from stainless steel sheets using wire electrical discharge machining (EDM) by colleagues within Cardiff University. The arrays were subsequently electropolished in a solution of 60% glycerine, 30% ortho-phosphoric acid (85% solution) and 10% distilled-deionised water (ddH_2O) under a current of 1.8 mA/mm2 at 70˚C for 15 minutes. A copper rod acted as the cathode and the microneedles as the anode. A magnetic stirrer was used to agitate the electropolishing solution and the anode was vibrated using a custom sonication device to prevent build-up of gas bubbles at the anode's surface. Following electropolishing, needle arrays were washed thoroughly in alternating ddH_2O and nitric acid (25% solution) for three repeats before a final wash in ddH_2O. Needles were allowed to air dry for 1 hour, wrapped in lens tissue and stored in airtight containers prior to use. The length and width of individual microneedles was reduced as a result of the polishing process. This was consistent between arrays, giving a final length of 640µm with 1mm spacing between microneedle tips (Figure 2.3).

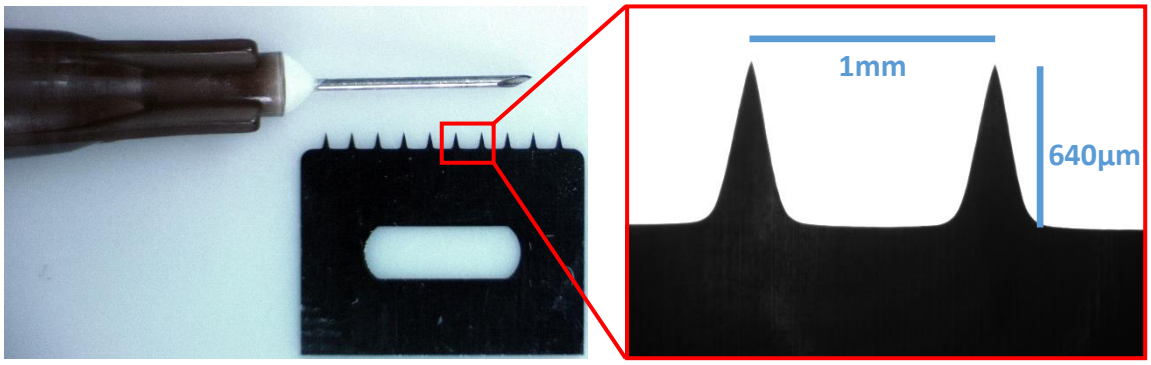

Figure 2.3: Solid stainless steel microneedle arrays after electropolishing. Arrays consist of 10 needles of 640µm length with 1mm spacing at the needle tips. BD Microlance 26G 10mm hypodermic needle (BD Biosciences, UK) included for scale.

2.3.2 Fluorescent Protein Formulation

To assess the capability of coating solid microneedle arrays with a protein-containing formulation, ovalbumin protein with Alexa Fluor™ 555 Conjugate (Fl-OVA; Invitrogen, UK) was utilised. A coating solution containing 1.25% w/v Fl-OVA plus 15%

w/v trehalose, 1% w/v carboxymethylcellulose sodium salt (average molecular weight: 90,000 Daltons) and 0.5% w/v Lutrol F-68 NF (all Sigma-Aldrich, UK) in ddH_2O was prepared and stored at 4˚C prior to use.

Two methods were used to coat microneedle arrays. In the first (method A), 0.6µl of coating solution was drawn up into a fine-tipped gel-loading pipettor tip. The tip was then removed from the pipettor body and pressure applied to the top of the pipettor tip by a gloved finger, forcing the coating solution out of the fine end of the tip a small volume at a time- forming a small droplet due to surface tension of the viscous coating solution. This droplet was applied to the surface of the needle to coat a layer of solution onto it over approximately 75% of the needle length. All needles were coated, the coating was allowed to air dry for 2 minutes and then coating repeated until all of the solution had been used. The volume used (0.6µl) was divided between 3 microneedles arrays- i.e. approximately 0.2µl was applied to each array of 10 needles.

The second coating method (method B), involved drawing 10µl of coating solution into a standard 200µl pipettor tip, which has had the end cut off to increase the bore diameter. Rather than expelling the liquid from the pipettor tip (as in method A), each needle on the array was individually inserted into the formulation *in situ* in the pipettor tip then removed to apply formulation to the needle surface. The coated needles were allowed to air dry for two minutes before repeating. The 10µl volume was used to coat three arrays (i.e. approximately 3.33µl was applied to each array).

Coated arrays were stored in a sealed container with silica gel desiccant at 4˚C prior to use. Coating success was determined by imaging needles using a DM IRB epifluorescence microscope (Leica, Germany) with Retiga Exi Fast digital camera (QImaging, Canada). Image post-processing was performed using ImageJ software (National Institutes of Health, USA).

2.3.3 Fluorescent Nanoparticle Formulation

A fluorescent model for influenza virions was assessed for its ability to be incorporated into a formulation, coated onto microneedles and then delivered into skin. Fluorescent red sulphate-modified polystyrene nanoparticles (Fl-NPs) (Sigma-Aldrich,

UK) with a mean diameter of 100nm were selected based on their similarity in size to influenza virions, which have a diameter of 80-120nm (Kang et al., 2009). A coating solution containing 1.25% w/v Fl-NPs, 15% w/v trehalose, 1% w/v carboxymethylcellulose sodium salt and 0.5% w/v Lutrol F-68 NF in ddH_2O was produced and stored at 4˚C prior to use. Coating was performed using Method B as described in Section 2.3.2.

2.3.4 Insertion of Microneedles into *Ex Vivo* Human Skin

Human skin samples were obtained from female patients undergoing mastectomy or breast reduction surgery under informed written patient consent and local ethical committee approval (South East Wales Research Ethics Committees Panel C, Reference: 08/WSE03/55). Skin was collected immediately following surgery and transported to the laboratory in Dulbecco's Modified Eagle's medium (DMEM) supplemented with 1% penicillin and streptomycin (100 IU/ml each) at 4˚C. Samples used in this study were frozen upon arrival and defrosted prior to use. Skin tissue was prepared for use by removal of subcutaneous fat tissue by blunt dissection. Skin was then pinned, epidermis uppermost, to cork board ready for microneedle treatment.

Microneedle arrays, coated with either Fl-NP or Fl-OVA coating formulations, were inserted into human skin explants by manual application using downward pressure perpendicular to the skin surface and held in place for 60s to allow dissolution of the formulation from the microneedle surface and deposition into the skin. Arrays were then removed from the skin and imaged as described in Section 2.3.2 to visualise the amount of formulation remaining on the microneedle arrays.

2.3.5 Microneedle Skin Penetration and Formulation Release in Skin

Microneedle-treated skin areas were excised, embedded in Optimal Cutting Temperature (OCT) embedding media and snap frozen in hexane cooled by an outer dry ice-methanol bath. Samples were stored at -80˚C prior to sectioning. Sections of 10µm thickness were generated using a Cryotome FSE (ThermoFisher Scientific, UK) onto SuperFrost™ Plus microscope slides (ThermoFisher Scientific, UK). Following fixing in

acetone at -20˚C for 20 minutes, skin sections treated with Fl-OVA-coated microneedles were mounted using PBS under glass cover slips and imaged using the DM IRB epifluorescent microscope (Leica, Germany) with Retiga Exi Fast digital camera (QImaging, Canada) in both fluorescent and brightfield imaging modes to visualise delivery within the skin. The cover slips were removed and the slides washed before staining using H&E. For H&E staining, slides were held in haematoxylin for 5 minutes then rinsed in tap water for 2 minutes. Sections were then differentiated by immersing the slides in 1% v/v acid alcohol (1% v/v HCl in 70% v/v ethanol in water) for 1 second. Finally, slides were held in eosin stain aqueous solution for 10 seconds before rinsing in running water. Slides were then re-mounted in PBS under glass cover slips and imaged using light microscopy with digital image capture as above. The resulting images were processed using ImageJ software (National Institutes of Health, USA).

Skin sections treated with Fl-NP-coated microneedles were fixed in acetone at -20˚C for 20 minutes before being stained with phycoerythrin-conjugated anti-CD207 mouse IgG1 antibody (Beckman Coulter, UK) and Hoechst stain solution (Sigma-Aldrich, UK) to visualise the epidermal LCs and cell nuclei respectively. Sections were then mounted on slides using ProLong® Diamond Antifade Mountant (Invitrogen, UK) according to the manufacturer's protocol. Image capture and processing was performed as above.

2.3.6 Changes in Langerhans Cell Numbers After Intradermal Vaccination

Previous studies (Pearton et al., 2010b, Pearton et al., 2010c) identified changes in Langerhans cell numbers in the epidermis at 24 and 48 hours after inactivated and VLP influenza vaccine delivery into *ex vivo* human skin. In this study, inactivated influenza virus (A/California/7/2009 (H1N1) pdm09-like virus), as used in the commercially-available trivalent influenza vaccine each season since the 2010-11 influenza season, was used to assess the response of *ex vivo* human skin to influenza vaccine delivery at earlier time points (pre-24 hours). The inactivated virus vaccine was formulated in a coating solution containing trehalose, carboxymethylcellulose sodium salt and Lutrol F-68 NF as described in Section 2.3.2 to produce a final concentration of 1 mg/ml inactivated virus and was coated onto microneedle arrays using Method B as

described in Section 2.3.2. Coated arrays were stored in a sealed container with silica gel desiccant at 4˚C prior to use. The arrays used were obtained from collaborators at Georgia Institute of Technology, Atlanta GA, USA and were identical to those used in the previously published work (Pearton et al., 2010b, Pearton et al., 2010c). These arrays were produced from stainless steel sheets, possessed a needle length of 700µm and a spacing of 1.5mm between needle tips. Skin was obtained and prepared for treatment as described in Section 2.3.4.

Inactivated influenza virus was then delivered either by application of the coated microneedles as described in Section 2.3.4 or by a traditional Mantoux-style ID injection into the upper dermis (Norman et al., 2014). Control samples received either an equivalent volume of sterile phosphate-buffered saline (PBS) by ID injection or MN array coated in coating formulation without virus. Six-millimetre punch biopsies were isolated from the treated areas and these were cultured at the media-air interface using a previously described method (Ng et al., 2009) for 2 or 4 hours. Following culture, the epidermis was removed from the skin biopsies using heat separation by submersing the tissue in ddH_2O at 60°C for 55 seconds. This allowed manual removal of the epidermis from the dermis as a single, intact sheet. Sheets were briefly rinsed in PBS before being fixed in -20°C acetone for 20 minutes. Following a further PBS rinse, the sheets were incubated in 1/200 anti-CD207 mouse monoclonal antibody (mAb; Abcam, UK) at 4°C overnight. An EnVision+ system-HRP (DAB) kit (Dako UK Ltd, UK) was used to detect the presence of the primary mAb according to the kit's included protocol. Stained epidermal sheets were dehydrated and mounted using xylene-based mounting media before being imaged by a digital microscope camera (VWR, UK). The field of view for images was 850µm x 640µm. Three skin samples (aged 53, 73 and 81) were used, with two full visual fields analysed per sample.

LC counts were performed using ImageJ software. In line with previously published protocols (Pearton et al., 2010a), the total number of LCs were counted and then this number divided by the area analysed to determine the LC density (as number of LCs per 1000µm^2). The data were compared between treated and untreated skin biopsies at both 2 and 4 hours to determine whether LC density changes were significantly different between the two. Statistical tests comprised one-way analysis of

variance (ANOVA) followed by Tukey's post hoc analysis performed using IBM SPSS Statistics (IBM, USA).

2.4 Results and Discussion

2.4.1 Formulation Coating onto Solid Microneedles

Characterisation of the microneedles coated with Fl-OVA coating solution by the two methods (Figure 2.4) revealed that both were able to produce visibly uniform coating of the formulation which did not change the overall shape of the needle tips (important to maintain sharpness so as to allow skin penetration). There was, however, a marked difference in the formulation coverage area of the two coating processes- method A coated formulation at the terminal end of the needles as shown in Figure 2.4 (A & B). Method B covered a much larger area of the array with formulation- coating the entire needle from tip to base. It was also evident that a large amount of the coating

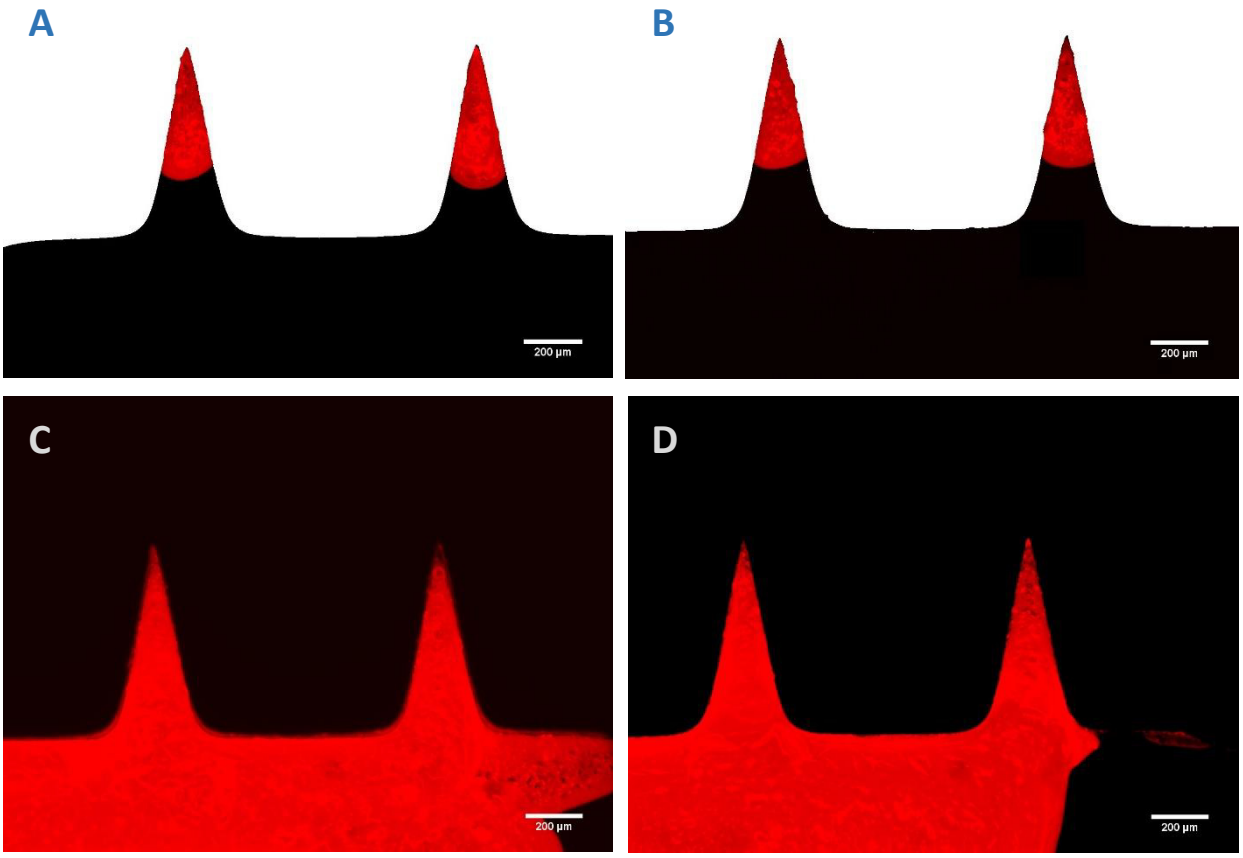

Figure 2.4: Solid stainless steel microneedles coated with Fl-OVA-containing coating solution using either method A (A, B) which deposited formulation specifically on the needle tips or method B (C, D) which distributed formulation across the entirety of the needle and also the base of the array. Each image is representative of the coating of a separate array of 10 needles each. Scale bars = 200µm

solution had been applied to the base of the array (Figure 2.4 C & D). This represents lost formulation as the base will not be inserted into the skin and so the formulation will not dissolve off of the array.

2.4.2 Insertion of Microneedles into *Ex Vivo* Human Skin

Re-imaging the microneedle arrays following insertion into *ex vivo* human skin explants allowed visual assessment of formulation which had failed to dissolve from the needle surface. Figure 2.5 indicates that the Fl-OVA-containing formulation was dissolved preferentially from the tip of the needles, the portion of the needle being inserted deepest into the skin. The natural water gradient of the skin, from its dry exterior to aqueous internal environment (Bjorklund et al., 2010) means that the needle tips are most likely to encounter sufficient fluid to dissolve the needle coating. The insertion depth of needles was therefore important. It appeared that the natural elastic property of skin acted to resist needle insertion as the arrays were applied firmly to the skin's surface. The needles at the edge of arrays (such as the leftmost needle in Figure

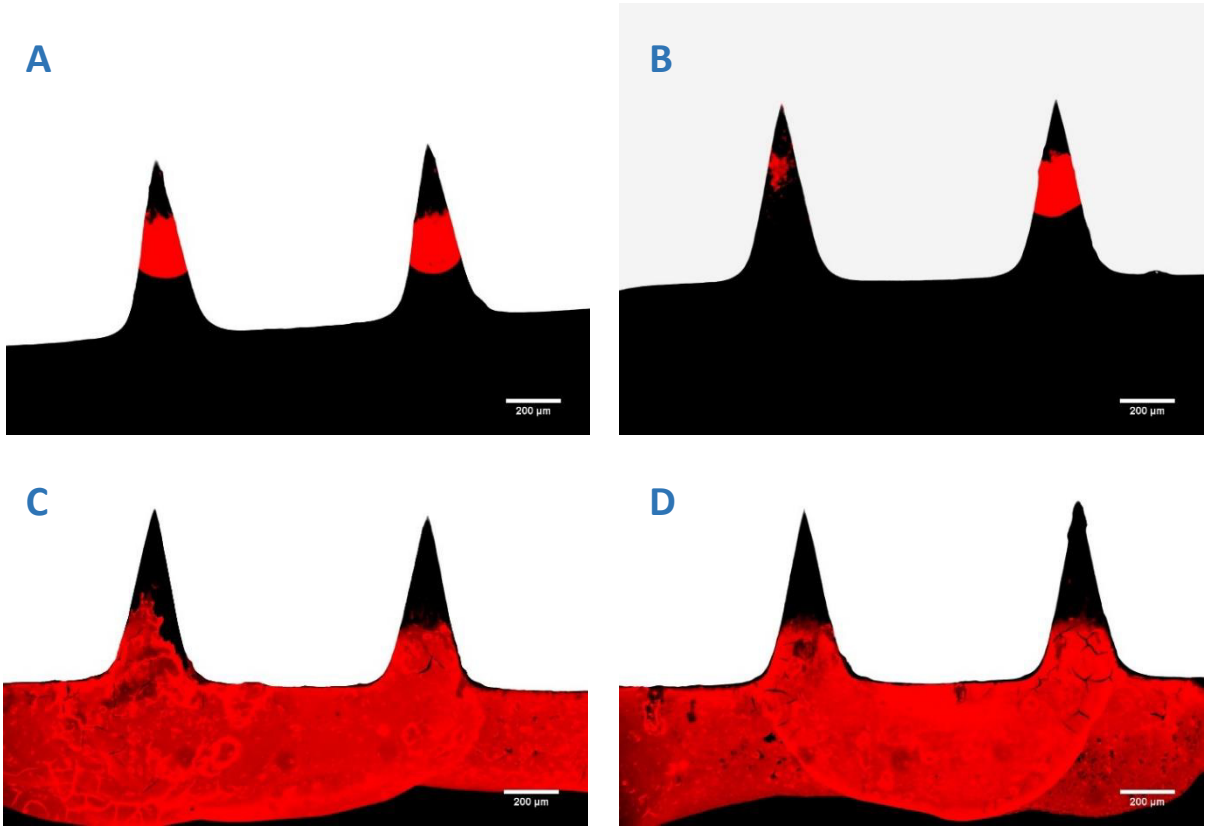

Figure 2.5: Microneedle arrays that had been coated with Fl-OVA-containing coating solution using either method A (A, B) or method B (C,D) following 60-second insertion into ex vivo human skin. Each image is representative of the removal of formulation from the needles' surface of a separate array of 10 needles each. Scale bars = 200µm

2.5 B) appeared to be able to penetrate the skin most fully and as a result showed the most complete dissolution of formulation. The inner needles on the array showed greater formulation retention on the needles. The fact that the *ex vivo* skin samples used had been previously frozen without cryoprotective media may have also reduced dissolution. The freezing process can dehydrate tissue (Pegg, 1987), particularly at the outermost surfaces. This will affect the water gradient by reducing the amount of interstitial fluid in outer layers of the skin which can rehydrate the microneedle coating and allow its deposition in skin. Finally, as a thin layer of formulation on the needles will still show fluorescence, it is not possible to determine whether some, rather than all, of the formulation had been deposited into the skin from the lower part of the needles.

2.4.3 Microneedle Skin Penetration and Formulation Deposition in Skin

Having determined that formulation had been removed from the microneedles' surface following insertion into skin, it was important to characterise the location of deposition in the skin. Fluorescence microscopy revealed that formulation was deposited in the area immediately surrounding the microneedle channel (Figure 2.6 A & B) i.e. mostly into the epidermis and papillary dermis. Haematoxylin and eosin staining of microneedle-treated skin confirmed this penetration profile. Some residual formulation (pink) could also be seen in the H&E stained sections (Figure 2.6 C & D). The formulation was retained within skin sections following the vigorous washing during H&E staining, suggesting association with the tissue if not internalisation into the skin cells.

Samples treated with fluorescent nanoparticles were stained with fluorescently-conjugated anti-CD207 antibody prior to imaging. This allowed the visualisation of Langerhans cells within the epidermis and confirmed that formulation released from microneedles was deposited adjacent to them (Figure 2.6 E & F). The depth and angle of microneedle channels, which are perpendicular to the skin's surface, meant that the majority of formulation was deposited in the upper dermis. The loose connective tissue of the dermis also allowed some permeation of protein or nanoparticle formulations away from the channel itself (visible in Figure 2.6 B & E).

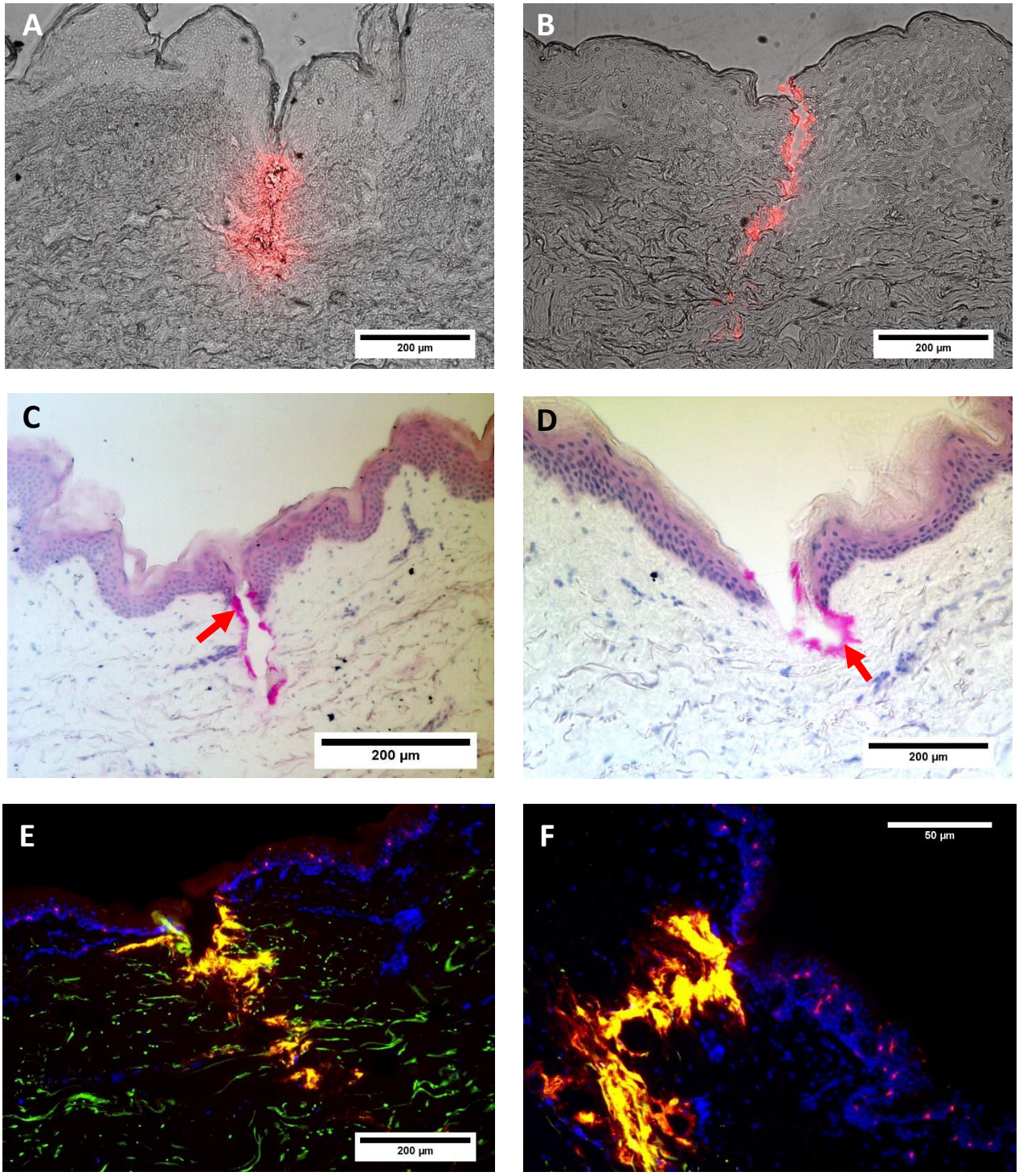

Figure 2.6: Representative images of deposition of fluorescent formulation from coated microneedle arrays into ex vivo human skin samples. A-B: Fl-OVA-containing formulation (red) overlaid with brightfield image of skin section. C-D: H&E stained skin sections showing the densely nucleated epidermal layer and microneedle channel with deposited pink Fl-OVA formulation (red arrows). E-F: Fl-NP deposition in skin (yellow) with nuclei (blue), LCs (red) and skin auto-fluorescence (green) also visible.

2.4.4 Changes in Langerhans Cell Numbers After Intradermal Vaccination

Submerging the *ex vivo* skin samples in water at 60°C for 55 seconds allowed for the mechanical separation of the epidermis from the dermis as a single sheet. Utilising the DAKO kit following staining with anti-CD207 antibody allowed for the Langerhans cells to be imaged in situ within the epidermis (Figure 2.7). The Langerhans cells appear as a central rounded cell body with a number of dendritic processes extending from it, creating a network across the skin's surface.

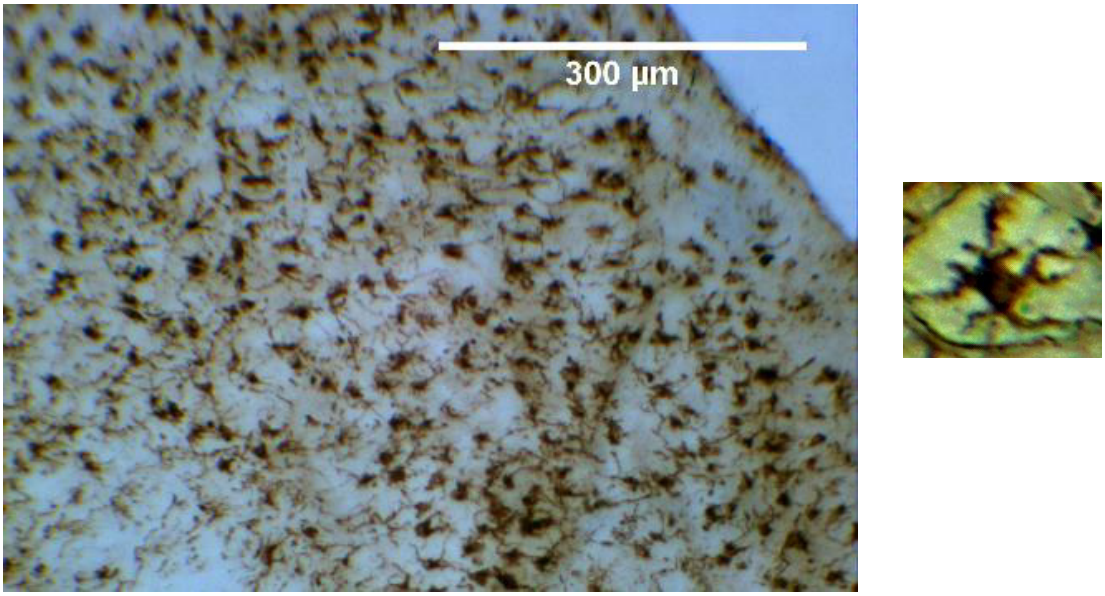

Figure 2.7: Epidermal sheet stained for CD207 showing the dendritic nature of LCs within epidermal sheets (left) and example of LC morphology (right).

Following treatment by inactivated influenza virus vaccine delivered either by standard intradermal injection or coated onto microneedle arrays, the density of LCs within epidermal sheets was assessed. The difference in density of LCs present in the sheets at 2 and 4 hours was not statistically significant between the control samples and those to which influenza vaccine was delivered by MN array or hypodermic needle (Figure 2.8). There was also no significant difference in LC density in any sample between the 2- and 4-hour time points. There was also a high level of variance between images from samples receiving identical treatments. This compared to the previously published

data at 24 hours (Pearton et al., 2010b) where LC density in vaccine-treated skin was 70% less than untreated controls.

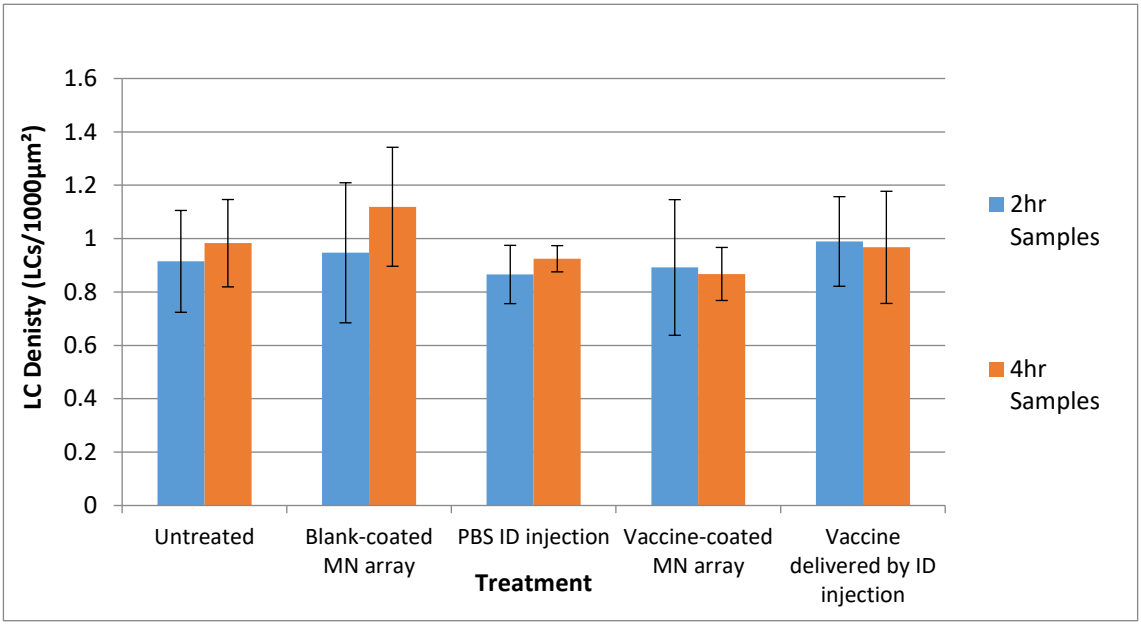

Figure 2.8: LC densities in treated samples and controls at 2 and 4 hours. Error bars at 2hrs are ±SD (2hrs: n = 3; 4hrs: n=2)

2.5 General Discussion

The results of this investigation provide further evidence that microneedles are a potentially viable delivery method for intradermal vaccines. Stainless steel arrays can be reproducibly produced to specifications of microneedle shape and length (Gill and Prausnitz, 2007a). The reproducible coating of solid microneedles, however, is a challenging area both in process development and regulatory approval (Zehrung, 2009). This chapter utilised a model protein and nanoparticle which were fluorescently conjugated to allow for straightforward visualisations of formulation coated on microneedles and delivered to skin.

The first of the two coating processes used in this chapter (method A) required a high level of operator skill to ensure that needles were coated consistently on the needle tips only. It is also a time-consuming process, with a set of three arrays taking approximately 30 minutes to coat. The second method tested (method B) reduces both the coating time and the level of operator skill required. Method B also involved much less efficient coating onto needle tips with a large proportion of the formulation ending up on the base of the array where it will not be delivered to skin. With vaccine antigen,

which can be costly to produce, this would represent an unacceptable cost to a pharmaceutical manufacturer. Method B was similar to previously described methods which use a reservoir for coating solution (Gill and Prausnitz, 2007a), which is also associated with a large amount of formulation loss remaining within the reservoir. The reproducibility of the coating process is also important, to ensure that equivalent amounts of vaccine are coated onto each needle. The nature of coated microneedles means that they require reformulation of vaccines into coating formulation which must then be approved along with the coating process by regulatory authorities (Ita, 2015). Compared to hollow microneedles, which after approval as a medical device may be used in combination with previously approved injectables, this represents a significant hurdle to getting coated microneedles into clinical use (Kim et al., 2012a).

The coating processes were able to leave a visually uniform layer of formulation on the needles regardless of whether the coating solution was loaded with nanoparticles or protein, suggesting neither significantly affected the physical properties of the formulation at the concentrations used. The even appearance of nanoparticle-containing formulation coating suggests that the viscosity of the formulation and the small size of the nanoparticles prevented them from undergoing sedimentation out of suspension over the time period required for coating. This is important as novel vaccines might be virion- or protein-based. These studies utilised simple formulations without adjuvants present. The addition of adjuvants may be necessary for immunisation, particularly in the case of a protein vaccine which will likely be non-immunogenic without them. Therapeutic proteins (for example botulinum toxin) do not require adjuvants and so the formulation used within this chapter may be a suitable vehicle for their intradermal delivery. Conjugation of peptide to nanoparticles may increase their immunogenicity, potentially avoiding the need for adjuvants.

One limitation of the microneedle technology is the low volumes that can be delivered. Method A requires the desired vaccine dose for an array to be contained in 0.2µl of formulation. Whilst a suspension can be used (for example the model nanoparticle vaccine) if the vaccine is poorly soluble, there will be a limit of vaccine concentration over which it will affect the physical properties and coating might be adversely affected. The volume limits can be overcome somewhat by the use of multiple arrays concurrently within an applicator device (Suh et al., 2014b), though this will also

possess an upper size limit over which the applicator will be too cumbersome to ensure consistent microneedle insertion. Though the limits may be feasible for vaccines, they have been a major obstacle to drug delivery via microneedles, where doses are normally in the mg rather than µg range (Bariya et al., 2012).

Following insertion into the skin, the amount of formulation left on microneedle arrays varied between needles on an array. The assessment of coating in this investigation was qualitative rather than quantitative which limits the conclusions that can be drawn. The differences in formulation deposition may have been due to the penetration depth of needles not being consistent, though it is difficult to assess the depth to which needles have been inserted or to match a channel in a skin section to the corresponding needle. The varying insertion depths of needles may be due to multiple factors. Firstly, the natural elasticity of the skin acts to resist penetration by the microneedles (Groves et al., 2012). The skin will deform with the force of array application until the microneedles breach the stratum corneum, after which applied pressure will force the needles deeper into the skin (Groves et al., 2012). The setup using *ex vivo* skin attempts to replicate natural skin elasticity by pinning it out taut on a cork board backing. Though this is more representative of skin in situ than an explant which is not pinned out, it is not able to fully recreate the natural tautness of skin. The flexibility of the cork board backing can allow the skin to deform rather than allowing full penetration. Thus, the performance of microneedles in *ex vivo* skin may not correspond accurately with *in vivo* tissue behaviour. Work is currently underway within the research group to produce support apparatus for *ex vivo* skin which better mimics the tautness of skin and the firm underlying tissue *in vivo*.

Studies also investigated the deposition of a model protein and model nanoparticle following application of coated microneedles. As could be predicted from the passive nature of microneedle formulation depositing in the skin following rehydration, the formulation was deposited in the vicinity of the microneedle channel only. The use of previously frozen skin meant that any active transport processes which might occur *in vivo* did not happen in this model. Thus, the results can be interpreted as a snapshot of initial deposition patterns rather than the true spatial kinetics of intradermal vaccine delivery into skin. The deposition patterns were similar between protein and nanoparticle formulations in the previously frozen skin. The soluble nature

of the protein means that it may distribute away from the delivery site more rapidly in tissue fluid than insoluble nanoparticles in fully hydrated live skin.

Whilst some formulation could be seen in the epidermis, a large proportion was deposited in the papillary dermis. Though this limits the amount of vaccine delivered to LCs, vaccine in the dermis may be internalised by dDCs. Delivery specifically to the epidermis is challenging due to the thinness of the skin layer and the densely packed cells contained within it which hinder the movement of formulation delivered there. It is possible that some formulation which had dissolved in the interstitial fluid could permeate up to the basement membrane where Langerhans cells might encounter it. Also, while this chapter focusses heavily on LCs' interaction with vaccine antigen, it is important to note that dDCs are also potent antigen-presenting cells that will also be involved in bringing about an immune response to vaccine antigen.

Assessing the density of Langerhans cells in epidermal sheets failed to show a response in the skin tissue cultured after 2 or 4 hours. It can be concluded that the early time points selected did not represent long enough for the LCs to uptake antigen, become activated and migrate out of the epidermis, hence the lack of significant difference between the numbers present in a given area of treated or untreated epidermis. It is likely that the differences between treated and control samples would become apparent after 24 hours based on previously published results using an identical protocol for vaccine delivery (Pearton et al., 2010a, Pearton et al., 2010c). Further work is required to determine when between 4 hours and 24 hours the LCs begin to migrate in significant numbers from the epidermis in response to vaccine delivery. This delay in migration out of the skin will increase the time taken for LCs to reach lymph nodes where they can present vaccine antigen and therefore increase the time it will take a person to develop immunity. This may partly explain the presence of resident memory CD8+ T-cells in the epidermis who can mount a response against previously encountered pathogens in a more rapid manner (Nomura et al., 2014). It is also possible that dDCs are able to transport vaccine antigen to the lymph nodes more quickly given their motile nature. Vaccines delivered to LCs may benefit from reformulation to increase residence time in the epidermis and improve exposure of LCs to the vaccine. As frozen skin was used in the delivery studies in this chapter, it was not possible to quantify co-localisation of fluorescent vaccine models with LCs or dDCs. The ability of both LCs and dDCs to raise

an immune response will need to be properly assessed before the relative importance of each immune cell type in vaccination can be concluded.

2.6 Potential for Publication

The work focussing on coating of microneedles with a model antigen formulation was performed to validate that formulation could be applied to the surface of a new design of microneedle array and then delivered into *ex vivo* human skin. This type of investigation has been performed (and published) many times previously and, as such, does not represent publishable work. The changes in numbers of LCs in *ex vivo* human epidermis to intradermally delivered inactivated influenza vaccine was not found to be significant. For this data to be publishable, further work is required to quantify the LC response at time points between 4 hours (studied in this chapter) and 24 hours (previously published (Pearton et al., 2010c)) to provide a more detailed timescale of LC activation and migration out of the skin following intradermal vaccination.

2.7 Conclusion

This chapter provided qualitative data on two coating methods for solid stainless steel microneedles. Both were shown to coat protein or nanoparticle onto needles which could then be delivered into skin. The quantities of formulation on the needles before and after skin were not quantified, limiting the conclusions that can be made on delivery efficiency. Whilst the dose of influenza vaccine that can be delivered into *ex vivo* human skin by microneedles had been previously shown to induce a response in LCs indicative of activation 24 hours after delivery, this chapter found the response did not develop after 2 or 4 hours. The implications of the timescale of LC responses within *ex vivo* human skin will be considered in later chapters as they may affect the optimal delivery kinetics for targeting these cells in intradermal vaccination.

2.8 Bibliography

BARIYA, S. H., GOHEL, M. C., MEHTA, T. A. & SHARMA, O. P. 2012. Microneedles: an emerging transdermal drug delivery system. *J Pharm Pharmacol,* 64**,** 11-29.

BERTON, A., GODEAU, G., EMONARD, H., BABA, K., BELLON, P., HORNEBECK, W. & BELLON, G. 2000. Analysis of the ex vivo specificity of human gelatinases A and B towards skin collagen and elastic fibers by computerized morphometry. *Matrix Biology,* 19**,** 139-148.

BILL, R. M. 2015. Recombinant protein subunit vaccine synthesis in microbes: a role for yeast? *Journal of Pharmacy and Pharmacology,* 67**,** 319-328.

BJORKLUND, S., ENGBLOM, J., THURESSON, K. & SPARR, E. 2010. A water gradient can be used to regulate drug transport across skin. *J Control Release,* 143**,** 191-200.

BRONAUGH, R. L., STEWART, R. F. & CONGDON, E. R. 1982. Methods for in vitro percutaneous absorption studies II. Animal models for human skin. *Toxicology and Applied Pharmacology,* 62**,** 481-488.

BUCHWALOW, I., SAMOILOVA, V., BOECKER, W. & TIEMANN, M. 2011. Non-specific binding of antibodies in immunohistochemistry: fallacies and facts. *Scientific Reports,* 1**,** 28.

CAUCHETEUX, S. M., MITCHELL, J. P., IVORY, M. O., HIROSUE, S., HAKOBYAN, S., DOLTON, G., LADELL, K., MINERS, K., PRICE, D. A., KAN-MITCHELL, J., SEWELL, A. K., NESTLE, F., MORIS, A., KAROO, R. O., BIRCHALL, J. C., SWARTZ, M. A., HUBBEL, J. A., BLANCHET, F. P. & PIGUET, V. 2016. Polypropylene Sulfide Nanoparticle p24 Vaccine Promotes Dendritic Cell-Mediated Specific Immune Responses against HIV-1. *J Invest Dermatol,* 136**,** 1172-81.

CHONG, R. H., GONZALEZ-GONZALEZ, E., LARA, M. F., SPEAKER, T. J., CONTAG, C. H., KASPAR, R. L., COULMAN, S. A., HARGEST, R. & BIRCHALL, J. C. 2013. Gene silencing following siRNA delivery to skin via coated steel microneedles: In vitro and in vivo proof-of-concept. *J Control Release,* 166**,** 211-9.

CHU, C. C., ALI, N., KARAGIANNIS, P., DI MEGLIO, P., SKOWERA, A., NAPOLITANO, L., BARINAGA, G., GRYS, K., SHARIF-PAGHALEH, E., KARAGIANNIS, S. N., PEAKMAN, M., LOMBARDI, G. & NESTLE, F. O. 2012. Resident CD141 (BDCA3)+ dendritic cells in human skin produce IL-10 and induce regulatory T cells that suppress skin inflammation. *J Exp Med,* 209**,** 935-45.

CODY, C. L., BARAFF, L. J., CHERRY, J. D., MARCY, S. M. & MANCLARK, C. R. 1981. Nature and rates of adverse reactions associated with DTP and DT immunizations in infants and children. *Pediatrics,* 68**,** 650-60.

COFFMAN, R. L., SHER, A. & SEDER, R. A. 2010. Vaccine Adjuvants: Putting Innate Immunity to Work. *Immunity,* 33**,** 492-503.

COULMAN, S. A., ANSTEY, A., GATELEY, C., MORRISSEY, A., MCLOUGHLIN, P., ALLENDER, C. & BIRCHALL, J. C. 2009. Microneedle mediated delivery of nanoparticles into human skin. *Int J Pharm,* 366**,** 190-200.

DANSO, M. O., BERKERS, T., MIEREMET, A., HAUSIL, F. & BOUWSTRA, J. A. 2015. An ex vivo human skin model for studying skin barrier repair. *Exp Dermatol,* 24**,** 48-54.

DEARMAN, R. J., BHUSHAN, M., CUMBERBATCH, M., KIMBER, I. & GRIFFITHS, C. E. 2004. Measurement of cytokine expression and Langerhans cell migration in human skin following suction blister formation. *Exp Dermatol,* 13**,** 452-60.

FISCHER, A. H., JACOBSON, K. A., ROSE, J. & ZELLER, R. 2008. Hematoxylin and eosin staining of tissue and cell sections. *CSH Protoc,* 2008**,** pdb.prot4986.

GALINSKI, M., SRA, K., HAYNES, J., II & NASPINSKI, J. 2015. Live Attenuated Viral Vaccines. *In:* NUNNALLY, B. K., TURULA, V. E. & SITRIN, R. D. (eds.) *Vaccine Analysis: Strategies, Principles, and Control.* Springer Berlin Heidelberg.

GILL, H. S. & PRAUSNITZ, M. R. 2007. Coated microneedles for transdermal delivery. *J Control Release,* 117**,** 227-37.

GROVES, R. B., COULMAN, S. A., BIRCHALL, J. C. & EVANS, S. L. 2012. Quantifying the mechanical properties of human skin to optimise future microneedle device design. *Comput Methods Biomech Biomed Engin,* 15**,** 73-82.

HANLEY, K. A. 2011. The double-edged sword: How evolution can make or break a live-attenuated virus vaccine. *Evolution,* 4**,** 635-643.

HANNOUN, C. 2013. The evolving history of influenza viruses and influenza vaccines. *Expert Rev Vaccines,* 12**,** 1085-94.

HOBOT, J. A. & NEWMAN, G. R. 1996. Immunomicroscopy: resin techniques and on-section labelling with immunocolloidal gold or immunoperoxidase--planning a protocol. *Scanning Microsc,* 10**,** 121-43; discussion 143-5.

ITA, K. 2015. Transdermal Delivery of Drugs with Microneedles-Potential and Challenges. *Pharmaceutics,* 7**,** 90-105.

JONES, P. S., ELIAS, J. M. & SCHECTER, N. 1986. An Improved Method for Embedding Retina for Cryosectioning. *Journal of Histotechnology,* 9**,** 181-182.

KANG, S.-M., YOO, D.-G., LIPATOV, A. S., SONG, J.-M., DAVIS, C. T., QUAN, F.-S., CHEN, L.-M., DONIS, R. O. & COMPANS, R. W. 2009. Induction of Long-Term Protective Immune Responses by Influenza H5N1 Virus-Like Particles. *PLoS ONE,* 4**,** e4667.

KANITAKIS, J. 2002. Anatomy, histology and immunohistochemistry of normal human skin. *Eur J Dermatol,* 12**,** 390-9; quiz 400-1.

KENNEY, R. T., FRECH, S. A., MUENZ, L. R., VILLAR, C. P. & GLENN, G. M. 2004. Dose sparing with intradermal injection of influenza vaccine. *N Engl J Med,* 351**,** 2295-301.

KHAN, M., DHANWANI, R., RAO, P. V. & PARIDA, M. 2012. Subunit vaccine formulations based on recombinant envelope proteins of Chikungunya virus elicit balanced Th1/Th2 response and virus-neutralizing antibodies in mice. *Virus Res,* 167**,** 236-46.

KIM, Y.-C., PARK, J.-H. & PRAUSNITZ, M. R. 2012. Microneedles for drug and vaccine delivery. *Advanced drug delivery reviews,* 64**,** 1547-1568.

MESTAS, J. & HUGHES, C. C. 2004. Of mice and not men: differences between mouse and human immunology. *J Immunol,* 172**,** 2731-8.

MURPHY, D. B. & DAVIDSON, M. W. 2012. Fundamentals of Light Microscopy. *Fundamentals of Light Microscopy and Electronic Imaging.* John Wiley & Sons, Inc.

NETZLAFF, F., SCHAEFER, U. F., LEHR, C. M., MEIERS, P., STAHL, J., KIETZMANN, M. & NIEDORF, F. 2006. Comparison of bovine udder skin with human and porcine skin in percutaneous permeation experiments. *Altern Lab Anim,* 34**,** 499-513.

NG, K. W., PEARTON, M., COULMAN, S., ANSTEY, A., GATELEY, C., MORRISSEY, A., ALLENDER, C. & BIRCHALL, J. 2009. Development of an ex vivo human skin model for intradermal vaccination: tissue viability and Langerhans cell behaviour. *Vaccine,* 27**,** 5948-5955.

NOMURA, T., KABASHIMA, K. & MIYACHI, Y. 2014. The panoply of αβT cells in the skin. *Journal of Dermatological Science,* 76**,** 3-9.

NORMAN, J. J., GUPTA, J., PATEL, S. R., PARK, S., JARRAHIAN, C., ZEHRUNG, D. & PRAUSNITZ, M. R. 2014. Reliability and accuracy of intradermal injection by Mantoux technique, hypodermic needle adapter, and hollow microneedle in pigs. *Drug Deliv Transl Res,* 4**,** 126-30.

PEARTON, M., KANG, S.-M., SONG, J.-M., ANSTEY, A. V., IVORY, M., COMPANS, R. W. & BIRCHALL, J. C. 2010a. Changes in Human Langerhans Cells Following Intradermal Injection of Influenza Virus-Like Particle Vaccines. *PLoS ONE,* 5**,** e12410.

PEARTON, M., KANG, S.-M., SONG, J.-M., KIM, Y.-C., QUAN, F.-S., ANSTEY, A., IVORY, M., PRAUSNITZ, M. R., COMPANS, R. W. & BIRCHALL, J. C. 2010b. Influenza Virus-Like Particles coated onto microneedles can elicit stimulatory effects on Langerhans cells in human skin. *Vaccine,* 28**,** 6104-6113.

PEARTON, M., PIRRI, D., KANG, S.-M., COMPANS, R. W. & BIRCHALL, J. C. 2013. Host responses in human skin after conventional intradermal injection or microneedle administration of virus-like-particle influenza vaccine. *Advanced healthcare materials,* 2**,** 1401-1410.

PEARTON, M., SALLER, V., COULMAN, S. A., GATELEY, C., ANSTEY, A. V., ZARNITSYN, V. & BIRCHALL, J. C. 2012. Microneedle delivery of plasmid DNA to living human skin: Formulation coating, skin insertion and gene expression. *J Control Release,* 160**,** 561-9.

PEGG, D. E. 1987. Mechanisms of freezing damage. *Symp Soc Exp Biol,* 41**,** 363-78.

RANI, Z. & HUSSAIN, I. 2003. Immunofluorescence in immunobullous diseases. *Journal of Pakistan Association of Dermatologists,* 13**,** 76-88.

RAVENSCROFT, N., COSTANTINO, P., TALAGA, P., RODRIGUEZ, R. & EGAN, W. 2015. Glycoconjugate Vaccines. *In:* NUNNALLY, B. K., TURULA, V. E. & SITRIN, R. D. (eds.) *Vaccine Analysis: Strategies, Principles, and Control.* Springer Berlin Heidelberg.

SAMJI, T. 2009. Influenza A: Understanding the Viral Life Cycle. *The Yale Journal of Biology and Medicine,* 82**,** 153-159.

SANDERS, B., KOLDIJK, M. & SCHUITEMAKER, H. 2015. Inactivated Viral Vaccines. *In:* NUNNALLY, B. K., TURULA, V. E. & SITRIN, R. D. (eds.) *Vaccine Analysis: Strategies, Principles, and Control.* Springer Berlin Heidelberg.

SCHMALFUß, U., NEUBERT, R. & WOHLRAB, W. 1997. Modification of drug penetration into human skin using microemulsions. *Journal of Controlled Release,* 46**,** 279-285.

SITRIN, R., ZHAO, Q., POTTER, C., CARRAGHER, B. & WASHABAUGH, M. 2015. Recombinant Virus-like Particle Protein Vaccines. *In:* NUNNALLY, B. K., TURULA, V. E. & SITRIN, R. D. (eds.) *Vaccine Analysis: Strategies, Principles, and Control.* Springer Berlin Heidelberg.

SRIVASTAVA, I. K. & LIU, M. A. 2003. Gene vaccines. *Ann Intern Med,* 138**,** 550-9.

STEIMER, K. S. & HAIGWOOD, N. L. 1991. Importance of conformation on the neutralizing antibody response to HIV-1 gp120. *Biotechnol Ther,* 2**,** 63-89.

STERN, A. M. & MARKEL, H. 2005. The history of vaccines and immunization: familiar patterns, new challenges. *Health Aff (Millwood),* 24**,** 611-21.

STOITZNER, P., HOLZMANN, S., MCLELLAN, A. D., IVARSSON, L., STOSSEL, H., KAPP, M., KAMMERER, U., DOUILLARD, P., KAMPGEN, E., KOCH, F., SAELAND, S. & ROMANI, N. 2003. Visualization and characterization of migratory Langerhans cells in murine skin and lymph nodes by antibodies against Langerin/CD207. *J Invest Dermatol,* 120**,** 266-74.

SUH, H., SHIN, J. & KIM, Y.-C. 2014. Microneedle patches for vaccine delivery. *Clinical and Experimental Vaccine Research,* 3**,** 42-49.

SWARBRICK, J., LEE, G. & BROM, J. 1982. Drug Permeation through Human Skin: I. Effects of Storage Conditions of Skin. *Journal of Investigative Dermatology,* 78**,** 63-66.

TAUBENBERGER, J. K. & KASH, J. C. 2010. Influenza Virus Evolution, Host Adaptation and Pandemic Formation. *Cell host & microbe,* 7**,** 440-451.

TAUBENBERGER, J. K. & MORENS, D. M. 2008. The Pathology of Influenza Virus Infections. *Annual review of pathology,* 3**,** 499-522.

TIWARI, T. S. P. & WHARTON, M. 2013. 12 - Diphtheria toxoid. *In:* OFFIT, S. A. P. A. O. A. (ed.) *Vaccines (Sixth Edition).* London: W.B. Saunders.

TORRISI, B. M., ZARNITSYN, V., PRAUSNITZ, M. R., ANSTEY, A., GATELEY, C., BIRCHALL, J. C. & COULMAN, S. A. 2013. Pocketed microneedles for rapid delivery of a liquid-state botulinum toxin A formulation into human skin. *J Control Release,* 165**,** 146-52.

VAN DAMME, P., OOSTERHUIS-KAFEJA, F., VAN DER WIELEN, M., ALMAGOR, Y., SHARON, O. & LEVIN, Y. 2009. Safety and efficacy of a novel microneedle device for dose sparing intradermal influenza vaccination in healthy adults. *Vaccine,* 27**,** 454-9.

VAN DEN BERG, J. H., NUJIEN, B., BEIJNEN, J. H., VINCENT, A., VAN TINTEREN, H., KLUGE, J., WOERDEMAN, L. A., HENNINK, W. E., STORM, G., SCHUMACHER, T. N. & HAANEN, J. B. 2009. Optimization of intradermal vaccination by DNA tattooing in human skin. *Hum Gene Ther,* 20**,** 181-9.

VAN DER WORP, H. B., HOWELLS, D. W., SENA, E. S., PORRITT, M. J., REWELL, S., O'COLLINS, V. & MACLEOD, M. R. 2010. Can animal models of disease reliably inform human studies? *PLoS Med,* 7**,** e1000245.

VANDESANDE, F. 1979. A critical review of immunocytochemical methods for light microscopy. *Journal of Neuroscience Methods,* 1**,** 3-23.

WANG, X., UTO, T., AKAGI, T., AKASHI, M. & BABA, M. 2008. Poly(gamma-glutamic acid) nanoparticles as an efficient antigen delivery and adjuvant system: potential for an AIDS vaccine. *J Med Virol,* 80**,** 11-9.

WHO. 2014. *Influenza (Seasonal)* [Online]. Switzerland. Available: http://www.who.int/mediacentre/factsheets/fs211/en/ [Accessed July 9th 2016].

WINSOR, L. 1994. Tissue processing. *Laboratory histopathology. New York: Churchill Livingstone***,** 4-2.

WRAITH, D. C., GOLDMAN, M. & LAMBERT, P. H. 2003. Vaccination and autoimmune disease: what is the evidence? *Lancet,* 362**,** 1659-66.

WU, S. J., GROUARD-VOGEL, G., SUN, W., MASCOLA, J. R., BRACHTEL, E., PUTVATANA, R., LOUDER, M. K., FILGUEIRA, L., MAROVICH, M. A., WONG, H. K., BLAUVELT, A., MURPHY, G. S., ROBB, M. L., INNES, B. L., BIRX, D. L., HAYES, C. G. & FRANKEL, S. S. 2000. Human skin Langerhans cells are targets of dengue virus infection. *Nat Med,* 6**,** 816-20.

XU, W., JONG HONG, S., JIA, S., ZHAO, Y., GALIANO, R. D. & MUSTOE, T. A. 2012. Application of a partial-thickness human ex vivo skin culture model in cutaneous wound healing study. *Lab Invest,* 92**,** 584-99.

ZEHRUNG, D. 2009. Intradermal Delivery of Vaccines: A review of the literature and the potential for development for use in low- and middle income countries. *In:* KRISTENSEN, D. (ed.). Program for Appropriate Technology in Health (PATH).

ZELLER, R. 2001. Fixation, Embedding, and Sectioning of Tissues, Embryos, and Single Cells. *Current Protocols in Molecular Biology.* John Wiley & Sons, Inc.

Chapter 3- The *Ex Vivo* Human Skin Immune Cell Model

3.1 Introduction

The previous chapter explored the *ex vivo* human skin model as a useful tool for assessing intradermal vaccine delivery. This chapter will consider the limitations of the model and explore the possibility of a cellular model derived from *ex vivo* skin as a complementary means of preclinical vaccine testing.

3.1.1 Limitations of the Human *Ex Vivo* Skin Model

Whilst full thickness *ex vivo* human skin allows the behaviour of skin immune cells to be studied *in situ*, there are limitations to the analysis techniques that can be used with the model. The thickness of skin prevents visible or laser light penetration, so it must be sectioned (Wu et al., 2000) or the epidermis isolated (Larsen et al., 1990) in order to allow imaging via microscopy. Immunofluorescence can allow for clear distinction of markers within a tissue but has limitations with photobleaching, tissue autofluorescence (Jensen, 2012)and spectral overlap if multiple fluorophores are used (Lichtman and Conchello, 2005). Spectral overlap is inconsequential if imaging a single marker e.g. Langerhans cells (LCs), which can be visualised by staining for CD207 (Pearton et al., 2010b). However, it is a significant issue for visualising subsets of dermal dendritic cells (dDCs) that possess more complex phenotypes (Nestle et al., 1993).

There are also practical issues related to the spatial distribution of immune cells within the *ex vivo* human skin samples. To deliver vaccine to a high number of cells, delivery must occur across a large area of skin. Many intradermal delivery methods only deliver formulation to a limited area proximal to the site of injection however (Witting et al., 2000). Delivery to large areas of skin also requires large amounts of reagents, which in the case of vaccines can represent significant cost (Kenney et al., 2004). The amount of excised skin obtained from each surgical procedure is also variable and therefore is not always large enough to complete such studies. Thus, to enable more intricate experiments, which allow for the observation of numerous cellular factors

concurrently, isolation of viable immune cells from the skin for downstream experimentation was explored.

3.1.2 Methods of Obtaining Cells from Skin

There have been three main methods previously reported for obtaining cells from skin. The first is a direct walkout from skin, where skin is floated on media directly after collection and the migratory cells collected from media 48 hours later (Goddard et al., 2004, Segura et al., 2012). This utilises split-thickness skin i.e. full thickness skin that has had a proportion of the dermis mechanically removed, to reduce the migratory distance for cells to exit the tissue and ensures the skin floats on the media. Because only migratory cells will actively move into the media, this technique represents an enrichment of these cells compared to their purity in the skin. Whilst this involves a minimal amount of skin processing, it does not allow for separation of epidermal and dermal migratory cells and also does not produce high yields of cells. The lengthy walkout process may also reduce the viability of migratory cells which are terminally differentiated and will not proliferate in culture. A longer walkout period was reported to increase yield but at a cost of lower viability (Nestle et al., 1993), so a balance must be struck between the two factors.

The second reported method uses enzyme treatment of skin to allow mechanical separation of the epidermis from the dermis. The two can then be cultured separately and the migratory cells collected from each. The enzymes used vary but normally involve dispase (Pena-Cruz et al., 2001) or collagenase (Hentzer and Kobayasi, 1978). Enzyme incubation time also varies from 30 mins at 37°C (McCully et al., 2012) to overnight at 4°C (Klechevsky et al., 2008a). The shortest incubation time reported used a combination of Dispase II, collagenase D and DNase (McCully et al., 2012). The walkout times reported tend to be similar, with 48-72 hours being commonly used. This possesses an advantage over the split thickness skin walkout as it allows dermal and epidermal migratory cells to be studied separately. The separated skin layers also possess a greater surface area from which cells can migrate and reduces the migration distance of LCs, which no longer have to migrate through the dermis into media. The

increased handling time and exposure to enzymes compared to the direct walkout method may affect cell viability or phenotype negatively though.

The final method involves enzymatic and/or mechanical dissociation of the skin to produce a complete cell suspension (Bigley et al., 2015, Haniffa et al., 2012). This may be done after enzymatic separation of the epidermis and dermis to produce separate epidermal and dermal cell suspensions. The method allows for the collection of immune cells within a few hours of collecting the tissue and thus is a relatively rapid method for cell isolation. As the entire tissue is processed it is possible to collect the complete immune cell populations present in the skin. The purity of cells will be reduced compared to the walkout method though, as non-migratory cells will also be included in the suspension. Again, the exposure to enzymes and/or mechanical stress may affect the viability/phenotype of the cells collected, which must be considered in any results obtained.

3.1.3 The Skin Cell Walkout Method

It was identified that allowing migratory cells to migrate from the skin was the favoured method of isolation due to the resulting increase in purity which will reduce reagent usage over a smaller cell population. Enzymatic pre-treatment would be performed to allow dermal and epidermal cells to be studied separately but in parallel from a given donor and to increase the yield of cells. Due to its short incubation time (30 mins at 37°C), the enzyme cocktail used by McCully et al (2012) was selected to separate the dermis and epidermis. This utilises a combination of Dispase II and collagenase to catalyse the breakdown of the basement membrane (Stenn et al., 1989) alongside DNase I which reduces clumping caused by DNA released from lysed cells (Stenn et al., 1989).

3.1.4 Assessing Dendritic Cell Responsiveness

The ability to recognise and be activated by foreign antigen is central to LCs and dDCs' ability to initiate an immune response (Banchereau and Steinman, 1998). They do so with a range of cell membrane and cytoplasmic receptors which bind to specific

antigens in the extra- and intra-cellular environments respectively (Dudziak et al., 2007). These receptors recognise certain structural sequences specific to pathogens, pathogen-associated molecular patterns (PAMPs), and are termed pattern recognition receptors (Reis e Sousa, 2004). One subset of pattern recognition receptors are toll-like receptors (TLRs) (Aderem and Ulevitch, 2000). This family of receptors can bind a variety of PAMPs, after which the TLR initiates a signal transduction pathway which can mediate a range of effects including gene expression, production of cytokines or cell maturation (Medzhitov, 2001). The antigen-induced signal transduction pathway varies with the PAMP and the TLR that binds it (Reis e Sousa, 2004). This investigation will focus on two TLRs that recognise bacterial cell wall components and viral double-stranded RNA.

Lipopolysaccharide (LPS) is a component of Gram-negative bacterial cell walls made up of fatty acids bound to a polysaccharide structure (Gangloff et al., 1999). It is one of the most potently immunostimulatory substances in nature (Beutler, 2000). DCs are able to detect LPS via Toll-like receptor 4 (TLR4) on their surface membranes (Lu et al., 2008). Signalling via TLR4 in the presence of LPS leads to maturation and the release of cytokines such as tumour necrosis factor-α (TNF-α) and interleukin 12 (IL-12) (Duraes et al., 2009). Polyinosinic:polycytidylic acid (poly(I:C)) comprises two repeating sequences of nucleotides, a chain of inosinic acid and a chain of cytidylic acid bound to one another, and is used as a synthetic analogue of viral double-stranded RNA (Ichinohe et al., 2005). On immune cells, this is recognised by TLR3 (Lee et al., 2006) which also signals the expression of cytokines such as TNF-α (Reimer et al., 2008). This investigation aims to vindicate the responsiveness of skin-derived DCs to stimulation by LPS and poly(I:C) to assess the usefulness of these cells as a model for immune system stimulation *in vivo*.

3.1.5 Human Immunodeficiency Virus (HIV)

HIV is part of the *Lentivirus* genus and is classified into two species: Human immunodeficiency virus 1 (HIV-1) and Human immunodeficiency virus 2 (HIV-2). Both species are further subdivided into multiple groups and subtypes based on genetic differences, with prevalence of the various subtypes varying across geographical regions (Perrin et al., 2003). HIV-1, and more specifically its subtype 'M', is responsible for the

vast majority of HIV infections in humans (Murphy et al., 2012). There are currently over 34 million people worldwide who are HIV-positive and the virus has been responsible for over 25 million deaths in the last 30 years (WHO, 2012a). It is transmitted via infected bodily fluids during sexual activity, from mother to child in childbirth/breastfeeding or in intravenous drug users sharing needles (Gouws et al., 2006). HIV possesses RNA as its genetic material which must be transcribed to DNA by reverse transcriptase before mRNA coding for viral replication can be produced (hence it is referred to as a retrovirus) (Murphy et al., 2012). Infection by the virus leads to depletion of CD4+ T-cells over a number of years. This leads to acquired immunodeficiency syndrome (AIDS), which occurs when the CD4+ cell count falls below 200/µl blood (Lindback et al., 1994). The inability of an AIDS patient's body to mount an effective immune response leads to opportunistic infections and cancers, which are the primary cause of mortality in the infected population (WHO, 2012a). Whilst there are effective anti-retroviral treatments available that can suppress a patient's viral load, they are not able to completely eliminate the infection. A vaccine would represent an extremely useful tool, allowing people to avoid initial infection altogether. Though some candidate vaccines have shown promise in clinical trials, no vaccine has made it to market yet. The extremely high mutation rate of HIV and the broad range of subtypes represent significant challenges to the creation of an effective vaccine (Johnston and Fauci, 2008).

One of the major challenges within laboratory HIV research is poor entry of the virus into cultured cells. It requires binding of two cell surface receptors, CD4 and a co-receptor such as CCR5 or CXCR4, to be internalised (Wilen et al., 2012). A low entry and therefore low infection rate in experiments can affect the robustness of readouts when assessing treatments. This has led to models of HIV infection being developed utilising pseudotyped virus models that increase the infectivity of the virions themselves by improving cell entry.

Another hurdle to the study of HIV infection in the laboratory is the lack of infectivity in species commonly used as animal models. Outside of humans, HIV only infects certain primate species that are associated with high research costs (Hatziioannou and Evans, 2012). These are therefore controversial models (Goodman and Check, 2002). It is also possible to produce humanised mouse models that can be infected with HIV (Rizza et al., 1996, Aldrovandi et al., 1993), though these models do

not possess multi-lineage human haematopoiesis or a functional human immune system (Berges et al., 2006). Human *ex vivo* skin presents a potentially useful tool in the study of HIV, particularly due to its populations of LCs. LCs are present on genital mucosa, the most common route of HIV infection, and have been implicated in the transmission of the virus to T-cells (Miller and Shattock, 2003). CD207 has also been shown to bind HIV and internalise it, though it has been shown to be involved in the degradation of the virus within LCs (de Witte et al., 2007). As human *ex vivo* genital mucosa is not readily available, skin provides an alternative source for these cells for use in HIV infection studies.

3.1.6 Pseudotyped Virus Models

Pseudotyped viruses are those where the envelope of one virus is combined with the viral core of another, usually to tailor the cell entry properties of the virus and deliver the viral core to the cells of interest (Sanders, 2002). For the purpose of this investigation, the HIV-1 virus will be pseudotyped to broaden its tropism and therefore provide a greater population of infected cells that can be studied. Using pseudotyped virus to negate the limited capacity of HIV to enter cells allows post-entry HIV restriction to be studied.

3.1.6.1 Vesicular Stomatitis Virus (VSV)

The Vesicular stomatitis Indiana virus (VSV) is a member of the viral family *Rhabdoviridae*. In the wild, it mainly affects animals such as horses and cattle but has the potential to zoonotically infect humans (Quiroz et al., 1988). It enters cells via the binding of glycoprotein G molecules on its viral envelope to low-density lipoprotein (LDL) receptors on target cells (Finkelshtein et al., 2013). It passes through the endocytic machinery in a clathrin-dependent pathway before delivering its nucleocapsid into the cytosol where it can infect the host cell (Albertini Aé et al., 2012). The LDL receptor is highly retained across cell types, allowing the virus to enter a wide range of unrelated cells (Superti et al., 1987). For this reason, viral envelopes containing VSV glycoprotein

G (VSV-G) are often used in pseudotyped retroviruses to broaden the range of cells which they can infect (Zufferey et al., 1997).

3.1.6.2 GFP-Encoding VSV-G-Pseudotyped HIV

This investigation will utilise a HIV-1 lentiviral vector pseudotyped with VSV-G envelope to remove the receptor binding requirements that normally limits HIV entry into DCs (Aiken, 1997). This will allow post-entry behaviour of the virus to be studied more robustly by improving delivery of the HIV nucleocapsid into cells. The vector is replication-deficient so only a single round of infection will occur (infected cells will not produce further virus) (Da Costa et al., 1999). This means viral titre remains directly proportional to the starting dose throughout the experiment, whereas wild type virus would replicate and titre would vary with culture time. The insertion of a green fluorescent protein (GFP) gene into the vector means that cells that are infected will fluoresce with laser excitation, allowing for a straightforward means of quantifying infection without the need for staining viral antigen in cells (Auewarakul et al., 2001).

3.1.7 SAM and HD Domain-Containing Protein 1 (SAMHD1)

The sterile alpha motif and histidine-aspartate domain-containing protein 1 (SAMHD1) is an antiviral factor within dDCs and LCs that allows them to resist infection by retroviruses (Laguette et al., 2011). Its expression is induced by interferon-γ (IFN-γ), a cytokine released in response to viral infection (Li et al., 2000). SAMHD1 catalyses hydrolysis of deoxynucleoside triphosphates (dNTPs) in the cytosol into their constituent nucleoside and phosphate components (Ji et al., 2014). This decreases dNTP availability to viral reverse transcriptase (which utilises dNTPs for transcribing viral RNA to DNA), thereby reducing viral replication (Pauls et al., 2013).

3.1.7.1 Simian Immunodeficiency Virus and Vpx Protein

Simian immunodeficiency virus (SIV) is a retrovirus from the genus *Lentivirus* along with HIV-1 and HIV-2. As the name suggests, it infects non-human primates. In

many host species, it does not present with clinical symptoms but in a small number it can cause a depletion in the immune system similar to AIDS in humans (Melby and Altman, 1974). Structurally, SIV and HIV possess a number of similarities. Of interest to this investigation is the accessory proteins Vif, Vpx, Vpr, Vpu, and Nef, which are expressed by lentiviruses that allow them to counteract intrinsic antiviral factors in cells and allow reverse transcription to proceed (Goujon et al., 2007). Vpx will be utilised in particular due to its ubiquitin-proteasome-dependent degradation of SAMHD1. Vpx is present on a number of strains of SIV and HIV-2 but not HIV-1 (Hrecka et al., 2011). Exposing cells to SIV before infection with a HIV-1 lentiviral vector will allow the effect of SAMHD1 protection on HIV-1 infection to be quantified.

3.1.8 Flow Cytometry

Chapter 2 utilised immunofluorescence to visualise cell markers within the skin. Flow cytometry also uses fluorescently-conjugated antigen-specific antibodies or other fluorescent substrates to bind to the target cells and thus enable their detection and/or quantification. However, instead of the sample being a tissue section it is a cell suspension. This allows labelling of individual cells extracellularly or, if the cell membrane is permeabilised before the addition of antibodies, intracellularly (Foster et al., 2007). Analysis is also different from immunofluorescence. In flow cytometry, the labelled cell suspension is passed in a single-file stream past a number of lasers which interrogate each cell individually. The use of dichromatic mirrors and filters means multiple wavelengths of excitation and emission can be analysed on each cell (Wang et al., 2010). Thus, multiple antibodies and/or substrates can be used concurrently and multiple marker expression analysed on each cell. Common flow cytometers have the ability to distinguish between 8 different fluorophores though systems exist that can analyse a greater number (Chattopadhyay et al., 2006).

Flow cytometry also has the ability to quantify the fluorescence signal present from different fluorophores. It does so by measuring the intensity of output light after excitation with a defined laser intensity. The intensity of light output is proportional to the number of fluorophores i.e. if staining is performed with an excess of antibody, it can be used to quantify cell marker or cytokine expression (Chen et al., 1999). This is

useful both in terms of distinguishing between positive and negative populations but can also show the up- or down-regulation of a particular marker/cytokine in a cell population. Flow cytometers also have the ability to measure the size and complexity of cells. Size is measured by the forward scatter (FSC), which is determined by the amount of refraction that occurs along the same axis as the original laser path (Shapiro, 2005). The larger a cell is, the greater the level of refraction and the higher the FSC signal will be. Complexity, mainly granularity and membrane roughness, is measured by the side scatter (SSC) that occurs in a cell i.e. the amount of light that is reflected at a right angle to the direction of the original laser (Shapiro, 2005). The more complex a cell, the greater the amount of light will be scatted at 90° angle and the greater the SSC signal will be.

3.1.8.1 Compensation Controls

Though the fluorophores used in flow cytometry analysis panels have fluorescence emission peaks at different wavelengths, some possess slight spectral overlap. Figure 3.1 shows a common example of the overlap between fluorescein isothiocyanate (FITC) and phycoerythrin (PE) spectra. Both fluorophores are excited by the 488nm laser and excitation of FITC produces a weak signal in the PE 575nm bandpass filter (Baumgarth and Roederer, 2000). To compensate for this, samples are analysed which are stained for each fluorophore individually and the 'spillover' signal detected in

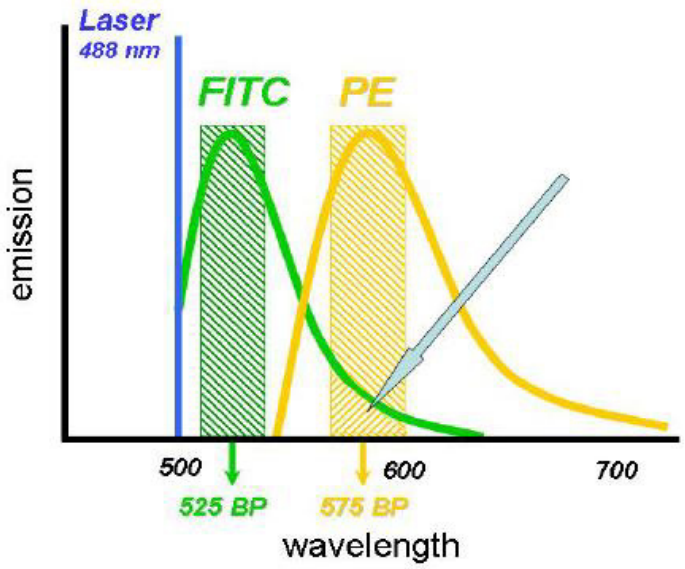

Figure 3.1: Fluorescence emission spectra overlap between fluorescein isothiocyanate (FITC) and phycoerythrin (PE) [Taken from: http://flowbook.denovosoftware.com/chapter-5-immunofluorescence-and-colour-compensation]

other channels is quantified. This can then be subtracted from the signals in the experimental samples, ensuring only fluorophore-specific signal is measured in each channel (Shapiro, 2005). The cells that will be used in the investigation may be used for compensation controls or, if this is not possible, polymer beads with antibody binding sites can be used (Roederer, 2002).

3.1.8.2 Isotype Control Antibodies

In flow cytometry it is important to negate the effects within results of non-specific binding of antibodies to cells, this can either be due to binding to Fc receptors on the cell surface or entrapment of the antibody on/in the cell. To control for this it is common to use isotype antibodies to create staining controls. These are antibodies conjugated with the fluorophores being used but not possessing antigen specificity to any marker that is present on the cells (Maecker and Trotter, 2006). Thus, the only antibody staining that will occur will be due to non-specific binding. The flow cytometric data can then be gated based on the isotype controls to determine the fluorescence levels (a combination of autofluorescence and non-specific antibody staining) of marker-negative populations.

3.1.8.3 Live/Dead Cell Staining

As well as antibody staining of cells, it is possible to chemically label cells with fluorescence. One particularly useful staining technique is the use of live/dead cell stains. These substances will not pass through intact cell membranes on viable cells but can easily pass into the permissive membranes of dead cells (King, 2000). This creates two populations: the non-fluorescent live cells where no dye has entered and the fluorescent dead cells which contain the stain, the proportions of which represent the viability of the cells at the time of staining. Some dyes are also fixable, meaning the cells can be fixed with paraformaldehyde or a similar fixative after live/dead staining and then stained with fluorophore-conjugated antibodies subsequently without degrading the viability dye staining.

3.1.8.4 Fluorescence-Activated Cell Sorting

Fluorescence-activated cell sorting (FACS) is a variation on flow cytometry that allows for the pooling of cell populations based on their fluorescence after staining. The staining protocol used is similar to flow cytometry apart from cells are not fixed and sterile conditions maintained. Gating is then applied to the sample in real time and cells possessing the characteristics of choice selected. The stream of cells passes out of the machine, forming droplets, each of which contains a single cell. The cytometer applies an electrical charge to the liquid at the moment it forms a droplet, creating a charged droplet which can be directed by a charge gate into the receptacle of choice (Herzenberg et al., 2002). The use of different charge polarity and deflection charge allow cells to be sorted into multiple directions. Highly pure viable cell populations can then be collected and used in downstream experimentation.

3.2 Aims and Objectives

This chapter aims to extend use of human *ex vivo* human skin beyond the full thickness skin model by extracting immune cells from it. The phenotype, viability and functionality of these cells will then be assessed. The specific practical objectives are:

1. Optimise a protocol for obtaining dDCs and epidermal LCs from skin which maximises yield, viability and purity of the cells.
2. Characterise the cell populations using flow cytometry to identify phenotypic markers.
3. Utilise live/dead cell staining to assess the viability of cells in combination with antibody staining to determine viability within immune cell populations specifically.
4. Utilise TLR agonists to assess the capacity of skin immune cells to respond to immune challenge representative of bacterial and viral pathogens.
5. Utilise SIV virus to knockdown SAMHD1 in dDCs and LCs obtained from skin.
6. Apply the skin cell model to validate results of a study on the effect of SAMHD1 on post-entry HIV-1 viral infection. Initial results were obtained

by a colleague using monocyte-derived DCs and so the skin cell model should provide data that is more representative of the *in vivo* situation.

3.3 Materials and Methods

[All reagents were obtained from Fisher Scientific, UK unless otherwise stated]

3.3.1 Isolation of Dermal and Epidermal Walkout Cells from Skin

Human skin samples were collected following mastectomy or breast reduction surgery at the Royal Gwent Hospital, Newport and transported to the laboratory for use as described in Section 2.3.2. Subcutaneous fat was removed using surgical scissors and the skin pinned, epidermis uppermost, onto a corkboard. The uppermost 300µm of the skin was isolated using a dermatome (Nouvag AG, Switzerland), a surgical instrument used to harvest skin from patients during skin graft surgery. The remaining skin (lower dermis) was discarded. The 300µm-thickness skin was then cut into pieces, roughly $1cm^2$ in size, using a scalpel and placed in Roswell Park Memorial Institute medium (RPMI; Sigma-Aldrich, UK) plus 10 mg/ml collagenase (Invitrogen, UK), 20 U/ml DNase I (Sigma-Aldrich, UK) and 10 mg/ml Dispase II (Invitrogen, UK) and incubated with agitation in a shaking water bath (at 175 strokes/min) for 30 mins at 37°C. Following removal from the enzyme solution, mechanical separation of the epidermal and dermal regions at the basement membrane using forceps was possible. Dermal and epidermal tissue were then washed briefly in PBS and divided between wells of a 6-well plate containing RPMI supplemented with 10% human AB serum (Sigma-Aldrich, UK) and 1% Pen/Strep/Fungizone solution (Sigma-Aldrich, UK) (DC-RPMI). The plate was then incubated at 37°C for 48 hours to allow the migration of cells out of the tissue and into the media. Following incubation, media was collected, passed through a 100µm cell strainer and spun down to collect cells. Cells were counted using a haemocytometer prior to use.

3.3.2 Characterisation of LCs and dDCs

Dermal and epidermal walkout cells were fixed in 1% paraformaldehyde (PFA) in PBS at room temperature for 10 mins then washed in PBS. Fixed cells were aliquoted at

1 x 10^5 cells per well of a round-bottomed 96-well plate, spun down and then resuspended in 50µl FACS buffer (1% bovine serum albumin (Sigma-Aldrich, UK) and 0.025% sodium azide in PBS) containing manufacturer's recommended concentration of the antibodies shown in Table 3.1.

Table 3.1: Antibodies used to assess phenotype of skin walkout cells via flow cytometry

	Antibody	**Conjugated Fluorophore**	**Manufacturer**
Dermal Dendritic Cell Panel	Anti-CD3	Fluorescein isothiocyanate (FITC)	BD Biosciences, UK
	Anti-CD19	FITC	Dako, Denmark
	Anti-CD20	FITC	BioLegend, UK
	Anti-CD56	FITC	BioLegend, UK
	Anti-CD45	Phycoerythrin (PE)	Miltenyi Biotec, UK
	Anti-HLA-DR	Allophycocyanin (APC)	BD Biosciences, UK
	Anti-CD14	Peridinin chlorophyll (PerCP)	Miltenyi Biotec, UK
	Anti-CD141	VioBlue®	Miltenyi Biotec, UK
	Anti-CD11c	Allophycocyanin-cyanine 7 (APC-Cy7)	BD Biosciences, UK
Epidermal Langerhans Cell Panel	Anti-CD1a	FITC	BD Biosciences, UK
	Anti-CD207	PE	Beckman Coulter, UK
	Anti-HLA-DR	APC	BD Biosciences, UK
Isotype Control Panel	IgG1 κ	FITC	BD Biosciences, UK
	IgG1 κ	PE	BD Biosciences, UK
	IgG1 κ	APC	BD Biosciences, UK
	IgG1 κ	PerCP	BD Biosciences, UK
	IgG1 κ	VioBlue®	Miltenyi Biotec, UK
	IgG1 κ	APC-Cy7	BD Biosciences, UK

Cells were incubated in antibody solutions and protected from light for 60 mins at 4°C. After staining, cells were washed and resuspended in 300µl FACS buffer per 1 x 10^5 cells for flow cytometric analysis on FACSCanto II Flow Cytometer (BD Biosciences, UK). Anti-Mouse Ig, κ/Negative Control Compensation Plus Beads (BD Biosciences, UK) were used with an antibody for each fluorophore used to provide compensation controls for the flow cytometric analysis. Analysis of flow cytometric data was performed using FlowJo software (FlowJo LLC, USA).

3.3.3 Characterisation of Dermal T-cells

Walkout cells were fixed as described in Section 3.3.2 then aliquoted at 1 x 10^5 cells per well of a round-bottomed 96-well plate, spun down and then resuspended in 50µl FACS buffer (1% bovine serum albumin (Sigma-Aldrich, UK) and 0.025% sodium azide in PBS) containing the manufacturer's recommended concentration of the antibodies listed in Table 3.2.

Table 3.2: Antibodies used to identify T-cells amongst skin walkout cells via flow cytometry

	Antibody	**Conjugated Fluorophore**	**Manufacturer**
Dermal T-cell Panel	Anti-CD8	FITC	BD Biosciences, UK
	Anti-CD3	PE	BD Biosciences, UK
	Anti-CD4	APC	BD Biosciences, UK
Isotype Control Panel	IgG1 κ	FITC	BD Biosciences, UK
	IgG1 κ	PE	BD Biosciences, UK
	IgG1 κ	APC	BD Biosciences, UK

Cells were incubated in antibody solutions protected from light for 60 mins at 4°C. After staining, cells were washed and resuspended in 300µl FACS buffer per 1 x 10^5 cells for flow cytometric analysis.

3.3.4 Walkout Cell Viability Staining

To assess the viability of skin walkout cells, LIVE/DEAD® Fixable Far Red Dead Cell Stain Kit, for 633 or 635 nm excitation (ThermoFisher Scientific, UK) was used. Cells were collected from skin following 48-hour walkout, as in Section 3.3.1. An aliquot of 1 x 10^6 each dermal or epidermal cells was heated to 65°C for 10 mins then cooled on ice to create a dead cell control for staining. All cells were washed with PBS before being stained for 30 mins with 1µl per 1 x 10^6 cells on ice. Following staining, cells were washed with PBS and fixed with 1% PFA for 10 mins at room temperature before being stained with the antibodies shown in Table 3.3.

Table 3.3: Antibodies used to assess viability of immune cells amongst skin walkout cells via flow cytometry

	Antibody	Conjugated Fluorophore	Manufacturer
Dermal Dendritic Cell Panel	Anti-HLA-DR	PE	BD Biosciences, UK
	Anti-CD141	VioBlue®	Miltenyi Biotec, UK
	Anti-CD11c	APC-Cy7	BD Biosciences, UK
Epidermal Langerhans Cell Panel	Anti-CD1a	FITC	BD Biosciences, UK
	Anti-CD207	PE	Beckman Coulter, UK
Isotype Control Panel	IgG1 κ	FITC	BD Biosciences, UK
	IgG1 κ	PE	BD Biosciences, UK
	IgG1 κ	APC	BD Biosciences, UK
	IgG1 κ	PerCP	BD Biosciences, UK
	IgG1 κ	VioBlue®	Miltenyi Biotec, UK
	IgG1 κ	APC-Cy7	BD Biosciences, UK

Following staining, flow cytometry and data analysis were performed as described in Section 3.3.2.

3.3.5 Stimulation of Skin LCs and dDCs with TLR Agonists

To assess the potential of the skin walkout cell model for measuring immune cell activation, walkout cells were collected from the dermis and epidermis as described in Section 3.3.1 before being plated at 2 x 10^6 cells per well of a 96 well plate. Cells were spun down and resuspended in Iscove's Modified Dulbecco's Medium (IMDM) plus 1 µg/ml lipopolysaccharide (LPS), IMDM plus 10 µg/ml poly-I:C or IMDM alone. One hour after plating, brefeldin-A was added to a final concentration of 10 µg/ml to wells designated for intracellular cytokine staining. Cells were then incubated overnight at 37°C.

The next morning, cells were fixed and stained for CD83 or intracellular cytokine expression. Intracellular staining was completed using using Perm/Wash Kit (BD Biosciences) according to the manufacturer's protocol. The antibodies used are listed in Table 3.4.

Table 3.4: Antibodies used to assess maturation and cytokine expression amongst skin walkout cells via flow cytometry

	Antibody	Conjugated Fluorophore	Manufacturer
Maturation Panel	Anti-HLA-DR	Phycoerythrin-cyanine 7 (PE-Cy7)	BD Biosciences, UK
	Anti-CD83	APC	Miltenyi Biotec, UK
ICC Panel	Anti-HLA-DR	PE-Cy7	BD Biosciences, UK
	Anti- TNF-α	APC	BD Biosciences, UK
	Anti-IL-12	APC	BD Biosciences, UK
Isotype Control Panel	IgG2a	PE-Cy7	BD Biosciences, UK
	IgG1 κ	APC	BD Biosciences, UK

Following staining, flow cytometry and data analysis were performed as described in Section 3.3.2. Statistical tests comprised one-way analysis of variance (ANOVA) followed by Tukey's post hoc analysis performed using IBM SPSS Statistics (IBM, USA).

3.3.6 Functional Testing of Skin Walkout Cells

The functionality of the walkout cells was also tested to further assess the *ex vivo* skin cell model. Previous work in the lab indicated differences in the infectability of monocyte-derived dendritic and LC models with a HIV-1 lentiviral vector, following knockdown of the antiviral factor SAM domain and HD domain-containing protein 1 (SAMHD1), which is common to skin-resident LCs and dDCs (Czubala et al., 2016). This investigation aimed to replace the monocyte-derived cells used in this series of experiment with *ex vivo* human skin cells in order to provide data that is more representative of *in vivo* cell behaviours.

3.3.6.1 Production of Lentiviral Vectors

[All plasmids were gifts from Prof. Didier Trono, EPFL, Switzerland]

Human embryonic kidney 293 cells expressing the simian vacuolating virus 40 large tumour antigen (HEK293T cells) were seeded at 10-15x 10^6 cells per T175 culture flask in 15mls Dulbecco's Modified Eagle Medium (DMEM) and incubated at 37°C

overnight to allow cell adherence onto the flask. A confluence of 70-80% was optimal for transfection using this protocol.

The following DNA plasmids (Figure 3.2) were combined in 2.5mM 4-(2-hydroxyethyl)-1-piperazineethanesulfonic acid (HEPES) buffered ddH_2O (Sigma-Aldrich, UK):

VSV-G-HIV-GFP Virus

1. 11.25µg pMD.G - envelope plasmid encoding G protein from VSV (Salmon et al., 2000b)
2. 33.75µg pLOX-EWgfp - HIV-1-derived transfer gene encoding GFP (Salmon et al., 2000a)
3. 45µg pR8.91 - lentiviral packaging plasmid which encodes HIV-1 group-specific antigen (Gag) and viral enzyme (Pol) polyproteins as well as the regulatory proteins Tat and Rev (acronyms for 'trans-activator of transcription' and 'regulator of expression of virion proteins' respectively) (Pollard and Malim, 1998, Salmon et al., 2000a)

SIV-Vpx Virus

1. 20µg pMD.G - as above, envelope plasmid encoding G protein from VSV
2. 40µg pSIV3+ - simian immunodeficiency virus-derived packaging plasmid (including Vpx) (Negre et al., 2000)

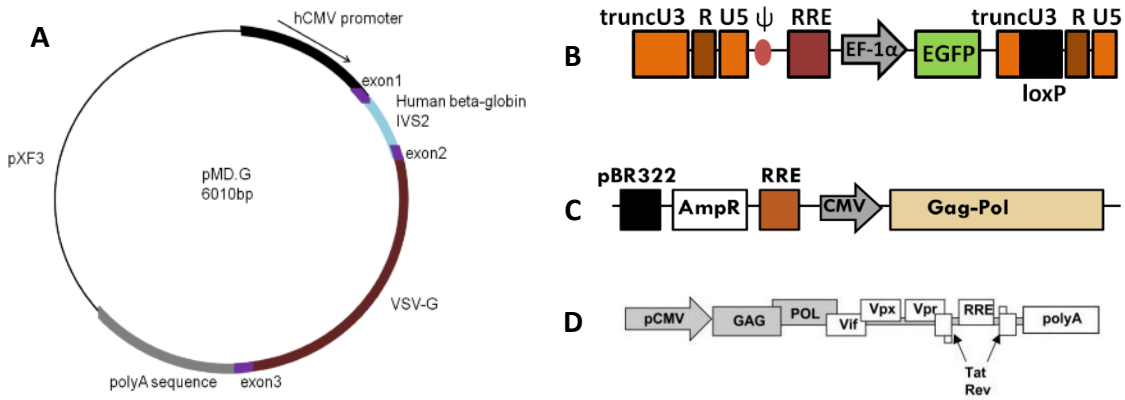

Figure 3.2: Schematic representations of the pMD.G (A), pLOX-EWgfp (B), pR8.91 (C) and pSIV3+ (D) plasmids used in the production of VSV-G-HIV-GFP and SIV-Vpx viruses

Plasmids were added to HEPES buffer to a final volume of 750µl and mixed gently for 5 mins at room temperature. The plasmid solution was then combined with 750µl 500mM $CaCl_2$. The resulting solution was added dropwise to 1.5ml of 2x HEPES-buffered saline (HBS) under gentle vortex to facilitate mixing. The mixture was then allowed to stand at room temperature for 30 mins. It was then added dropwise to the HEK293T cells in T175 flasks (3ml per flask), ensuring to distribute it across the entire culture surface. Gently tilting the flask further distributed the plasmids. Cells were then incubated at 37°C overnight. After this media was removed from the flasks, cells were washed gently with 20ml sterile phosphate-buffered saline (PBS) and 25ml DMEM was added before the flasks were returned to the incubator for a further overnight incubation at 37°C.

Cell supernatant was then removed, passed through a 0.45µm sterile filter and pelleted through a solution of 20% sucrose in PBS using an ultracentrifuge (Beckman Coulter, UK) at 26,000RPM at 4°C for 90 mins. After centrifugation, supernatant was aspirated and the lentiviral vector resuspended in DMEM and stored at -80°C until use. Viral titres were determined by a colleague using a Lenti-X p24 titre ELISA kit (Clontech, France) and titration of virus followed by western blot to assess SAMHD1 knockdown to establish the viral yield of VSV-G-HIV-GFP and SIV-Vpx viruses respectively.

3.3.6.2 Knockdown of SAMHD1 in LCs/dDCs

LCs and dDCs were isolated from skin using the walkout protocol (Section 3.3.1). A total of 3 x 10^5 dermal walkout cells and 1 x 10^6 epidermal walkout cells were plated at 1 x 10^5 cells per well with or without SIV-Vpx in a 96 round-bottomed well plate. Three hours after initial plating, cells were lysed by incubation for 30 mins at 4°C in lysis buffer (1mM $MgCl_2$, 1mM EDTA, Roche cOmplete™ Mini Protease Inhibitor Cocktail (Sigma Aldrich, UK), 1% IGEPAL® CA-630 (Sigma Aldrich, UK), 20mM Tris base and 150mM NaCl in ddH_2O in 1.5ml microcentrifuge tubes. Tubes were then vortexed before centrifugation at 13,000RPM for 18 mins. NuPAGE® LDS Sample Buffer and Reducing Agent were added to the supernatant and heated to 80°C for 10 mins to denature proteins ready for gel electrophoresis.

Gel electrophoresis was performed on NuPAGE™ Novex™ 4-12% Bis-Tris Protein Gels according to the manufacturer's protocol. SeeBlue® Pre-stained and Mark12™ Unstained protein standards were run concomitantly as per manufacturer's protocol to allow determination of protein size. Following gel electrophoresis, proteins were transferred to nitrocellulose membrane via electroblotting. Transfer success was determined via staining with 0.1% Ponceau S in 5% acetic acid in ddH_2O. The membrane was washed to remove Ponceau S staining then blocked using 5% milk protein in PBS. Antibody staining was performed overnight at 4°C on a rocking platform using the manufacturer-recommended concentrations of mouse anti-actin (Millipore, UK) and mouse anti-SAMHD1 (Abcam, UK) antibodies in 1% BSA, 0.025% sodium azide and 0.1% Tween 20 in PBS. After overnight incubation, membranes were washed then stained with anti-mouse HRP-conjugated secondary antibody (Bio-Rad, UK) as per manufacturer's protocol. SuperSignal West Pico Chemiluminescent Substrate (ThermoFisher, UK) was then added and the membrane imaged using x-ray film to detect light produced. SAMHD1 knockdown by SIV-Vpx was assessed by absence of a band on the developed film compared to the untreated control cells.

3.3.7 Infection of LCs/dDCs with VSV-G-HIV-GFP

LCs and dDCs were isolated from skin using the walkout protocol. Cells were plated at 1 x 10^5 cells per well with or without SIV-Vpx in a 96 round-bottomed well plate. Three hours after initial plating, VSV-G-HIV-GFP (17-63ng p24 per well) was added to the appropriate wells. Cells were fixed 96 hours after initial plating in 2% paraformaldehyde at room temperature for 10 mins prior to staining for flow cytometric analysis. Antibodies listed in Table 3.1 were used to characterise the cell populations based on CD141, CD45, CD11c, CD14, HLA-DR, CD1a and CD207 expression. Cells were incubated with antibodies for 60 mins at 4°C followed by two washes before analysis using a FACSCanto II flow cytometer (BD Biosciences, UK). GFP-expressing cells were analysed in the FITC channel. Statistical tests comprised one-way analysis of variance (ANOVA) followed by Tukey's post hoc analysis performed using IBM SPSS Statistics (IBM, USA).

3.3.8 Sorting of LCs and dDCs from Skin

Analysis of infection by VSV-G-HIV-GFP in dDC subsets following 96-hour incubation proved to be difficult due to CD141 and CD11c downregulation during culture (probably due to reduced viability of cells towards the end of culture). To assess whether differences in infectability post-SAMHD1 knockdown existed between dDC subsets, cell sorting was used to isolate the various subpopulations of dDCs. The walkout protocol was followed as described in Section 3.3.1 up until cell counting. After counting, cells were stained in sterile FACS buffer without sodium azide with the antibodies listed in Table 3.5.

Table 3.5: Antibodies used to sort dDC subsets and LCs from skin walkout cells

	Antibody	**Conjugated Fluorophore**	**Manufacturer**
dDC Panel	Anti-CD45	Phycoerythrin (PE)	Miltenyi Biotec, UK
	Anti-HLA-DR	Allophycocyanin (APC)	BD Biosciences, UK
	Anti-CD141	VioBlue®	Miltenyi Biotec, UK
	Anti-CD11c	Allophycocyanin-cyanine 7 (APC-Cy7)	BD Biosciences, UK
LC Panel	Anti-CD207	PE	Beckman Coulter, UK
	Anti-HLA-DR	APC	BD Biosciences, UK

Cell sorting was performed on a FACSAria III cell sorter (BD Biosciences, UK). Following sorting, cells were counted using a haemocytometer and viability assessed using Fixable Viability Dye eFluor® 450 (Affymetrix eBioscience, UK) following the manufacturer's protocol. Sorted cells were plated and SIV-Vpx and/or VSV-G-HIV-GFP added as described in Section 3.3.7. Following incubation, cells were fixed and stained as described in Section 3.3.7 to assess the infectability of LCs and dDC subsets in the presence and absence of SAMHD1 based on GFP expression.

3.4 Results and Discussion

3.4.1 Isolation of epidermal LCs and dDCs from skin

Preliminary work using enzymatic separation of the dermis and epidermis of full thickness human *ex vivo* skin was unsuccessful, with the dermis forming a gelatinous mass that could not be easily separated from the epidermis. Manual removal of excess dermis using surgical scissors was performed and allowed more efficient enzymatic separation but was extremely time-consuming, especially with larger skin samples. The inclusion of a dermatome in the protocol allowed rapid processing of large areas of skin to a consistent thickness. Lower skin thickness reduced the enzyme incubation time required and allowed easier separation of the dermis and epidermis. The 48-hour incubation time derived from the literature was adequate for the collection of migratory cells from the media in numbers suitable for downstream use.

Flow cytometric analysis of dermal walkout cells revealed that dDCs existed in a separate FSC-A/SSC-A region from T-cells and cell debris (Figure 3.3 A). Analysing the HLA-DR+/CD45+ cells from this region revealed the existence of three distinct subsets based on CD141 and CD11c expression (Figure 3.3 D). The mean proportions of each subset within the dDCs analysed (n=10) were: 17.3% CD11c+/CD141+ (SD: 8.4), 60.3% CD11c+/CD141- (SD: 7.8) and 21.6% CD11c-/CD141- (SD: 9.1). CD11c+/CD141+ dDCs also showed CD14 expression in line with the literature (Chu et al., 2012) (Figure 3.3 E).

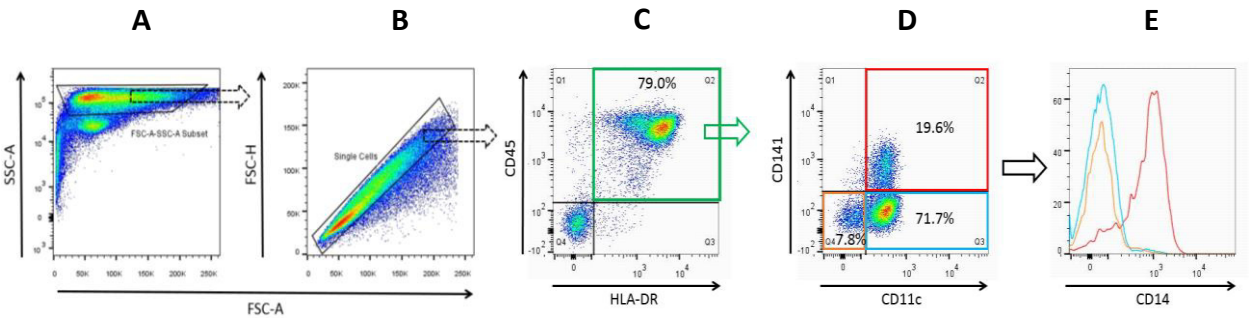

Figure 3.3: Gating strategy for migratory dermal cells. Gates: (A) exclude cell debris and T-cells (B) eliminate cell doublets (C) select total dDCs [CD45+/HLA-DR+] (D) distinguish between the three major dDC subsets [CD11c+/CD141+, CD11c+/CD141- and CD11c-/CD141-] and (E) confirm the CD14 expression within CD11c+/CD141+ dDCs only.

It had been previously reported that B-cells, T-cells and macrophages are also present in human skin (Haniffa et al., 2012, Geherin et al., 2012, McCully et al., 2012). For this reason, the lineage markers CD3, CD19, CD20 and CD56 were analysed in walkout cells. It was found that isolating dDCs based on FSC-A/SSC-A region and HLA-DR positivity was adequate to exclude these other cells and allow analysis of dDCs alone (Figure 3.4).

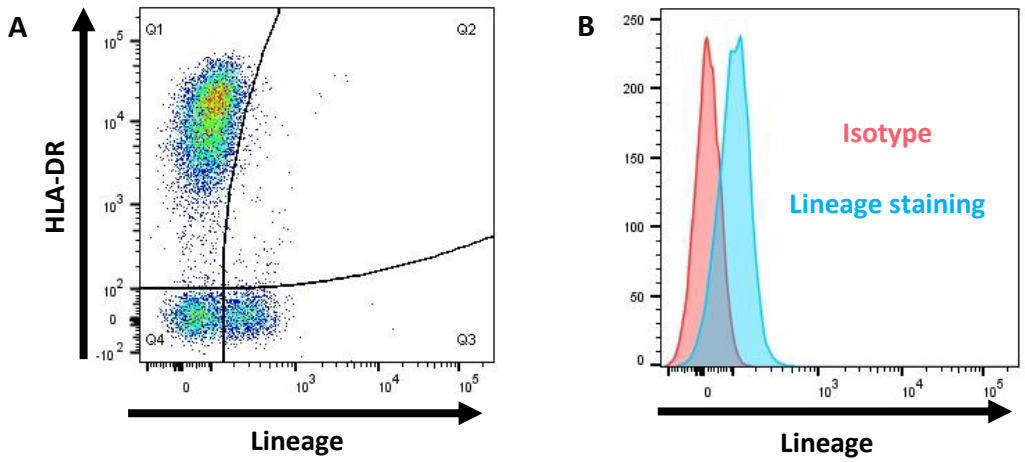

Figure 3.4: Lineage staining of cells in the dDC FSC-A/SSC-A region, showing that HLA-DR+ dDCs do not stain for lineage markers (A) and the shift in Lineage-FITC MFI compared to isotype due to increased concentration of antibodies leading to increased non-specific staining (B)

Phenotypically, LCs expressed HLA-DR, CD1a and CD207 (Langerin) (Figure 3.5) - the latter of which is a distinguishing marker of the cells from dDCs in human skin (Klechevsky et al., 2008a).

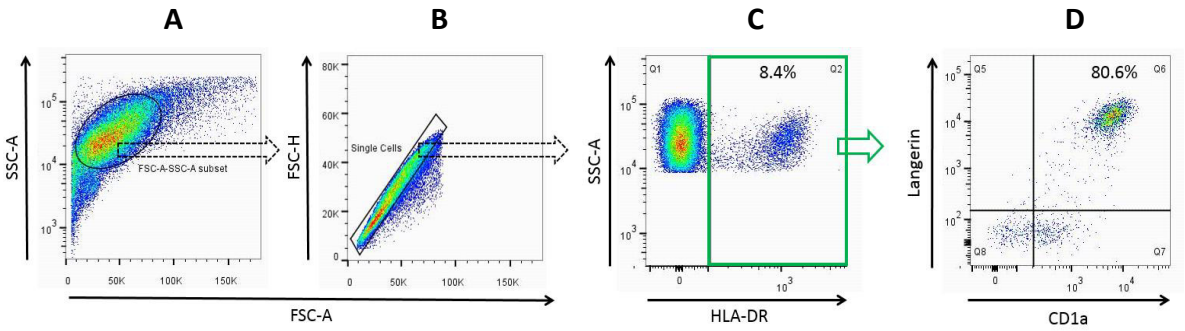

Figure 3.5: Gating strategy for migratory epidermal cells. Gates (A) eliminate cell debris (B) eliminate cell doublets (C) select HLA-DR+ cells present and (D) confirm the cells are LCs based on their CD1a/Langerin (CD207) double positivity.

Given that LCs migrate into the dermis to enter the dermal lymphatic vessels (Pearton et al., 2010b), it was likely that LCs would be found in dermal walkout cells. As Figure 3.6 shows, CD1a+/CD207+ cells made up a small fraction of the HLA-DR+ dermal walkout cells (less than 2% in the skin samples tested) and so do not represent a meaningful contamination of the dDCs in dermal walkout cells. Yields of epidermal LCs and dDCs varied with the size of the sample. The mean yield of LCs was over 5.25 x 10^5 cells per sample with values ranging from 4.5 x 10^4 to 3.06 x 10^6 across the samples tested (n=16). The mean yield of dDCs was greater than 1.23 x 10^6 per sample with values ranging from 1.81 x 10^5 to 4.98 x 10^6 (n=16). The purity of LCs amongst epidermal cells was typically lower than that of dDCs amongst dermal cells; 7.31% versus 34.11% respectively. This is most likely the result of a combination of connective dermal tissue

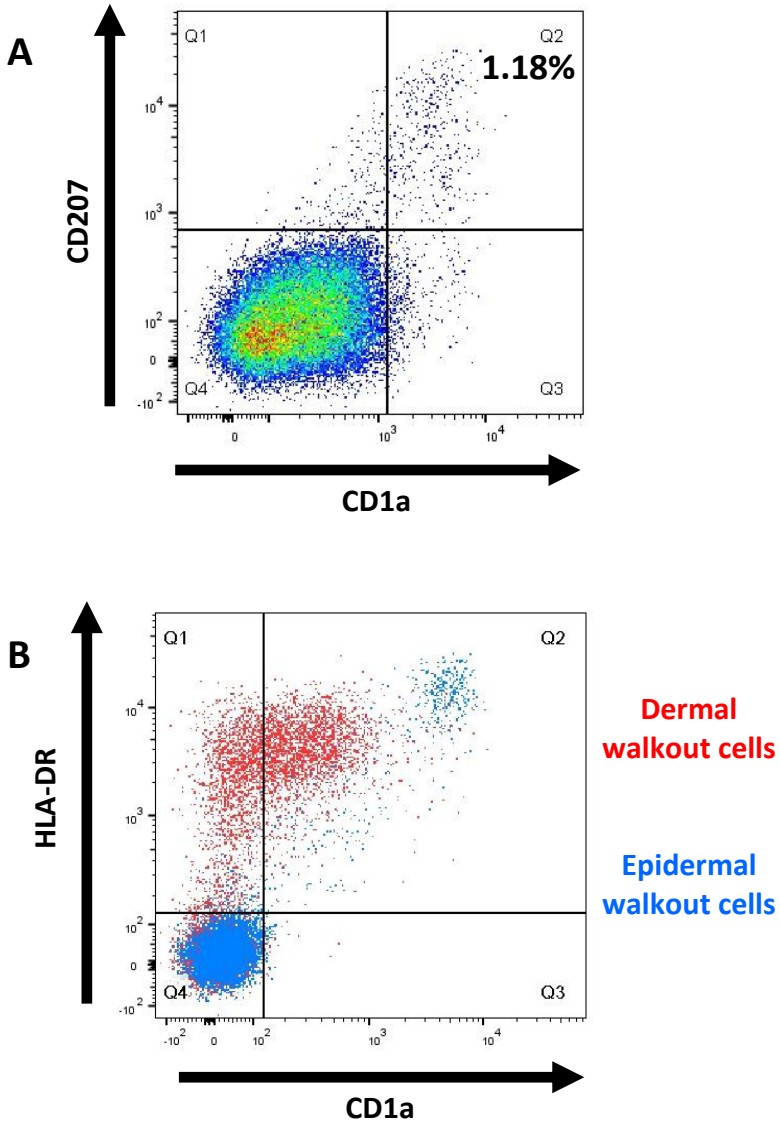

Figure 3.6: CD1a+/CD207+ LCs amongst dermal walkout cells (A) and the difference in HLA-DR and CD1a expression between dDCs and LCs amongst walkout cells from skin (B).

being more resistant to dispersion following enzyme treatment (thus not contaminating walkout cells), the motility of immature dDCs and the proliferative nature of epidermal stem cells leading to an increase in the proportion of non-immunological cells collected from the epidermis.

Cell viability was determined by fixable viability dye staining of walkout cells, with dead control cells and unstained cells allowing for validation (Figure 3.7). The viability of dermal walkout cells was consistently over 90%, while overall epidermal cell viability was much lower (below 50% in the samples tested).

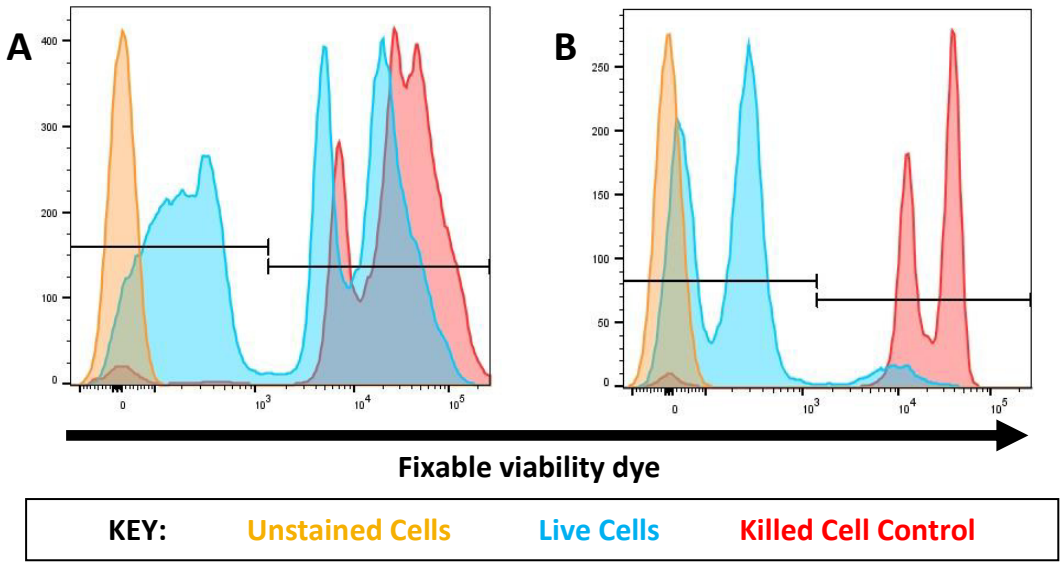

Figure 3.7: Cell viability staining of epidermal walkout cells (A) and dermal walkout cells (B)

Concurrent staining of walkout cells with antibodies alongside the fixable viability dye allowed the viability of the immune cells to be observed independently. The viability of the immune cells at over 95% in the samples tested was much higher than the mean values of the walkout cells (Figure 3.8). It is likely that amongst epidermal walkout cells a large amount of keratinocytes, which lose viability as they move towards the stratum corneum in natural turnover (Fore, 2006), formed the majority of the dead cells seen. Their non-migratory nature means they likely dissociated from the epidermis following enzymatic treatment. Dermal cells contained less contaminating cells, perhaps due to the gel-like state of the dermal tissue after enzyme exposure acting to better retain non-migratory cells. Thus it was concluded that although cell viability was generally poor amongst walkout cells, the immune cells appeared to be viable and therefore suitable for use in downstream experimentation.

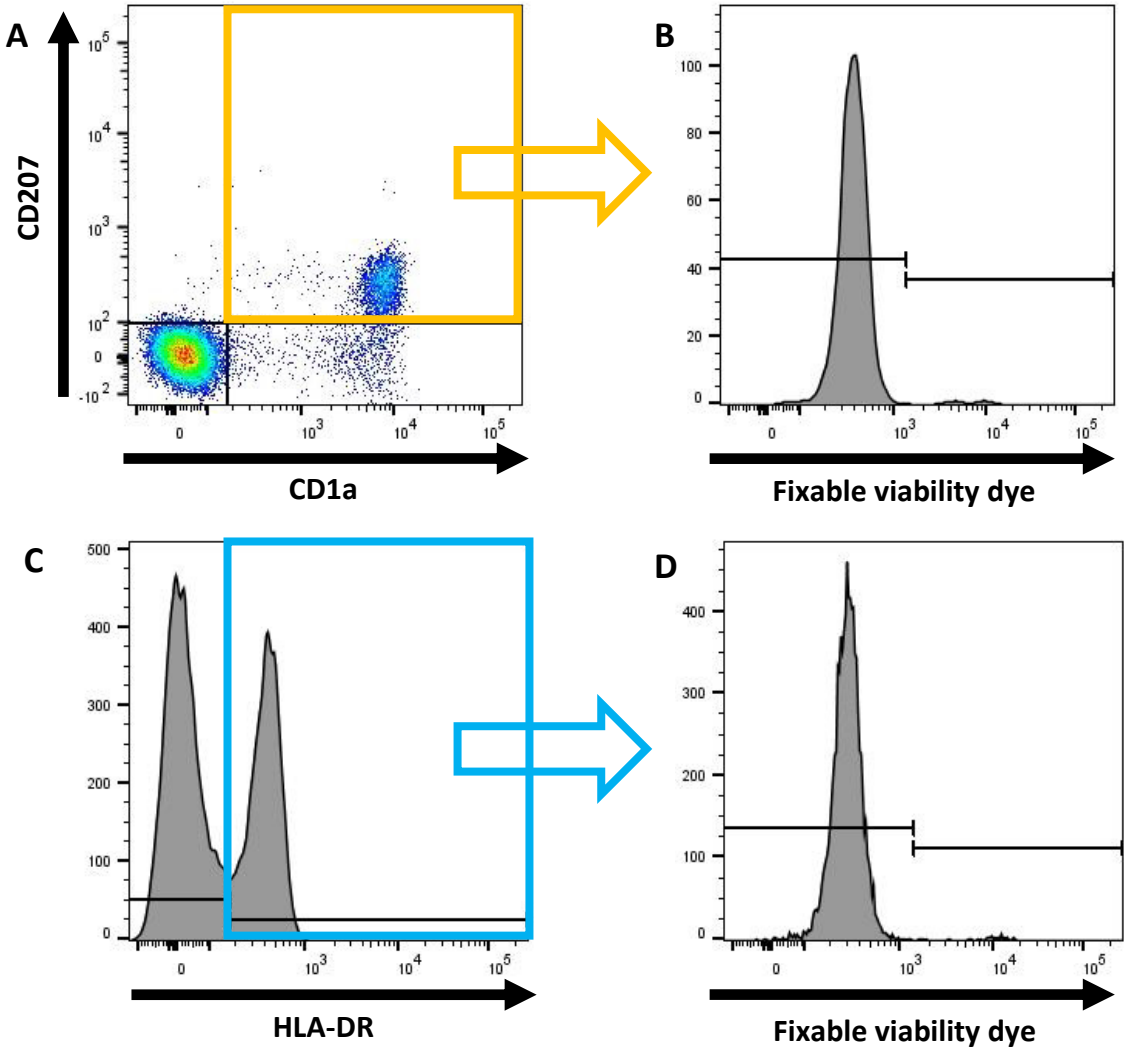

Figure 3.8: Viability of walkout immune cells. Plots show gating for LCs on CD207 [PE] and CD1a [FITC] (A) and dDCs on HLA-DR [PE] (C) and their viability by viability dye exclusion- 97.7% for LCs (B) and 98.7% for dDCs (D).

3.4.2 Characterisation of dermal T-cells

Flow cytometric analyses revealed that T-cells occupied a distinct FSC-A/SSC-A region proximal to the dDC FSC-A/SSC-A region (Figure 3.9 A) (Chu et al., 2012). Epidermal walkout cells did not show significant numbers of T-cells (Figure 3.9 C). The majority of cells (91%) in the T-cell region were CD3+ compared to only 2.2% in the dDC region confirming the location of the total T-cell population (Figure 3.10). Within the CD3+ T-cell population, CD4+ helper T-cells made up the majority of the cells. The ratio of CD4+:CD8+ T-cells obtained from the dermis varied between patients but was on average approximately 2:1. This is roughly equivalent to the ratio of T-cell populations that exists within the blood (McCully et al., 2012).

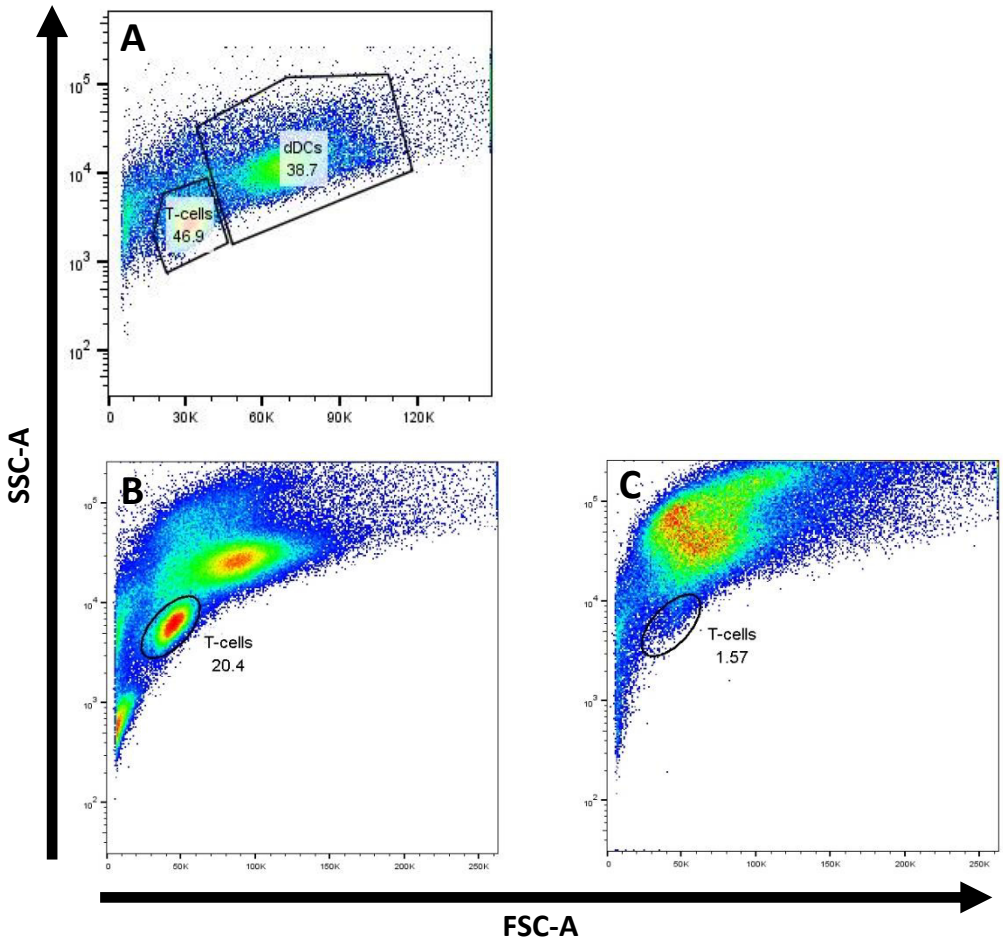

Figure 3.9: FSC-A/SSC-A regions occupied by T-cells and dDCs, the two major constituents of total dermal walkout cells (A). Proportion of cells found in the T-cell FSC-A/SSC-A region of dermal (B) and epidermal (C) walkout cells

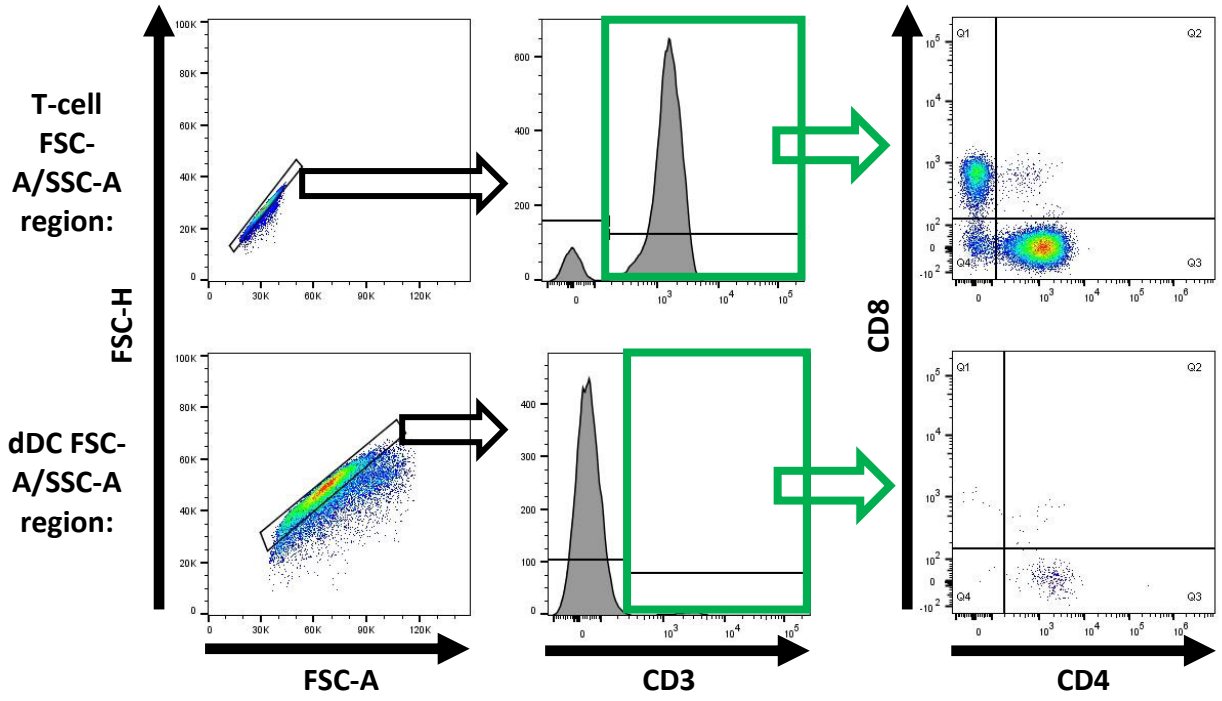

Figure 3.10: Staining of dermal walkout cells to characterise T-cells using PE anti-CD3, APC anti-CD4 and FITC anti-CD8 antibodies

3.4.3 Stimulation of Skin LCs and dDCs with TLR Agonists

Attempts to stimulate walkout dDCs and LCs with the TLR agonists LPS and poly(I:C) failed to elicit a meaningful upregulation of maturation marker CD83 with untreated cells already showing expression, suggesting walkout cells were already partly matured (Figure 3.11 A). There was also no distinguishable cytokine expression in TLR agonist-treated cells versus untreated controls (Figure 3.11 B). Thus, it was concluded that walkout cells exist in a partially-matured state and therefore are not responsive enough to stimuli to make the model a useful readout for immune stimuli.

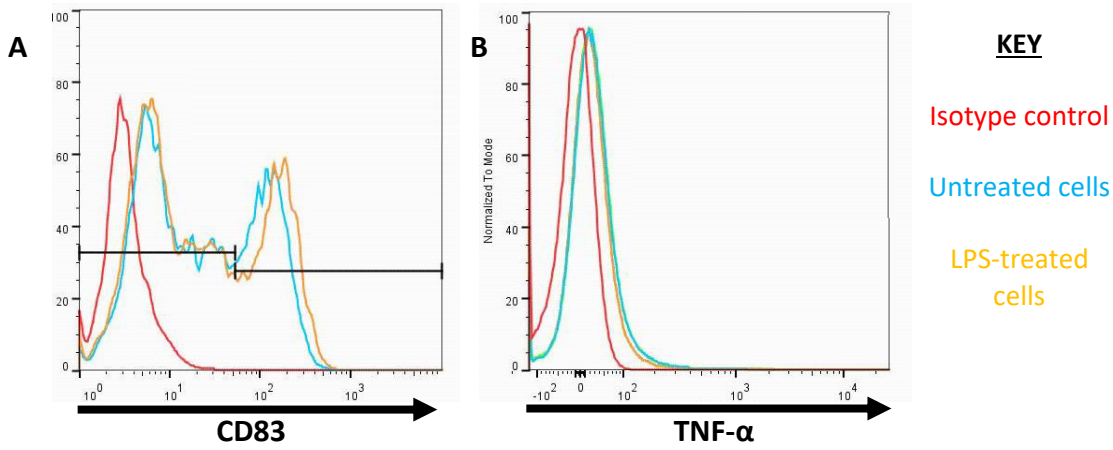

Figure 3.11: CD83 (A) and TNF-α/IL-12 (B) expression in dDCs treated with TLR agonists. LCs showed a similar lack of response to stimulation.

3.4.4 Knockdown of SAMHD1 in LCs/dDCs

Knockdown of SAMHD1 by exposing walkout cells to SIV-Vpx virus proved successful, with a reduction in the protein visible on western blot (Figure 3.12). Unlike SAMHD1 knockdown in mdDCs (as completed by a colleague), it was not possible to fully eliminate the antiviral factor. This may be due to viral uptake and SAMHD1 degradation being active processes, meaning dead or dying walkout cells will not show SAMHD1 knockdown. Thus, the Western blot shows a reduction rather than elimination in the levels of the protein in the cell population. This should not affect downstream investigations adversely as only the viable cells will be able to be integrate and express the GFP gene in the VSV-G-HIV-GFP lentiviral vector.

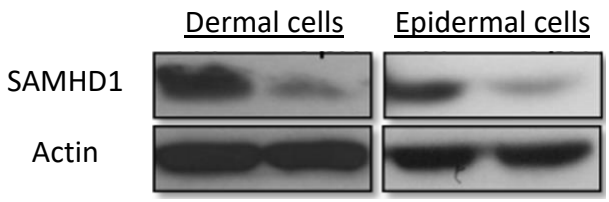

Figure 3.12: SAMHD1 knockdown in dermal and epidermal walkout cells from human ex vivo skin following incubation with SIV-Vpx virus

3.4.5 Infection of LCs/dDCs with VSV-G-HIV-GFP

Infection of primary skin LCs and dDCs with VSV-G-HIV-GFP alone showed low levels of GFP expression, mean values of 1.54% and 1.64% respectively (n = 4), which was not significantly different between the cell types. Following pre-treatment for 3 hours with Vpx-encoding SIV3, mean GFP expression rose to 3.99% in LCs and 14.04% in dDCs (Figure 3.13). The inherent variability in baseline and post-SAMHD1 knockdown infectability of dDCs from the skin samples used compromised the ability to detect statistically significant differences between the infection conditions Figure 3.14 A). LC baseline infectivity was more consistent between donors, with significant differences existing between control and infected cells with or without SIV3 ($p \leq 0.05$ in both cases). Eliminating the variability in baseline infectivity between donors by normalising the data to baseline infectivity (VSV-G-HIV-GFP infection without SIV3 pre-treatment) revealed the effect of SAMHD1 inhibition and revealed statistically significant differences in fold-change of infection between untreated cells, cells infected with VSV-G-HIV-GFP alone and those infected following SAMHD1 knockdown (Figure 3.14 B). Normalised data also confirmed the significant increase in infectability of dDCs over LCs (mean increases of 11.1- and 2.5-fold respectively; $p \leq 0.05$). This agreed with results in monocyte-derived dDC and LC equivalents and appears to suggest that LCs possess some extra post-entry

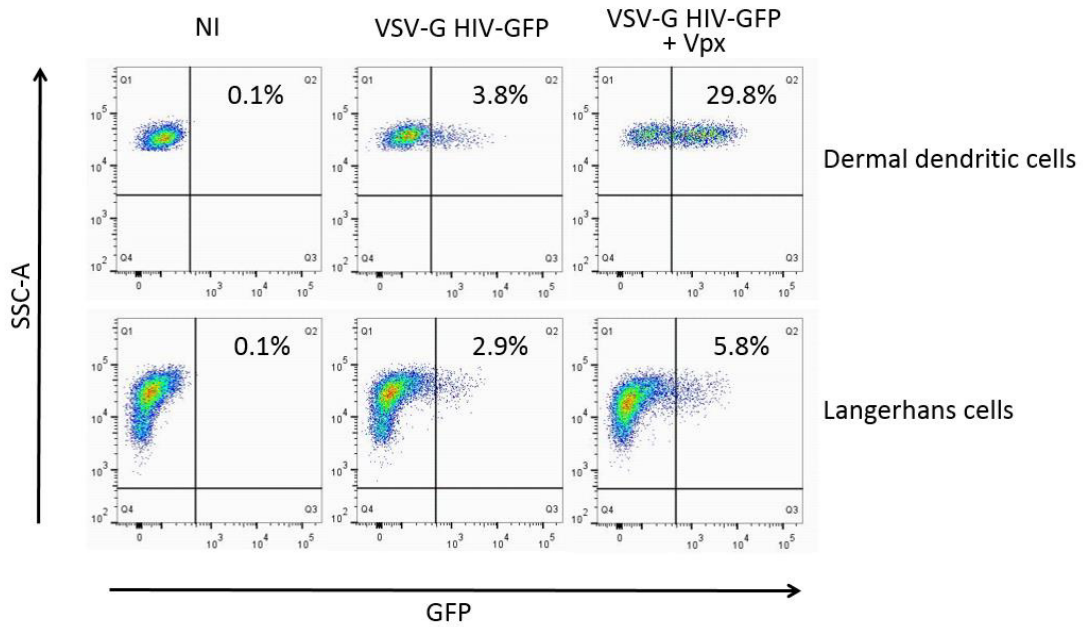

Figure 3.13: Flow cytometric plots from a single skin sample showing GFP expression in dDCs and LCs after infection with VSV-G-HIV-GFP ± SIV-Vpx .

viral restriction factor over dDCs that allow them to remain resistant to infection even after SAMHD1 degradation.

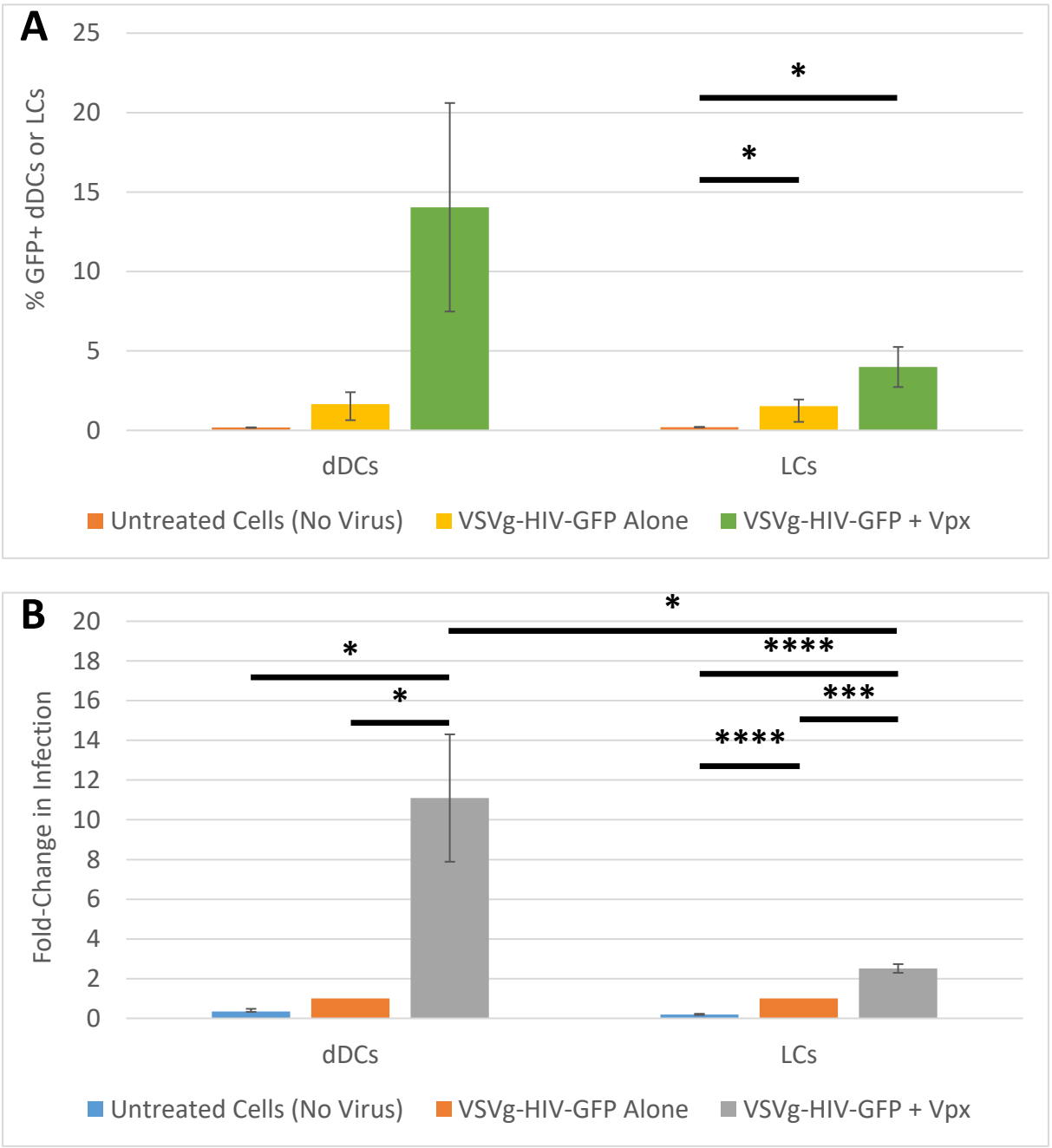

Figure 3.14: Infection of skin walkout immune cells by VSV-G-HIV-GFP with and without prior exposure to SIV-Vpx to knock down SAMHD1. Graphs present data as mean % GFP+ cells (A) and normalised within each skin sample to show fold-change in infection following SIV-Vpx pre-treatment (B). Error bars ± SD.

3.4.6 Sorting of LCs and dDCs from Skin

Sorting was attempted on walkout cells from two separate skin samples. The first skin sample was particularly large and yielded a high number of cells - 16.5 x 10^6 total dermal cells and 46 x 10^6 total epidermal cells. Antibody concentrations were reduced from the standard protocol by 50% to reduce the reagent usage of staining such large cell populations. As a result, the HLA-DR+/CD207+ population was less distinct than usual (Figure 3.15 A) - though the double positive population should still represent LCs. The staining of dDC subsets produced data in line with previous results despite the reduction antibody concentration (Figure 3.15 B). The quantitative data from the FACSAria cell sorter gave the figures for cells sorted listed in Table 3.6.

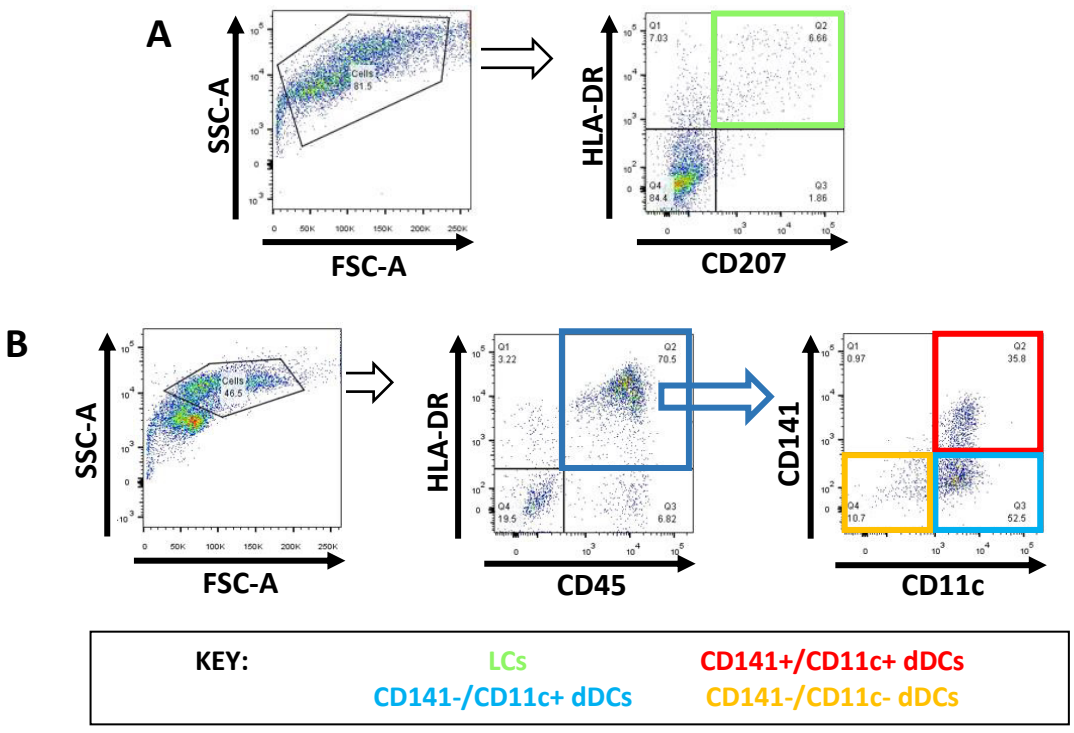

Figure 3.15: Phenotypic analysis of sorted epidermal migratory cells (A) and of dermal migratory cells (B)

Table 3.6: Skin walkout cell numbers sorted into dDC subset and LC populations

Cell Type	Sorted Cell Number (FACSAria Software Readout)
++ dDCs	9.5 x 10^5
+- dDCs	4.1 x 10^5
-- dDCs	1.8 x 10^6
LCs	3.0 x 10^5

The analysis of cells for GFP expression following the 5-day incubation post-sort is shown in Figure 3.16. The low levels of GFP expression with any treatment condition suggests the cells did not possess functionality after sorting. There were also fewer cells during analysis than expected based on readouts from the cell sorter. This led to unreliable data, with high levels of signal noise in untreated samples. As a result, there was no distinguishable difference in GFP expression between treated and untreated cells.

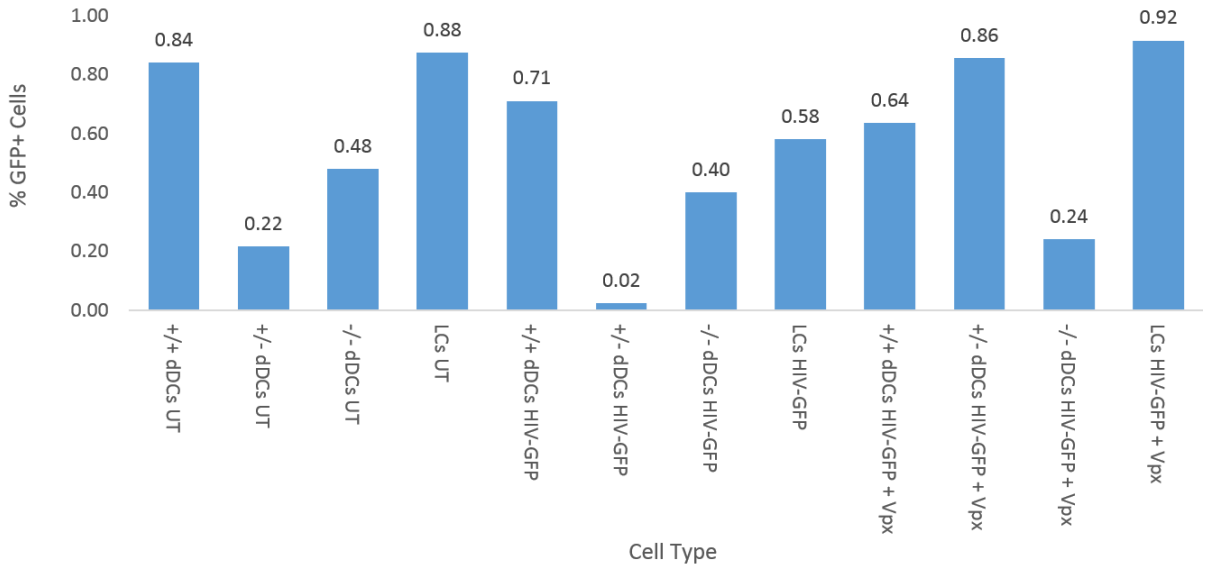

Figure 3.16: GFP-expressing cells amongst sorted dDC subsets and LCs from skin sample 324. Key: +/+ = CD11c+/CD141+ dDCs, +/- = CD11c+/CD141- dDCs and -/- = CD11c-/CD141- dDCs.

Given that the first attempt at sorting suffered practical setbacks, with a breakdown of the first choice cell sorter necessitating storage of cells on ice for an extended period of time (both of which might have adversely affected cell viability and functionality), a second skin sample was processed for cell sorting. The second skin sample was markedly smaller than the first and as a result the yield of total dermal (2.7 x 10^6) and epidermal (2.2 x 10^6) cells was lower. Staining was clearer, perhaps due to the lower cell number. LCs formed a distinct population that was 9.85% of the total epidermal cell events whilst dDCs accounted for 43.2% of the dermal cell events (Figure 3.17). Cell numbers from the second sample were assessed using a haemocytometer after sorting (Table 3.7). The cell numbers were too low for lentiviral vector infection of the cells was not feasible. Therefore, cell viability was utilised as an endpoint. Viability was measured 24 hours after sorting to allow any cells which had become apoptotic during sorting to progress to cell death and give a more accurate readout of cell viability.

Of all the cells, -- dDCs were the only sorted cell population with a viability over 10%. Thus, it was concluded that the large number of cells required and the poor viability after sorting meant that cell sorting was unsuitable for use in this investigation.

Table 3.7: Walkout cell numbers from ex vivo human skin at the various stages of cell sorting

Cell Type	Predicted Number (Subset Frequency x Pre-Sort Haemocytometer Count)	Sorted Cell Number (Software Readout)	Sorted Cell Number (Post-Sort Haemocytometer Count)
++ dDCs	1.8×10^5	8.3×10^4	3×10^4
+- dDCs	5.7×10^5	2.9×10^4	8×10^4
-- dDCs	2.2×10^4	8.4×10^3	No cells in countable area
LCs	1.1×10^5	7.6×10^4	2×10^4

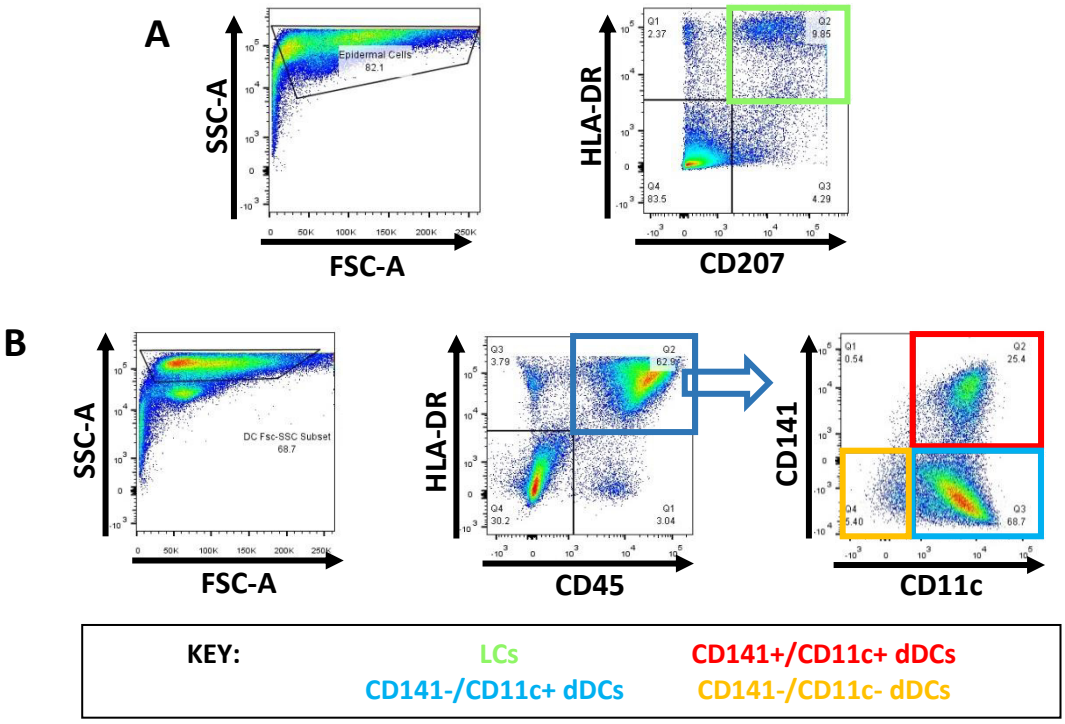

Figure 3.17: Phenotypic analysis of sorted epidermal migratory cells (A) and of dermal migratory cells (B) from second sorted skin sample

3.5 General Discussion

The human *ex vivo* skin immune cell model was developed to address some of the limitations of the full thickness skin model. The initial challenge was processing skin to separate dermis from epidermis, so that walkout cells from each could be used separately. The thickness of dermis on the skin samples when they are received impedes enzyme cocktail access to the basement membrane and so increases the incubation time required. The connective tissue of the dermis, which contains collagen fibrils, is also partly broken down by the enzyme cocktail (which contains collagenase) and forms a gelatinous substance, making separation from the epidermis more difficult after extended incubation periods in enzyme cocktail. The use of surgical scissors to remove excess lower dermis reduced the required incubation time, though increased processing time as skin needed to be divided into punch biopsies initially before trimming away the lower dermis. Given the limited time window of viability of *ex vivo* skin tissue and the fact that manual handling occurs at room temperature, any steps to reduce the processing time will benefit tissue (and downstream cell) viability.

The use of a dermatome to remove excess lower dermis allowed large areas of the skin to be processed more quickly than could be achieved using the previous biopsy punch method. This reduced the time that skin was out of media and thereby helped to maintain its viability. The reduced thickness of the skin after the dermatome was used also helped to minimise enzyme incubation time, protecting the structural integrity of the dermis and epidermis and reducing the contamination from non-migratory cells in the walkout media. The differences in purity observed between cells from the dermis and epidermis is most likely the result of a combination of connective dermal tissue being more resistant to dispersion following enzyme treatment (limiting non-dDC presence in the walkout media) and the proliferative nature of epidermal stem cells which fall out of the epidermal tissue leading to an increase in the proportion of non-immunological cells collected from the epidermis.

It was possible to collect walkout cells from both the epidermis and dermis. Phenotypically, LCs were straightforward to characterise given their HLA-DR/CD1a/CD207 triple positivity, which is unique amongst skin cells (Klechevsky et al., 2008a). Though dDCs have been reported to probe the epidermis (Rattanapak et al.,

2014), they do not migrate into it and so LCs are the lone HLA-DR+ cell type present in the upper layer of skin, confirmed by CD207 expression. Identifying dDCs was more challenging, given their diverse subsets.

The ability to separate dDCs from dermal T-cells by their size/granularity (quantified as FSC-A and SSC-A respectively) proved advantageous in analysing dDCs. They could then be gated specifically based on their HLA-DR/CD45 double positivity (dermal T-cells are CD45+/HLA-DR- (Koretzky et al., 1990)). This then allowed the total dDC population to be analysed for the various subset markers. Subset classification varies by group along with the method used to isolate the dDCs, some groups lyse the dermis completely (Haniffa et al., 2012) whilst others perform a walkout similar to the one described (Chu et al., 2012). The lysis protocol means that all cells from the dermis are present, whether migratory or not. This leads to a lower purity of dDCs. Also, it allows for the analysis of other skin-resident cells, such as macrophages, which do not spontaneously migrate from dermal tissue (Haniffa et al., 2009). It has also been reported that macrophages are adherent cells (Haniffa et al., 2009), so will not be collected during the harvesting of walkout media, where the plate is only gently washed to collect non-adherent dDCs. The walkout protocol produced two major cell populations, dDCs and dermal T-cells, as confirmed by lineage marker staining. The gating strategy used to classify dDC subsets was adapated from the work of the Nestle lab, due to the similar protocols used in obtaining cells from the dermis. Their work identified CD141+ dDCs as a cell type of particular interest (Chu et al., 2012) and so it was important that this subset could be reliably identified.

The frequency of T-cells amongst migratory dermal cells were in line with those observed by Bernhard Moser's group, who utilise a comparable isolation protocol (frequencies around 30% are routine) (McCully et al., 2012). Their work also normally obtains CD4:CD8 ratios like those in blood (a ratio of 2:1 CD4:CD8 exists in average blood samples). The usefulness of these cells, given their broad antigen-specificity as a population, is limited in intradermal injection studies (as a very small proportion will be responsive to any given antigen, making assays less robust) (Murphy et al., 2012). It is however useful data in the characterisation of the overall *ex vivo* skin cell model obtained using this protocol. A number of studies reported using skin T-cells (Clark et

al., 2006, Watanabe et al., 2015), so it could also represent an interesting avenue for future work.

Overall cell viability in walkout cells was found to be much lower in the epidermis than the dermis, less than 50% versus more than 90% respectively. Further analysis of the cells, however, revealed that both LC and dDC viabilities were consistently over 95% and that the contaminating cells (e.g. keratinocytes from the epidermis and fibroblasts from the dermis) were responsible for the vast majority of dead cells. As well as being viable, it was also necessary to characterise the functionality of LCs and dDCs obtained from skin. Attempted stimulation proved fruitless, with both sets of immune cells exhibiting partial maturation at the time of collection, which meant further stimulation with LPS or poly(I:C) was difficult. The small increases in CD83+ cell population and CD83 median fluorescence intensity (MFI) when exposed to potent TLR agonists highlighted the lack of robustness in the model for this use. It is possible that the use of bacterially-derived enzymes in the enzyme cocktail, which will likely be recognised as foreign antigen, may lead to this activation of the immune cells in skin. The tissue damage during patient surgery and dermatome processing of skin may also release damage-associated molecular patterns (DAMPs) which can mature DCs (Bianchi, 2007). Other separation methods that have been published tend to expose the skin to harsh thermal (60°C water) (Kligman and Christophers, 1963) or chemical (ammonium thiocyanate) (Pearton et al., 2010c) conditions which would likely drastically affect the viability of cells so do not represent usable alternatives.

The functionality of the cells was therefore assessed in a different manner. The recent results from a colleague within the group utilising monocyte-derived DC models to test lentiviral vector HIV models provided a unique opportunity for model validation. The work confirmed that both skin LCs and dDCs remained functional as well as viable, expressing the GFP gene following infection with the lentiviral vector. It was not expected that the cells would retain viability to the end of the 5-day infection period but the persistence of GFP within the cells following cell death allowed for the analysis of infection rates regardless. The overall infectivity levels witnessed were lower than in monocyte-derived models, potentially due to the improved viability of blood-derived cells or due to the partial maturity of *ex vivo* skin immunological cells reducing their infectability. The pattern of infectability between primary cells and the equivalent

models was consistent though, thus prompting the conclusion that LCs possess an extra antiviral factor over dDCs. Work to identify this factor is ongoing.

Analysis of the infection rates in the various dDC subsets proved to be difficult due to the down-regulation of subset markers CD11c and CD141 during cell culture. There appeared to be a greater increase in infectability following degradation of SAMHD1 in CD11c+/CD141+ dDCs than in the other two subsets, though this could not be confirmed with any reliability. The most feasible solution to this subset identification problem was sorting of the dDCs into their subsets prior to infection with VSV-G-HIV-GFP, eliminating doubt of the subsets present at time of analysis.

Attempted infection of sorted skin cells with VSV-G-HIV-GFP revealed that cell functionality was greatly reduced by the sorting process and that sorted cells were not usable for this experiment. There were discrepancies between the sorted cell number recorded by the sorting software and the cell number quantified by haemocytometer count, highlighting the cell loss that occurs during sorting. The results also showed an inversely proportional relationship between dDC subset frequency and cell viability. Given that each subset was sorted into the same volume of media, this might suggest that the tubes receiving more cell-containing droplets accumulate levels of sheath fluid that adversely affect cell viability (as it contains sodium azide). To eliminate this possibility, larger vessels containing a greater volume of media will be used to collect cells in future. It was also apparent that cell viability was poor 24 hours after sorting, the extra stresses placed on LCs and dDCs in staining and sorting meaning that a large proportion of cells are dead after 24 hours in culture post-sort. Optimisation of sorting conditions is clearly required and it is likely that even under optimal conditions, cells may only have a brief period of usability. This would make them unusable for studies that require extended culture and cell activity such as the lentiviral vector studies but could still allow them to be useful in antigen presentation experiments where less than 24 hours of cell functionality is required. Future work will explore the model to assess the antigen processing capacity of the skin cells. If sorting is possible in these experiments, it will allow for the comparison of dDC subsets against LCs, properties of skin immune cells that are not currently understood.

3.6 Potential for Publication

The isolation of dDCs and LCs from *ex vivo* human skin, knockdown of SAMHD1 using SIV-Vpx virus and subsequent infection of these cells has been published already (Czubala et al., 2016). The quantitative data regarding dDC subsets found in this and subsequent studies may be publishable if enough repeats are obtained to allow comparison of subset frequencies to factors such as patient age. The identification of dermal T-cells amongst walkout skin cells has been published previously so would require further development to allow publication- perhaps with downstream experimentation looking at responses of skin-resident T-cells to immunostimulatory substrates.

3.7 Conclusion

The work in this chapter achieved its primary objective of producing a protocol for obtaining immune cells from *ex vivo* human skin samples. The LCs and dDCs could then be characterised by flow cytometry, revealing a phenotype in line with previously published work in the field (Chu et al., 2012, Haniffa et al., 2012). It was also possible to divide the dDCs into subsets based on CD11c and CD141 expression. The dDC subset proportions found were also consistent with the literature. Two potential uses for the model were explored- a TLR agonist stimulation assay and a HIV lentiviral vector study. Whilst the former generated little success, with the cells being partially matured at the time of collection and difficult to stimulate further, the latter proved to be an appropriate use for the model. It was possible to provide supporting data for results obtained in monocyte-derived DC models, increasing the reliability of the conclusions drawn from the work and leading to a publication (Czubala et al., 2016). The next step will be to assess the potential use of the *ex vivo* skin cell model to study the processing of vaccine by skin-resident immune cells, with the aim of informing intradermal vaccine design and delivery strategies at a cellular level.

3.7 Bibliography

ADEREM, A. & ULEVITCH, R. J. 2000. Toll-like receptors in the induction of the innate immune response. *Nature,* 406**,** 782-7.

AIKEN, C. 1997. Pseudotyping human immunodeficiency virus type 1 (HIV-1) by the glycoprotein of vesicular stomatitis virus targets HIV-1 entry to an endocytic pathway and suppresses both the requirement for Nef and the sensitivity to cyclosporin A. *J Virol,* 71**,** 5871-7.

ALBERTINI AÉ, A. V., BAQUERO, E., FERLIN, A. & GAUDIN, Y. 2012. Molecular and Cellular Aspects of Rhabdovirus Entry. *Viruses.*

ALDROVANDI, G. M., FEUER, G., GAO, L., JAMIESON, B., KRISTEVA, M., CHEN, I. S. & ZACK, J. A. 1993. The SCID-hu mouse as a model for HIV-1 infection. *Nature,* 363**,** 732-6.

AUEWARAKUL, P., PAUNGCHAROEN, V., LOUISIRIROTCHANAKUL, S. & WASI, C. 2001. Application of HIV-1-green fluorescent protein (GFP) reporter viruses in neutralizing antibody assays. *Asian Pac J Allergy Immunol,* 19**,** 139-44.

BANCHEREAU, J. & STEINMAN, R. M. 1998. Dendritic cells and the control of immunity. *Nature,* 392**,** 245-252.

BAUMGARTH, N. & ROEDERER, M. 2000. A practical approach to multicolor flow cytometry for immunophenotyping. *Journal of Immunological Methods,* 243**,** 77-97.

BERGES, B. K., WHEAT, W. H., PALMER, B. E., CONNICK, E. & AKKINA, R. 2006. HIV-1 infection and CD4 T cell depletion in the humanized Rag2(-/-)γc(-/-)(RAG-hu) mouse model. *Retrovirology,* 3**,** 76-76.

BEUTLER, B. 2000. Tlr4: central component of the sole mammalian LPS sensor. *Current Opinion in Immunology,* 12**,** 20-26.

BIANCHI, M. E. 2007. DAMPs, PAMPs and alarmins: all we need to know about danger. *J Leukoc Biol,* 81**,** 1-5.

BIGLEY, V., MCGOVERN, N., MILNE, P., DICKINSON, R., PAGAN, S., COOKSON, S., HANIFFA, M. & COLLIN, M. 2015. Langerin-expressing dendritic cells in human tissues are related to CD1c+ dendritic cells and distinct from Langerhans cells and CD141high XCR1+ dendritic cells. *J Leukoc Biol,* 97**,** 627-34.

CHATTOPADHYAY, P. K., PRICE, D. A., HARPER, T. F., BETTS, M. R., YU, J., GOSTICK, E., PERFETTO, S. P., GOEPFERT, P., KOUP, R. A., DE ROSA, S. C., BRUCHEZ, M. P. & ROEDERER, M. 2006. Quantum dot semiconductor nanocrystals for

immunophenotyping by polychromatic flow cytometry. *Nat Med,* 12**,** 972-7.

CHEN, R., LOWE, L., WILSON, J. D., CROWTHER, E., TZEGGAI, K., BISHOP, J. E. & VARRO, R. 1999. Simultaneous Quantification of Six Human Cytokines in a Single Sample Using Microparticle-based Flow Cytometric Technology. *Clin Chem,* 45**,** 1693-1694.

CHU, C. C., ALI, N., KARAGIANNIS, P., DI MEGLIO, P., SKOWERA, A., NAPOLITANO, L., BARINAGA, G., GRYS, K., SHARIF-PAGHALEH, E., KARAGIANNIS, S. N., PEAKMAN, M., LOMBARDI, G. & NESTLE, F. O. 2012. Resident CD141 (BDCA3)+ dendritic cells in human skin produce IL-10 and induce regulatory T cells that suppress skin inflammation. *J Exp Med,* 209**,** 935-45.

CZUBALA, M. A., FINSTERBUSCH, K., IVORY, M. O., MITCHELL, J. P., AHMED, Z., SHIMAUCHI, T., KAROO, R. O., COULMAN, S. A., GATELEY, C., BIRCHALL, J. C., BLANCHET, F. P. & PIGUET, V. 2016. TGFbeta Induces a SAMHD1-independent Post-Entry Restriction to HIV-1 Infection of Human Epithelial Langerhans Cells. *J Invest Dermatol*.

DA COSTA, X. J., BROCKMAN, M. A., ALICOT, E., MA, M., FISCHER, M. B., ZHOU, X., KNIPE, D. M. & CARROLL, M. C. 1999. Humoral response to herpes simplex virus is complement-dependent. *Proc Natl Acad Sci U S A,* 96**,** 12708-12.

DE WITTE, L., NABATOV, A., PION, M., FLUITSMA, D., DE JONG, M. A., DE GRUIJL, T., PIGUET, V., VAN KOOYK, Y. & GEIJTENBEEK, T. B. 2007. Langerin is a natural barrier to HIV-1 transmission by Langerhans cells. *Nat Med,* 13**,** 367-71.

DUDZIAK, D., KAMPHORST, A. O., HEIDKAMP, G. F., BUCHHOLZ, V. R., TRUMPFHELLER, C., YAMAZAKI, S., CHEONG, C., LIU, K., LEE, H.-W. & PARK, C. G. 2007. Differential antigen processing by dendritic cell subsets in vivo. *Science,* 315**,** 107-111.

DURAES, F. V., CARVALHO, N. B., MELO, T. T., OLIVEIRA, S. C. & FONSECA, C. T. 2009. IL-12 and TNF-alpha production by dendritic cells stimulated with Schistosoma mansoni schistosomula tegument is TLR4- and MyD88-dependent. *Immunol Lett,* 125**,** 72-7.

FINKELSHTEIN, D., WERMAN, A., NOVICK, D., BARAK, S. & RUBINSTEIN, M. 2013. LDL receptor and its family members serve as the cellular receptors for vesicular stomatitis virus. *Proc Natl Acad Sci U S A,* 110**,** 7306-11.

FORE, J. 2006. A review of skin and the effects of aging on skin structure and function. *Ostomy Wound Manage,* 52**,** 24-35; quiz 36-7.

FOSTER, B., PRUSSIN, C., LIU, F., WHITMIRE, J. K. & WHITTON, J. L. 2007. Detection of intracellular cytokines by flow cytometry. *Curr Protoc Immunol,* Chapter 6**,** Unit 6.24.

GANGLOFF, S. C., HIJIYA, N., HAZIOT, A. & GOYERT, S. M. 1999. Lipopolysaccharide structure influences the macrophage response via CD14-independent and CD14-dependent pathways. *Clin Infect Dis,* 28**,** 491-6.

GEHERIN, S. A., FINTUSHEL, S. R., LEE, M. H., WILSON, R. P., PATEL, R. T., ALT, C., YOUNG, A. J., HAY, J. B. & DEBES, G. F. 2012. The skin, a novel niche for recirculating B cells. *J Immunol,* 188**,** 6027-35.

GODDARD, S., YOUSTER, J., MORGAN, E. & ADAMS, D. H. 2004. Interleukin-10 secretion differentiates dendritic cells from human liver and skin. *Am J Pathol,* 164**,** 511-9.

GOODMAN, S. & CHECK, E. 2002. The great primate debate. *Nature.* England.

GOUJON, C., RIVIERE, L., JARROSSON-WUILLEME, L., BERNAUD, J., RIGAL, D., DARLIX, J. L. & CIMARELLI, A. 2007. SIVSM/HIV-2 Vpx proteins promote retroviral escape from a proteasome-dependent restriction pathway present in human dendritic cells. *Retrovirology,* 4**,** 2.

GOUWS, E., WHITE, P. J., STOVER, J. & BROWN, T. 2006. Short term estimates of adult HIV incidence by mode of transmission: Kenya and Thailand as examples. *Sex Transm Infect,* 82 Suppl 3**,** iii51-55.

HANIFFA, M., GINHOUX, F., WANG, X. N., BIGLEY, V., ABEL, M., DIMMICK, I., BULLOCK, S., GRISOTTO, M., BOOTH, T., TAUB, P., HILKENS, C., MERAD, M. & COLLIN, M. 2009. Differential rates of replacement of human dermal dendritic cells and macrophages during hematopoietic stem cell transplantation. *J Exp Med,* 206**,** 371-85.

HANIFFA, M., SHIN, A., BIGLEY, V., MCGOVERN, N., TEO, P., SEE, P., WASAN, P. S., WANG, X. N., MALINARICH, F., MALLERET, B., LARBI, A., TAN, P., ZHAO, H., POIDINGER, M., PAGAN, S., COOKSON, S., DICKINSON, R., DIMMICK, I., JARRETT, R. F., RENIA, L., TAM, J., SONG, C., CONNOLLY, J., CHAN, J. K., GEHRING, A., BERTOLETTI, A., COLLIN, M. & GINHOUX, F. 2012. Human tissues contain CD141hi cross-presenting dendritic cells with functional homology to mouse CD103+ nonlymphoid dendritic cells. *Immunity,* 37**,** 60-73.

HATZIIOANNOU, T. & EVANS, D. T. 2012. Animal models for HIV/AIDS research. *Nat Rev Microbiol,* 10**,** 852-67.

HENTZER, B. & KOBAYASI, T. 1978. Enzymatic liberation of viable cells of human skin. *Acta Derm Venereol,* 58**,** 197-202.

HERZENBERG, L. A., PARKS, D., SAHAF, B., PEREZ, O. & ROEDERER, M. 2002. The history and future of the fluorescence activated cell sorter and flow cytometry: a view from Stanford. *Clin Chem,* 48**,** 1819-27.

HRECKA, K., HAO, C., GIERSZEWSKA, M., SWANSON, S. K., KESIK-BRODACKA, M., SRIVASTAVA, S., FLORENS, L., WASHBURN, M. P. & SKOWRONSKI, J. 2011. Vpx relieves inhibition of HIV-1 infection of macrophages mediated by the SAMHD1 protein. *Nature,* 474**,** 658-61.

ICHINOHE, T., WATANABE, I., ITO, S., FUJII, H., MORIYAMA, M., TAMURA, S., TAKAHASHI, H., SAWA, H., CHIBA, J., KURATA, T., SATA, T. & HASEGAWA, H. 2005. Synthetic double-stranded RNA poly(I:C) combined with mucosal vaccine protects against influenza virus infection. *J Virol,* 79**,** 2910-9.

JENSEN, E. C. 2012. Types of imaging, Part 2: an overview of fluorescence microscopy. *Anat Rec (Hoboken),* 295**,** 1621-7.

JI, X., TANG, C., ZHAO, Q., WANG, W. & XIONG, Y. 2014. Structural basis of cellular dNTP regulation by SAMHD1. *Proc Natl Acad Sci U S A,* 111**,** E4305-14.

JOHNSTON, M. I. & FAUCI, A. S. 2008. An HIV vaccine--challenges and prospects. *N Engl J Med,* 359**,** 888-90.

KENNEY, R. T., FRECH, S. A., MUENZ, L. R., VILLAR, C. P. & GLENN, G. M. 2004. Dose sparing with intradermal injection of influenza vaccine. *N Engl J Med,* 351**,** 2295-301.

KING, M. A. 2000. Detection of dead cells and measurement of cell killing by flow cytometry. *Journal of Immunological Methods,* 243**,** 155-166.

KLECHEVSKY, E., MORITA, R., LIU, M., CAO, Y., COQUERY, S., THOMPSON-SNIPES, L., BRIERE, F., CHAUSSABEL, D., ZURAWSKI, G., PALUCKA, A. K., REITER, Y., BANCHEREAU, J. & UENO, H. 2008. Functional specializations of human epidermal Langerhans cells and CD14+ dermal dendritic cells. *Immunity,* 29**,** 497-510.

KLIGMAN, A. M. & CHRISTOPHERS, E. 1963. PREPARATION OF ISOLATED SHEETS OF HUMAN STRATUM CORNEUM. *Arch Dermatol,* 88**,** 702-5.

KORETZKY, G. A., PICUS, J., THOMAS, M. L. & WEISS, A. 1990. Tyrosine phosphatase CD45 is essential for coupling T-cell antigen receptor to the phosphatidyl inositol pathway. *Nature,* 346**,** 66-8.

LAGUETTE, N., SOBHIAN, B., CASARTELLI, N., RINGEARD, M., CHABLE-BESSIA, C., SEGERAL, E., YATIM, A., EMILIANI, S., SCHWARTZ, O. & BENKIRANE, M. 2011. SAMHD1 is the dendritic- and myeloid-cell-specific HIV-1 restriction factor counteracted by Vpx. *Nature,* 474**,** 654-7.

LARSEN, C. P., STEINMAN, R. M., WITMER-PACK, M., HANKINS, D. F., MORRIS, P. J. & AUSTYN, J. M. 1990. Migration and maturation of Langerhans cells in skin transplants and explants. *J Exp Med,* 172**,** 1483-93.

LEE, H.-K., DUNZENDORFER, S., SOLDAU, K. & TOBIAS, P. S. 2006. Double-Stranded RNA-Mediated TLR3 Activation Is Enhanced by CD14. *Immunity,* 24**,** 153-163.

LI, N., ZHANG, W. & CAO, X. 2000. Identification of human homologue of mouse IFN-gamma induced protein from human dendritic cells. *Immunol Lett,* 74**,** 221-4.

LICHTMAN, J. W. & CONCHELLO, J.-A. 2005. Fluorescence microscopy. *Nature methods,* 2**,** 910-919.

LINDBACK, S., BROSTROM, C., KARLSSON, A. & GAINES, H. 1994. Does symptomatic primary HIV-1 infection accelerate progression to CDC stage IV disease, CD4 count below 200× 106/l, AIDS, and death from AIDS? *Bmj,* 309**,** 1535-1537.

LU, Y.-C., YEH, W.-C. & OHASHI, P. S. 2008. LPS/TLR4 signal transduction pathway. *Cytokine,* 42**,** 145-151.

MAECKER, H. T. & TROTTER, J. 2006. Flow cytometry controls, instrument setup, and the determination of positivity. *Cytometry A,* 69**,** 1037-42.

MCCULLY, M. L., LADELL, K., HAKOBYAN, S., MANSEL, R. E., PRICE, D. A. & MOSER, B. 2012. Epidermis instructs skin homing receptor expression in human T cells. *Blood,* 120**,** 4591-8.

MEDZHITOV, R. 2001. Toll-like receptors and innate immunity. *Nat Rev Immunol,* 1**,** 135-45.

MELBY, E. C. & ALTMAN, N. H. 1974. *Handbook of laboratory animal science. Volume 2*, CRC Press Inc.

MILLER, C. J. & SHATTOCK, R. J. 2003. Target cells in vaginal HIV transmission. *Microbes and Infection,* 5**,** 59-67.

MURPHY, K., TRAVERS, P., WALPORT, M. & JANEWAY, C. 2012. *Janeway's Immunobiology (8th ed.),* New York, Garland Science.

NEGRE, D., MANGEOT, P. E., DUISIT, G., BLANCHARD, S., VIDALAIN, P. O., LEISSNER, P., WINTER, A. J., RABOURDIN-COMBE, C., MEHTALI, M., MOULLIER, P., DARLIX, J. L. & COSSET, F. L. 2000. Characterization of novel safe lentiviral vectors derived from simian immunodeficiency virus (SIVmac251) that efficiently transduce mature human dendritic cells. *Gene Ther,* 7**,** 1613-23.

NESTLE, F. O., ZHENG, X. G., THOMPSON, C. B., TURKA, L. A. & NICKOLOFF, B. J. 1993. Characterization of dermal dendritic cells obtained from normal human skin reveals phenotypic and functionally distinctive subsets. *J Immunol,* 151**,** 6535-45.

PAULS, E., BALLANA, E. & ESTÉ, J. A. 2013. Nucleotide embargo by SAMHD1: A strategy to block retroviral infection. *Antiviral Research,* 97**,** 180-182.

PEARTON, M., KANG, S.-M., SONG, J.-M., ANSTEY, A. V., IVORY, M., COMPANS, R. W. & BIRCHALL, J. C. 2010a. Changes in Human Langerhans Cells Following Intradermal Injection of Influenza Virus-Like Particle Vaccines. *PLoS ONE,* 5**,** e12410.

PEARTON, M., KANG, S.-M., SONG, J.-M., KIM, Y.-C., QUAN, F.-S., ANSTEY, A., IVORY, M., PRAUSNITZ, M. R., COMPANS, R. W. & BIRCHALL, J. C. 2010b. Influenza Virus-Like Particles coated onto microneedles can elicit stimulatory effects on Langerhans cells in human skin. *Vaccine,* 28**,** 6104-6113.

PENA-CRUZ, V., ITO, S., OUKKA, M., YONEDA, K., DASCHER, C. C., VON LICHTENBERG, F. & SUGITA, M. 2001. Extraction of human Langerhans cells: a method for isolation of epidermis-resident dendritic cells. *J Immunol Methods,* 255**,** 83-91.

PERRIN, L., KAISER, L. & YERLY, S. 2003. Travel and the spread of HIV-1 genetic variants. *Lancet Infect Dis,* 3**,** 22-7.

POLLARD, V. W. & MALIM, M. H. 1998. The HIV-1 Rev protein. *Annu Rev Microbiol,* 52**,** 491-532.

QUIROZ, E., MORENO, N., PERALTA, P. H. & TESH, R. B. 1988. A human case of encephalitis associated with vesicular stomatitis virus (Indiana serotype) infection. *Am J Trop Med Hyg,* 39**,** 312-4.

RATTANAPAK, T., BIRCHALL, J. C., YOUNG, K., KUBO, A., FUJIMORI, S., ISHII, M. & HOOK, S. 2014. Dynamic visualization of dendritic cell-antigen interactions in the skin following transcutaneous immunization. *PLoS One,* 9**,** e89503.

REIMER, T., BRCIC, M., SCHWEIZER, M. & JUNGI, T. W. 2008. poly(I:C) and LPS induce distinct IRF3 and NF-kappaB signaling during type-I IFN and TNF responses in human macrophages. *J Leukoc Biol,* 83**,** 1249-57.

REIS E SOUSA, C. 2004. Activation of dendritic cells: translating innate into adaptive immunity. *Current Opinion in Immunology,* 16**,** 21-25.

RIZZA, P., SANTINI, S. M., LOGOZZI, M. A., LAPENTA, C., SESTILI, P., GHERARDI, G., LANDE, R., SPADA, M., PARLATO, S., BELARDELLI, F. & FAIS, S. 1996. T-cell dysfunctions in hu-PBL-SCID mice infected with human immunodeficiency

virus (HIV) shortly after reconstitution: in vivo effects of HIV on highly activated human immune cells. *J Virol,* 70**,** 7958-64.

ROEDERER, M. 2002. Compensation in flow cytometry. *Curr Protoc Cytom,* Chapter 1**,** Unit 1.14.

SALMON, P., KINDLER, V., DUCREY, O., CHAPUIS, B., ZUBLER, R. H. & TRONO, D. 2000a. High-level transgene expression in human hematopoietic progenitors and differentiated blood lineages after transduction with improved lentiviral vectors. *Blood,* 96**,** 3392-8.

SALMON, P., OBERHOLZER, J., OCCHIODORO, T., MOREL, P., LOU, J. & TRONO, D. 2000b. Reversible immortalization of human primary cells by lentivector-mediated transfer of specific genes. *Mol Ther,* 2**,** 404-14.

SANDERS, D. A. 2002. No false start for novel pseudotyped vectors. *Current opinion in biotechnology,* 13**,** 437-442.

SEGURA, E., VALLADEAU-GUILEMOND, J., DONNADIEU, M. H., SASTRE-GARAU, X., SOUMELIS, V. & AMIGORENA, S. 2012. Characterization of resident and migratory dendritic cells in human lymph nodes. *J Exp Med,* 209**,** 653-60.

SHAPIRO, H. M. 2005. *Practical flow cytometry*, John Wiley & Sons.

STENN, K. S., LINK, R., MOELLMANN, G., MADRI, J. & KUKLINSKA, E. 1989. Dispase, a neutral protease from Bacillus polymyxa, is a powerful fibronectinase and type IV collagenase. *J Invest Dermatol,* 93**,** 287-90.

SUPERTI, F., SEGANTI, L., RUGGERI, F. M., TINARI, A., DONELLI, G. & ORSI, N. 1987. Entry pathway of vesicular stomatitis virus into different host cells. *J Gen Virol,* 68 (Pt 2)**,** 387-99.

WANG, Y., HAMMES, F., DE ROY, K., VERSTRAETE, W. & BOON, N. 2010. Past, present and future applications of flow cytometry in aquatic microbiology. *Trends Biotechnol,* 28**,** 416-24.

WHO. 2012. *Fact Sheet No. 360: HIV/AIDS* [Online]. Geneva: World Health Organisation. Available: http://www.who.int/mediacentre/factsheets/fs360/en/ [Accessed 28 April 2016].

WILEN, C. B., TILTON, J. C. & DOMS, R. W. 2012. HIV: cell binding and entry. *Cold Spring Harb Perspect Med,* 2.

WITTING, N., SVENSSON, P., GOTTRUP, H., ARENDT-NIELSEN, L. & JENSEN, T. S. 2000. Intramuscular and intradermal injection of capsaicin: a comparison of local and referred pain. *Pain,* 84**,** 407-412.

WU, S. J., GROUARD-VOGEL, G., SUN, W., MASCOLA, J. R., BRACHTEL, E., PUTVATANA, R., LOUDER, M. K., FILGUEIRA, L., MAROVICH, M. A., WONG, H. K., BLAUVELT, A., MURPHY, G. S., ROBB, M. L., INNES, B. L., BIRX, D. L., HAYES, C. G. & FRANKEL, S. S. 2000. Human skin Langerhans cells are targets of dengue virus infection. *Nat Med,* 6**,** 816-20.

ZUFFEREY, R., NAGY, D., MANDEL, R. J., NALDINI, L. & TRONO, D. 1997. Multiply attenuated lentiviral vector achieves efficient gene delivery in vivo. *Nat Biotechnol,* 15**,** 871-5.

Chapter 4- Cross-Presentation of Influenza Vaccine Antigen

4.1 Introduction

The previous chapters explored the *ex vivo* human skin tissue and cellular models. One of the limitations of the skin cell model was that isolated cells show a partially mature phenotype and thus are not able to respond to TLR-agonist stimulation (Section 3.4.3). The purposes of this chapter are therefore twofold: (i) to explore the use of a monocyte-derived dendritic cell model as an alternative to skin-derived immune cells and (ii) to explore the use of skin-derived cells in antigen cross-presentation studies.

4.1.1 Monocyte-Derived Dendritic Cell Models

Whilst a useful model, the irregular availability of *ex vivo* human skin samples (which relies on surgical lists and informed patient consent) and the unpredictable size of samples means that this model has practical disadvantages. *Ex vivo* human skin is also not widely available, with many groups lacking the ethical approval and access to a clinician to obtain samples. This has led to the development of cellular models of the immunological cells of the skin utilising monocytes obtained from blood donations by a number of groups (Sallusto and Lanzavecchia, 1994, Piemonti et al., 2000, Albert et al., 1998). Monocyte-derived dendritic cell (mdDC) models have been widely used for a number of years and are well understood (Leon et al., 2005), providing insight into the behaviour of dendritic cells (DCs).

Monocytes can be isolated from donated blood, following removal of erythrocytes and plasma (Repnik et al., 2003). Monocytes form part of the peripheral blood mononuclear cells (PBMCs) which consist of lymphocytes (B-cells, T-cells and natural killer cells) along with macrophages (Murphy et al., 2012). Centrifugation over a density gradient (for example an aqueous cell suspension layered over a more dense Ficoll solution (Repnik et al., 2003)) can be used to isolate the PBMCs from the erythrocytes, remaining leukocytes and plasma. After this, magnetic-activated cell sorting (MACS) is often used to isolate the monocytes from the PBMC population (Caucheteux et al., 2016, Mayer et al., 2011). This involves labelling cells with antibodies conjugated to magnetic nanoparticles (Schmitz et al., 1994). In the case of isolating

monocytes, anti-CD14 antibodies are used. The entire population is then passed through a magnetic column, which will retain cells labelled with the magnetic nanoparticle-conjugated antibody, whilst unlabelled cells can pass freely through. The column is then removed from the magnetic housing and the labelled cells eluted, providing a purified CD14+ monocyte population (El-Sahrigy et al., 2015).

Monocytes require cytokine stimulation to develop a DC-like phenotype. A general model for DCs is most commonly used, where interleukin 4 (IL-4) and granulocyte-macrophage colony-stimulating factor (GM-CSF) are utilised to develop mdDCs from monocytes over 7 days' culture (Leon et al., 2005). The derivation process can also be tailored to produce DC subset models- for example CD141+ dermal DC-like cells which are derived by the addition of vitamin D3 to the culture medium (Chu et al., 2012) and Langerhans like cells, which are produced by the addition of transforming growth factor-beta (TGF-β) to the culture medium (Geissmann et al., 1998).

4.1.2 T-cells

As their name suggests, one of the major functions of antigen-presenting cells (APCs) such as epidermal Langerhans cells (LCs) and dermal DCs (dDCs) within the immune system is presentation of antigenic epitopes to T-cells. Naïve T-cells lack cell surface receptors to extracellular antigen and so can only become activated by presentation of antigen on the surface of APCs (Ni and O'Neill, 1997). Antigen is presented via one of two types of receptor, the major histocompatibility complex (MHC) type I or type II molecules. MHC molecules differ from the other major antigen-binding molecule, antibodies, in that they can only bind peptide antigen (Turley et al., 2000). They also do not bind peptides in their native form (i.e. after folding), but instead bind linear peptide sequences. Thus, their specificity is to amino acids which are proximal to one another in a peptide sequence rather than those that only exist in proximity in a folded protein (Murphy et al., 2012).

The MHC molecules each have a number of subtypes, for example MHC class I includes HLA-A, HLA-B and HLA-C (where HLA refers to human leukocyte antigen, synonymous with MHC). Each subtype then contains a number of different molecules

(e.g. HLA-A1 and HLA-A2 amongst HLA-A molecules) (Makhatadze et al., 1997). T-cells possess T-cell receptors (TCRs) on their surface that allow them to interact with MHC molecules. Each TCR is specific to a MHC molecule with a specific peptide sequence bound within it (Baker et al., 2012), for example a given T-cell may only respond to binding a HLA-A2 molecule containing an influenza peptide 9mer (Clement et al., 2011). The assorted MHC molecules possess different specificities to antigens that relies on a number of 'anchoring' amino acids within a peptide, as defined by their physicochemical properties (e.g. an aromatic side chain or polar group). This allows them to bind a range of antigenic peptides with common characteristics (Murphy et al., 2012). Thus, a broad range of peptide sequences can be bound by the limited number of MHC receptor subtypes each person possesses (Engelhard, 1994). MHC-I molecules normally only bind peptide sequences which are 8-10 bases long, whilst MHC-II can bind peptide with its terminal ends extending beyond the molecule, allowing it to present much longer peptides (Murphy et al., 2012).

Binding of the TCR to the MHC:antigen complex requires the involvement of a co-receptor to stabilise the interaction and to increase the response within the T-cell. For MHC-I and II the co-receptors are CD8 and CD4 respectively (Campanelli et al., 2002, Janeway, 1991). These co-receptors have long been used to define the two major subsets of T-cells; cytotoxic T-cells express CD8 whilst helper T-cells express CD4 on their surface (Amadori et al., 1995). MHC-II is expressed on APCs and mediates the induction of CD4+ helper T-cell responses to antigen taken up from the extracellular environment (Santambrogio et al., 1999). Conversely, MHC-I is found on the surface of all nucleated cells within the body (Murphy et al., 2012). Its main function is to present viral antigens synthesised within the cell on the cell's surface, thereby alerting CD8+ cytotoxic T-cells to their infection and triggering cell death signalling to prevent the further viral production or spread of infection to further cells (Bedoui et al., 2009).

4.1.3 Cross-Presentation

Whilst presentation of antigen on MHC-I is vital for alerting CD8+ T-cells to the presence of infection in a cell, infected cells are unable to activate naïve T-cells directly (Murphy et al., 2012). APCs are able to present exogenous antigen on MHC-I molecules

via endosomal processing without direct infection in a process known as cross-presentation (Heath and Carbone, 2001). This is a vital part of the immune response to pathogens, both live and in their antigenic state within vaccines (Ruedl et al., 2002). The different cross-presentational abilities of human DC subsets are not yet fully understood (Joffre et al., 2012) and so it is vital in intradermal vaccination research that the antigen used and its delivery are tailored to best suit the most potent cross-presenting cells of the skin. This investigation therefore aimed to compare the cross-presentation of influenza vaccine antigen by the LCs and various dDC subsets of the skin.

4.1.4 T-Cell Response Testing

Given their important role in the adaptive immune system, investigating the response of T-cells to a novel vaccine can provide useful pre-clinical data. Animal models are often used in pre-clinical studies and possess the advantage of allowing the response of the immune system as a whole to be studied (Mestas and Hughes, 2004). There are, however, differences in animal and human immune systems, which mean that human cell models remain a useful laboratory tool. There are two main options for laboratory T-cell experimentation. The first is to use the total T-cell population from human blood, with its broad range of peptide-MHC complex specificities. The T-cells are then mixed with APCs and those T-cells possessing the correct antigen specificity will be 'primed' by the APCs- becoming activated and undergoing proliferative clonal expansion (Wölfl and Greenberg, 2014). T-cells may be stained with carboxyfluorescein succinimidyl ester (CFSE) to show proliferation (Quah and Parish, 2010). T-cells of a single specificity can also be quantified via tetramer staining, which utilises 4 MHC molecules, bound to a streptavidin core, each containing the peptide of interest (Dolton et al., 2015). The use of multiple peptide-MHC complexes on a single tetramer increases the binding affinity of the tetramer, thus increasing the success of staining for the cells of interest. The tetramer is often fluorescently-conjugated, allowing for flow cytometric analysis (Sims et al., 2010). This allows the proportion of a particular T-cell clone within the overall T-cell population to be quantified and the effect of a treatment or vaccine measured. This method possesses advantages in that T-cells may be obtained from blood buffy coats alongside monocytes, using MACS (Caucheteux et al., 2016). This allows monocyte-

derived DCs to be produced that are HLA-matched to the T-cells being used. It is also very similar to the *in vivo* situation, where T-cells exist as a heterogeneous population that APCs must interact with (Murphy et al., 2012). Its drawbacks include the extremely diverse nature of TCR specificity. Even epitopes that can be recognised by multiple TCRs tend not to prime more than 0.05% of the overall T-cell population (Challier et al., 2013). The alternative to this is to utilise a pure population of a single T-cell clone.

4.1.4.1 T-Cell Clones

T-cell clones are a population of T-cells which possess uniform TCR expression i.e. they will only successfully interact with a specific peptide-MHC complex (Mariotti and Nisini, 2009). They are obtained by the isolation and proliferation of T-cells, often by tetramer staining and FACS (Matthis and Reijonen, 2013). Using a pure population allows the stimulation of T-cells that important to a certain immune response to be quantified, with theoretical responses between 0 and 100% of the cells possible. However, since they are produced from T-cells from a single donor, any APCs that are used must be HLA-matched to the clones. Each MHC molecule type has differing prevalence within the general human population with prevalence varying between geographical and ethnic populations (Makhatadze et al., 1997, Arnaiz-Villena et al., 1995). This can provide an obstacle to experimentation if the HLA-type is particularly rare in the geographical location that is used to source APC donors (blood or skin). T-cell clones also only permit the assessment of vaccines containing the specific peptide sequence that the clones recognise. However, the use of T-cell clones does allow for a straightforward quantitative readout. Following co-culture with vaccine-treated APCs and the addition of brefeldin-A (to prevent the release of cytokines from the cell), the T-cell clones can be analysed for interferon-γ (IFN-γ) expression by flow cytometry as a marker of activation (Caucheteux et al., 2016, Norris et al., 2001). The uniformity of the clone population means that the frequency of activated cells can theoretically be detected in up to 100% of the cell population used, providing a robust readout for comparative experiments.

4.2 Aims and Objectives

This chapter aims to explore the use of monocyte-derived DC models as an alternative to skin-derived cells for immunological studies. It also aims to investigate the abilities of skin immune cells to cross-present an influenza vaccine. The specific practical objectives are:

1. Isolate monocytes from blood using previously established protocols and derive a number of DC models from them, assessing success of derivation using flow cytometry.
2. Use monocyte-derived DCs (mdDCs) to assess the concentration of LPS that is required to stimulate ex vivo human skin LCs/dDCs
3. Assess ALF3 T-cell clone for specificity to influenza A matrix protein (M1)-derived peptide (residues 58-66; GILGFVFTL).
4. Use mdDCs to develop a protocol for a T-cell clone activation experiment which assesses the cross-presentation of inactivated virus and virus-like particle influenza vaccines and transition this protocol to utilise *ex vivo* human skin dDCs and LCs to assess the cross-presentational ability of these cells.
5. Assess the differences in cross-presentation of antigen between the subsets of dDCs (based on CD11c and CD141 expression) and LCs using fluorescence-activated cell sorting to purify the cell subsets prior to co-culture with vaccine and ALF3 cells.

4.3 Materials and Methods

[All reagents were obtained from Fisher Scientific, UK unless otherwise stated]

4.3.1 Derivation of Monocyte-Derived Cell Models

4.3.1.1 Isolation of CD14+ Monocytes

Buffy coats were produced by the removal of erythrocytes and plasma from whole blood donations (obtained from Welsh Blood Service). After collection, they were diluted to a total volume of 180ml with sterile PBS. Next, 30ml of the diluted buffy coat was layered over 15ml Ficoll-Paque density gradient media in 50ml centrifuge tubes. Tubes were spun at 800 x g for 30 minutes and the rotor allowed to stop without application of the brake to preserve the density gradient. Peripheral blood mononuclear

cells (PBMCs) formed a distinct white layer within the density gradient, which was isolated by gentle pipetting. PBMCs were then labelled using anti-human CD14 MicroBeads and passed through a magnetic-assisted cell sorting (MACS) column (both Miltenyi Biotec, UK), according to manufacturer guidelines, to isolate CD14+ monocytes.

4.3.1.2 Monocyte-Derived Dendritic Cells

Monocytes were plated at 2 x 10^6 cells per well on a 6-well plate in 3ml complete IMDM (IMDM with 50U/ml penicillin, 50µg/ml streptomycin, 10% foetal bovine serum (FBS), 10mM 4-(2-hydroxyethyl)-1-piperazineethanesulfonic acid (HEPES) and 1mM sodium pyruvate (all Sigma-Aldrich, UK)). The following were also added: 500U/ml granulocyte-macrophage colony-stimulating factor (GM-CSF) (Miltenyi Biotec, UK), 500U/ml interleukin 4 (IL-4) (Miltenyi Biotec, UK) and 50µM 2-mercaptoethanol (β-2M) to stimulate the differentiation of monocytes towards a DC phenotype. 1ml of media was removed and replaced with complete IMDM containing 1500U/ml each of GM-CSF and IL-4 every 2 days until day 7 when the cells were visually assessed for dendritic morphology and phenotyped using flow cytometry to establish success of DC derivation.

4.3.1.3 Monocyte-Derived CD141 Dendritic Cells (CD141 mdDCs)

Monocytes were cultured in an identical manner to deriving mdDCs (section 4.3.1.2) until day 4 of culture, when 100nM vitamin D3 was added to the culture media. Cell culture was then continued as described in Section 4.3.1.2 until day 7 when cells were collected for use.

4.3.1.4 Monocyte-Derived Langerhans Cells (mdLCs)

Monocytes were cultured in T25 cell culture flasks at a concentration of 1 x 10^6 cells/ml in RPMI-1640 growth medium (supplemented with 2mM L-glutamine, 50U/ml penicillin, 50µg/ml streptomycin and 10% FBS) plus 500U/ml each of GM-CSF and IL-4 plus 10ng/ml transforming growth factor-beta (TGF-β). Media and cytokines were refreshed every 2 days. Cells were harvested for use on day 7 of culture.

4.3.2 Responsiveness of Monocyte Models to LPS Stimulation

Given the lack of meaningful stimulation of *ex vivo* human skin walkout cells in the previous chapter using Toll-like receptor (TLR) agonists, the mdDC model was used to determine whether a sub-optimal dose of TLR agonist had been used. The immature state of blood monocytes cultured in a sterile environment allows them to show marked upregulation of maturation markers and cytokine production from baseline when stimulated. LPS was used due to its potent immunostimulatory properties and the optimal dose for DC stimulation sought.

The mdDCs were plated at 1 x 10^5 cells per well of a 96-well plate in 100µl complete IMDM containing 10ng/ml, 100ng/ml, 1µg/ml or 2µg/ml LPS or 100µl complete IMDM alone. Three hours after plating, brefaldin A was added to a final concentration of 10µg/ml to cells that were designated for analysis of cytokine expression. Cells were fixed in 1% paraformaldehyde at room temperature for 10 minutes after either 24 or 48 hours in culture. Cytokine expression was analysed in cells exposed to LPS for 24 hours and maturation markers analysed after 24 and 48 hours' exposure.

Cells to be analysed for cytokine expression were stained using Perm/Wash Kit (BD Biosciences) according to the manufacturer's protocol to allow intracellular staining. The 3-colour panels listed in Table 4.1 were used to stain cells.

Flow cytometry was performed using a BD FACSCanto II cytometer. Statistical tests comprised one-way analysis of variance (ANOVA) followed by Tukey's post hoc analysis performed using IBM SPSS Statistics (IBM, USA).

Table 4.1: Antibodies used to assess intracellular cytokine (ICC) and maturation marker expression on mdDCs via flow cytometry

	Antibody	Conjugated Fluorophore	Manufacturer
Maturation Panel	Anti-HLA-DR	Allophycocyanin (APC)	BD Biosciences, UK
	Anti-CD1a	Fluorescein isothiocyanate (FITC)	BD Biosciences, UK
	Anti-CD83	Phycoerythrin (PE)	Beckman Coulter, UK
ICC Panel	Anti-CD1a	FITC	BD Biosciences, UK
	Anti-DC-SIGN	PE	BD Biosciences, UK
	Anti- TNF-α	APC	BD Biosciences, UK
	Anti-IL-12	APC	BD Biosciences, UK
Isotype Control Panel	IgG1 κ	FITC	BD Biosciences, UK
	IgG1 κ	PE	BD Biosciences, UK
	IgG1 κ	APC	BD Biosciences, UK

4.3.3 ALF3 T-Cell clones

This investigation utilised a pair of influenza A vaccines against the H1N1 influenza A/Puerto Rico 8/1934 virus. One vaccine was an inactivated whole virion (IV) vaccine, produced by formalin inactivation of virions produced in chicken eggs, in a manner similar to that used for producing the commercial vaccine (Furuya et al., 2010). The second vaccine was a virus-like particle (VLP) vaccine consisting of hemagglutinin and matrix M1 peptides in the absence of viral genetic material (Quan et al., 2011). Both vaccines were provided by Sang-Moo Kang's laboratory in the Centre for Inflammation Immunity & Infection, Georgia State University. As discussed in Chapter 2, VLP vaccines are a developing vaccine technology which eschews the need for inactivation of virus and the risk of reversion to wild-type virus, whilst still delivering viral peptides in a similar way to virions (Kang et al., 2009). The investigation sought to study the ability of skin immune cells to cross-present the two vaccines, comparing the results between dDCs and LCs and IV and VLP vaccines.

HLA A*0201-restricted CD8+ T-cell clones (ALF3 clones) specific for the influenza A matrix protein (M1)-derived epitope GILGFVFTL (residues 58-66) were kindly provided by David Price's laboratory in the department of Infection and Immunity, Cardiff University. ALF3 cells were propagated in advance of planned experimentation by the

Price group and were collected in a ready-to-use cell suspension on the morning of each experiment.

4.3.3.1 Validation of ALF-3 Peptide Specificity

ALF3 clones were tested for specific responsiveness to the 9mer peptide of interest to validate their use in this investigation. ALF3 clones were plated at 6 x10^4 cells per well in complete RPMI in a round-bottomed 96 well plate with:

1. 1µg of HLA A*0201-restricted influenza A matrix protein (M1)-derived peptide (residues 58-66; GILGFVFTL)
2. 1µg of irrelevant HLA-A*0201-restricted HIV-1 p17 Gag-derived peptide (residues 77-85; SLYNTVATL)
3. 1µg formaldehyde-inactivated H1N1 influenza A/Puerto Rico 8/1934 virus
4. 1µg H1N1 influenza A/Puerto Rico 8/1934 virus-like particles
5. Media alone (untreated control)

ALF-3 cells were incubated for 1 hour prior to the addition of brefaldin-A to a final concentration of 10µg/ml then incubated overnight. Cells were fixed after overnight culture and stained intracellularly utilising FITC anti-CD3 and PE anti-IFN-γ antibodies (both BD Biosciences, UK) before analysis on a BD FACSCanto II flow cytometer (BD Biosciences, UK) to quantify IFN-γ expression amongst ALF3 cells. Analysis of flow cytometric data was performed using FlowJo software (FlowJo LLC, USA). Statistical tests comprised one-way analysis of variance (ANOVA) followed by Tukey's post hoc analysis performed using IBM SPSS Statistics (IBM, USA).

4.3.4 Cross-Presentation by Monocyte-Derived DCs/LCs

Initial studies utilised mdDCs in the place of primary skin cells to generate preliminary data and optimise the protocol without the constraints of infrequent skin samples. HLA-A*0201 expressing monocytes were selected by flow cytometric analysis of FITC anti-HLA-A2 (BD Biosciences, UK) antibody-stained monocytes following isolation from buffy coats. The mdDC models (mdDCs, CD141 mdDCs and mdLCs) were

then produced as described in Section 4.3.1. To assess the cross-presentation ability of the DC models, they were plated at 2 x 10^4 cells per well of a 96-well plate and treated with one of the vaccines (either VLP or IV) at 1µg per well. Then they were incubated for 4-6 hours to allow uptake and processing of the vaccines. 6 x 10^4 ALF3 cells were then added, mixed thoroughly and incubated for 1 hour. Brefaldin-A was then added (to 10µg/ml) and the cells incubated overnight. Cells were fixed the next morning and stained/analysed to quantify IFN-γ expression as described in Section 4.3.3.1.

4.3.5 Cross-Presentation by Skin-Derived DCs/LCs

Given *ex vivo* skin cells' closer representation of *in vivo* cell behaviour, compared to monocyte-derived models, the investigation utilising ALF3 T-cell clones was extended to utilise primary skin LCs and dDCs as the APCs.

Human skin was collected, processed and dermal and epidermal walkout cells collected separately as described in Section 3.3.1. An identical protocol to that used for monocyte-derived cells was used, with the exception that dermal walkout cells were plated out at 7.5 x 10^4 cells per well and epidermal walkout cells at 2 x 10^5 to account for the differing purities of the immunological cells obtained from each skin region. Cells were processed, co-cultured with ALF3 cells and analysed as described in Section 4.3.4.

4.3.6 Sorted Skin Cell Subset Cross-Presentation Investigation

The two human skin samples used in this study were obtained from patients undergoing abdominoplasty surgery at Spire Hospital, Cardiff under informed written patient consent and local ethical committee approval (South East Wales Research Ethics Committees Panel C, Reference: 08/WSE03/55). Sample transport and processing for cell walkout were performed in an identical manner to that described in Section 3.3.1. Following 48 hours' walkout, the walkout cells were collected, counted and then plated with either 10µg/ml IV vaccine or 10µg/ml VLP vaccine in 6-well cell culture plates. Cells were incubated overnight at 37°C to allow vaccine uptake and processing. The next day they were washed and re-suspended in sodium azide-free sterile FACS buffer (1% BSA in PBS) at 2 million cells/ml. The antibodies listed in Table 4.2 were then added.

Table 4.2: Antibodies used to identify dDC subsets and LCs from dermal and epidermal walkout cells respectively by FACS

	Antibody	Conjugated Fluorophore	Manufacturer
Dermal Dendritic Cell Panel	Anti-HLA-DR	Allophycocyanin (APC)	BD Biosciences, UK
	Anti-CD141	VioBlue®	Miltenyi Biotec, UK
	Anti-CD11c	Allophycocyanin-cyanine 7 (APC-Cy7)	BD Biosciences, UK
Epidermal LC Panel	Anti-HLA-DR	APC	BD Biosciences, UK

Cells were stained at 4°C for 1 hour then washed and re-suspended at 50 million cells/ml in sterile FACS buffer for sorting. Cell sorting was performed on a custom FACSAria cell sorter (BD Biosciences, UK). Dermal cells were gated for size/granularity (FSC-A/SSC-A), singlets and HLA-DR positivity (i.e. total dDCs) before being sorted into CD141+/CD11c+ (++ dDCs), CD141-/CD11c+ (+- dDCs) and CD141-/CD11c- (--dDCs) subsets. Epidermal cells were gated for size/granularity, singlets and HLA-DR positivity to sort LCs from epidermal walkout cells. After sorting, cells were counted and plated at 2 x 10^4 cells per well of a 96-well plate. Immediately after plating, 6 x 10^4 ALF3 cells were added to each well and the plate incubated for 60 minutes at 37°C before the addition of brefeldin-A (to 10µg/ml), then returned to incubation overnight. The next morning cells were fixed, stained and analysed for IFN-γ expression amongst ALF3 cells as described in Section 4.3.3.1. A portion of epidermal and dermal cells were also stained for HLA-A2 expression.

4.4 Results and Discussion

4.4.1 Derivation of Monocyte-Derived Cell Models

Flow cytometric analyses of the three mdDC models are shown in Figure 4.1. Analysis revealed mdDCs continued to express HLA-DR (as was the case on monocytes). The cells also showed expression of CD1a and DC-SIGN which are not expressed on monocytes, indicating successful transformation from monocytes into the classic mdDC phenotype (Leon et al., 2005). There was notably no CD141 expression on mdDCs. CD141 mdDCs displayed similar HLA-DR, CD1a and DC-SIGN marker expression to mdDCs with the addition of CD141 expression which was induced by the addition of vitamin D3 to the media during culture (Chu et al., 2012). The mdLCs produced higher CD1a expression than mdDCs or CD141 mdDCs, much like LCs in skin which express high levels of CD1a (Pena-Cruz et al., 2001). There was also CD207 expression in mdLCs, which is indicative of an mdLC phenotype (Guironnet et al., 2002) though expression was not ubiquitous. The partial CD207 expression shows that although some monocytes were displaying a LC-like phenotype, many failed to transition into full LC-like cells, a fact that will be taken into account when interpreting results.

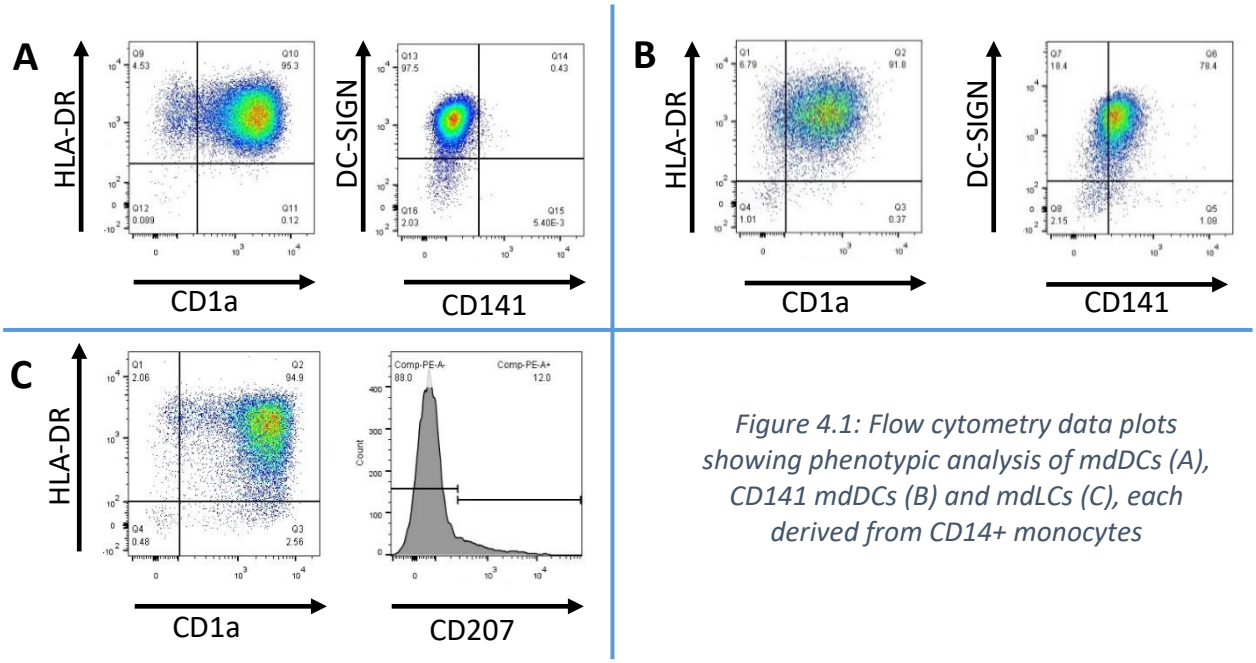

Figure 4.1: Flow cytometry data plots showing phenotypic analysis of mdDCs (A), CD141 mdDCs (B) and mdLCs (C), each derived from CD14+ monocytes

4.4.2 Responsiveness of Monocyte Models to LPS Stimulation

The cytokine expression and maturation of mdDCs in response to LPS is shown in Figure 4.2. The data were normalised to the maximal response from each donor, negating the biological variance and allowing comparison between blood donors. The mean maxima for maturation and cytokine responses are shown in Figure 4.2 (B, D & F). The greatest cytokine expression occurred with 1µg/ml LPS, though the normalised response was not significantly different from 100ng/ml or 2µg/ml LPS ($p = 0.098$ and 0.195 respectively).

Maturation of mdDCs at 24 hours displayed a positive correlation between LPS concentration and CD83 expression, with the highest expression occurring with 2µg/ml LPS. Again, however, the difference in expression in the cells exposed to 100ng/ml and 1µg/ml LPS was not significantly different. After a 48-hour exposure to LPS the maturation profile was different, with maximal CD83 expression occurring in the cells treated with 100ng/ml LPS. Maturation tailed off above 100ng/ml, with cells exposed to 2µg/ml LPS showing a similar proportion of mature cells as those with 10ng/ml LPS. This may be due to higher LPS concentrations possessing some cytotoxic activity over the 48-hour culture period.

The results in both maturation and cytokine expression suggest that 1µg/ml LPS is either optimal, or not significantly different from the optimal, concentration for DC stimulation. This supports the conclusion that skin LCs and dDCs are partially matured following their walkout from skin and so are unresponsive to Toll-like receptor agonist stimulation.

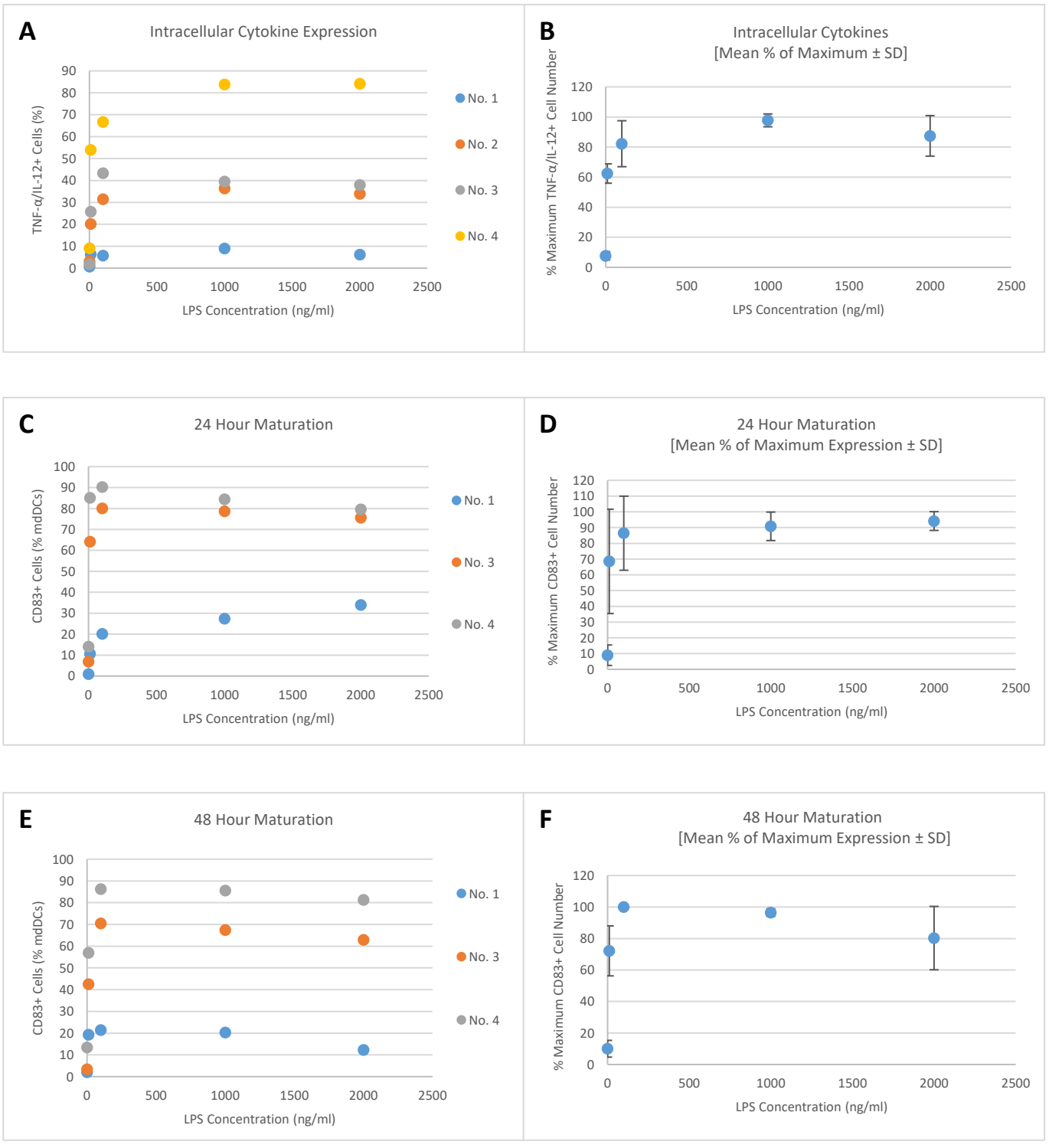

Figure 4.2: Intracellular cytokine expression [A,B], 24 hours [C,D] and maturation at 48 hours [E,F] in mdDCs treated with varying concentrations of LPS; all expressed as raw data [A,C,E] and normalised to maximal staining within each sample [B,D,F]. Legends on graphs A, C and E indicate buffy coat donor number.

4.4.3 Validation of ALF-3 T-Cell Clones

Prior to their use in combination with monocyte- or skin-derived antigen-presenting cells, the ALF3 T-cell clones were assessed for their response to the influenza matrix peptide 9mer GILGFVFTL. As MHC-I molecules are expressed on all nucleated cells (Murphy et al., 2012), it was possible to add the peptide to the cells and allow them to 'self-present' the peptide to one another and become activated. The results of the experiment are shown in Figure 4.3. There was a statistically significant ($p < 0.0001$) activation of ALF3 cells, as determined by intracellular staining for IFN-γ expression, following treatment with the influenza matrix peptide of interest. There was no significant stimulation following treatment with an irrelevant peptide 9mer or with either vaccine type. This shows that the ALF3 cells are functional and only activated in a sequence-specific manner and that the vaccines must be processed to allow the influenza matrix 9mer to be liberated and presented on MHC-I molecules. Thus, any ALF3 activation by the influenza vaccines will depend on the cross-presentation of vaccine antigen by either LCs or dDCs.

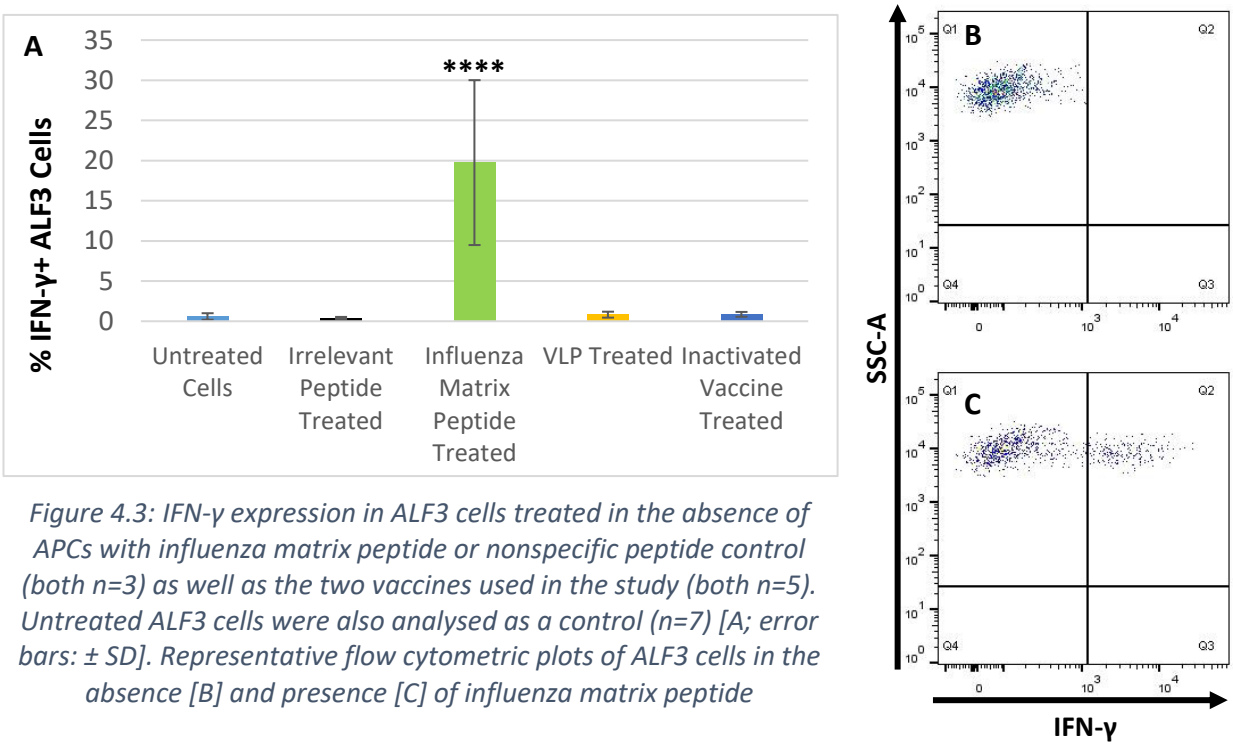

Figure 4.3: IFN-γ expression in ALF3 cells treated in the absence of APCs with influenza matrix peptide or nonspecific peptide control (both n=3) as well as the two vaccines used in the study (both n=5). Untreated ALF3 cells were also analysed as a control (n=7) [A; error bars: ± SD]. Representative flow cytometric plots of ALF3 cells in the absence [B] and presence [C] of influenza matrix peptide

4.4.4 Cross-Presentation by Monocyte-Derived DCs/LCs

The three different mdDC models were assessed for their ability to cross-present inactivated H1N1 influenza A/Puerto Rico 8 (II) vaccine and the equivalent virus-like particle (VLP) vaccine, the results of which are shown in Figure 4.4. The results showed that both the VLP and IV vaccines were able to stimulate marked IFN-γ production in ALF3 via APCs. Untreated APCs did not stimulate the ALF3 cells, showing that the response was antigen-specific. Both mdDCs and CD141 mdDCs elicited a much greater response with the VLP vaccine than the IV vaccine (a 2-fold increase in mean with mdDCs). The mdLCs showed almost identical levels of ALF3 stimulation with both

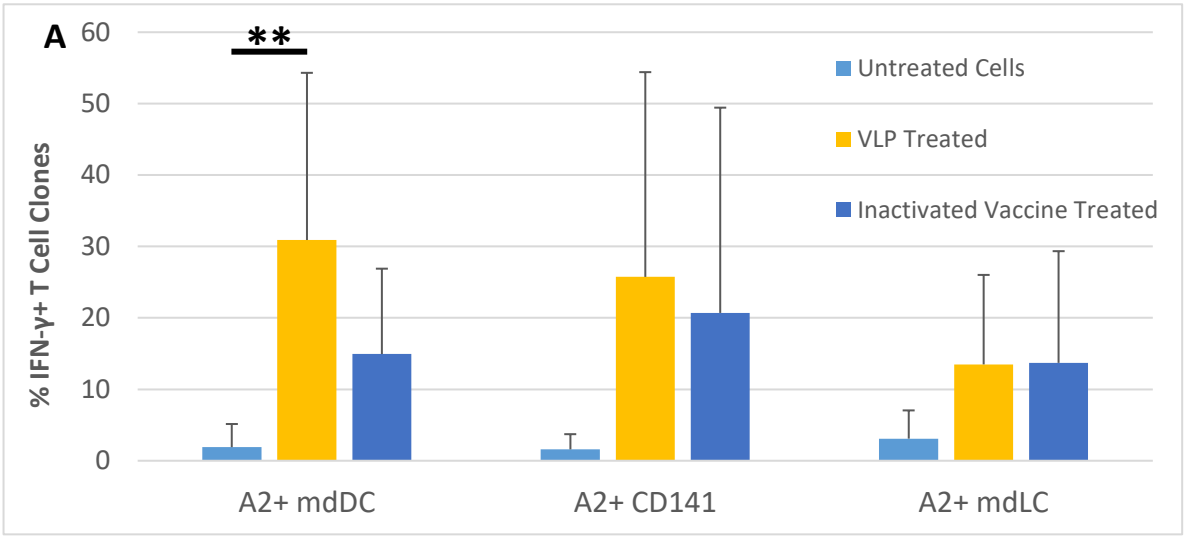

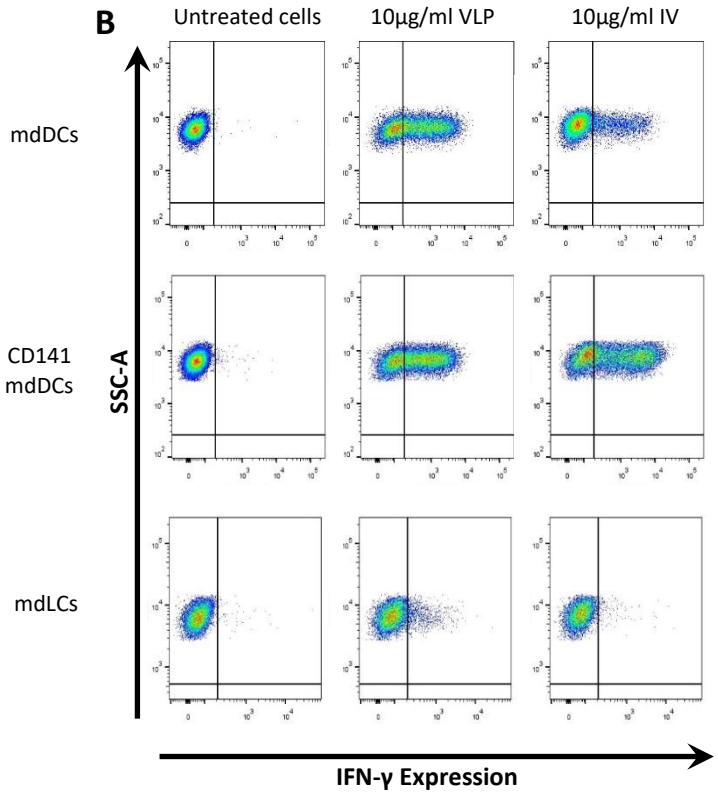

Figure 4.4: IFN-γ expression in ALF3 cells co-cultured with vaccine-treated monocyte-derived dendritic cell models. Mean data (A) is shown from experiments using mdDCs (n=6), CD141 mdDCs (n=4) and mdLCs (n=3); error bars: ±SD. Representative flow cytometry plots for each cell type are also shown (B).

vaccines, both of which were lower than the levels seen with mdDCs or CD141 mdDCs. As with the stimulation with TLR agonists, there was high inter-donor variability seen within the results meaning mdDCs treated with VLP vaccines were the only treatment condition that had a significantly significant difference in IFN-γ+ ALF3 cells compared to the untreated control ($p < 0.01$). The overall pattern appeared to be that both mdDCs and CD141 mdDCs were able to cross-present the vaccine antigen more readily than the mdLCs. It is possible that the incomplete conversion of monocytes to mdLCs (based on low CD207 expression) meant that the mdLCs used still possessed some mdDC-like characteristics and so differences were perhaps diminished. Skin-derived LCs will possess the full LC phenotype and provide a truer representation of the *in vivo* situation. This protocol was transitioned into the *ex vivo* skin cell model to benefit from its comparability to the *in vivo* behaviour of cells.

4.4.5 Cross-Presentation by Skin-Derived DCs/LCs

Figure 4.5 and Figure 4.6 show the pattern of ALF-3 stimulation achieved using *ex vivo* skin dDCs and LCs as the APCs. The skin APCs performed differently to monocyte-derived cell models, with IV vaccine-treated APCs eliciting significantly greater responses than VLPs or untreated cells with both dDCs and LCs. The IV vaccine also elicited the greatest overall response in combination with dDCs. LCs showed reduced cross-presentation of both vaccine types, in line with the preliminary work done in monocyte-derived models. HLA-A2- controls also showed no stimulation with either VLPs or IV vaccines. The skin samples used were largely HLA-A2+ (HLA-A2+ cells: n=5; HLA-A2- cells: n=1), meaning statistical differences could not be determined between HLA-A2 positive and negative cells. However, IFN-γ levels in HLA-mismatched cells were almost identical to untreated cells, suggesting that the stimulation was specifically linked to the HLA-A2 MHC-I molecule on APCs.

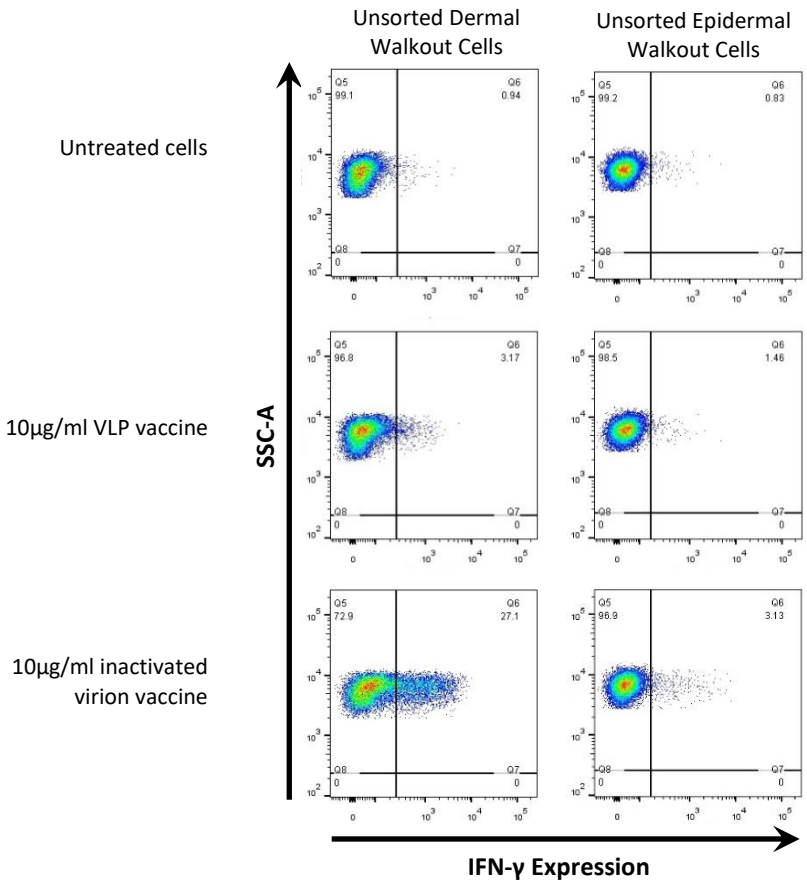

Figure 4.5: Flow cytometry plots showing ALF3 cell IFN-γ expression following co-culture with vaccine treated skin walkout cells from a single donor

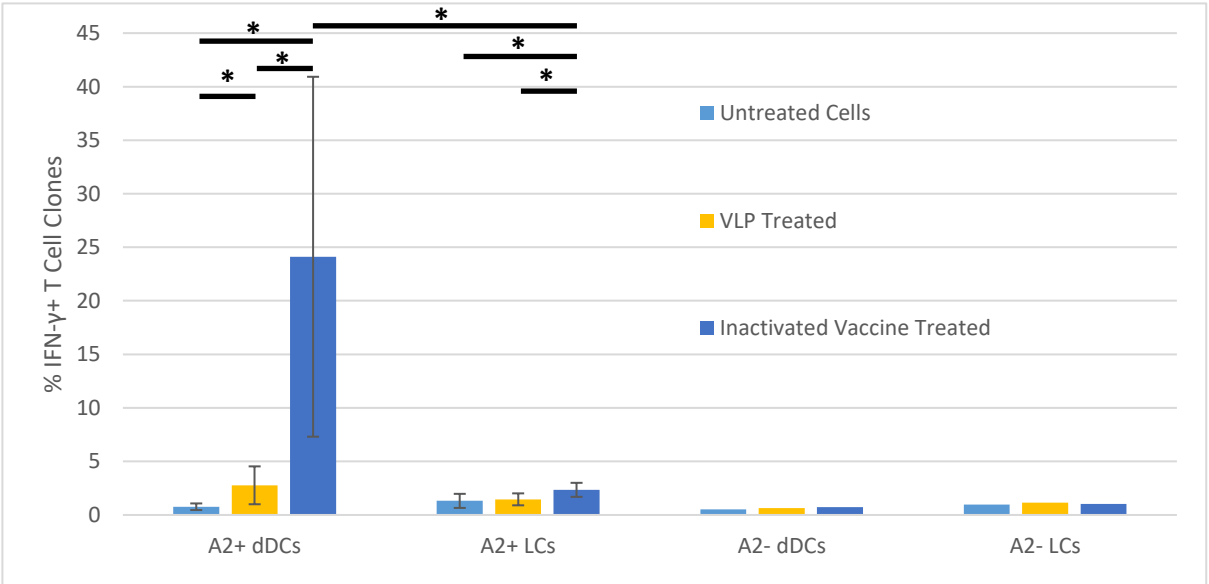

Figure 4.6: IFN-γ expression in ALF-3 cells following co-culture with VLP or IV vaccine-treated unsorted walkout skin dDCs or LCs. Error bars: ± SD

4.4.6 Sorted Skin Cell Subset Cross-Presentation Investigation

The final portion of the investigation aimed to distinguish the differences in cross-presentation between the different subsets of dermal DCs rather than the population as a whole. The sorting of skin cells also allows for the effects of non-APC contamination (especially in walkout epidermal cells) on ALF3 stimulation to be eliminated as a pure APC population will be used. This was an important part of the investigation as the subsets of dDCs have only recently begun to be characterised and their properties are still not fully understood. As discussed in Chapter 3, cell sorting involves a high level of cell loss. Thus, a high number of cells must be sorted to ensure adequate cell numbers can be used in downstream experimentation. The acquisition of abdominoplasty skin samples, which were much larger than the mastectomy or breast reduction skin samples normally obtained, enabled this. The donors were also younger than normal, 32 and 31 years old versus a mean age of 66 years for breast skin samples used in this study. These two factors allowed a large pool of viable cells to be collected for sorting and meant that a cell sorting experiment was possible.

The results of the investigation are shown in Figure 4.7. Only two abdominoplasty samples were available and therefore results are limited. There was, however, one HLA-A2+ and one HLA-A2- sample, allowing for an internal control with a single batch of T-cell clones. The size of skin samples also meant that each treatment condition could be tested in duplicate, granting some reliability to the data. The overall pattern was similar to the results seen in unsorted walkout cells, with only HLA-A2+ cells able to elicit a response from the ALF3 cells. Within the HLA-A2+ skin cells, IV vaccine produced a markedly stronger response than VLP vaccine. The greatest stimulation was observed with dDCs treated with IV vaccine, both ++ and +- dDCs producing strong ALF3 stimulation (58% and 66% respectively). -- dDCs produced a much lower response, though this was still greater than the response with LCs. Previously published literature (Jongbloed et al., 2010, Chu et al., 2012, Haniffa et al., 2012) reported that CD141+ dDCs are able to cross-present antigen, but little work had been done to compare the three subsets of dDCs in parallel. Only limited conclusions can be drawn from the experiment due to low N values but initial data appears to show that both ++ and +- dDCs are able

to cross present antigen and that +- dDCs may even be able to do so more readily than ++ dDCs.

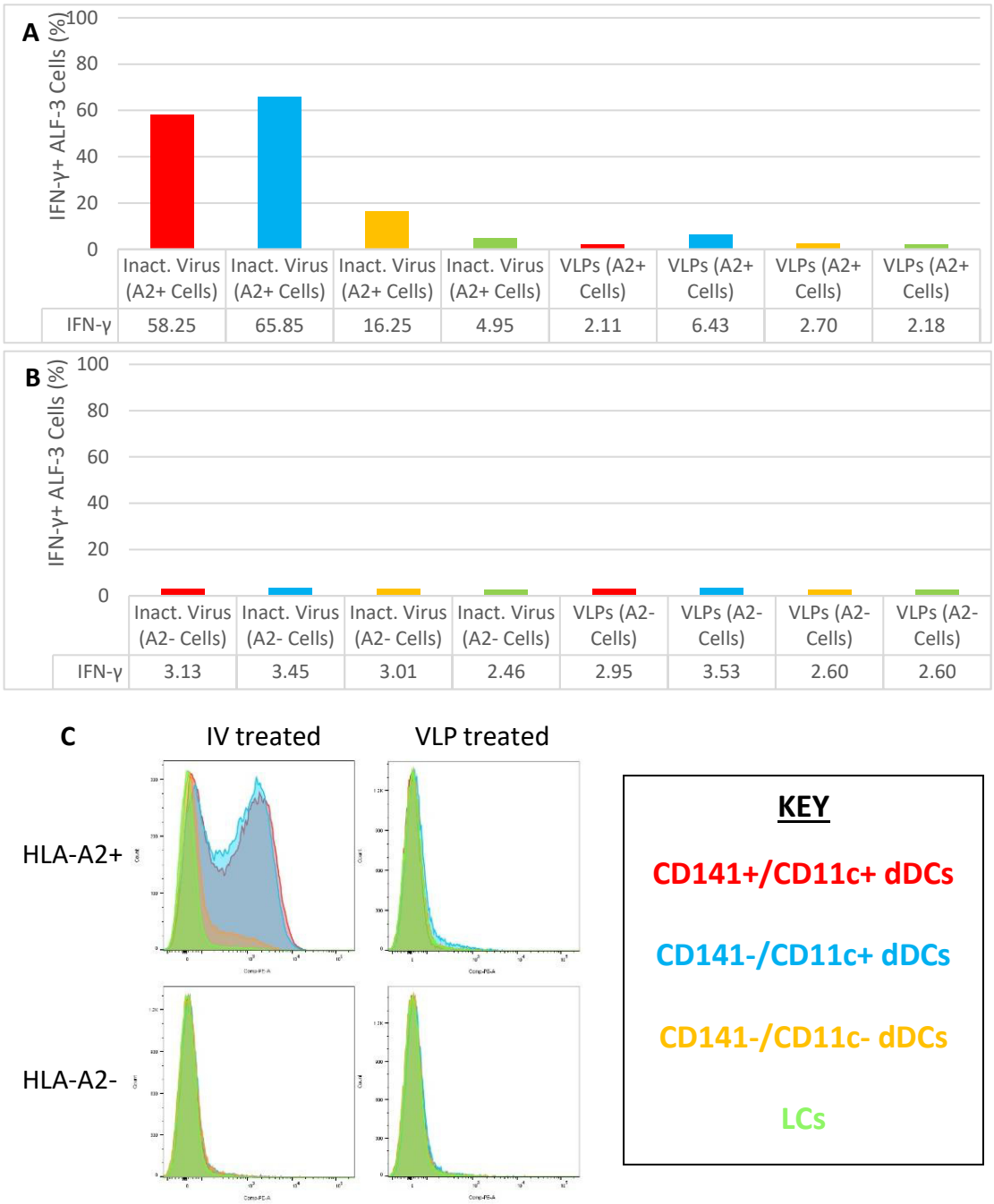

Figure 4.7: Results of the sorted skin cell cross presentation investigation. Graphs show IFN-γ expression amongst ALF3 cells co-cultured with vaccine treated skin cells which have been sorted to provide pure DC subset and LC populations. Cells were from an HLA-A2+ donor (A) and an HLA-A2- donor (B). Data is also presented in histogram format to allow comparison between the DC and LC populations (C)

4.5 General Discussion

The mdDC model proved to hold a number of practical advantages over cells that are isolated from *ex vivo* human skin samples. Firstly, the buffy coats that are used are available much more frequently than *ex vivo* human skin samples as they do not rely on irregular surgery dates. This provides greater flexibility in planning experiments and allows the completion of experimental repeats in a much shorter timeframe than experiments that rely on skin samples. It is also possible to isolate a large number of monocytes; yields of tens of millions of CD14+ cells from a single buffy coat are routine (Schwanke et al., 2006). Thus, the model was ideal for the optimisation of LPS stimulation of DCs protocol, which had yielded poor results in skin cells. The results confirmed that an optimal LPS concentration was used to try and stimulate the skin walkout cells in Section 3.3.5. Thus, skin walkout cells will not be used for stimulation assays of this type in the future. The high yield of cells from buffy coats can be used flexibly; monocytes can be cultured to produce a number of different DC models. This means equal numbers of the various models can be produced for experiments, unlike skin-derived cells, which exist in predefined subsets (Nestle et al., 1993) which are unequal in proportion to one another. This can allow better controlled comparative experiments, with equal numbers of cell types of each subset in comparable purities to one another to be used in parallel from a single donor.

Conversely, there are a number of drawbacks to mdDC models. They are less representative of the *in vivo* cells than skin-derived cells, as they do not receive the full milieu of environmental signals that an immature DC would encounter in the skin (Leon et al., 2005). The derivation process from monocytes into DC-like cells also introduces a source of variability, as monocytes from different donors may respond differently to the cytokines used, as exemplified by different levels of DC markers on cells from different donors. This may amplify differences in responsiveness to stimuli in downstream experimentation and explain the range of results seen in the LPS concentration titration study, where maximal stimulation ranged from less than 10% to over 90% of cells between donors. The fact that monocytes are obtained from blood, which is a sterile environment, may mean that they are more responsive to pathogens than skin APCs, which may encounter PAMPs more regularly. This may account for the partial maturity of skin cells witnessed in the Chapter 3. The complex ontogeny of DCs (Shortman and

Naik, 2007) means it is unlikely that the model will be truly representative of DCs until this is resolved. The protocols for producing monocyte-derived models also vary between groups. For example, when producing mdLCs some protocols only add IL-4 at the outset (day 0) (Peiser et al., 2004) whilst others do not use it at all (Guironnet et al., 2002). The use of IL-4 in this investigation may account for the low CD207 expression on mdLCs and their retained ability to cross-present antigen, both of which are mdDC-like characteristics. It may be prudent in future work to optimise the mdLC derivation process to improve the reliability of the model. Cell sorting to purify CD207+ cells would also improve the model by eliminating cells which had not developed the full mdLC phenotype.

The ALF3 clones used proved to be an extremely useful tool in the study of cross-presentation of vaccine antigen. The ubiquity of the M1 protein (Ito et al., 1991) meant that the vaccines from a relevant strain of influenza could be used without worries on compatibility. The conserved structure of the matrix protein between influenza strains has led to its use in candidate universal influenza vaccines (De Filette et al., 2005, Neirynck et al., 1999). ALF3 cells proved to be specific to the peptide of interest, showing no stimulation with irrelevant peptide or either unprocessed vaccine. This meant that any stimulation resulting from the co-culture of ALF3 cells with APCs and vaccines would be a result of vaccine being processed and presented and that false positive results from direct ALF3 stimulation by the vaccines used were not possible.

The results of T-cell clone experiments with the monocyte-derived cells showed all three models were able to process antigen from both vaccine types and produce mean ALF-3 activation levels higher than untreated cells. Unfortunately, the high level of variability in the responses between donors meant that significance could only be attached to the difference between untreated mdDCs and mdDCs treated with the VLP vaccine. The monocyte models were also able to produce numbers of activated ALF3 cells that were comparable or greater than stimulating the clones with the readily-processed M1 peptide 9mer, perhaps due to the presence of costimulatory molecules on the APCs, which enhance the response versus presentation of the peptide between ALF3 cells alone. Interestingly, the response was reduced when using mdLCs in place of mdDCs, which suggests less cross-presentation of vaccine with these cells. The results were validated when using skin cells, with LCs being unable to produce anywhere near

the same response from ALF3 cells as dDCs. These results suggest that LCs are less able to cross-present antigen derived from influenza virus matrix protein than dDCs.

A lower level of T-cell clone activation using primary skin APCs was predicted as they possess a lower responsiveness to stimulation than their monocyte-derived counterparts. In actuality, the dermal walkout cells were able to produce a greater level of ALF3 activation than either of the mdDC models, perhaps due to the more mature phenotype of skin cells than mdDC models. There was also much less inter-donor variability, allowing statistically significant differences to be observed between the treatment conditions. Notably though, the cross presentation of VLPs was much lower than that of inactivated virus. This was the opposite of monocyte-derived models, where VLPs tended to produce a stronger response. The main difference between inactivated virus and VLPs is the presence of viral genetic material in the inactivated viral particles (Sitrin et al., 2015). Thus, it may be speculated that the RNA present is essential for skin dDCs to cross-present the viral antigen. As the main sensors of viral genetic material, TLR3 (for dsRNA) or TLR7/8 (for ssRNA) might be involved in this immune cell activation. These PRRs have been found to be involved in cross presentation previously (Davey et al., 2010, Le Goffic et al., 2007, Oh et al., 2011). However, further work is required to confirm this from this data. The monocyte-derived models may detect VLPs by some other receptor not found on skin LCs/dDCs, allowing them to eschew the requirement for activation by viral RNA, meaning they can uptake and cross-present antigen from VLPs as well as inactivated virus. Further work is required to determine whether this is a true property of monocyte-derived models over skin-derived cells.

The results were in contrast to studies utilising mice (Stoitzner et al., 2006) or human (Klechevsky et al., 2008b) tissue that found that epidermal LCs readily cross-present antigen. It has been speculated that LCs may perform more of an immune-regulatory function, controlling tolerance rather than initiating immune responses (Stoitzner, 2010). This is logical, given their location closest to the external environment and ability to sample the stratum corneum (Yoshida et al., 2014). If LCs brought about inflammatory immune responses, they would likely cause responses to commensal organisms which do not present a pathogenic threat (van der Aar et al., 2013). The response of the dermal cells on the other hand, is in line with the literature, which found that dDCs (Segura et al., 2013), and more specifically the CD141+ dDC subset (Joffre et

al., 2012, Chu et al., 2012, Jongbloed et al., 2010), are potent cross-presenting APCs. The use of cell sorting allowed concurrent testing of the three dDC subsets (classified by CD11c and CD141 expression). It found that whilst the CD141+/CD11c+ dDCs could present vaccine antigen and elicit a strong response from the T-cell clones, the CD141-/CD11c+ dDCs proved to be equally able to do so. This has been found in previous studies using DCs from human lymph nodes (Segura et al., 2013). It is also possible that whilst the relatively small CD141+ subset of dDCs is more prone to cross-presentation, the other subsets are also able to do so in certain circumstances, thus providing a 'back up' system for immune response generation (Bachy et al., 2013). For example, following 48 hours' culture to induce maturation, human skin LCs have been shown to be able to cross-present influenza antigen (van der Aar et al., 2011). It is likely that the cross-presentational abilities of skin immune cells depends on the antigen type and method of DC exposure (Lee et al., 2009), antigen receptor expression (Burgdorf et al., 2007) or activation state (Schulz et al., 2005). Thus, the results should not be considered a universal property for all skin DCs with all antigen as only the cross-presentation of a single peptide from one strain of influenza virus was studied. The lack of available abdominoplasty skin samples meant that repeats could not be obtained, rather the data can be taken as a starting point for further work. One limitation of the work was the high cell loss associated with cell sorting and the relative scarcity of CD11c-/CD141- and CD11c+/CD141+ dDCs within the overall dDC population also meant that insufficient cell numbers were available for post-sorting purity validation. Thus, there was no way of determining whether the sorting gates displayed on the software correlated to the final cell purity. The results instead represent an interesting starting point of an investigation which has implications for the intradermal delivery of vaccines, especially in conditions such as influenza, where $CD8^+$ T-cell responses are critical for viral clearance from the lungs (Helft et al., 2012).

It was also noted that HLA-A2 frequency in the general population is roughly 50% (Ellis et al., 2000) but five of the six donors used in the unsorted cell experiment were positive for HLA-A2. The results with the single HLA-A2- sample obtained appear to validate the HLA-A2 specificity of the T-cell clone response though further repeats may be necessary to provide full confirmation. The sorted cell experiment, which had one HLA-A2+ and one HLA-A2- sample provided further confirmation of initial results and

allowed an initial insight into the behaviour of each subset in isolation but again further repeats would confer greater reliability on the conclusions that can be drawn. The limited supply of abdominoplasty tissues of the size needed for these experiments meant that further repeats could not be obtained during the period of this study.

The next stage of investigation will aim to combine the immunological study with vaccine delivery optimisation. This will involve delivery of vaccine via a number of candidate microneedle devices as well as via the currently used hypodermic delivery route. Skin can then be cultured to allow vaccine uptake and then the tissue processed for cell walkouts. The walkout cells can then be immediately co-cultured with T-cell clones to measure cross-presentation of antigen. Histological studies of the tissue will also be utilised to show both delivery site and tracking of the antigen in tissue following uptake.

4.6 Potential for Publication

The work investigating the cross-presentation of influenza virus matrix peptide by *ex vivo* human skin cells is currently being prepared for submission for publication. Monocyte-derived models were used mainly for protocol validation and so will not form part of the publication, though may be useful as supplementary data. The sorted skin cell data represents an interesting initial result, though the lack of post-sort purity validation will limit its usefulness in a publication.

4.7 Conclusion

This chapter explored monocyte-derived DC models, which proved to be a flexible and useful model to study DC functions, though less representative of actual DCs *in vivo* than the *ex vivo* skin-derived walkout cells. Monocyte-derived DCs were utilised to optimise protocols for both cell stimulation and antigen presentation assays. The protocols could then be applied to walkout *ex vivo* skin cells. The walkout *ex vivo* skin cell model proved to be well-suited to an antigen cross-presentation experiment using influenza vaccines and CD8+ T-cell clones. The results showed that concerning the

inactivated influenza A virus-derived matrix protein (M1)-derived peptide GILGFVFTL, *ex vivo* human skin dDCs were more potent cross-presenting cells than LCs. The results confirm that targeting the dermis is a good strategy for intradermal delivery technologies, as the epidermis is thin and tightly packed which acts as a barrier to delivery there and LCs in our model had a more limited capacity to mount an effective immune response compared to dDCs. Future work should investigate other viral peptides that are integral to an antiviral immune response against influenza.

4.7 Bibliography

ALBERT, M. L., SAUTER, B. & BHARDWAJ, N. 1998. Dendritic cells acquire antigen from apoptotic cells and induce class I-restricted CTLs. *Nature,* 392**,** 86-9.

AMADORI, A., ZAMARCHI, R., DE SILVESTRO, G., FORZA, G., CAVATTON, G., DANIELI, G. A., CLEMENTI, M. & CHIECO-BIANCHI, L. 1995. Genetic control of the CD4/CD8 T-cell ratio in humans. *Nat Med,* 1**,** 1279-83.

ARNAIZ-VILLENA, A., BENMAMAR, D., ALVAREZ, M., DIAZ-CAMPOS, N., VARELA, P., GOMEZ-CASADO, E. & MARTINEZ-LASO, J. 1995. HLA allele and haplotype frequencies in Algerians. Relatedness to Spaniards and Basques. *Hum Immunol,* 43**,** 259-68.

BACHY, V., HERVOUET, C., BECKER, P. D., CHORRO, L., CARLIN, L. M., HERATH, S., PAPAGATSIAS, T., BARBAROUX, J. B., OH, S. J., BENLAHRECH, A., ATHANASOPOULOS, T., DICKSON, G., PATTERSON, S., KWON, S. Y., GEISSMANN, F. & KLAVINSKIS, L. S. 2013. Langerin negative dendritic cells promote potent CD8+ T-cell priming by skin delivery of live adenovirus vaccine microneedle arrays. *Proc Natl Acad Sci U S A,* 110**,** 3041-6.

BAKER, B. M., SCOTT, D. R., BLEVINS, S. J. & HAWSE, W. F. 2012. Structural and dynamic control of T-cell receptor specificity, cross-reactivity, and binding mechanism. *Immunol Rev,* 250**,** 10-31.

BEDOUI, S., WHITNEY, P. G., WAITHMAN, J., EIDSMO, L., WAKIM, L., CAMINSCHI, I., ALLAN, R. S., WOJTASIAK, M., SHORTMAN, K., CARBONE, F. R., BROOKS, A. G. & HEATH, W. R. 2009. Cross-presentation of viral and self antigens by skin-derived CD103+ dendritic cells. *Nat Immunol,* 10**,** 488-95.

BURGDORF, S., KAUTZ, A., BOHNERT, V., KNOLLE, P. A. & KURTS, C. 2007. Distinct pathways of antigen uptake and intracellular routing in CD4 and CD8 T cell activation. *Science,* 316**,** 612-6.

CAMPANELLI, R., PALERMO, B., GARBELLI, S., MANTOVANI, S., LUCCHI, P., NECKER, A., LANTELME, E. & GIACHINO, C. 2002. Human CD8 co-receptor is strictly involved in MHC-peptide tetramer-TCR binding and T cell activation. *Int Immunol,* 14**,** 39-44.

CAUCHETEUX, S. M., MITCHELL, J. P., IVORY, M. O., HIROSUE, S., HAKOBYAN, S., DOLTON, G., LADELL, K., MINERS, K., PRICE, D. A., KAN-MITCHELL, J., SEWELL, A. K., NESTLE, F., MORIS, A., KAROO, R. O., BIRCHALL, J. C., SWARTZ, M. A., HUBBEL, J. A., BLANCHET, F. P. & PIGUET, V. 2016. Polypropylene Sulfide Nanoparticle p24 Vaccine Promotes Dendritic Cell-Mediated Specific Immune Responses against HIV-1. *J Invest Dermatol,* 136**,** 1172-81.

CHALLIER, J., BRUNIQUEL, D., SEWELL, A. K. & LAUGEL, B. 2013. Adenosine and cAMP signalling skew human dendritic cell differentiation towards a tolerogenic phenotype with defective CD8(+) T-cell priming capacity. *Immunology,* 138**,** 402-10.

CHU, C. C., ALI, N., KARAGIANNIS, P., DI MEGLIO, P., SKOWERA, A., NAPOLITANO, L., BARINAGA, G., GRYS, K., SHARIF-PAGHALEH, E., KARAGIANNIS, S. N., PEAKMAN, M., LOMBARDI, G. & NESTLE, F. O. 2012. Resident CD141 (BDCA3)+ dendritic cells in human skin produce IL-10 and induce regulatory T cells that suppress skin inflammation. *J Exp Med,* 209**,** 935-45.

CLEMENT, M., LADELL, K., EKERUCHE-MAKINDE, J., MILES, J. J., EDWARDS, E. S., DOLTON, G., WILLIAMS, T., SCHAUENBURG, A. J., COLE, D. K., LAUDER, S. N., GALLIMORE, A. M., GODKIN, A. J., BURROWS, S. R., PRICE, D. A., SEWELL, A. K. & WOOLDRIDGE, L. 2011. Anti-CD8 antibodies can trigger CD8+ T cell effector function in the absence of TCR engagement and improve peptide-MHCI tetramer staining. *J Immunol,* 187**,** 654-63.

DAVEY, G. M., WOJTASIAK, M., PROIETTO, A. I., CARBONE, F. R., HEATH, W. R. & BEDOUI, S. 2010. Cutting edge: priming of CD8 T cell immunity to herpes simplex virus type 1 requires cognate TLR3 expression in vivo. *J Immunol,* 184**,** 2243-6.

DE FILETTE, M., MIN JOU, W., BIRKETT, A., LYONS, K., SCHULTZ, B., TONKYRO, A., RESCH, S. & FIERS, W. 2005. Universal influenza A vaccine: Optimization of M2-based constructs. *Virology,* 337**,** 149-161.

DOLTON, G., TUNGATT, K., LLOYD, A., BIANCHI, V., THEAKER, S. M., TRIMBY, A., HOLLAND, C. J., DONIA, M., GODKIN, A. J., COLE, D. K., THOR STRATEN, P., PEAKMAN, M., SVANE, I. M. & SEWELL, A. K. 2015. More tricks with tetramers: a practical guide to staining T cells with peptide–MHC multimers. *Immunology,* 146**,** 11-22.

EL-SAHRIGY, S. A., MOHAMED, N. A., TALKHAN, H. A. & RAHMAN, A. M. 2015. Comparison between magnetic activated cell sorted monocytes and monocyte adherence techniques for in vitro generation of immature dendritic cells: an Egyptian trial. *Cent Eur J Immunol,* 40**,** 18-24.

ELLIS, J. M., HENSON, V., SLACK, R., NG, J., HARTZMAN, R. J. & KATOVICH HURLEY, C. 2000. Frequencies of HLA-A2 alleles in five U.S. population groups: Predominance of A∗02011 and identification of HLA-A∗0231. *Human Immunology,* 61**,** 334-340.

ENGELHARD, V. H. 1994. Structure of peptides associated with class I and class II MHC molecules. *Annu Rev Immunol,* 12**,** 181-207.

FURUYA, Y., REGNER, M., LOBIGS, M., KOSKINEN, A., MULLBACHER, A. & ALSHARIFI, M. 2010. Effect of inactivation method on the cross-protective immunity induced by whole 'killed' influenza A viruses and commercial vaccine preparations. *J Gen Virol,* 91**,** 1450-60.

GEISSMANN, F., PROST, C., MONNET, J.-P., DY, M., BROUSSE, N. & HERMINE, O. 1998. Transforming Growth Factor β1, in the Presence of Granulocyte/Macrophage Colony-stimulating Factor and Interleukin 4, Induces Differentiation of Human Peripheral Blood Monocytes into Dendritic Langerhans Cells. *The Journal of Experimental Medicine,* 187**,** 961-966.

GUIRONNET, G., DEZUTTER-DAMBUYANT, C., VINCENT, C., BECHETOILLE, N., SCHMITT, D. & PEGUET-NAVARRO, J. 2002. Antagonistic effects of IL-4 and TGF-beta1 on Langerhans cell-related antigen expression by human monocytes. *J Leukoc Biol,* 71**,** 845-53.

HANIFFA, M., SHIN, A., BIGLEY, V., MCGOVERN, N., TEO, P., SEE, P., WASAN, P. S., WANG, X. N., MALINARICH, F., MALLERET, B., LARBI, A., TAN, P., ZHAO, H., POIDINGER, M., PAGAN, S., COOKSON, S., DICKINSON, R., DIMMICK, I., JARRETT, R. F., RENIA, L., TAM, J., SONG, C., CONNOLLY, J., CHAN, J. K., GEHRING, A., BERTOLETTI, A., COLLIN, M. & GINHOUX, F. 2012. Human tissues contain CD141hi cross-presenting dendritic cells with functional homology to mouse CD103+ nonlymphoid dendritic cells. *Immunity,* 37**,** 60-73.

HEATH, W. R. & CARBONE, F. R. 2001. Cross-presentation, dendritic cells, tolerance and immunity. *Annu Rev Immunol,* 19**,** 47-64.

HELFT, J., MANICASSAMY, B., GUERMONPREZ, P., HASHIMOTO, D., SILVIN, A., AGUDO, J., BROWN, B. D., SCHMOLKE, M., MILLER, J. C., LEBOEUF, M., MURPHY, K. M., GARCIA-SASTRE, A. & MERAD, M. 2012. Cross-presenting CD103+ dendritic cells are protected from influenza virus infection. *J Clin Invest,* 122**,** 4037-47.

ITO, T., GORMAN, O. T., KAWAOKA, Y., BEAN, W. J. & WEBSTER, R. G. 1991. Evolutionary analysis of the influenza A virus M gene with comparison of the M1 and M2 proteins. *Journal of Virology,* 65**,** 5491-5498.

JANEWAY, C. A., JR. 1991. The co-receptor function of CD4. *Semin Immunol,* 3**,** 153-60.

JOFFRE, O. P., SEGURA, E., SAVINA, A. & AMIGORENA, S. 2012. Cross-presentation by dendritic cells. *Nat Rev Immunol,* 12**,** 557-569.

JONGBLOED, S. L., KASSIANOS, A. J., MCDONALD, K. J., CLARK, G. J., JU, X., ANGEL, C. E., CHEN, C. J., DUNBAR, P. R., WADLEY, R. B., JEET, V., VULINK, A. J., HART,

D. N. & RADFORD, K. J. 2010. Human CD141+ (BDCA-3)+ dendritic cells (DCs) represent a unique myeloid DC subset that cross-presents necrotic cell antigens. *J Exp Med,* 207**,** 1247-60.

KANG, S.-M., YOO, D.-G., LIPATOV, A. S., SONG, J.-M., DAVIS, C. T., QUAN, F.-S., CHEN, L.-M., DONIS, R. O. & COMPANS, R. W. 2009. Induction of Long-Term Protective Immune Responses by Influenza H5N1 Virus-Like Particles. *PLoS ONE,* 4**,** e4667.

KLECHEVSKY, E., MORITA, R., LIU, M., CAO, Y., COQUERY, S., THOMPSON-SNIPES, L. A., BRIERE, F., CHAUSSABEL, D., ZURAWSKI, G., PALUCKA, A. K., REITER, Y., BANCHEREAU, J. & UENO, H. 2008. Functional Specializations of Human Epidermal Langerhans Cells and CD14(+) Dermal Dendritic Cells. *Immunity,* 29**,** 497-510.

LE GOFFIC, R., POTHLICHET, J., VITOUR, D., FUJITA, T., MEURS, E., CHIGNARD, M. & SI-TAHAR, M. 2007. Cutting Edge: Influenza A virus activates TLR3-dependent inflammatory and RIG-I-dependent antiviral responses in human lung epithelial cells. *J Immunol,* 178**,** 3368-72.

LEE, H. K., ZAMORA, M., LINEHAN, M. M., IIJIMA, N., GONZALEZ, D., HABERMAN, A. & IWASAKI, A. 2009. Differential roles of migratory and resident DCs in T cell priming after mucosal or skin HSV-1 infection. *J Exp Med,* 206**,** 359-70.

LEON, B., LOPEZ-BRAVO, M. & ARDAVIN, C. 2005. Monocyte-derived dendritic cells. *Semin Immunol,* 17**,** 313-8.

MAKHATADZE, N. J., FRANCO, M. T. & LAYRISSE, Z. 1997. HLA class I and class II allele and haplotype distribution in the Venezuelan population. *Hum Immunol,* 55**,** 53-8.

MARIOTTI, S. & NISINI, R. 2009. Generation of human T cell clones. *Methods Mol Biol,* 514**,** 65-93.

MATTHIS, J. & REIJONEN, H. 2013. Production of Primary Human CD4+ T Cell Lines and Clones. *Methods in molecular biology (Clifton, N.J.),* 960**,** 545-555.

MAYER, A., LEE, S., LENDLEIN, A., JUNG, F. & HIEBL, B. 2011. Efficacy of CD14(+) blood monocytes/macrophages isolation: positive versus negative MACS protocol. *Clin Hemorheol Microcirc,* 48**,** 57-63.

MESTAS, J. & HUGHES, C. C. 2004. Of mice and not men: differences between mouse and human immunology. *J Immunol,* 172**,** 2731-8.

MURPHY, K., TRAVERS, P., WALPORT, M. & JANEWAY, C. 2012. *Janeway's Immunobiology (8th ed.),* New York, Garland Science.

NEIRYNCK, S., DEROO, T., SAELENS, X., VANLANDSCHOOT, P., JOU, W. M. & FIERS, W. 1999. A universal influenza A vaccine based on the extracellular domain of the M2 protein. *Nat Med,* 5**,** 1157-63.

NESTLE, F. O., ZHENG, X. G., THOMPSON, C. B., TURKA, L. A. & NICKOLOFF, B. J. 1993. Characterization of dermal dendritic cells obtained from normal human skin reveals phenotypic and functionally distinctive subsets. *J Immunol,* 151**,** 6535-45.

NI, K. & O'NEILL, H. C. 1997. The role of dendritic cells in T cell activation. *Immunol Cell Biol,* 75**,** 223-30.

NORRIS, P. J., SUMAROKA, M., BRANDER, C., MOFFETT, H. F., BOSWELL, S. L., NGUYEN, T., SYKULEV, Y., WALKER, B. D. & ROSENBERG, E. S. 2001. Multiple Effector Functions Mediated by Human Immunodeficiency Virus-Specific CD4(+) T-Cell Clones. *Journal of Virology,* 75**,** 9771-9779.

OH, J. Z., KURCHE, J. S., BURCHILL, M. A. & KEDL, R. M. 2011. TLR7 enables cross-presentation by multiple dendritic cell subsets through a type I IFN-dependent pathway. *Blood,* 118**,** 3028-3038.

PEISER, M., WANNER, R. & KOLDE, G. 2004. Human epidermal Langerhans cells differ from monocyte-derived Langerhans cells in CD80 expression and in secretion of IL-12 after CD40 cross-linking. *J Leukoc Biol,* 76**,** 616-22.

PENA-CRUZ, V., ITO, S., OUKKA, M., YONEDA, K., DASCHER, C. C., VON LICHTENBERG, F. & SUGITA, M. 2001. Extraction of human Langerhans cells: a method for isolation of epidermis-resident dendritic cells. *J Immunol Methods,* 255**,** 83-91.

PIEMONTI, L., MONTI, P., SIRONI, M., FRATICELLI, P., LEONE, B. E., DAL CIN, E., ALLAVENA, P. & DI CARLO, V. 2000. Vitamin D3 affects differentiation, maturation, and function of human monocyte-derived dendritic cells. *J Immunol,* 164**,** 4443-51.

QUAH, B. J. C. & PARISH, C. R. 2010. The Use of Carboxyfluorescein Diacetate Succinimidyl Ester (CFSE) to Monitor Lymphocyte Proliferation. *J Vis Exp***,** 2259.

QUAN, F. S., KIM, Y., LEE, S., YI, H., KANG, S. M., BOZJA, J., MOORE, M. L. & COMPANS, R. W. 2011. Viruslike particle vaccine induces protection against respiratory syncytial virus infection in mice. *J Infect Dis,* 204**,** 987-95.

REPNIK, U., KNEZEVIC, M. & JERAS, M. 2003. Simple and cost-effective isolation of monocytes from buffy coats. *J Immunol Methods,* 278**,** 283-92.

RUEDL, C., STORNI, T., LECHNER, F., BACHI, T. & BACHMANN, M. F. 2002. Cross-presentation of virus-like particles by skin-derived CD8(-) dendritic cells: a dispensable role for TAP. *Eur J Immunol,* 32**,** 818-25.

SALLUSTO, F. & LANZAVECCHIA, A. 1994. Efficient presentation of soluble antigen by cultured human dendritic cells is maintained by granulocyte/macrophage colony-stimulating factor plus interleukin 4 and downregulated by tumor necrosis factor alpha. *J Exp Med,* 179**,** 1109-18.

SANTAMBROGIO, L., SATO, A. K., CARVEN, G. J., BELYANSKAYA, S. L., STROMINGER, J. L. & STERN, L. J. 1999. Extracellular antigen processing and presentation by immature dendritic cells. *Proceedings of the National Academy of Sciences of the United States of America,* 96**,** 15056-15061.

SCHMITZ, B., RADBRUCH, A., KUMMEL, T., WICKENHAUSER, C., KORB, H., HANSMANN, M. L., THIELE, J. & FISCHER, R. 1994. Magnetic activated cell sorting (MACS)--a new immunomagnetic method for megakaryocytic cell isolation: comparison of different separation techniques. *Eur J Haematol,* 52**,** 267-75.

SCHULZ, O., DIEBOLD, S. S., CHEN, M., NASLUND, T. I., NOLTE, M. A., ALEXOPOULOU, L., AZUMA, Y. T., FLAVELL, R. A., LILJESTROM, P. & REIS E SOUSA, C. 2005. Toll-like receptor 3 promotes cross-priming to virus-infected cells. *Nature,* 433**,** 887-92.

SCHWANKE, U., NABEREIT, A. & MOOG, R. 2006. Isolation of monocytes from whole blood-derived buffy coats by continuous counter-flow elutriation. *J Clin Apher,* 21**,** 153-7.

SEGURA, E., DURAND, M. & AMIGORENA, S. 2013. Similar antigen cross-presentation capacity and phagocytic functions in all freshly isolated human lymphoid organ-resident dendritic cells. *J Exp Med,* 210**,** 1035-47.

SHORTMAN, K. & NAIK, S. H. 2007. Steady-state and inflammatory dendritic-cell development. *Nat Rev Immunol,* 7**,** 19-30.

SIMS, S., WILLBERG, C. & KLENERMAN, P. 2010. MHC-peptide tetramers for the analysis of antigen-specific T cells. *Expert Rev Vaccines,* 9**,** 765-74.

SITRIN, R., ZHAO, Q., POTTER, C., CARRAGHER, B. & WASHABAUGH, M. 2015. Recombinant Virus-like Particle Protein Vaccines. *In:* NUNNALLY, B. K., TURULA, V. E. & SITRIN, R. D. (eds.) *Vaccine Analysis: Strategies, Principles, and Control.* Springer Berlin Heidelberg.

STOITZNER, P. 2010. The Langerhans cell controversy: are they immunostimulatory or immunoregulatory cells of the skin immune system[quest]. *Immunol Cell Biol,* 88**,** 348-350.

STOITZNER, P., TRIPP, C. H., EBERHART, A., PRICE, K. M., JUNG, J. Y., BURSCH, L., RONCHESE, F. & ROMANI, N. 2006. Langerhans cells cross-present antigen derived from skin. *Proc Natl Acad Sci U S A,* 103**,** 7783-8.

TURLEY, S. J., INABA, K., GARRETT, W. S., EBERSOLD, M., UNTERNAEHRER, J., STEINMAN, R. M. & MELLMAN, I. 2000. Transport of peptide-MHC class II complexes in developing dendritic cells. *Science,* 288**,** 522-7.

VAN DER AAR, A. M., DE GROOT, R., SANCHEZ-HERNANDEZ, M., TAANMAN, E. W., VAN LIER, R. A., TEUNISSEN, M. B., DE JONG, E. C. & KAPSENBERG, M. L. 2011. Cutting edge: virus selectively primes human langerhans cells for CD70 expression promoting CD8+ T cell responses. *J Immunol,* 187**,** 3488-92.

VAN DER AAR, A. M., PICAVET, D. I., MULLER, F. J., DE BOER, L., VAN CAPEL, T. M., ZAAT, S. A., BOS, J. D., JANSSEN, H., GEORGE, T. C., KAPSENBERG, M. L., VAN HAM, S. M., TEUNISSEN, M. B. & DE JONG, E. C. 2013. Langerhans cells favor skin flora tolerance through limited presentation of bacterial antigens and induction of regulatory T cells. *J Invest Dermatol,* 133**,** 1240-9.

WÖLFL, M. & GREENBERG, P. D. 2014. Antigen-specific activation and cytokine-facilitated expansion of naive, human CD8+ T cells. *Nat. Protocols,* 9**,** 950-966.

YOSHIDA, K., KUBO, A., FUJITA, H., YOKOUCHI, M., ISHII, K., KAWASAKI, H., NOMURA, T., SHIMIZU, H., KOUYAMA, K., EBIHARA, T., NAGAO, K. & AMAGAI, M. 2014. Distinct behavior of human Langerhans cells and inflammatory dendritic epidermal cells at tight junctions in patients with atopic dermatitis. *Journal of Allergy and Clinical Immunology,* 134**,** 856-864.

Chapter 5- Delivery of Peptide Antigen into Skin Utilising Cubosomes

5.1 Introduction

5.1.1 Colloidal Formulations for Intradermal Vaccine Delivery

The hydrophobic stratum corneum (SC) is a significant barrier to the delivery of vaccines into the skin (Desai et al., 2010). Chapter 2 explored mechanical SC disruption using microneedle arrays to allow vaccine delivery into the skin. An alternative strategy is chemical negation of the barrier properties of the SC to allow antigen penetration into the skin (Benson and Namjoshi, 2008, Williams and Barry, 2012). One such technology that has been explored is formulation of the vaccine into an emulsion- colloidal systems where antigen is entrapped within lipid droplets that are dispersed in an aqueous continuous phase (Watson et al., 2012). The mechanism by which colloidal systems improve transdermal delivery are not fully understood. There are four methods that have been described - intact vesicles penetrating the skin, vesicles acting as penetration enhancers by fluidising skin lipids, exchange between the vesicles and skin lipids termed 'collision complex transfer' and enhanced delivery via appendages such as sweat glands (Hua, 2015). The mechanism(s) by which a given formulation will enhance delivery into the skin are a function of the lipid components and the lipid droplet size contained in the formulation (Verma et al., 2003, Pierre and dos Santos Miranda Costa, 2011).

Historically, vesicular systems have most commonly been used for the intradermal delivery of small molecule drugs (Cevc, 1996, Hua, 2014, Honeywell-Nguyen and Bouwstra, 2003) into the skin rather than biological macromolecules. There have however been a number of studies that utilised lipid colloid formulations to aid the delivery of DNA (Alexander and Akhurst, 1995), protein (Weiner et al., 1989) or peptide (Fleisher et al., 1995) into the skin. Colloidal formulations not only improve the movement of molecules across the stratum corneum but can also improve the presentation of antigen (Schwendener, 2014) and favour retention within the skin (Cevc, 1996)- both of which can help to improve the immune response brought about by the subsets of skin-resident immune cells. The delivery characteristics of colloidal systems can be tailored by altering the type and proportions of lipid components used to form their dispersed phase (Schwendener, 2014). This provides a level of design flexibility to

the delivery technology so that delivery kinetics, depth of delivery in the skin and retention at the site of delivery can all be optimised.

The lipid components and manufacturing processes used determine the structure of the dispersed phase. The earliest systems described were liposomes, where an amphiphilic dispersed phase spontaneously arranges into spherical particles contained by a bilayer. This allows the entrapment of hydrophilic substances within the particle's aqueous interior or entrapment within the bilayer of hydrophobic drugs. Other technologies that have developed from conventional liposomes are shown in Figure 5.1. Transfersomes® and ethosomes are 'ultradeformable' particles, being able to alter shape to fit through the tight junctions in the skin without losing structural integrity (Hua, 2015). Niosomes are composed of a single chain surfactant molecule and cholesterol; their surfactant properties make the stratum corneum more permeable to the delivery of the drug within it (Kazi et al., 2010). All three of these liposomal formulations have improved stability compared to conventional liposomes (Hua, 2015).

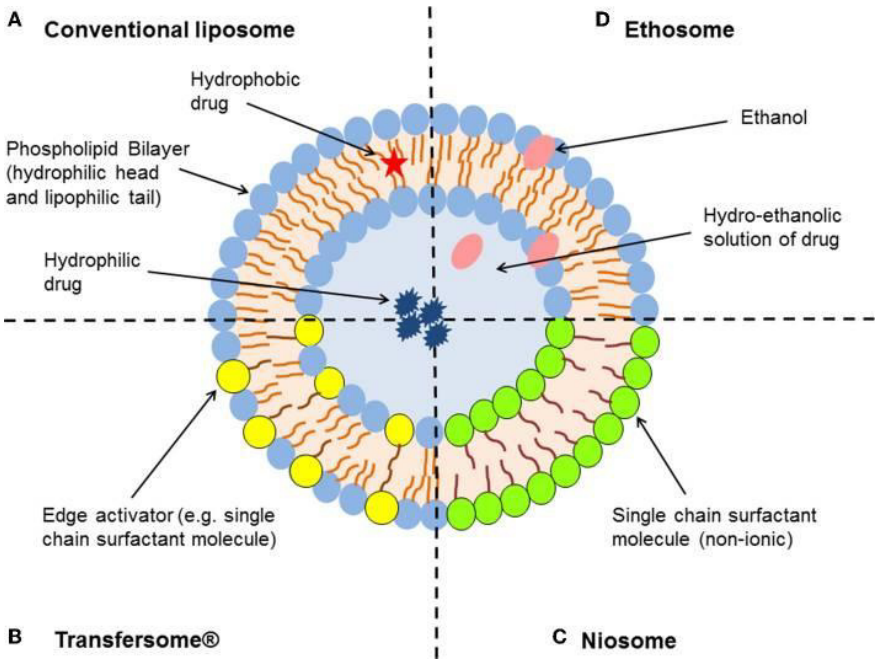

Figure 5.1: Structure of liposomal delivery technologies (taken from (Hua, 2015))

5.1.1.1 Cubosomes

A further colloidal formulation which shows potential for use in intradermal delivery of biological macromolecules such as vaccines is cubosomes. The lipid components of cubosomes arrange into an ordered liquid crystalline structure Figure 5.2 termed the 'cubic phase' (Karami and Hamidi, 2015). This cubic structure led to the coining of the term cubosomes to describe the cubic liposomes. It is possible to disperse the lipid phase in an aqueous medium, producing lipid nanoparticles which retain the cubic phase characteristics at the nanostructural level (Demurtas et al., 2015). Within the particles, the cubosome lipid phase forms a continuous bilayer that separates two non-intersecting channels containing the aqueous phase (Karami and Hamidi, 2015). This property allows them to entrap a range of hydrophilic, hydrophobic and amphiphilic molecules or macromolecules (Pan et al., 2013). The tortuous water channels contained within the dispersed phase give cubosomes potential use in controlled release applications also (Clogston and Caffrey, 2005).

Cubosomes have been studied by a number of groups, using various lipid components including glycerol monooleate (Lopes et al., 2006) and phytantriol (Bender et al., 2008). This chapter builds upon the work of Professor Sarah Hook's lab in the University of Otago who produced cubosomes using phytantriol as the lipid phase, propyleneglycol as a hydrotrope and poloxamer 407 to stabilise the particulate system (Kojarunchitt et al., 2011, Rattanapak et al., 2014). Two methods of producing cubosomes have been described- top-down and bottom-up techniques (Garg and Saraf, 2007). The top-down method involves the assembly of the cubic lipid phase first before dispersion in the aqueous medium by some high-energy process such as vortexing. The bottom-up technique involves dispersing the components of cubosomes into water at

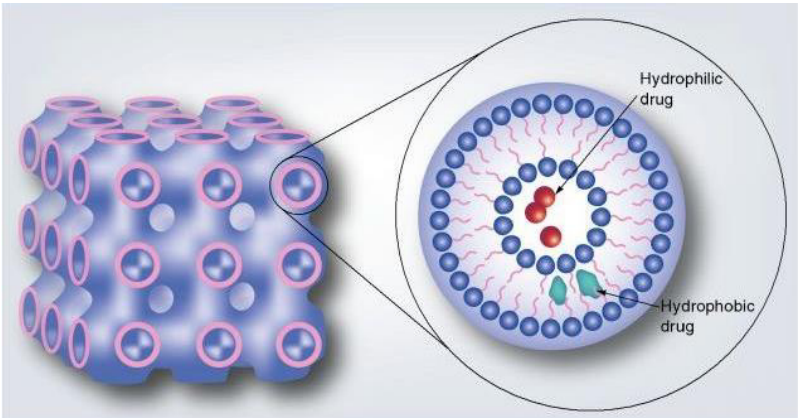

Figure 5.2: The structure of cubosomes- a liposomal formulation that spontaneously arranges into a cubic liquid crystal structure (adapted from (Bei et al., 2010))

80°C before cooling the water to allow the components to crystallise into cubosomes. Most work to date uses the top-down technique though this requires high energy input and the viscosity of the bulk cubic phase makes scaling-up the process difficult (Prashar and Sharma, 2011). Care must also be taken to ensure the compatibility of entrapped drugs or vaccines in the formulation to ensure they do not disrupt the cubic phase structure.

Previous work by the Hook lab (Rattanapak et al., 2013) and others (Bender et al., 2005, Lopes et al., 2007) has shown that when applied to intact stratum corneum, cubosomes can improve the permeation of protein, peptide or drug into the skin. They speculated that the nanostructural similarities between lipids in cubosomes and the stratum corneum can allow the cubosomes to 'fluidise' the stratum corneum and improve the movement of substances across it (Esposito et al., 2005). A synergistic improvement was seen when cubosomes were applied to skin following microneedle pre-treatment (Rattanapak et al., 2014). It was also shown that cubosomes tended to aggregate at the site of delivery, creating a depot of formulation which can improve retention within the skin (Rattanapak et al., 2013, Clogston and Caffrey, 2005). This may increase the time immune cells are exposed to antigen and therefore increase the number of cells that can transport antigen to the lymph nodes and increase the likelihood of immunity being established.

5.1.2 Formulation Characterisation

Though cubosome studies had been performed previously in collaboration with Cardiff University, the earlier formulation work had been completed in the labs in New Zealand. With no guarantee of consistency of formulation manufacture between the two labs, it was essential to establish that formulations of an acceptable standard could be produced in Cardiff. It was also vital that stability testing was performed to verify the timescales over which formulations could be used in experimentation. Two methods are commonly used to characterise the cubosome formulations - transmission electron microscopy, to provide visual characterisation, and particle analysis, to provide quantitative data on the diameter, polydispersity and surface charge of lipid particles.

5.1.2.1 Transmission Electron Microscopy

Transmission electron microscopy (TEM) is a powerful tool for imaging samples at high resolution. For liquid formulations, such as the cubosomes used in this chapter, sample preparation requires snap freezing of the sample at a thickness of less than 500nm and maintenance at low temperature throughout imaging (Almgren et al., 2000). The sample is then exposed to a beam of electrons and a detector underneath the sample monitors electrons which are 'transmitted' through the sample- the absorption of electrons is a function of the sample density in a given area (Reimer, 2013). The electrons which are transmitted through the sample are detected and an image can be produced with density differences apparent. TEM's high magnification is possible due to the wavelength of electrons being smaller than the wavelength of visible light, thus making the resolution much greater (Williams and Carter, 1996). TEM can provide an insight into the structural appearance of lipid particles, the arrangement of particles within the aqueous phase and by comparing images of cubosomes with and without incorporated antigen, providing qualitative data on the effects of vaccine incorporation into cubosomes.

5.1.2.2 Malvern Zetasizer Nano

The Malvern Zetasizer Nano utilises two analyses- dynamic light scattering (DLS) and zeta potential analysis- to provide quantitative data on particle size and surface charge of particles in colloidal liquids. DLS passes a beam of laser light through a sample, which will undergo refraction as it passes from aqueous phase through the dispersed phase. The angle of refraction varies proportionally with the size of the dispersed phase particles and so can be used to calculate mean particle size (Berne and Pecora, 1976). The software uses a simple 2 parameter fit to the cumulants analysis of particle size data to calculate the polydispersity index (PDI)- a measure of size distribution of particles within the sample (Malvern Instruments, 2011). PDI values calculated by the software normally fall between 0.05 (monodispersity) and 0.7 (an extremely polydisperse system) (Malvern Instruments, 2011). With respect to cubosome synthesis, a low PDI is desirable as it shows consistency in the synthesis process. It is also important to monitor size and PDI following storage, to provide a measure of the tendency of the colloidal system to flocculate or coalesce.

Zeta potential is a measurement of the electrical potential at the effective outer surface of particle within a colloidal system. As shown in Figure 5.3, the effective outer surface of a charged particle is not simply the edge of the dispersed phase particle but instead includes a layer of adsorbed ions of opposite charge (the Stern layer) and a layer of ions with mixed charges which are less strongly attracted to the particle (the diffuse layer) (Hunter, 2013). Together the Stern layer and diffuse layer form the electrical double layer. The zeta potential is a measurement of the potential difference between the outer edge of the electrical double layer (the 'slipping plane') and the bulk phase at a distal point (Figure 5.3). Zeta potential can be used as a predictor of colloid stability- a large zeta potential confers charge at the outer surface of the colloid particles (Hunter, 2013). Particles with similar charge at their surface will be repelled from one another, thus reducing the likelihood of aggregation and improving the stability of the system (Riddick, 1968). A zeta potential greater than 30mV (either +30mV or -30mV) is considered adequate to ensure particles do not aggregate (Mandzy et al., 2005, Li et al., 2008). Whether the dispersed phase possesses a positive or negative zeta potential depends on the characteristics of both dispersed and continuous phases.

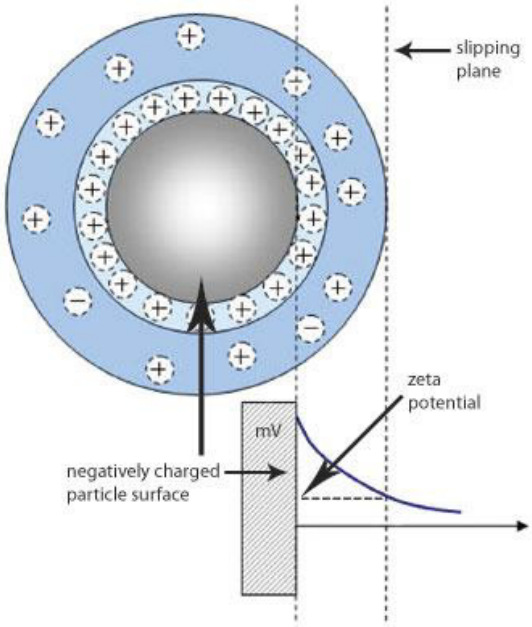

Figure 5.3: Zeta potential of a particle with a negative surface charge and therefore a positive zeta potential when suspended in a continuous phase (from http://www.horiba.com/scientific/products/particle-characterization/applications/colloids/)

5.1.3 Intravital Two-Photon Microscopy

As discussed in previous chapters, immunofluorescence is a powerful tool for the visualisation of cells and formulation following delivery into *ex vivo* human skin. There are a number of limitations in using immunofluorescence to study the excised human skin model. Whilst the *ex vivo* human skin model is useful for generating data on the delivery of substances into skin and the behaviour of skin immune cells, it exists in isolation of the patient (and their complex body processes which may influence the skin) and only has a limited time frame of use (Ng et al., 2009). Imaging of *ex vivo* skin requires fixed samples- thus can only provide a snapshot of skin processes at the time of fixing. The penetration depth of imaging is limited in both fluorescence and confocal microscopy (Helmchen and Denk, 2005), meaning tissue sectioning is often required- thus only a small area of tissue can be imaged at one time.

One technique which overcomes some of the limitations of visualising tissue with immunofluorescence microscopy is two-photon microscopy (2PM). This is similar in principle to classic fluorescence microscopy, where laser light is used to excite fluorophores in a sample which will then emit light at a longer wavelength, allowing visualisation. 2PM differs from fluorescence microscopy in its excitation wavelength which is longer and thus the excitation photons possess lower energy- half of the energy of a standard fluorescence microscopy laser's excitation photons (Denk et al., 1990). Concurrent excitation by two photons is therefore required to elicit fluorescence from a fluorophore (So et al., 2000). This difference leads to greatly reduced background fluorescence (Denk et al., 1995), improved depth of imaging (Helmchen and Denk, 2005) and less chance of photobleaching or damage to the sample from the laser (Patterson and Piston, 2000).

The use of excitation and emission filters in 2PM imaging allows for the visualisation of multiple fluorophores concurrently. Imaging via 2PM also offers an advantage over fluorescence microscopy due to second-harmonic generation (SHG)- a phenomenon whereby laser light passing through a molecule with a non-centrosymmetric structure will have its wavelength halved (Mohler et al., 2003). This is particularly useful in the imaging of skin where SHG can be used to visualise the non-centrosymmetric structure of collagen fibrils (Williams et al., 2005). As it does not

involve the excitation of a fluorophore, SHG requires no pre-imaging staining and is less susceptible to photobleaching (Campagnola et al., 1999).

Transgenic *in vivo* models are particularly useful in combination with 2PM imaging. This investigation utilises a transgenic mouse model that expresses enhanced yellow fluorescent protein (eYFP) under the transcriptional control of the CD11c promoter (Lindquist et al., 2004). CD11c, also known as integrin α-x (ITGAX), is a protein which forms part of the integrin complement receptor 4 (CR4) along with CD18 (Sadhu et al., 2007). Within murine skin, CD11c is found exclusively on DCs- both epidermal LCs and dDCs (Lindquist et al., 2004). Thus, both types of skin immune cells can be observed concurrently without the need for staining with a fluorophore. The structural detail of the collagen fibrils within the dermis can be concurrently distinguished via SHG. The epidermis does not contain collagen fibrils and so will not produce SHG signal, allowing distinction between the two skin layers to be made. Finally, the 2PM equipment possesses a further two fluorescence channels which will be utilised to visualise fluorescently-conjugated peptide and cubosome lipid phase. Thus, the delivery of peptide, distribution of the lipid phase and immune cell behaviours can be studied concurrently.

5.1.4 Mouse Skin Model

Mice are the most widely used model species in immunological research due to their ready availability, low cost and similarities with human immune systems (Mestas and Hughes, 2004). However, mouse skin is structurally very different to human skin- mouse fur is more coarse and densely packed than the vellus hair found on human skin (Pasparakis et al., 2014) (especially on female breast skin, the major source of the *ex vivo* human skin used in previous chapters). Mouse skin is also much thinner than human skin. Murine epidermis is between 10-20µm thick (cf. 80µm in humans) (Hansen et al., 1984). Immunologically, mice share a number of characteristics with humans (Haley, 2003). Both possess LCs which whilst immature occupy the epidermis (Kel et al., 2010, de Jong et al., 2010). In both, the dermis also contains a heterogeneous population of dDCs (Klechevsky et al., 2008b, Malissen et al., 2014). It is believed that subsets can be aligned between the two species based on function rather than surface markers, where

a number of differences exist (Shortman and Liu, 2002). The discrepancies between authors on how to classify dDC subsets based on marker expression mean that work is still required before consensus is reached on the subsets of dDCs (Malissen et al., 2014). This investigation will utilise the mouse model to take advantage of being able to visualise the immune response in the skin of a live organism. We will also be able to examine the DCs of the skin and lymph nodes of the mouse after imaging to further examine the movements of mouse skin DCs and their uptake of fluorescent peptide after encountering peptide antigen, something not possible in the human *ex vivo* skin model. The results will be interpreted in the context of vaccine processing by the human DC subsets found in Chapter 4. The 2PM studies using CD11c-eYFP mice will be completed in the laboratories of Professor Masaru Ishii at Osaka University, Japan. His group has completed a large amount of work using the 2PM technique to image osteoclasts (Kowada et al., 2011), tumour cells (Kagawa et al., 2012) and skin DCs (Rattanapak et al., 2014) *in vivo* with murine models.

5.2 Aim and Objectives

The overall aim of this chapter is to produce a cubosome formulation for intradermal vaccine delivery, establish whether it is stable following a period of storage and to test how it affects delivery of ovalbumin peptide antigen into the skin of an *in vivo* mouse model. Whilst the mouse work utilises the fluorescently-conjugated peptide, a lack of availability meant that preliminary work in human *ex vivo* skin was completed using fluorescently-conjugated ovalbumin protein. The specific practical objectives are:

1. Produce cubosome formulations using a protocol previously optimised by Sarah Hook's group in the University of Otago (Rizwan et al., 2011) and characterise the formulations by TEM and using particle size, PDI and zeta potential analysis to indicate consistency with formulations from the literature.
2. Establish stability of the cubosomes following storage by assessing changes in size, PDI and zeta potential after storage times of up to 28 days.
3. Measure ovalbumin protein entrapment within cubosome formulations.

4. Use *ex vivo* human skin for preliminary testing of ovalbumin protein delivery into the skin using cubosomes in combination with solid coated microneedles and hollow microneedle devices.
5. Deliver fluorescently-labelled ovalbumin peptide (residues 257–264; SIINFEKL) into mice and characterise microneedle channel healing and skin immune cell behaviour following treatment.
6. Analyse murine immune cells isolated from skin and skin-draining lymph nodes to quantify peptide uptake and transport to lymph nodes by different skin-resident immune cells.

5.3 Materials and Methods

[All equipment and reagents obtained from Fisher Scientific, UK unless otherwise stated]

The work in this chapter focusses on the delivery of antigen into skin using cubosome formulations. It aimed to build on work previously done by a collaborator utilising cubosome formulations containing 5(6)-tetramethylcarboxy rhodamine labelled $OVA_{257–264}$ (SIINFEKL-TAMRA) as a vaccine antigen model delivered using a microneedle device (Rattanapak et al., 2013, Rattanapak et al., 2014). Before skin delivery studies *in vivo* could be completed, it was necessary to establish whether cubosome formulations could be consistently synthesised and whether they were stable following storage. It was also important to establish whether formulation could be delivered into the skin using the range of delivery methods that would be used in the *in vivo* study. Given that the *in vivo* work was to be carried out in Japan and the fluorescently-conjugated peptide that we would be utilising was unavailable for the months leading up to the work, fluorescently-conjugated ovalbumin protein was used in its place in the early characterisation studies.

5.3.1 Synthesis of Cubosomes

Cubosome formulations were synthesised using a previously published method (Rizwan et al., 2011). The lipid phase components- 100mg phytantriol (Tokyo Chemical Industry UK Ltd, UK), 268.3mg propyleneglycol (Sigma Aldrich, UK) and 15mg poloxamer

407 (Sigma Aldrich, UK)- were weighed into a 25ml round-bottomed flask and 10ml chloroform added to dissolve them. The flask was then attached to a rotary evaporator (BÜCHI Labortechnik AG, Switzerland) and mixed at 45°C for approximately 30 minutes until the chloroform had fully evaporated, leaving a visually homogeneous lipid phase. Next, 100µl of a 10mg/ml solution of ovalbumin protein with Alexa Fluor™ 555 Conjugate (Fl-OVA; Invitrogen, UK) in ddH_2O was added dropwise to the lipid phase whilst vortexing. Finally, the volume was made up to 5ml by the addition of ddH_2O in two stages under vortex. This produced final concentrations of 200µg/ml Fl-OVA, 20mg/ml phytantriol, 53.66mg/ml propyleneglycol and 3mg/ml poloxamer 407 in ddH_2O. The formulation was then homogenised by vortexing for 10 minutes. Cubosomes without Fl-OVA were synthesised as above but with 100µl ddH_2O being added to the lipid phase before being made up to the 5ml final volume. Cubosomes were stored under nitrogen at room temperature and protected from light prior to their use.

5.3.2 Physical Characterisation of Cubosomes

5.3.2.1 Zeta Potential and Particle Size Analysis

Prior to analysis, cubosome formulations either containing Fl-OVA (CuFl) or without fluorescent protein (Cu0) were diluted 1 in 50 by making 20µl of the cubosome formulation up to 1ml using ddH_2O. Particle size (z-average diameter) and size distribution of particles (polydispersity index; PDI) of colloidal particles within the cubosome formulation were measured using dynamic light scattering on a Zetasizer Nano ZS (Malvern Instruments, UK) in disposable polystyrene cuvettes with a 10mm light path. Three samples were taken from each formulation batch 24hrs after initial synthesis and size/PDI measured in triplicate at 25°C.

The zeta potential of the colloidal particles was also measured using the Zetasizer Nano ZS, this time with Folded Capillary Zeta Cells (Malvern Instruments, UK). Again three samples were taken from each batch and diluted 1 in 50 before the zeta potential was measured in triplicate.

5.3.2.2 *Transmission Electron Microscopy (TEM)*

Aliquots of 20µl each of the CuFl and Cu0 formulations were submitted to a collaborator in the School of Optometry & Vision Sciences, Cardiff University for analysis by cryogenic TEM using a JEM-2100 LaB6 Transmission Electron Microscope (JEOL, USA) with a high-resolution digital camera (Gatan, UK) utilised for image capture.

5.3.3 Protein Entrapment in Cubosomes

Fluorescence absorption/emission spectra for Fl-OVA were obtained using a Cary Eclipse fluorescence spectrophotometer (Agilent Technologies Inc., USA)- the absorption and emission maxima were determined to be 553nm and 572nm respectively (Figure 5.4).

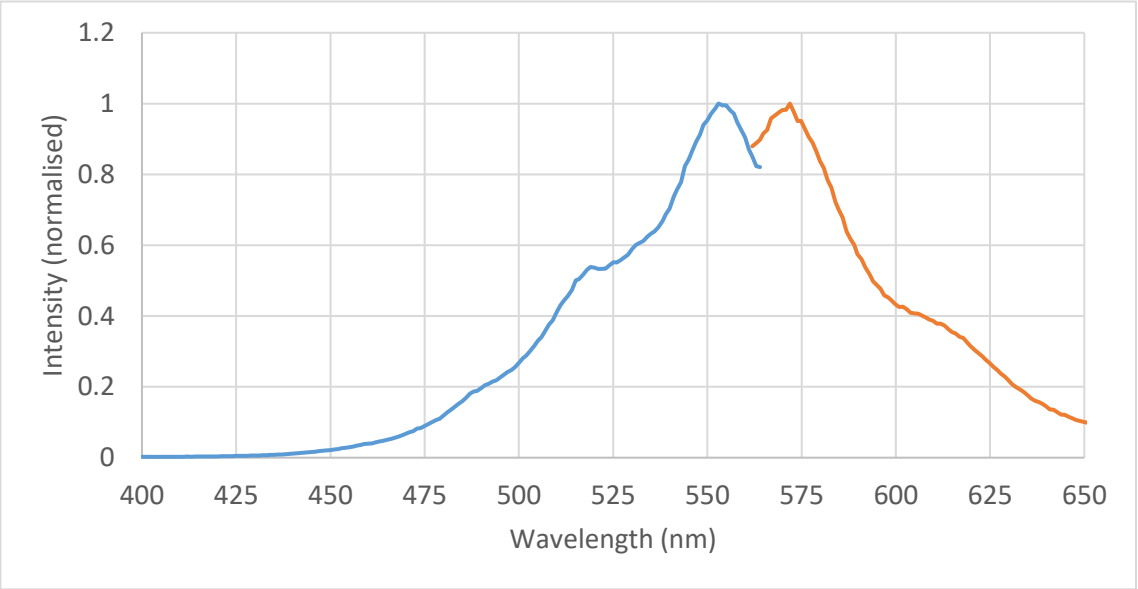

Figure 5.4: Absorbance (blue line) and emission (orange line) spectra for Fl-OVA in ddH_2O

A concentration calibration curve was produced for the concentration range 0-150µg/ml (Figure 5.5).

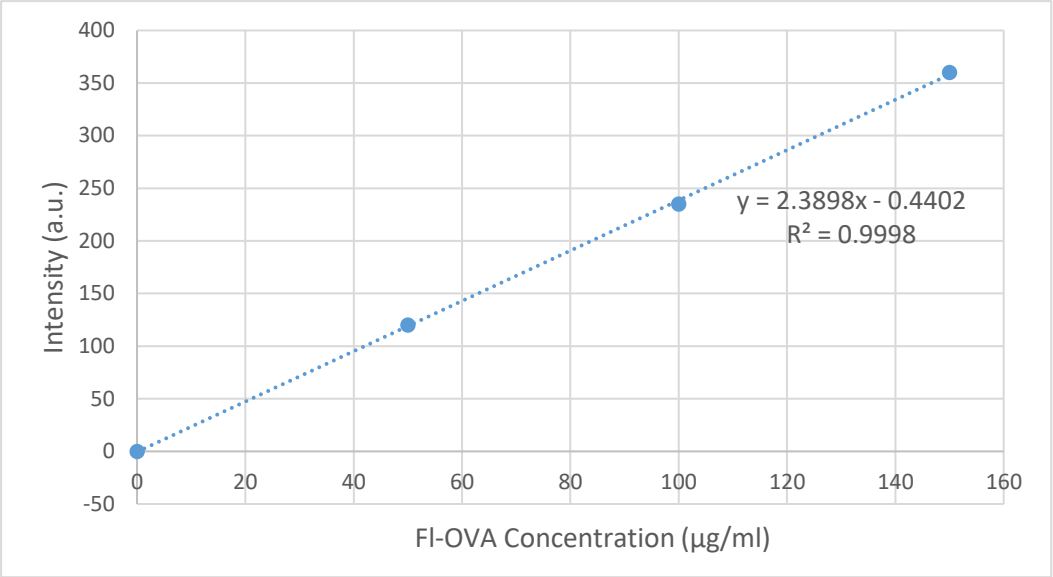

Figure 5.5: Concentration-calibration curve for Fl-OVA in ddH_2O with absorbance: 553nm and emission: 572nm

To determine the protein entrapment within cubosomes, 200µl of CuFl was centrifuged at 20,800 x g for 30 minutes, leading to the separation of the lipid and aqueous phases. The aqueous phase was then removed and diluted 1:1 with ddH_2O before fluorescence analysis with absorption and emission set to 553nm and 572nm respectively. The intensity reading could then be converted into the protein concentration using the following formula:

$$\text{Concentration of Fl-OVA in aqueous phase } (conc^{aq}) = \frac{(\text{intensity} + 0.4402)}{2.3898}$$

This provided the concentration of FL-OVA in the aqueous phase (which had been diluted 1:1). The mass of protein in the aqueous phase was then calculated:

$$\text{Mass of Fl-OVA in aqueous phase } (m^{aq}) = 2 \times conc^{aq} \times \text{volume of aqueous phase}$$

Finally, the percentage of protein entrapment could then be calculated from the mass of protein present in the 200µl cubosome formulation (m^{for}):

$$\% \text{ protein entrapment} = \left(\frac{m^{for} - m^{aq}}{m^{for}} \right) \times 100$$

5.3.4 Stability Testing of Formulations

To assess the stability of cubosomes in storage, four 500µl aliquots of CuFl and Cu0 formulations were taken and stored under nitrogen in 1.5ml microcentrifuge tubes protected from light at room temperature. At 7, 14, 21 and 28 days after initial storage, an aliquot of each formulation was analysed for size, PDI, and zeta potential using the analysis protocols described in Section 5.3.2.1.

5.3.5 Effects of Hollow Microneedle Delivery on Cubosome Formulations

The effects of two methods of cubosome delivery into the skin using microneedles were assessed to inform the *in vivo* study design- delivery as a liquid dispersion through hollow microneedle arrays or dry-coated onto solid microneedles. The MicronJet™ device (NanoPass Technologies Ltd, Israel) was selected for hollow microneedle delivery due to its prior regulatory approval supporting its use for intradermal delivery. Should promising results be found in this work with pre-clinical models using the devices, they would be available for use in clinical trials. The device is available in two needle lengths: 450µm and 600µm (MicronJet450™ and MicronJet600™ respectively). The devices possess either three 600µm or four 450µm hollow microneedles attached to a solid base (Figure 5.6) which attached to a syringe via a Luer fit connection. The microneedles can then be used in a similar fashion to hypodermic needle, with the needles inserted into the skin and pressure being applied to the plunger of the syringe to force liquid formulation into the skin.

Figure 5.6: NanoPass's MicronJet device (image taken from http://www.nanopass.com/content-e.asp?cid=19&itemid=335#;)

To ensure that the cubosome formulations were not adversely affected by delivery through the microneedle devices, CuFl and Cu0 formulations were passed through the microneedle array three times and analysed for changes in size, PDI and zeta potential as described in Section 5.3.2.1. Both MicronJet450™ and MicronJet600™ array types were assessed.

5.3.6 Coating of Cubosome Formulation onto Stainless Steel Microneedles

The potential for coating cubosome formulations onto solid stainless steel microneedles was also assessed. It was hoped that cubosome formulation could be coated onto the needles' surface and the aqueous phase allowed to evaporate. After delivery, the rehydration of the formulation would allow its release from the needles surface and the reconstitution of the cubosome formulation in the skin where it could mediate its slow release of protein or peptide. The needle design and coating method used were both as described in Section 2.3.1. Briefly, 0.6µl of CuFl formulation was drawn up into a gel-loading pipette tip before being forced out gradually to form a small droplet of liquid which could be applied to the tips of needles. The formulation was allowed to dry before subsequent layers were added until the entire volume had been used to coat 3 microneedle arrays. Coating success was assessed using a Leica DM IRB epifluorescence microscope (Leica Microsystems Ltd, UK) with Retiga Exi Fast digital camera (QImaging, Canada).

5.3.7 Protein Delivery into the Skin by Injection of Cubosome Formulation

Cubosome delivery into the skin by hollow microneedles or coated solid stainless steel microneedle arrays was assessed using *ex vivo* human skin. Hollow microneedle delivery was performed using MicronJet450™ and MicronJet600™ arrays attached to 1ml syringes to deliver 50µl of undiluted CuFl formulation in the skin according to the microneedle manufacturer's injection technique instructions. Treated skin areas, as determined by the 'bleb' that formed due to hydrostatic pressure of the injection volume within the upper layers of the skin, were excised using an 8mm biopsy punch and snap frozen in Optimal Cutting Temperature (OCT) embedding media and stored at -80°C prior to use.

The protocol for testing microneedle coating release in human skin described in Section 2.3.2 was used for cubosome-coated needles. The needles were inserted into previously frozen *ex vivo* human skin samples using a downward force perpendicular to the skin's surface and held in place for 60 seconds to allow rehydration of the formulation on the needles' surface. The needles were then removed and reimaged as described above to assess formulation removal from their surface. The treated areas of skin were excised, embedded and snap frozen as described above and stored at -80°C prior to use.

Sections of 10µm were produced, mounted and fixed on SuperFrost Ultra Plus slides before being imaged as described in Section 2.3.3 to visualise fluorescent protein deposition in the skin.

5.3.8 Antigen Uptake by Skin APCs

The early kinetics of antigen delivery into skin and interaction with skin-resident immune cells was assessed using two-photon microscopy (2PM) in a fluorescent *in vivo* immune cell model.

Given the lack of success of coating stainless steel microneedle arrays with cubosome formulation for delivery into human skin, this study used a liquid cubosome formulation applied to the skin after microneedle channels had been made by uncoated needle arrays to allow entry into the skin- this had been used in previous studies with

different microneedle arrays and cubosome formulation (Rattanapak et al., 2013, Rattanapak et al., 2014). Microneedles coated with an aqueous formulation of peptide and adjuvant or an intradermal injection of liquid cubosome formulation were also assessed as potential delivery methods.

5.3.8.1 Cubosome Formulations

Three formulations were produced for use in 2PM studies:

I. Cubosomes produced as described in Section 5.3.1- with 20mg/ml phytantriol (Tokyo Chemical Industry UK Ltd, UK), 53.66mg/ml propyleneglycol (Sigma Aldrich, UK) and 3mg/ml poloxamer 407 (Sigma Aldrich, UK)- plus 0.2mg/ml SIINFEKL-TAMRA (Peptides and Elephants, Germany), 0.4mg/ml Quil-A and 0.1mg/ml monophosphoryl lipid A (MPL-A) (CuPQM) (both Sigma Aldrich, UK).
II. Cubosomes produced as described in Section 5.3.1 with 38.325µg/ml Nile red (to create a 1:2000 ratio with the lipid phase in cubosomes) (CuNQM).
III. An aqueous solution of the SIINFEKL-TAMRA, Quil-A and MPL-A as above without lipid cubosome components present (AqPQM).

Nile red is a lipophilic dye which fluoresces when it is in a nonpolar environment (Greenspan et al., 1985)- in this case, within the lipid phase of the cubosome formulation. Nile red was selected to allow the visualisation of the lipid phase's behaviour after delivery into the skin; its distinct fluorescence spectra in combination with eYFP, TAMRA and SHG allowing visualisation of lipid phase, immune cells, peptide and collagen concurrently.

5.3.8.2 Transgenic Mice

The mice utilised in this study were B6.Cg-Tg (ITGAX-eYFP) 1 Mnz/J mice (Jackson Laboratory, USA) which were purchased and maintained by collaborators under specific pathogen-free conditions in the animal facility of Osaka University, Japan. Experimental work was performed under an approved protocol from the Animal Experimental Committee of Osaka University.

Mice were anaesthetised with isoflurane prior to treatment- 3% isoflurane for induction and 1-2% for maintenance (both vaporised in 100% oxygen). First, one or both flanks of the mouse were trimmed using electric hair clippers to remove the bulk of the fur. Depilatory cream (Church & Dwight Co. Inc., USA) was then applied to the trimmed area and left for 5 minutes to degrade the remaining hair, which could then be wiped away using a cotton swab. The hairless area was wiped clean using a tissue soaked with PBS and subsequently patted dry with a dry tissue prior to treatment.

5.3.8.3 Treatment with SIINFEKL-TAMRA Formulation

The microneedles used in these studies were stainless steel needle arrays of a design similar to those described in Section 2.3.1.1 (10 needles in a single row) with a length of 500µm after elctropolishing. Each hairless flank was treated with one of the following treatments:

a) **Microneedle poke-through (MNPT):** mouse flank was first treated with uncoated microneedles - one array applied three times in succession in parallel with 1mm spacing to create 30 channels in the skin. Immediately after MN application. 50µl of formulation was applied to the surface of the skin over the area with the microneedle channels. After 2 minutes, excess formulation was removed using tissue.

b) **Coated microneedle (coated MN):** 1.3µl of an aqueous solution containing 3.84mg/ml SIINFEKL-TAMRA, 7.68mg/ml Quil-A and 1.92mg/ml MPL-A was coated onto microneedle arrays as described in Section 2.3.1.2. Two arrays were applied at a time in parallel using a custom microneedle array holder, using downward pressure and held in place in the skin for 60 seconds to allow dissolution of the coating and then removed.

c) **Intradermal injection (IDInj):** 50µl of CuSQP or AqSQP formulation was delivered intradermally using the Mantoux technique with a 26-guage needle. Nanopass needles were initially used but difficulties were found in reproducibly injecting the live mice so the hypodermic needle injection method was utilised instead.

d) **Untreated control (UT):** flank was left untreated to allow imaging of LCs and dDCs in the absence of antigen or cubosomes.

To prepare the mouse for imaging, a glass microscope cover slip was attached to the flank of the mouse using tissue glue (3M, USA). The mouse was then inverted so that the cover slip could be fixed onto a heated microscope stage using adhesive tape. Total time to prepare the mouse and set up the microscope for imaging was approximately 15-45 minutes. Mice were divided into two groups- the first of which was treated and then imaged immediately to allow the analysis of early events following treatment. The second group were treated as described above and then returned to the animal facility for 48hrs before imaging- to allow analysis of changes in LCs after this extended time period.

5.3.8.4 Two-Photon Microscopy

The heated stage was fitted onto a motorised stage holder within a custom-built housing. The housing served to protect the stage from external light and also contained an air heating unit. Both the heated stage apparatus and the air heater within the housing were set to 37°C to maintain the body temperature of the anaesthetised mouse. Isoflurane was used to maintain anaesthesia at 1-2% in 100% oxygen, adjusted to keep the mice's breathing rate and depth steady so as not to introduce movement whilst imaging.

Two-photon microscope imaging of treated areas of mouse flank was performed using an A1RMP multiphoton microscope (Nikon, Japan) driven by a Chameleon Vision II Ti:Sapphire laser (Coherent, USA) tuned to 920 nm with an inverted microscope equipped with a 206 oil immersion objective (CFIPlan-Fluor, N.A. 0.75, Nikon). Collagen was detected through SHG at 446nm, eYFP was detected at 525nm and SIINFEKL-TAMRA detected at 575nm. Images were acquired with 3µm spacing between z-planes starting from the surface of the skin downwards to the depth where signal became diminished (ranging from 30-50 z-planes). Images were acquired either as a snapshot (with one complete set of z-plane images) or over a time course (with sets of z-plane images being taken at 5-minute intervals to allow the visualisation of movement of immune cells) depending on whether the mouse was being imaged 48hrs after treatment or

immediately following treatment respectively. Mice being studied immediately following treatment were imaged for up to 4 hours. Raw imaging data were processed with a combination of NIS-Elements AR (Nikon, Japan) and Imaris (Bitplane AG, Switzerland) software.

5.3.8.5 Antigen Uptake Analysis by Flow Cytometry

Following imaging, mice were sacrificed by cervical dislocation. The glass cover slip was gently removed and the mouse's flank washed with PBS to remove any residual formulation. The treated skin areas and the local inguinal lymph nodes were then harvested. The skin was incubated in a 1mg/ml collagenase (Wako Chemicals, Japan) solution in Hanks buffered salt solution (Nacalai Tesque, Japan) at 37°C in a shaking water bath for 1 hour to allow for dispersion of the tissue. The resulting cell suspension was passed through a 100µm cell strainer to eliminate cell clumps. A single cell suspension was also prepared from inguinal lymph nodes by mechanical disruption and washing through a 100µm cell strainer using PBS. After collection, skin and lymph node cell suspensions were fixed in 1% paraformaldehyde for 10 minutes at room temperature. Fixed cells were stored in FACS buffer at 4°C prior to use.

Skin and lymph cells were initially incubated in Fc Block (Nippon Becton Dickinson, Japan) according to manufacturer's protocol. They were then washed in FACS buffer before being stained with the following panel:

- Brilliant Violet 421™ anti-mouse/human CD11b antibody (Biolegend, USA)
- APC anti-mouse/human CD207 (Langerin) Antibody (Biolegend, USA)

Analysis was performed on a FACSCantoII (Nippon Becton Dickinson, Japan) with the Brilliant Violent 421 fluorophore being visualised in the Pacific Blue channel, eYFP in the FITC channel and SIINFEKL-TAMRA in the PE channel. Compensation was performed using BD CompBead compensation beads (Nippon Becton Dickinson, Japan) with FITC- and PE-conjugated antibodies used in the place of eYFP and TAMRA in the absence of antibodies conjugated with these fluorophores (Figure 5.7). The raw data were analysed using FlowJo software (FlowJo LLC, USA). Statistical tests comprised one-way analysis of

variance (ANOVA) followed by Tukey's post hoc analysis performed using IBM SPSS Statistics (IBM, USA).

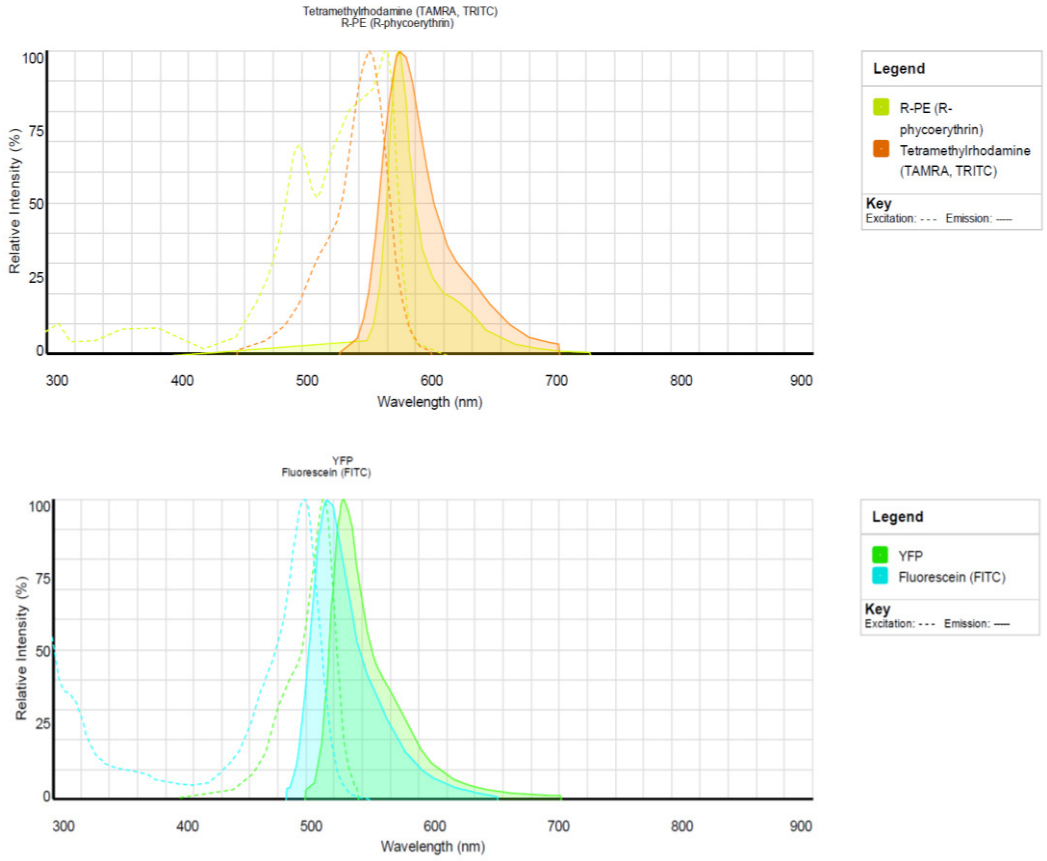

Figure 5.7: Fluorescence excitation and emission spectra for R-phycoerythrin, TAMRA, YFP and FITC used to inform analysis by flow cytometry

5.4 Results and Discussion

5.4.1 Characterisation of Cubosomes

5.4.1.1 Zeta Potential and Particle Size Analysis

Analysis of cubosome batches 24hrs after synthesis revealed an average particle size of 169.5nm (SD ±12.5, n = 4). The insertion of Fl-OVA or Nile red into the formulations did not alter the particle size significantly- mean particle size was 167.7nm and 152.9nm with insertion of Fl-OVA and Nile red respectively. The particle distribution index was low for all the samples measured, with a mean PDI of 0.164 (SD ±0.022, n = 4), indicating that relatively homogeneous particles had been produced. Both the particle size and PDI values seen were consistent with the values published by Rattanapak et al. (2013) who reported particle sizes ranging from 158-182nm and PDI <

0.3. The zeta potential of cubosomes differed from those previously reported. Whereas Rattanapak et al. (2013) reported a zeta potential range of -21 to -25mV, the mean zeta potential observed in this study was -16.3mV (SD ± 3.4, n = 4)- the significance of this difference will be determined in the stability investigation.

5.4.1.2 Transmission Electron Microscopy (TEM)

TEM imaging of Cu0 formulation produced the images in Figure 5.8. Based on previously published TEM images of cubosome formulations (Bu et al., 2015, Fraser et al., 2011), it was determined that the lighter areas represented the continuous aqueous phase, with the dark spots representing the lipid particles. The presence of other lipid structures was also noted, with unilamellar and multilamellar liposomes both visible.

The addition of ovalbumin protein to the cubosome formulation led to a reduction in the quality of TEM images that were obtained. In a small proportion of the images obtained, areas of light aqueous background with darker, rounded areas the size of Cu0 lipid particles could be distinguished (Figure 5.9). Unlike images of the Cu0 formulation, the continuous phase contained lighter coloured particulate material- most likely the Fl-OVA protein precipitated from solution following freezing of the formulation. This material made distinguishing cubosome particles very difficult and so

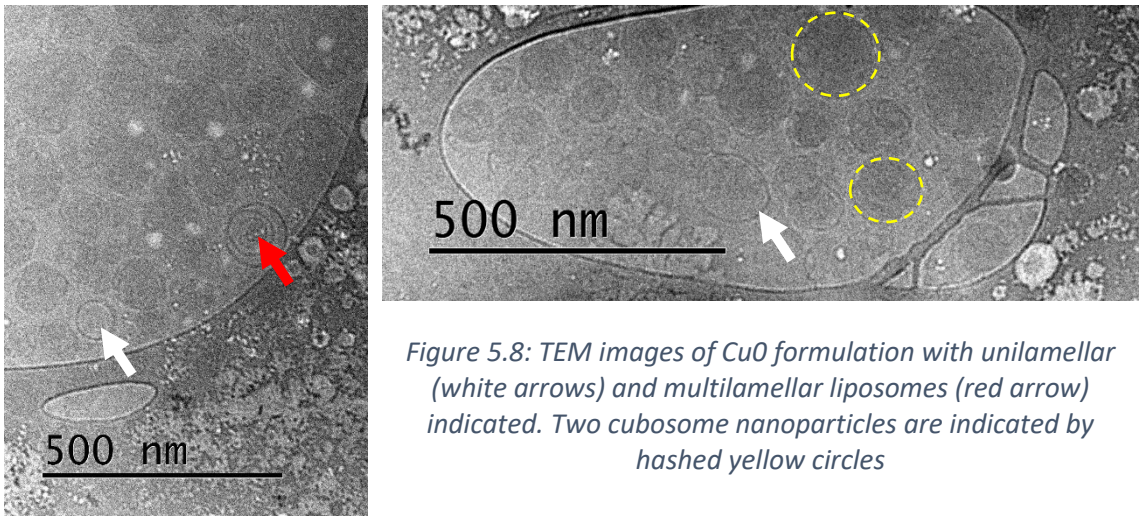

Figure 5.8: TEM images of Cu0 formulation with unilamellar (white arrows) and multilamellar liposomes (red arrow) indicated. Two cubosome nanoparticles are indicated by hashed yellow circles

particle size and zeta potential analysis will be used to reliably characterise particles in the place of TEM.

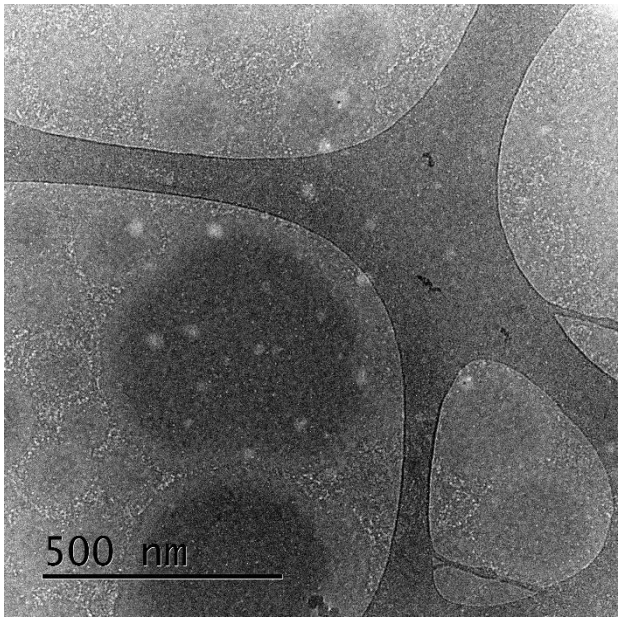

Figure 5.9: TEM image of CuFl formulation

5.4.2 Protein Insertion into Cubosomes

The mean entrapment of protein within the lipid phase was 28.54% (SD ± 1.63, n = 3). This was higher than the 23% entrapment reported for fluorescent peptide in the literature (Rattanapak et al., 2013) but lower than the entrapment reported for the full length ovalbumin protein of 73% (Rizwan et al., 2011). The results showed that ovalbumin protein could be entrapped in cubosomes despite its size, approximately 7.0nm × 3.6nm × 3.0nm (Erickson, 2009), exceeding that of the peptide. Whilst the low entrapment efficiency is a limitation, the formulation may provide for a bolus dose of protein from the continuous phase followed by sustained release of protein entrapped the lipid phase providing a greater overall exposure time.

5.4.3 Stability Testing of Formulations

The stability tests of cubosome batches showed a similar trend across all of the batches analysed- particle size and PDI both reversibly increased upon storage. This was presumably due to lipid particle aggregation, perhaps due to the relatively low zeta potential values observed. There was no significant difference in the size or PDI of batches analysed after vortexing at 7, 14, 21 or 28 days after initial analysis (Figure 5.10). This suggests that there is a stable equilibrium size that lipid particles in the formulation tend towards between 180 and 220nm. Vortexing formulations reversed the changes in size in all samples, returning them to the reported ranges of particle size (158-182nm). Interestingly, the PDI values on extended storage did not exceed the reported value (>0.3) during storage before or after vortexing.

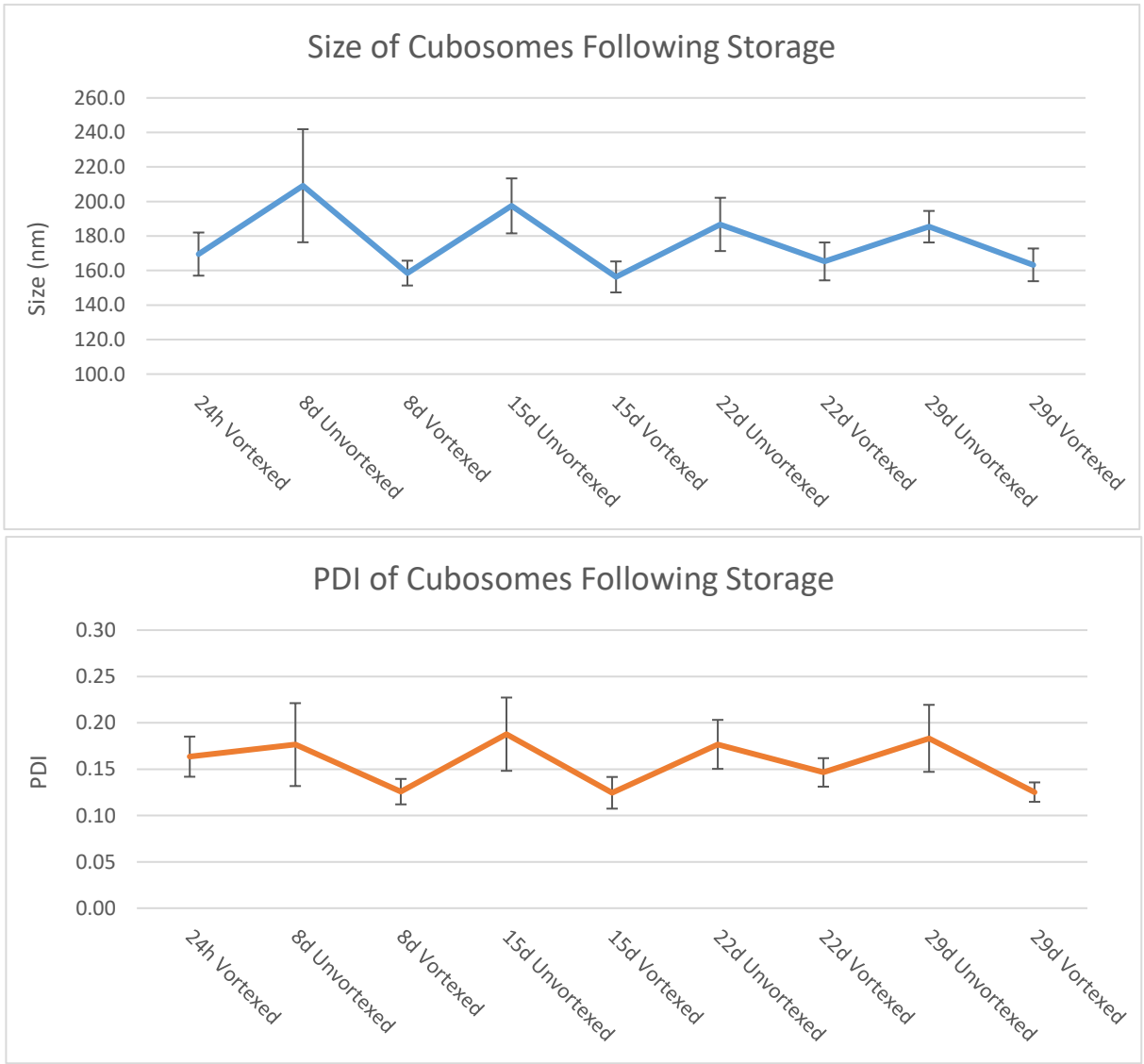

Figure 5.10: Mean size and PDI of lipid particles in cubosome formulations following extended storage at room temperature, protected from light and under nitrogen

The zeta potential of the formulations remained consistent with storage time, with samples tested at all time points not varying significantly from the -16.3mV value produced by the initial analysis (Figure 5.11). There was also no significant difference between Cu0 formulations and those with Nile red or Fl-OVA, suggesting that while they were inserted into the lipid particles, their low mass in the formulation relative to the mass of lipid meant they did not disturb the colloidal system.

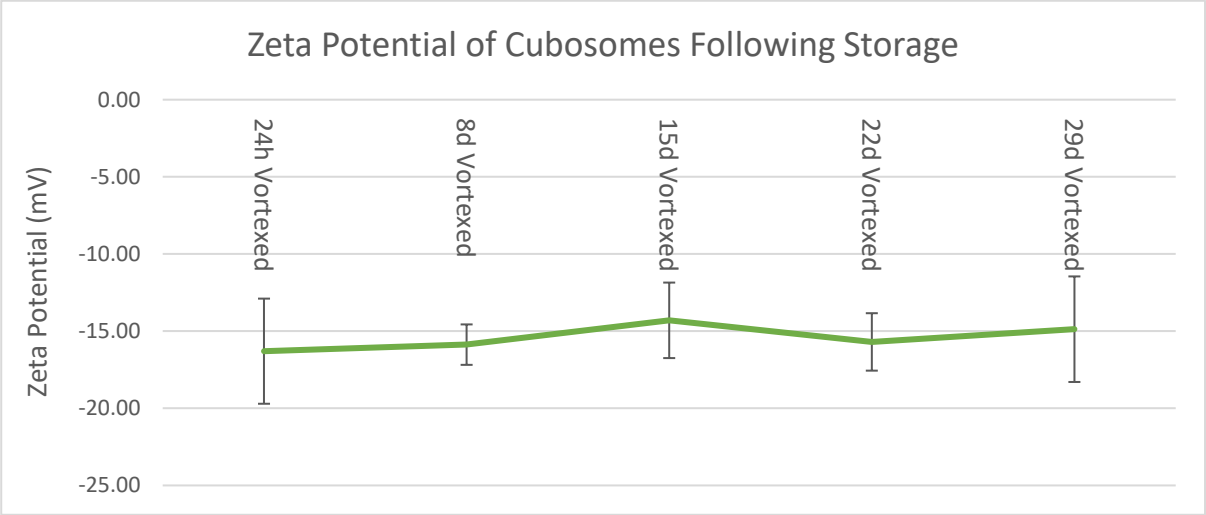

Figure 5.11: Mean zeta potential of lipid particles in cubosome formulations following extended storage at room temperature, protected from light and under nitrogen. All samples were vortexed for 10 minutes prior to analysis

5.4.4 Effects of Hollow Microneedle Delivery on Cubosome Formulations

Figure 5.12 shows the effect on cubosome characteristics of 5 consecutive passes through NanoPass hollow microneedle arrays. The particle size and PDI of the cubosomes showed only marginal increases after passing through either MicronJet450™ or MicronJet600™ array type- a mean increase of 7.6nm in particle size and 0.0145 in PDI. This represented mean changes of 3.9% and 6.6% for size and PDI respectively. The change in zeta potential were more marked, with decreases by both array types to approximately -25mV in all cases. This change may be due to the shear forces of the formulation being passed through the needle leading to a change in the alignment of components of cubosomes, altering the charge at the surface of the particles. It is also possible that passing the formulation through a plastic syringe and microneedle device will lead to adsorption of surfactant (Clint, 1998) from cubosomes, thus changing their composition which may have led to the difference in zeta potential seen. Further work is required to determine the source of this change in cubosome properties. The more

negative zeta potential might improve the long-term stability of formulations as particles are more repelled from one another, preventing aggregation. However, the delivery through microneedles will be the terminal use for the formulation so effects on stability will be inconsequential. Overall, the results support the use of hollow microneedle technology for delivery of cubosomes.

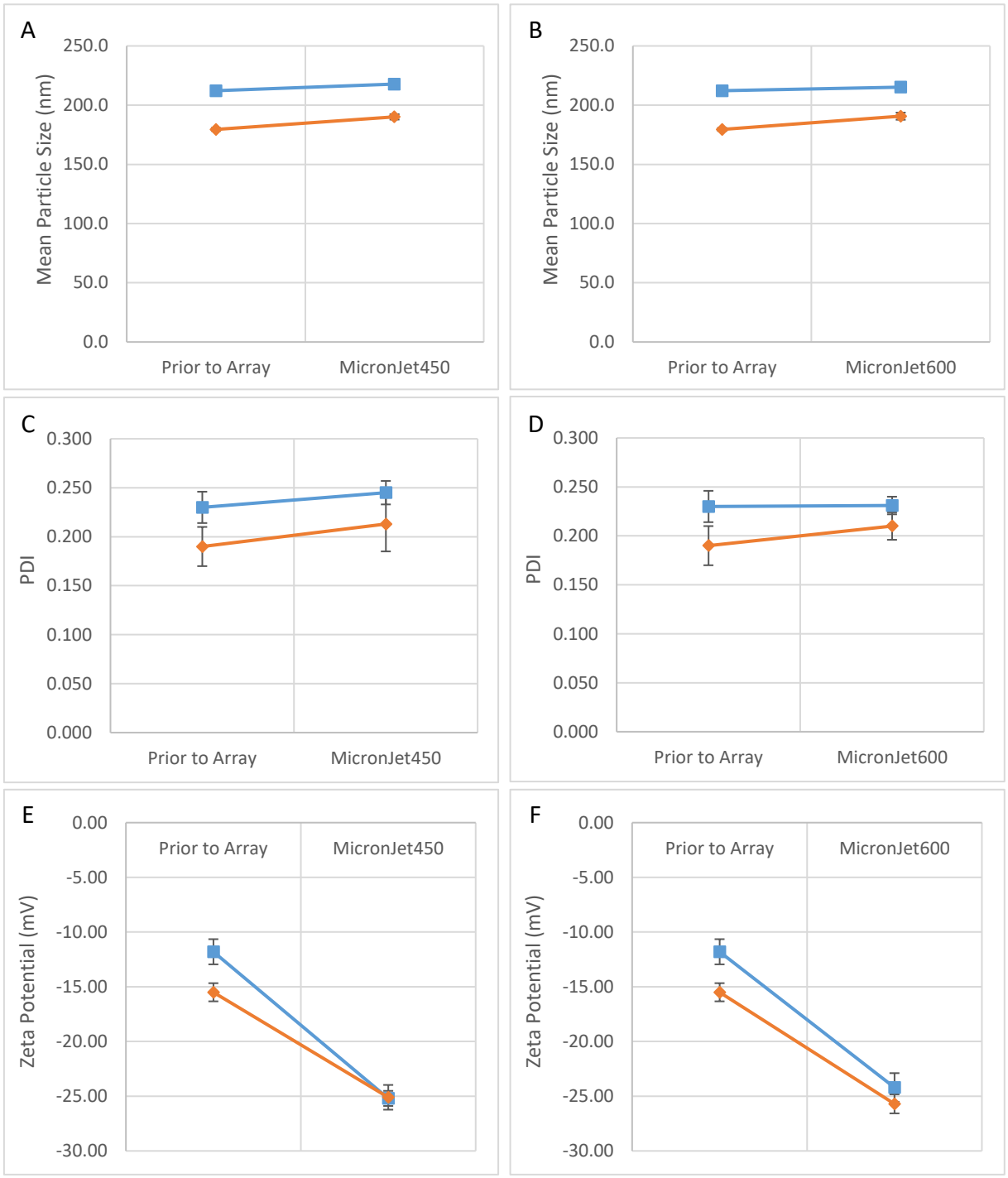

Figure 5.12: Effect of being passed through NanoPass hollow microneedle arrays on mean particle size (A,B), PDI (C,D) and zeta potential (E,F). Two formulations were tested: Cu0 (blue) and CuFl (orange). Three separate aliquots of each formulation were tested; error bars are ±SD.

5.4.5 Coating of Cubosome Formulation onto Stainless Steel Microneedles

Results of coating stainless steel microneedles with cubosome formulation are shown in Figure 5.13 (A & B). It was possible to achieve coverage of the needle tips comparable to that seen in Chapter 2 using an aqueous solution of Fl-OVA alone. The fluorescence was not evenly distributed across the area that was coated however. This was most likely due to the aqueous phase of the cubosome formulation evaporating preferentially from the needle edges, leading to aggregation of the dispersed phase at the centre of the needles due to the lyophobic nature of the dispersed phase. Reimaging the needles following insertion into the skin revealed that the coating on the needles was not physically resilient enough to insert into skin- some of the formulation appeared to be 'smeared' on the base of the arrays following skin insertion. This phenomenon was later confirmed by imaging *ex vivo* skin sections following microneedle treatment to determine where, if at all, the formulation had been deposited within the skin.

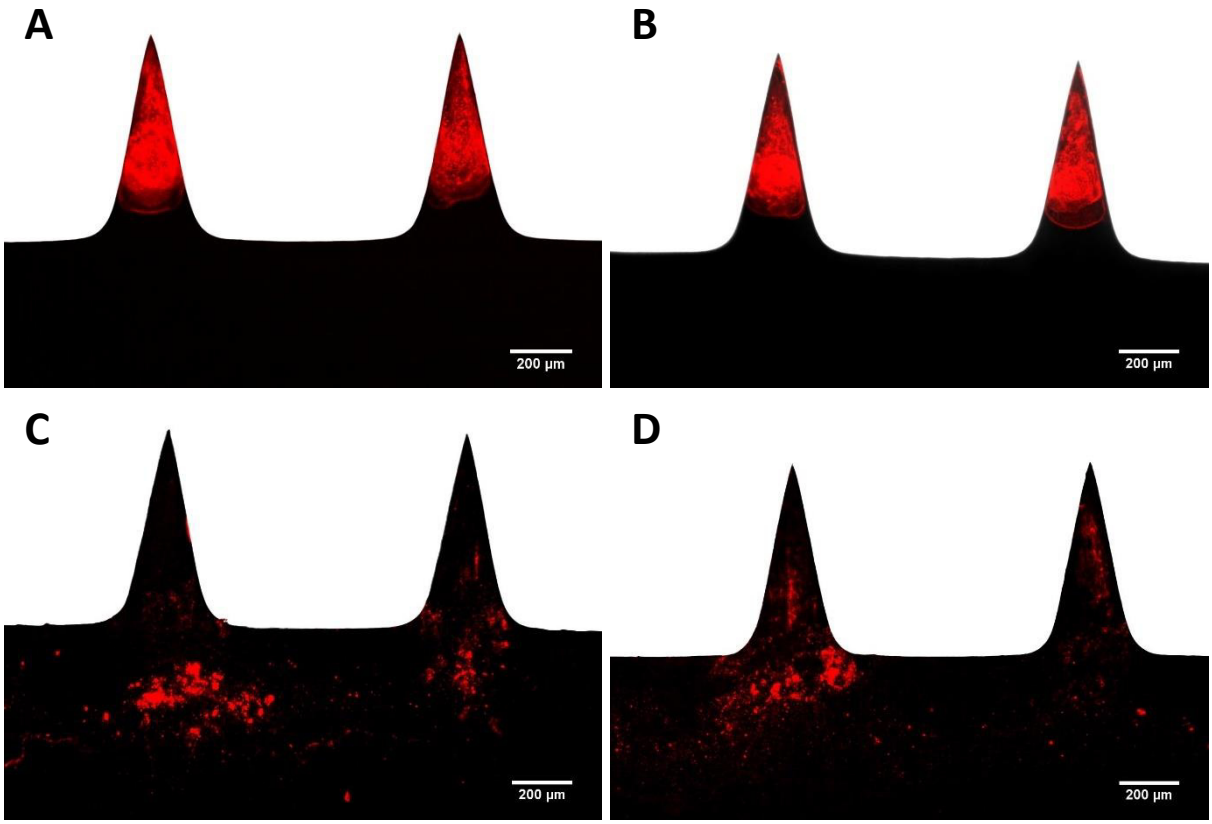

Figure 5.13: Microneedle arrays (black) coated with CuFL formulation (red) following coating showing uneven distribution on the needle surface (A,B) and following insertion into ex vivo human skin showing formulation spread onto the base of the needle array (C,D). Scale bar: 200µm

5.4.6 Protein Delivery into the Skin by Injection of Cubosome Formulation

As Figure 5.14 shows, both of the NanoPass hollow microneedle array devices were able to deliver cubosome formulation into skin. As is the case with intradermal injections using a hypodermic needle, the bulk of formulation was delivered into the fibrous dermis. Little formulation was seen in the epidermis, likely due to the densely cellular nature of the epidermis meaning that the hydrostatic pressure of injection is inadequate to distribute formulation into the epidermis, though delivery of formulation occurs adjacent to the needle channel in the epidermis (Figure 5.14 A, C & D). This preferential delivery to the lower dermis is likely exacerbated in *ex vivo* skin due to the lack of hypodermic tissue or muscle present, creating a path of least resistance out of the bottom of the skin samples which injected formulation will follow.

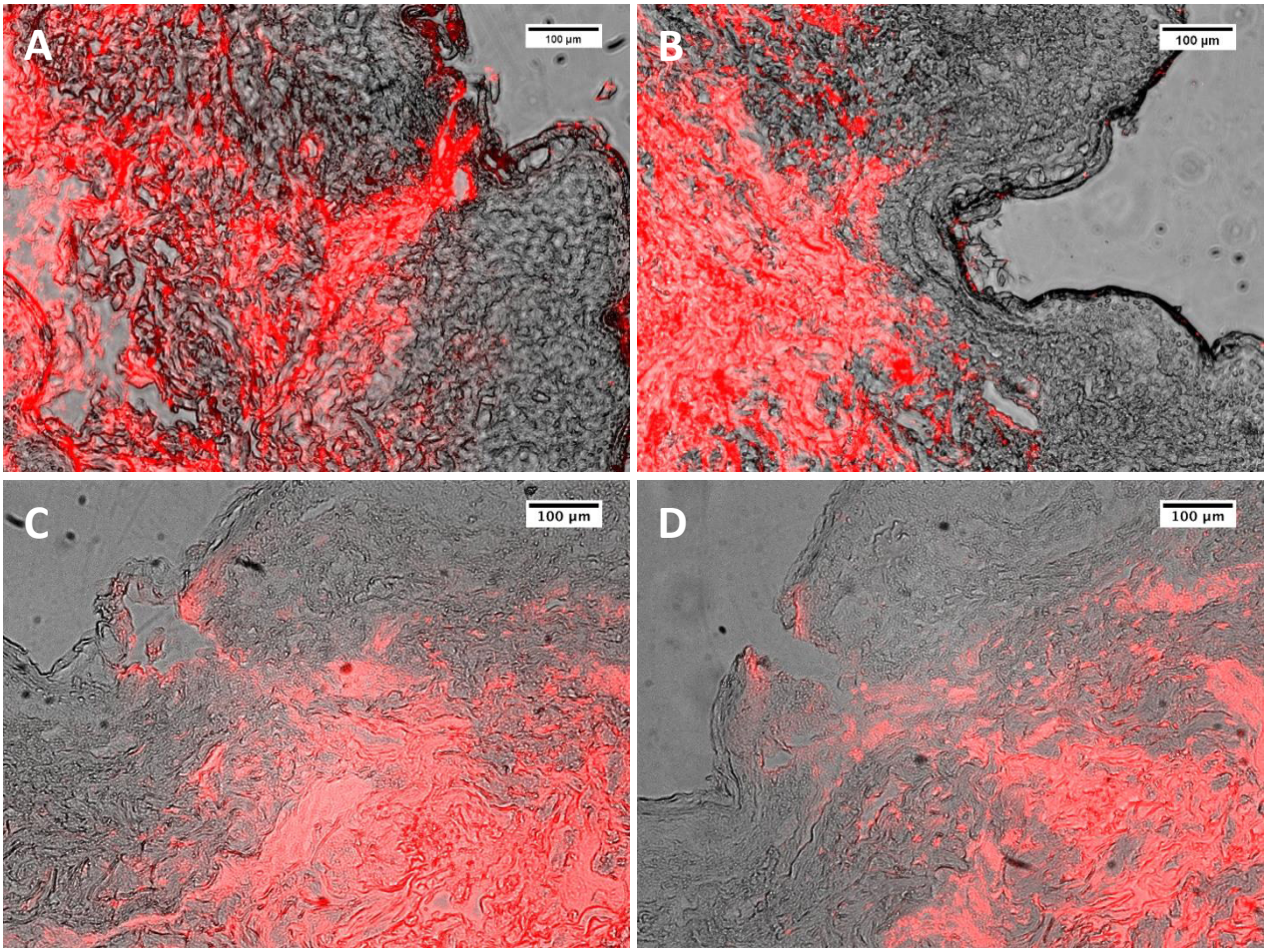

Figure 5.14: Delivery of CuFL formulation into ex vivo skin samples using NanoPass NP450 (A,B) and NP600 (C,D) hollow microneedle array devices. Scale bar: 100µm

Figure 5.15 shows the delivery of cubosome formulation into the skin using either cubosome-coated solid steel microneedles or by applying a liquid cubosome formulation to the skin after treatment with uncoated needles to create needle channels through which the formulation could enter the skin. There was a smaller area of fluorescent protein delivery into skin delivered into the using these methods than intradermal injection using microneedles. As expected from the images of microneedles coated with cubosome formulation following skin insertion, some of the coating was wiped off of the needles during insertion into skin and could be found on the skin's surface adjacent to the needle channel (Figure 5.15 B). Deposition below the stratum corneum was limited to the edges of the needle channel and so covered a very small area only. Delivery of liquid formulation onto needle pre-treated skin showed only a small improvement in delivery, with some formulation able to permeate down into the dermis (Figure 5.15 D), though not in all cases (Figure 5.15 C).

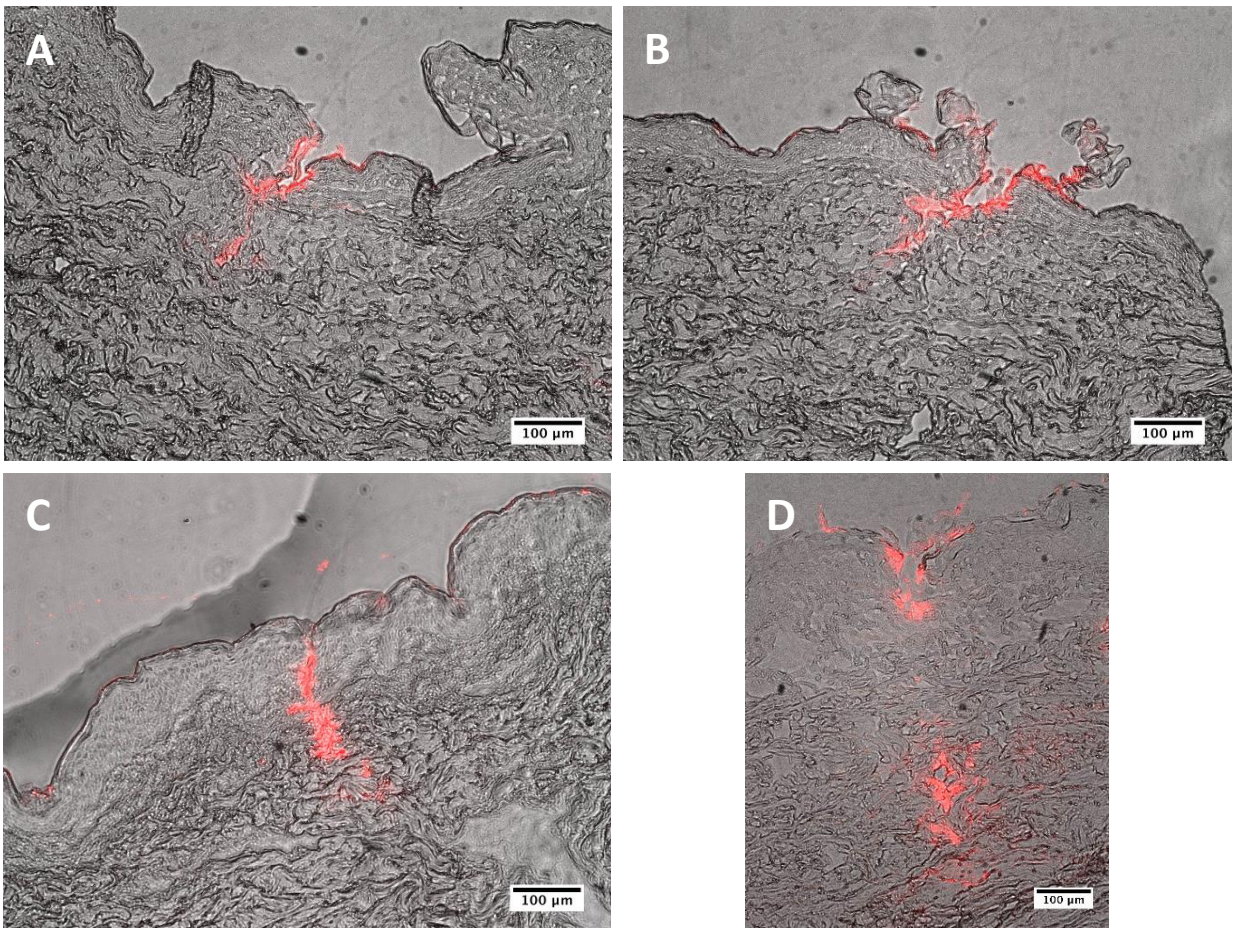

Figure 5.15: Delivery of CuFL formulation into ex vivo skin samples coated onto solid steel microneedles (A,B) and applied to the surface of skin which had previously been treated with uncoated microneedle arrays to create channels in the skin (C,D). Scale bar: 100µm

5.4.7 Two-Photon Microscopy

5.4.7.1 Structure of Skin

Figure 5.16 shows the skin of a B6.Cg-Tg (ITGAX-eYFP) 1 Mnz/J mouse visualised by 2PM after microneedle pre-treatment followed by application of a cubosome formulation containing fluorescent peptide, Quil-A and MPL (CuPQM MNPT). The stratum corneum is red due to the liquid formulation being applied to the skin's surface, with the undulations of the skin's surface causing areas of uneven fluorescence intensity. The dark region in the middle of the images is a microneedle channel in the skin. Just below the surface, the network of green LCs in the epidermis are clearly visible. Folds in the skin and the upper end of hair shafts containing formulation also appear red in the epidermis. At 21µm below the skin's surface, the collagen fibres of the dermis are visible in blue, along with the lower parts of hair shafts which are green due to autofluorescence on the 480/40 filter. At this depth, dDCs could also be seen. They are distinguishable by their bright green fluorescence, rounded morphology compared to

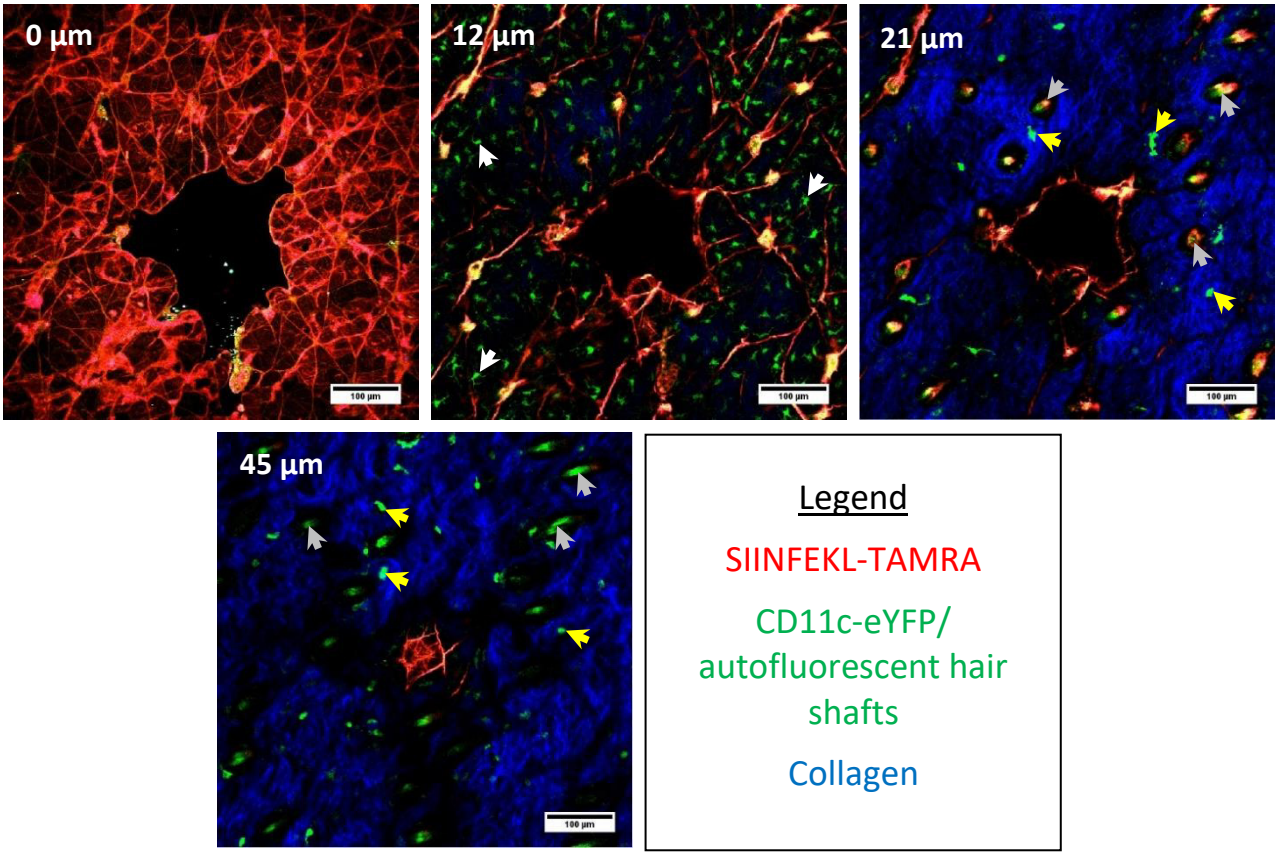

Figure 5.16: Visualisation of the skin of a CD11c-eYFP mouse using two-photon microscopy (2PM). The legend applies to all subsequent 2PM images in this chapter. Text on each image indicates depth of imaging relative to the skin's surface. Arrows indicate LCs (white arrows) at 12µm imaging depth and dDCs (yellow arrows)/autofluorescent hairs (grey arrows) at both 21µm & 45µm imaging depths. Scale bar: 100µm

LCs and motility within the dermis. The bottom of the microneedle channel could be seen at a depth of 45µm and was distinguishable by the presence of red formulation in the dermis. At depths of 70µm below the skin's surface, the laser power was attenuated by the skin and so signal was reduced- this varied between mice though, with some producing signal to depths of as much as 200µm. The depth at which the signal was fully attenuated varied between mice and with the presence of microneedle channels, which allowed penetration of the laser to greater depths in the skin.

Figure 5.17 shows further characteristics of the CD11c+ cells in mouse skin that could be observed using 2PM. Figure 5.17 (A) shows the non-motility of LCs over 2 hours of imaging- this was in support of the results seen in human skin in Chapter 2 where LCs require longer times to respond to stimuli and migrate out of the epidermis. This was not the case for the motile green dDCs within the dermis (Figure 5.17 B), which could be seen moving both laterally and vertically within the skin in the time lapse en face images. It was also noted that dDCs occasionally migrated to the basement membrane and extended dendrites into the epidermis (Figure 5.17 C). This is most likely to allow dDCs to 'sample' antigen that may be present in the epidermis. An accumulation of dDCs at the dermal-epidermal junction has been previously reported in response to herpes simplex virus infection of the epidermis (Eidsmo et al., 2009). This may be important in allowing antigen transport to lymph nodes more rapidly after pathogenic infiltration of the epidermis than can be achieved by LCs.

5.4.7.2 Microneedle Channel Healing

One of the advantages of 2PM is the ability to image the skin in real time- useful both for observing cellular behaviour and that of the skin as a whole. In particular in this study, the healing of microneedle channels could be observed. During the investigation, healing of microneedle channels occurred almost completely within an hour of the needles' removal as was apparent in 2PM images. This presented a challenge as the process of preparing the mouse for imaging after treatment and setting up the microscope to image the region of interest and initiating the imaging sequence took up to 45 minutes. This issue was particularly pronounced for CuPQM and AqPQM MNPT-treated mice, where formulation was applied, allowed to permeate skin and excess then

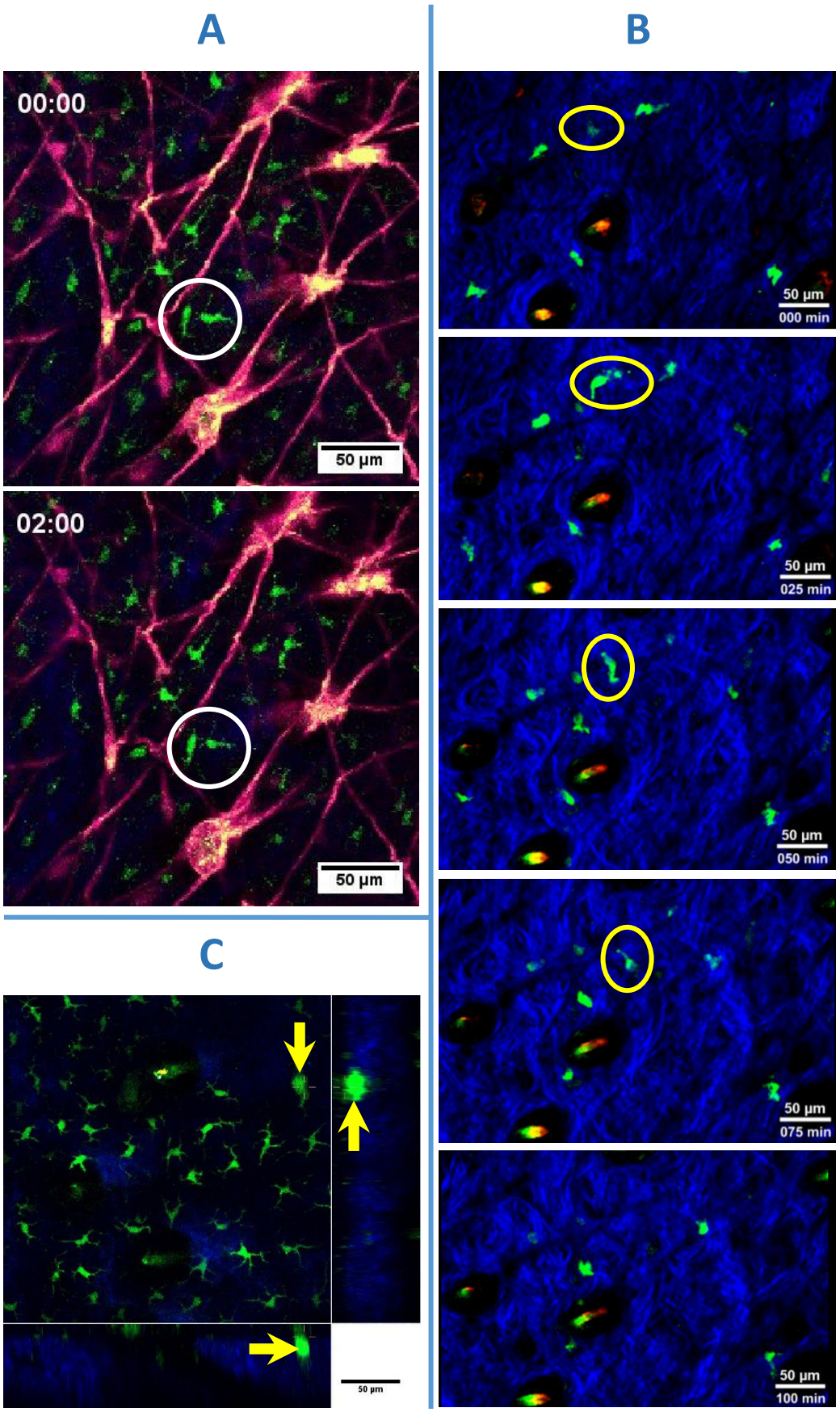

Figure 5.17: 2PM images that demonstrate the lack of motility of LCs over 2 hours (A) with white circles indicating a pair of stationary LCs, the motile nature of dDCs within the dermis (B) with yellow circles following a single dDC through the dermis and demonstrate a dDC's movement into the epidermis (C; z-depth 72µm) with yellow arrows. Scale bar: 50µm

removed before attaching the glass cover slip to the mouse. The coated MN studies provided the best opportunity to image microneedle channels due to the fact that mice could be prepared for imaging immediately following microneedle removal. The fact that the fluorescent formulation was only deposited where microneedle arrays came into direct contact with skin also made aligning the microscope to the region of interest much more straightforward. Figure 5.16 is an example of a MN channel that was imaged roughly 45 minutes after the MN array was removed from the skin and as a result, the needle channel is more shallow (at roughly 50µm) than would be expected from 500µm needles being inserted into the skin. Figure 5.18 shows a microneedle channel formed by a coated microneedle. Of the three repeats of mice treated with coated microneedles, this had the shortest elapsed time from treatment of the mouse to imaging run being commenced (15 minutes). Thus, it provides the best insight into the microneedle channel healing process. The black channel area on the images can be seen to decrease in width from 320µm (approximately the width of the microneedles) at 15 minutes' post-treatment to 63µm 60 minutes later. The depth of the channel also decreased from extending beyond the field of view at 15 minutes' post-treatment to 70µm at 60 minutes as the channel healed. It was interesting to note that the skin appears to close both inwards and move upwards to effectively 'close' the channel. At 75 minutes post-MN removal, the MN 'channel' appears as a shallow indentation in the skin, with the red coating formulation visible on its inner surface.

5.4.7.3 Antigen Retention at the Site of Injection

Another facet of vaccine delivery that was visualised using 2PM was retention of antigen at the injection site 48 hours' post-treatment and changes in the distribution of immune cells as a result of the vaccination. Figure 5.19 shows the increase in dDC numbers at one injection site following immunisation. Though the difference is striking between treated and untreated areas in Figure 5.19 (A & B), high variability existed in the numbers of dDCs seen in different areas both between mice and across areas on the same mouse. The constant movement of dDCs also made quantification unreliable.

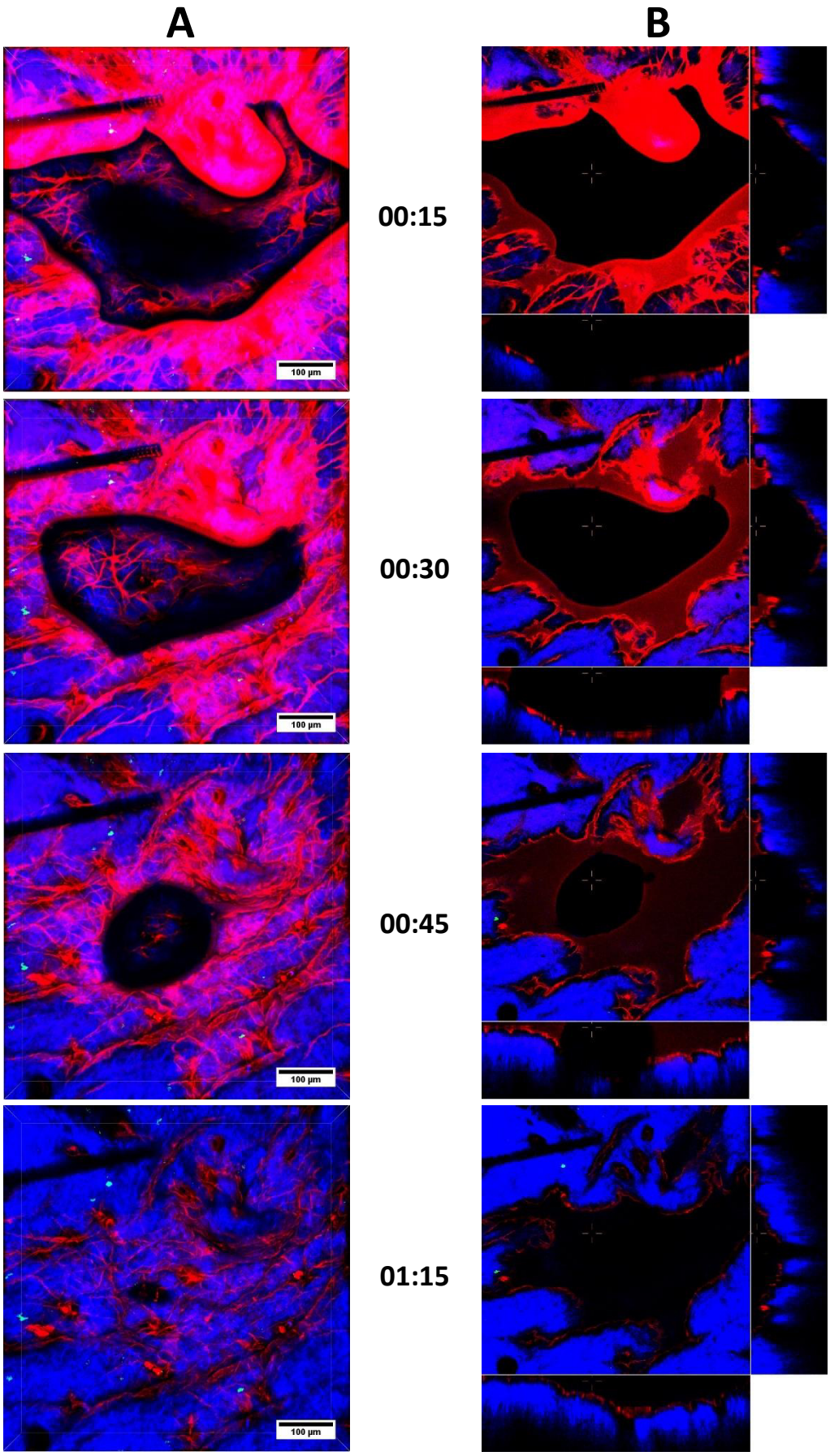

Figure 5.18: Time lapse imagery of a microneedle channel formed in mouse skin following treatment with coated microneedles. Images are shown both as a 3D projection (A) and as a 'slice view' showing a single z-plane with corresponding lateral views to allow channel visualisation (B; depth of z-plane 180um). Time elapsed expressed as hh:mm relative to removal of MN array. Scale bar: 100µm

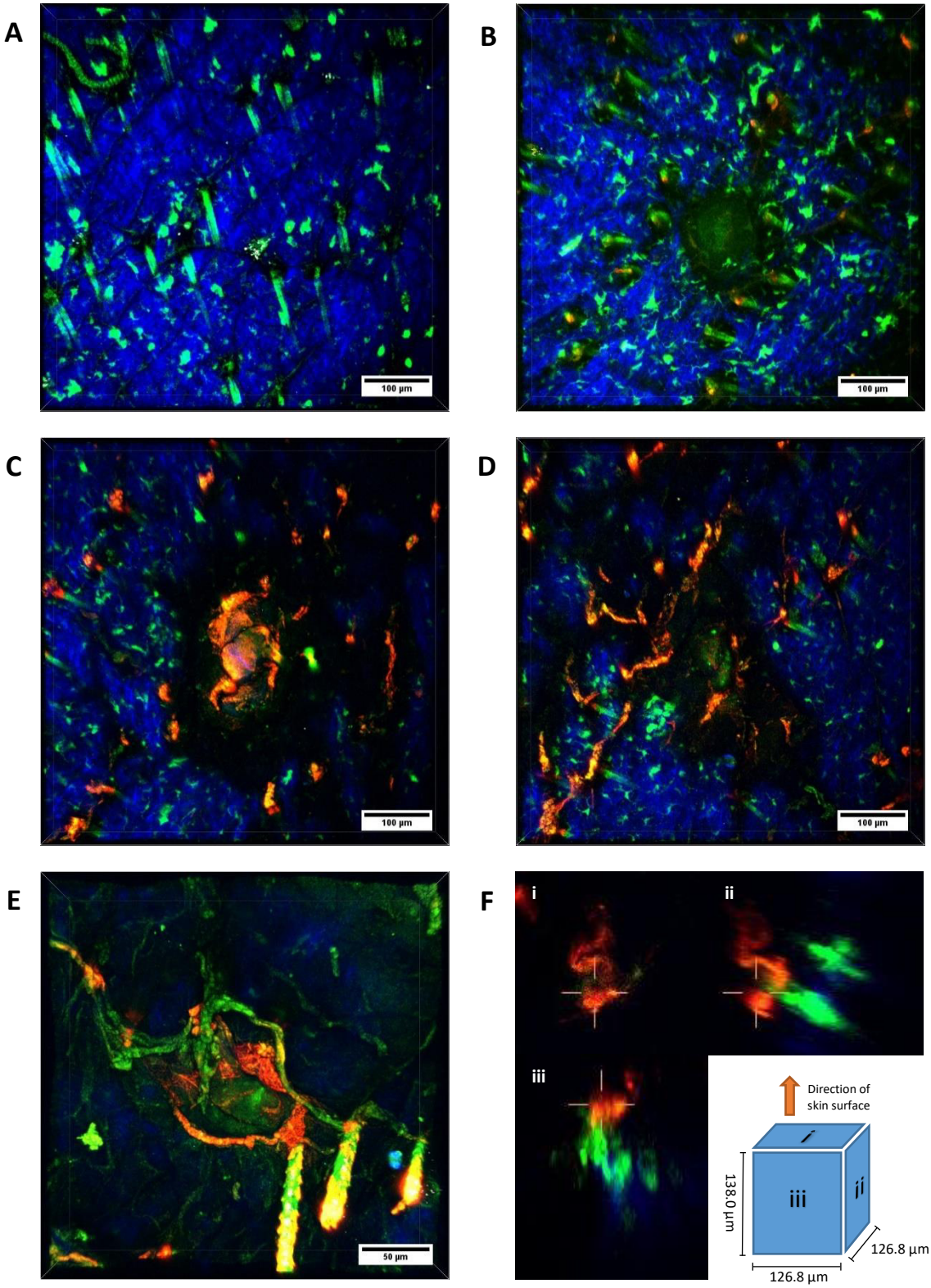

Figure 5.19: 2PM images showing dDCs in untreated mouse skin (A) and surrounding the site of a channel created by a coated microneedle (B). Antigen retention at the site of treatment was seen in mouse skin 48 hours after treatment with both aqueous antigen solution (C,D) and cubosome formulation (E) using the MNPT method described in Section 5.3.8.3. Finally, a 'slice view' of dDCs interacting with retained antigen in the skin 48 hours after treatment with aqueous peptide solution delivered by MNPT method (F). Scale bar (A-D): 100µm, (E): 50µm

For this reason, dDC density was not used as a quantitative output. Antigen retention was not consistently different between the three delivery methods used (CuPQM/AqPQM MNPT or coated MN). In cases where antigen remained on the skin 48 hours after treatment, it was limited to the border of healed channels in the skin Figure 5.19 (C - E). A characteristic autofluorescent region of tissue could be seen in the area where needle channels had healed, which may correspond to granulation tissue as the channel heals. Finally, evidence of dDCs (green) interacting with antigen (red) could be seen 48 hours after delivery Figure 5.19 (F).

5.4.7.4 Changes in LC Density Following Antigen Delivery

There were reductions in LC density in the skin of mice following treatment with CuPQM MNPT, PepAdj MNPT and coated MN of 43.18%, 29.48% and 13.19% respectively (Figure 5.20). Unfortunately, analysable images from a low number of treated (n=2) or control mice (n=1) were obtained, limiting the analyses that could be performed to ascertain statistical significance. The trend for the data obtained shows that the reduction was greatest with CuPQM MNPT treated mice and lowest in coated MN treated- it could be speculated that this was due to the delivery over a large area of the stratum corneum enhanced by cubosomes in the former. Following coated MN delivery antigen was delivered to a more limited area, likely meaning that fewer LCs were directly exposed to antigen. It is also possible that a greater proportion of antigen was delivered from coated needles into the dermis than with the two methods that involved application of liquid formulation, thus limiting the effect on LCs.

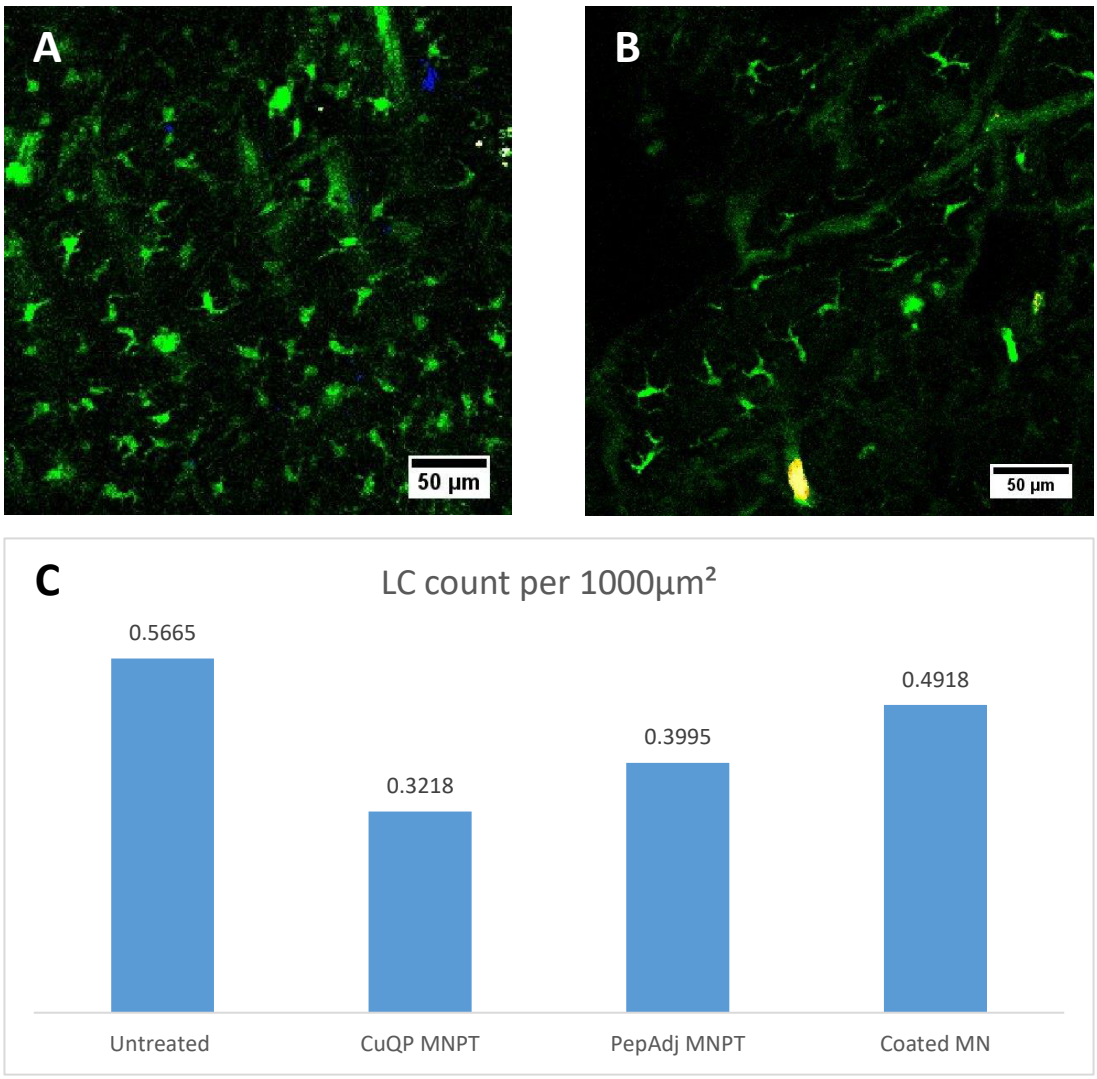

Figure 5.20: LCs in untreated mouse epidermis (A) and 48 hours after treatment with CuPQM MNPT (B). Density of LCs in the epidermis of mice 48 hours after treatment (C; n=1 for untreated, n=2 for all other treatments). Scale bar: 50µm

5.4.8 Antigen Uptake Analysis by Flow Cytometry

Cells from the treated area of skin and the inguinal lymph node proximal to the treated area were isolated from the mice following imaging and analysed by flow cytometry to determine SIINFEKL-TAMRA uptake. Based on the literature, the PE median fluorescence intensity (MFI) of $CD11c^+$ cells were used as the readout. Staining cells with anti-CD207 and anti-CD11b antibodies also allowed for analysis of peptide uptake within LCs and dDC subsets individually.

The yield of cells from mouse skin was poor and inconsistent, suggesting that the protocol required further optimisation. As a result, there was insufficient data to draw any meaningful conclusions and so this portion of the investigation was disregarded.

Lymph nodes isolated from mice, however, provided improved cell yields. There was no change in fluorescence in the cells isolated from mice treated and imaged on the same day, most likely due to longer than 5 hours being required for the dDCs to be able to uptake antigen and migrate to the lymph nodes. Data from lymph nodes isolated 48 hours' post-treatment are shown in (Figure 5.21). In total CD11c+ cells, CuPQM and coated MN-treated mice both showed significant increases in PE MFI, whilst variability in mice treated with AqPQM MNPT meant that no significant difference was present (Figure 5.21 A). Breaking this down into the cell subsets revealed that the subset of $CD207^{+}$ dDCs (CD11c+/CD207+/CD11b-) possessed the largest increase in PE MFI (Figure 5.21 B). This was in agreement with previous results (Rattanapak et al., 2014) and highlights the importance of these cells in antigen transport to lymph nodes in mice.

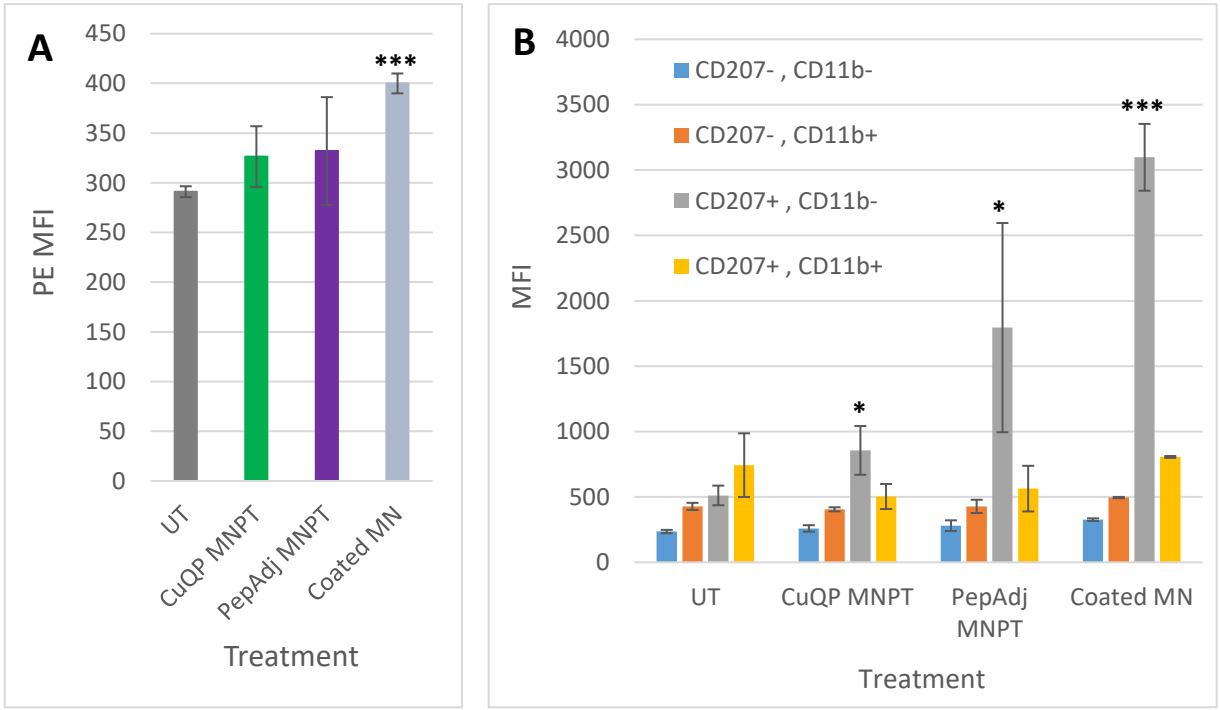

*Figure 5.21: TAMRA uptake in cells measured by median fluorescent intensity (MFI) in the PE channel. Values shown are in the overall YFP+ (CD11c+) population (A) and in the subsets of CD11c+ cells based on CD207 and CD11b expression. Error bars = ± SD. Significance indicated relative to untreated (UT) cells; * p<0.05, *** p<0.001*

5.4.9 Visualising Cubosome Lipid Phase Distribution

Nile red was used to track the movement of lipid from the formulation on a separate channel to the SIINFEKL-TAMRA with an emission wavelength of 629nm. As Figure 5.22 (A) shows, this emission wavelength is near to the emission maxima for the CuNQM formulation in isolation. In practice, however, fluorescence was seen across at 525nm and 575nm emission wavelengths also (Figure 5.22 B), making it impossible to properly visualise the CD11c+ cells and SIINFEKL-TAMRA peptide when Nile red was present. A possible explanation may arise from the fact that Nile red, which is not fluorescent alone or in polar environments, becomes fluorescent in a lipid environment (Greenspan et al., 1985). The fluorescence characteristics of Nile red are solvent-dependent- thus the spectra seen in Figure 5.22 are specific to Nile red within the lipid phase of cubosomes. It is likely that delivery into the skin, particularly the lipid-rich stratum corneum led to some sequestering of Nile red into a different lipid environment and leading to a change in its fluorescence emission. The diversity of lipids present in the skin could help to explain the broad fluorescence seen via 2PM.

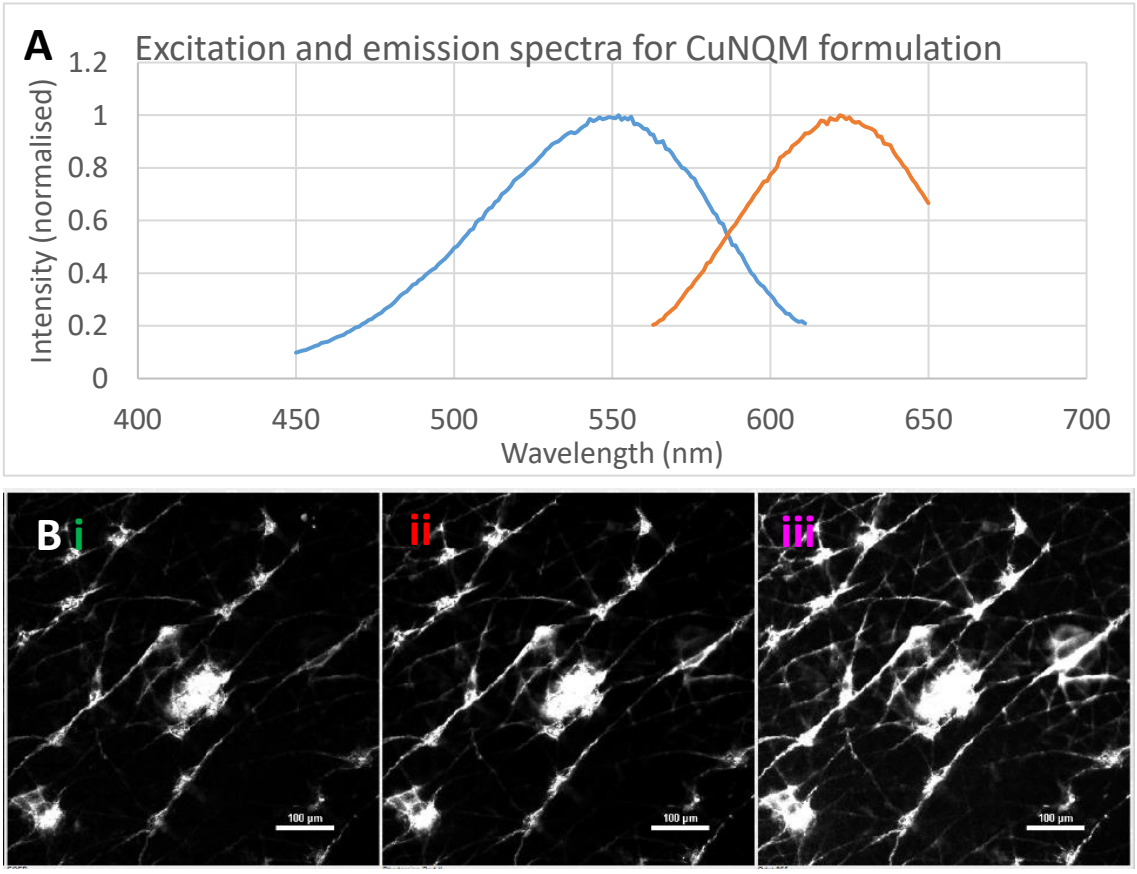

Figure 5.22: Fluorescence excitation and emission spectra for CuNQM formulation (A) and 2PM image (B) showing bleed-through of fluorescence from Nile red across the channels used to visualise EYFP (i), TAMRA (ii) and Nile red itself (iii). Scale bar: 100µm

5.5 General Discussion

This chapter aimed to build on previously published work using cubosomes and microneedles to facilitate the delivery of an ovalbumin peptide into the skin (Rattanapak et al., 2013, Rattanapak et al., 2014)- a collaborative project between Cardiff University, Osaka University and the University of Otago. Initial work focussed on the synthesis of the cubosome formulation to previously reported specifications. Wherever possible, reagents from the supplier indicated in the literature were used. One material that proved difficult to acquire was phytantriol as the manufacturer named in previous work was no longer producing it. As phytantriol comprises a mix of isomers, having to purchase from a new supplier meant that a potential source of variability was introduced. This was in addition to different synthesis equipment being used and the lack of availability of a stream of nitrogen, which was used in the previous publication to remove residual chloroform during the production of the homogeneous lipid phase.

Characterisation of cubosomes revealed that the particle diameter and size distribution (polydispersity index; PDI) of formulations were within the reported ranges (Rizwan et al., 2011). The zeta potential values obtained were slightly outside the range previously reported, though this did not affect the stability of cubosomes over the month-long storage test. There was coalescence within the dispersed phase, with both particle size and PDI increasing upon storage, though this was fully reversible with 10 minutes' vortexing. This stability is important to cubosome formulations that may be used clinically as a cracked emulsion will not possess the cubic structure desired and will show altered delivery properties compared to a monodisperse system. TEM imaging of cubosomes produced limited amounts of qualitative data, though the prohibitive cost of further TEM work and the characterisation data that could be rapidly obtained from the Malvern Nanosizer meant this avenue was not pursued further.

It was not possible to use the SIINFEKL-TAMRA peptide (to be used in later *in vivo* studies) for the early formulation work, so ovalbumin protein was used in its place. The incorporation of fluorescently-conjugated ovalbumin or Nile red into the cubosome formulation did not significantly alter its properties. The insertion of FITC-conjugated ovalbumin into cubosomes had been previously reported with 73% entrapment achieved (Rizwan et al., 2011). The entrapment efficiency obtained in our study (28.5%)

may be due to the use of AlexaFluor 555-conjugated ovalbumin in the place of FITC-conjugated protein. This was selected due to the autofluorescence of human skin sections in the FITC (488nm excitation) channel. AlexaFluor 555 is a much more polar fluorophore than FITC (LogP -1.06 and 4.90 respectively) (ChemAxon, 2016)- this could have reduced the protein's ability to partition into the lipid dispersed phase. The entrapment value was closer to the reported value for SIINFEKL-TAMRA (23%) (Rattanapak et al., 2013). The unavailability of the peptide before work in Japan meant that entrapment data could not be obtained for SIINFEKL-TAMRA, though the similarities of cubosomes produced in this investigation to those previously reported mean it is likely that comparable entrapment efficiencies were achieved.

Passing the cubosome formulations through NanoPass hollow microneedle arrays did not significantly alter the particle size of the lipid particles. This was to be expected, given that the bore of the microneedles was approximately 60µm, providing sufficient clearance for the 160nm lipid particles to pass through. This is important as the liposomal nanostructure of cubosomes is important both for its drug entrapment and for it to be able to form the cubic phase which aids skin retention. This method of delivery avoids altering water content of the formulation which could affect its stability. It is also efficient, delivering formulation into the skin without loss of formulation associated with topical application (Kim and Prausnitz, 2011, Norman et al., 2014, Wang et al., 2006). For a formulation that is difficult to scale up by the commonly used methods of manufacture (Garg and Saraf, 2007) (and therefore potentially expensive to produce in large quantities), this could reduce the formulation volume required to deliver a given dose and reduce costs for pharmaceutical manufacturers.

Coating the cubosomes onto microneedles proved to be more challenging than coating with an aqueous formulation (Chapter 2), with the lipid phase distributing itself unevenly on the needles' surface. The coating also proved ineffective for delivery into *ex vivo* human skin, with the soft lipid formulation failing to remain coated onto the needles' surface during insertion into skin. Given that the *ex vivo* skin was used at room temperature, it is possible that clinical application of these coated microneedles might be even less successful as warmer *in vivo* skin would further soften the formulation. This provides further evidence that although coated microneedles are a potentially useful delivery tool (Gill and Prausnitz, 2007a), the physical properties of the coating

formulation are important to ensure delivery into the skin. For this investigation, an aqueous formulation of peptide and adjuvant was coated onto microneedle arrays instead of cubosomes. The topical application of liquid cubosome formulation after microneedle pre-treatment was also tested to allow comparison with previous work (Rattanapak et al., 2014). Injection through hollow microneedles, solid microneedle pre-treatment followed by topical cubosome delivery and coated microneedles all showed successful delivery of Fl-OVA into human *ex vivo* skin in preliminary work before commencing *in vivo* mouse work in Osaka.

2PM allowed the real-time visualisation of immune cell behaviours in live skin, something that was not possible in the work to date in *ex vivo* human skin. One limitation of 2PM is that it cannot be performed in human skin as genetic manipulation is required to produce innately fluorescent DCs. It would most likely be extremely difficult to achieve fluorescent labelling of immune cells by another means, with technical challenges of specifically delivering a fluorophore by conjugated antibody or some other means. The equipment used would also be unsuited to the imaging of larger animals which could not be contained within the light-protective microscope housing. The murine model was useful however due to the similarities between mouse skin and human skin at a cellular level. Dermal DCs and epidermal LCs, which were morphologically similar to human LCs, were clearly visible in the images produced. There was a surprising disparity between the motility of the two immune cell populations in the mouse skin, with dDCs appearing more mobile than sessile LCs. This was in agreement with LCs in human ex vivo skin, where no change in LC density was seen in the epidermis 4 hours after vaccine delivery and dDCs migrated out of *ex vivo* skin in greater numbers than LCs.

Imaging the skin's structure was straightforward, with formulation on the stratum corneum allowing easy identification of the skin's surface. The stratum corneum was also faintly autofluorescent in the 480/80 filter, allowing its identification in untreated mice. The use of SHG made identification of the dermis (rich in collagen fibres) simple without the need for further staining or preparation. The depth of imaging proved to be a limiting factor in some of the treatments- in particular intradermal injection. The thinness of mouse skin increases the possibility that 'intradermal' injections were mistakenly subcutaneous rather than true intradermal injections. This

might explain why formulation could not be visualised despite depth of detection up to 200µm which is approximately the thickness of mouse skin (Calabro et al., 2011).

Another limitation of using 2PM in combination with live mice was the lengthy process of preparing the mice for imaging. This was especially important in microneedle-treated mice, where the channel began healing the moment that microneedles were removed from the skin and was mostly healed at approximately 90 minutes after treatment. The preparation process got more efficient with repeated attempts but a limit of speed was reached due to the delicate process of attaching the microscope cover glass to the mouse- attempting to remove it after initial application damaged the skin due to the adhesiveness of the glue used. Excess dried glue proximal to the treatment area also made it difficult to remount the cover glass accurately.

In cases where treatment and mounting of the mouse onto glass cover slip went as planned, there were still a number of issues which acted to the detriment of imaging. Firstly, the level of anaesthesia used played an important role in the quality of images acquired. The laboratory used a protocol with 3% isoflurane used to induce anaesthesia and 2% used for maintenance. Though this level was adequate for mouse work on the benchtop, it quickly became apparent that within the confines of the light-protective microscope housing that this was excessive. Excess anaesthesia presented in mice as respiratory depression- breathing became 'gasping', similar to agonal breathing. This was not only bad for the mouse's welfare but led to displacement of the mouse from the cover glass, affecting stability of the images. Thus, in subsequent experiments, the inner door was allowed to remain slightly open to improve air circulation. To avoid the mouse being affected by the cooler air in the room, a heated microscope stage was also included at this point.

The high number of treatments that were explored in this study, along with the fact that a mouse could only be used for one imaging session- either immediately after treatment or 48 hours later, after which it was sacrificed - meant that a low number of repeats could be obtained for the study. LCs were analysed at a later time point than the 4 hours used previously where no change was seen (Rattanapak et al., 2014). The results showed a trend of reduced LC numbers in treated skin, with the reduction greatest in mice treated with peptide-loaded cubosome formulation. This was in line

with the results found previously in human LCs at 48 hours following antigen delivery into the skin (Pearton et al., 2010b, Pearton et al., 2010c). Unfortunately, there were a low number of usable images due to poor images being acquired from some mice (due to movement from the slide or poor initial mounting) meaning that LCs could not be reliably quantified. This led to an n-number of 1 for untreated mice and 2 for each of the treatment conditions. This low number meant that statistical significance could not be assigned to the data and instead it can be stated that the data represents a potentially interesting trend, with further work required to determine the reliability of conclusions.

The low number of repeats due to inconsistent imaging also limited the quantitative data that could be drawn from other areas of the 2PM images. Post-imaging analysis software is able to track the movements of dDCs over time. Unfortunately, the majority of the time-lapse videos showed 'drift' over time whereby the movements brought about by the mouse's breathing (especially in cases where respiratory depression occurred) affected the microscope stage position and meant the plane of focus moved over time, making the movement of cells markedly more difficult to measure. It would also have been useful to obtain a greater number of videos of microneedle channels healing to try and quantify the process, but this proved impossible in the time available for the investigation.

The low number of repeats and variability of antigen retention within treatment groups meant that no conclusive statement could be made about whether cubosomes improved the retention of antigen. The depth of imaging meant that only the upper layers of skin could be visualised- thus any formulation which had been delivered to the deep reticular dermis could not be seen. Mice are prone to self-grooming and so the area of treatment would likely have been cleaned between treatment and imaging 48 hours later, potentially removing any antigen close to the skin's surface also. Thus, no conclusions could be drawn regarding cubosomes' ability to aid vaccine retention within the skin. This was unfortunate as cubosomes have shown promise in the retention of drugs (Peng et al., 2015) or vaccines (Gordon et al., 2012) within the skin and it may be one of their advantages over other liposomal formulations which only enhance overall delivery rather than alter kinetics (Clogston and Caffrey, 2005).

The analysis of antigen uptake by flow cytometry on inguinal lymph node cells confirmed that dDCs, the most motile DCs in the skin, were responsible for the greatest uptake of ovalbumin peptide antigen. The autofluorescence seen in untreated CD207+ dDCs from the mice was most likely the result of imperfect compensation as FITC and PE conjugated antibodies were used to compensate for eYFP and TAMRA respectively. In future work, compensation using untreated eYFP-expressing cells and cells stained with a TAMRA-conjugated antibody would likely reduce this fluorescence spill-over.

The data agreed with previous results which found the CD207+ dDC subset were responsible for the greatest internalisation of peptide (Rattanapak et al., 2014). This subset has been compared to the CD141+ subset of human dDCs (Chu et al., 2012, Bennett, 2015)- reinforcing the importance of this dDC subset in intradermal immunisation as seen in Chapter 4. The lack of complementary skin cell data from mice due to poor tissue lysis meant that no robust conclusions could be drawn as to whether the CD207+ dDCs were internalising the peptide in the skin or whether formulation had been carried in solution in the lymph vessels to the lymph nodes where resident DCs may internalise it. If the latter is true, retention in the skin may not be desirable for the formulation. It is of note that this investigation did not include immunological challenge, so it cannot be concluded that higher peptide uptake would translate to greater stimulation of T-cells by CD207+ dDCs in the mice. Also, this investigation does not distinguish between the protein processing capabilities of skin immune cells as the peptide was delivered to cells without the need for them to cleave it from a larger polypeptide as was the case with the influenza matrix peptide in Chapter 4.

Coated microneedle delivery led to the greatest amount of peptide internalised by CD207+ dDCs isolated from lymph nodes. Cubosome-based delivery, however, led to the greatest reduction in LCs in the epidermis- a sign of maturation which in this case will have been induced by the adjuvants present in the formulation as the peptide itself is non-immunogenic. Thus, it can be speculated that the coated microneedles represent the most efficient manner to deliver antigen to dDCs, which may well be responsible for priming early immune responses due to their more motile characteristics over LCs. However, if LCs prove to be more able to create an adaptive immune response against a certain pathogen and are to be targeted, a cubosome-based system may well prove

more beneficial. The retention properties of cubosomes remained untested due to the limitations of imaging via 2PM, though represent an interesting avenue for future work.

5.6 Potential for Publication

The work within this chapter aimed to build on previously published work (Rattanapak et al., 2013, Rattanapak et al., 2014) to create publishable collaborative data. The initial characterisation of cubosomes' physical properties was completed to ensure that the manufacturing process was implemented to the standards previously achieved. The physical stability study represents novel data that could potentially be publishable, as proven stability is an important characteristic of any formulation for clinical use. The 2PM studies did not yield sufficient replicates to allow for publishable data regarding LC density in the mouse skin or the motile behaviour of dDCs following antigen delivery. The antigen uptake study in lymph node cells is not publishable without corresponding skin cell data that would allow a distinction to be made between cells that internalised antigen in the skin and then migrated to the lymph node and those cells that internalised antigen in situ in the lymph node. Optimisation of the lipid staining protocol (using a fluorescent substrate other than Nile red) would allow the behaviour of the lipid phase of cubosomes in murine skin to be visualised which could potentially be publishable.

5.7 Conclusion

This work has provided further evidence that cubosomes are a physically stable liposomal formulation that can be used to entrap vaccine antigen. This chapter focussed on the protein ovalbumin and its peptide SIINFEKL. Both possess aqueous solubility and so are likely to insert into the aqueous continuous phase. It is likely that hydrophilic proteins/peptides will be compatible with a cubosome formulation as they will not interact with the lipid phase and thus the stability of the cubic phase will be maintained. A size limit will however exist, above which the macromolecules will not be able to insert into the 'nanopockets' that exist within the cubic phase (Angelov et al., 2012) and cubosomes will therefore not improve delivery. Hydrophobic antigen will instead insert

into the lipid phase. In this case, care must be taken that the antigen does not adversely affect the ability of the stabiliser (in this study poloxamer 407) to maintain the colloidal system. Further work is required to establish a comprehensive list of protein/peptide antigen which are compatible with the cubosome formulation used in this chapter.

Cubosomes were shown to improve delivery into the skin and can be used in combination with microneedles to provide a synergistic delivery improvement into the skin. The entrapment may also increase the immunogenicity of the antigen, though further work is needed to confirm this. Cubosomes appear to deliver preferentially to the upper layers of skin, where they stimulate LCs to mature and migrate out of the skin in a mouse model. However, LCs do not seem to be the most active immune cells of the skin, with dDCs (and CD207+ dDCs in mice in particular) being much more motile and internalising a greater amount of peptide antigen, even extending into the epidermis to sample antigen there. The work in the transgenic mouse model did not include assessment of responses in the T-cell compartment though, so no conclusions can be made about how the greater uptake of antigen by dDCs translates into an adaptive immune response. The data obtained in the human *ex vivo* skin cell model demonstrated a greater ability of dDCs to uptake and cross-present influenza virus-derived antigen, which in combination with the results within this chapter suggests that these cells are the optimal targets for intradermal immunisation as opposed to LCs.

5.7 Bibliography

ALEXANDER, M. Y. & AKHURST, R. J. 1995. Liposome-medicated gene transfer and expression via the skin. *Hum Mol Genet,* 4**,** 2279-85.

ALMGREN, M., EDWARDS, K. & KARLSSON, G. 2000. Cryo transmission electron microscopy of liposomes and related structures. *Colloids and Surfaces A: Physicochemical and Engineering Aspects,* 174**,** 3-21.

BEI, D., MENG, J. & YOUAN, B. B. 2010. Engineering nanomedicines for improved melanoma therapy: progress and promises. *Nanomedicine (Lond),* 5**,** 1385-99.

BENDER, J., ERICSON, M. B., MERCLIN, N., IANI, V., ROSÉN, A., ENGSTRÖM, S. & MOAN, J. 2005. Lipid cubic phases for improved topical drug delivery in photodynamic therapy. *Journal of Controlled Release,* 106**,** 350-360.

BENDER, J., SIMONSSON, C., SMEDH, M., ENGSTRÖM, S. & ERICSON, M. B. 2008. Lipid cubic phases in topical drug delivery: Visualization of skin distribution using two-photon microscopy. *Journal of Controlled Release,* 129**,** 163-169.

BENNETT, C. L. 2015. Editorial: Faux amis: Langerin-expressing DC in humans and mice. *J Leukoc Biol.* United States.

BENSON, H. A. E. & NAMJOSHI, S. 2008. Proteins and Peptides: Strategies for Delivery to and Across the Skin. *Journal of Pharmaceutical Sciences,* 97**,** 3591-3610.

BERNE, B. J. & PECORA, R. 1976. *Dynamic light scattering: with applications to chemistry, biology, and physics*, Courier Corporation.

BU, M., TANG, J., WEI, Y., SUN, Y., WANG, X., WU, L. & LIU, H. 2015. Enhanced bioavailability of nerve growth factor with phytantriol lipid-based crystalline nanoparticles in cochlea. *Int J Nanomedicine,* 10**,** 6879-89.

CALABRO, K., CURTIS, A., GALARNEAU, J.-R., KRUCKER, T. & BIGIO, I. J. 2011. Gender variations in the optical properties of skin in murine animal models. *Journal of Biomedical Optics,* 16**,** 011008-011008-8.

CAMPAGNOLA, P. J., WEI, M.-D., LEWIS, A. & LOEW, L. M. 1999. High-Resolution Nonlinear Optical Imaging of Live Cells by Second Harmonic Generation. *Biophysical Journal,* 77**,** 3341-3349.

CEVC, G. 1996. Transfersomes, Liposomes and Other Lipid Suspensions on the Skin: Permeation Enhancement, Vesicle Penetration, and Transdermal Drug Delivery. 13**,** 257-388.

CHEMAXON. 2016. *Chemicalize.org* [Online]. Available: http://www.chemicalize.org/structure/#!mol=Alexa+Fluor+555Available: http://www.chemicalize.org/structure/#!mol=S%3DC%3DN%2Fc5cc1c(C(%3DO)OC13c4ccc(O)cc4Oc2cc(O)ccc23)cc5 [Accessed 21st March 2016].

CHU, C. C., ALI, N., KARAGIANNIS, P., DI MEGLIO, P., SKOWERA, A., NAPOLITANO, L., BARINAGA, G., GRYS, K., SHARIF-PAGHALEH, E., KARAGIANNIS, S. N., PEAKMAN, M., LOMBARDI, G. & NESTLE, F. O. 2012. Resident CD141 (BDCA3)+ dendritic cells in human skin produce IL-10 and induce regulatory T cells that suppress skin inflammation. *J Exp Med,* 209**,** 935-45.

CLOGSTON, J. & CAFFREY, M. 2005. Controlling release from the lipidic cubic phase. Amino acids, peptides, proteins and nucleic acids. *Journal of Controlled Release,* 107**,** 97-111.

DE JONG, M. A., DE WITTE, L. & GEIJTENBEEK, T. B. 2010. Isolation of immature primary Langerhans cells from human epidermal skin. *Methods Mol Biol,* 595**,** 55-65.

DEMURTAS, D., GUICHARD, P., MARTIEL, I., MEZZENGA, R., HÉBERT, C. & SAGALOWICZ, L. 2015. Direct visualization of dispersed lipid bicontinuous cubic phases by cryo-electron tomography. *Nat Commun,* 6**,** 8915.

DENK, W., PISTON, D. W. & WEBB, W. W. 1995. Two-Photon Molecular Excitation in Laser-Scanning Microscopy. *In:* PAWLEY, J. B. (ed.) *Handbook of Biological Confocal Microscopy.* Boston, MA: Springer US.

DENK, W., STRICKLER, J. H. & WEBB, W. W. 1990. Two-photon laser scanning fluorescence microscopy. *Science,* 248**,** 73-76.

DESAI, P., PATLOLLA, R. R. & SINGH, M. 2010. Interaction of nanoparticles and cell-penetrating peptides with skin for transdermal drug delivery. *Mol Membr Biol,* 27**,** 247-59.

EIDSMO, L., ALLAN, R., CAMINSCHI, I., VAN ROOIJEN, N., HEATH, W. R. & CARBONE, F. R. 2009. Differential migration of epidermal and dermal dendritic cells during skin infection. *J Immunol,* 182**,** 3165-72.

ERICKSON, H. P. 2009. Size and shape of protein molecules at the nanometer level determined by sedimentation, gel filtration, and electron microscopy. *Biol Proced Online,* 11**,** 32-51.

ESPOSITO, E., CORTESI, R., DRECHSLER, M., PACCAMICCIO, L., MARIANI, P., CONTADO, C., STELLIN, E., MENEGATTI, E., BONINA, F. & PUGLIA, C. 2005. Cubosome dispersions as delivery systems for percutaneous administration of indomethacin. *Pharm Res,* 22**,** 2163-73.

FLEISHER, D., NIEMIEC, S. M., OH, C. K., HU, Z., RAMACHANDRAN, C. & WEINER, N. 1995. Topical delivery of growth hormone releasing peptide using liposomal systems: an in vitro study using hairless mouse skin. *Life Sci,* 57**,** 1293-7.

FRASER, S. J., ROSE, R., HATTARKI, M. K., HARTLEY, P. G., DOLEZAL, O., DAWSON, R. M., SEPAROVIC, F. & POLYZOS, A. 2011. Preparation and biological evaluation of self-assembled cubic phases for the polyvalent inhibition of cholera toxin. *Soft Matter,* 7**,** 6125-6134.

GARG, G. & SARAF, S. 2007. Cubosomes: an overview. *Biol Pharm Bull,* 30**,** 350-3.

GILL, H. S. & PRAUSNITZ, M. R. 2007. Coated microneedles for transdermal delivery. *J Control Release,* 117**,** 227-37.

GORDON, S., YOUNG, K., WILSON, R., RIZWAN, S., KEMP, R., RADES, T. & HOOK, S. 2012. Chitosan hydrogels containing liposomes and cubosomes as particulate sustained release vaccine delivery systems. *J Liposome Res,* 22**,** 193-204.

GREENSPAN, P., MAYER, E. P. & FOWLER, S. D. 1985. Nile red: a selective fluorescent stain for intracellular lipid droplets. *J Cell Biol,* 100**,** 965-73.

HALEY, P. J. 2003. Species differences in the structure and function of the immune system. *Toxicology,* 188**,** 49-71.

HANSEN, L. S., COGGLE, J. E., WELLS, J. & CHARLES, M. W. 1984. The influence of the hair cycle on the thickness of mouse skin. *Anat Rec,* 210**,** 569-73.

HELMCHEN, F. & DENK, W. 2005. Deep tissue two-photon microscopy. *Nat Methods,* 2**,** 932-40.

HONEYWELL-NGUYEN, P. L. & BOUWSTRA, J. A. 2003. The in vitro transport of pergolide from surfactant-based elastic vesicles through human skin: a suggested mechanism of action. *J Control Release,* 86**,** 145-56.

HUA, S. 2014. Comparison of in vitro dialysis release methods of loperamide-encapsulated liposomal gel for topical drug delivery. *Int J Nanomedicine,* 9**,** 735-44.

HUA, S. 2015. Lipid-based nano-delivery systems for skin delivery of drugs and bioactives. *Frontiers in Pharmacology,* 6**,** 219.

HUNTER, R. J. 2013. *Zeta potential in colloid science: principles and applications*, Academic press.

KAGAWA, Y., MAEDA, S., MORI, M. & ISHII, M. 2012. [Intravital imaging of cancer cell dynamics]. *Nihon Geka Gakkai Zasshi,* 113**,** 171-6.

KALE, M., SURUSE, P., SINGH, R., MALHOTRA, G. & RAUT, P. 2012. Effect of size reduction techniques on doxorubicin hydrochloride loaded liposomes. *Int J Biol Pharm Res,* 3**,** 308-316.

KARAMI, Z. & HAMIDI, M. 2015. Cubosomes: remarkable drug delivery potential. *Drug Discovery Today,* In press, corrected proof.

KAZI, K. M., MANDAL, A. S., BISWAS, N., GUHA, A., CHATTERJEE, S., BEHERA, M. & KUOTSU, K. 2010. Niosome: A future of targeted drug delivery systems. *Journal of Advanced Pharmaceutical Technology & Research,* 1**,** 374-380.

KEL, J. M., GIRARD-MADOUX, M. J., REIZIS, B. & CLAUSEN, B. E. 2010. TGF-beta is required to maintain the pool of immature Langerhans cells in the epidermis. *J Immunol,* 185**,** 3248-55.

KIM, Y.-C. & PRAUSNITZ, M. R. 2011. Enabling skin vaccination using new delivery technologies. *Drug Delivery and Translational Research,* 1**,** 7-12.

KLECHEVSKY, E., MORITA, R., LIU, M., CAO, Y., COQUERY, S., THOMPSON-SNIPES, L. A., BRIERE, F., CHAUSSABEL, D., ZURAWSKI, G., PALUCKA, A. K., REITER, Y., BANCHEREAU, J. & UENO, H. 2008. Functional Specializations of Human Epidermal Langerhans Cells and CD14(+) Dermal Dendritic Cells. *Immunity,* 29**,** 497-510.

KOJARUNCHITT, T., HOOK, S., RIZWAN, S., RADES, T. & BALDURSDOTTIR, S. 2011. Development and characterisation of modified poloxamer 407 thermoresponsive depot systems containing cubosomes. *International Journal of Pharmaceutics,* 408**,** 20-26.

KOWADA, T., KIKUTA, J., KUBO, A., ISHII, M., MAEDA, H., MIZUKAMI, S. & KIKUCHI, K. 2011. In vivo fluorescence imaging of bone-resorbing osteoclasts. *J Am Chem Soc,* 133**,** 17772-6.

LI, D., MULLER, M. B., GILJE, S., KANER, R. B. & WALLACE, G. G. 2008. Processable aqueous dispersions of graphene nanosheets. *Nat Nano,* 3**,** 101-105.

LINDQUIST, R. L., SHAKHAR, G., DUDZIAK, D., WARDEMANN, H., EISENREICH, T., DUSTIN, M. L. & NUSSENZWEIG, M. C. 2004. Visualizing dendritic cell networks in vivo. *Nature immunology,* 5**,** 1243-1250.

LOPES, L. B., LOPES, J. L. C., OLIVEIRA, D. C. R., THOMAZINI, J. A., GARCIA, M. T. J., FANTINI, M. C. A., COLLETT, J. H. & BENTLEY, M. V. L. B. 2006. Liquid crystalline phases of monoolein and water for topical delivery of cyclosporin A: Characterization and study of in vitro and in vivo delivery. *European Journal of Pharmaceutics and Biopharmaceutics,* 63**,** 146-155.

LOPES, L. B., SPERETTA, F. F. & BENTLEY, M. V. 2007. Enhancement of skin penetration of vitamin K using monoolein-based liquid crystalline systems. *Eur J Pharm Sci,* 32**,** 209-15.

MALISSEN, B., TAMOUTOUNOUR, S. & HENRI, S. 2014. The origins and functions of dendritic cells and macrophages in the skin. *Nat Rev Immunol,* 14**,** 417-28.

MANDZY, N., GRULKE, E. & DRUFFEL, T. 2005. Breakage of TiO2 agglomerates in electrostatically stabilized aqueous dispersions. *Powder Technology,* 160**,** 121-126.

MESTAS, J. & HUGHES, C. C. 2004. Of mice and not men: differences between mouse and human immunology. *J Immunol,* 172**,** 2731-8.

MOHLER, W., MILLARD, A. C. & CAMPAGNOLA, P. J. 2003. Second harmonic generation imaging of endogenous structural proteins. *Methods,* 29**,** 97-109.

NG, K. W., PEARTON, M., COULMAN, S., ANSTEY, A., GATELEY, C., MORRISSEY, A., ALLENDER, C. & BIRCHALL, J. 2009. Development of an ex vivo human skin model for intradermal vaccination: tissue viability and Langerhans cell behaviour. *Vaccine,* 27**,** 5948-5955.

NORMAN, J. J., GUPTA, J., PATEL, S. R., PARK, S., JARRAHIAN, C., ZEHRUNG, D. & PRAUSNITZ, M. R. 2014. Reliability and accuracy of intradermal injection by Mantoux technique, hypodermic needle adapter, and hollow microneedle in pigs. *Drug Deliv Transl Res,* 4**,** 126-30.

PAN, X., HAN, K., PENG, X., YANG, Z., QIN, L., ZHU, C., HUANG, X., SHI, X., DIAN, L., LU, M. & WU, C. 2013. Nanostructured cubosomes as advanced drug delivery system. *Curr Pharm Des,* 19**,** 6290-7.

PASPARAKIS, M., HAASE, I. & NESTLE, F. O. 2014. Mechanisms regulating skin immunity and inflammation. *Nature Reviews Immunology,* 14**,** 289-301.

PATTERSON, G. H. & PISTON, D. W. 2000. Photobleaching in Two-Photon Excitation Microscopy. *Biophysical Journal,* 78**,** 2159-2162.

PEARTON, M., KANG, S.-M., SONG, J.-M., ANSTEY, A. V., IVORY, M., COMPANS, R. W. & BIRCHALL, J. C. 2010a. Changes in Human Langerhans Cells Following Intradermal Injection of Influenza Virus-Like Particle Vaccines. *PLoS ONE,* 5**,** e12410.

PEARTON, M., KANG, S.-M., SONG, J.-M., KIM, Y.-C., QUAN, F.-S., ANSTEY, A., IVORY, M., PRAUSNITZ, M. R., COMPANS, R. W. & BIRCHALL, J. C. 2010b. Influenza Virus-Like Particles coated onto microneedles can elicit

stimulatory effects on Langerhans cells in human skin. *Vaccine,* 28**,** 6104-6113.

PENG, X., ZHOU, Y., HAN, K., QIN, L., DIAN, L., LI, G., PAN, X. & WU, C. 2015. Characterization of cubosomes as a targeted and sustained transdermal delivery system for capsaicin. *Drug Des Devel Ther,* 9**,** 4209-18.

PIERRE, M. B. R. & DOS SANTOS MIRANDA COSTA, I. 2011. Liposomal systems as drug delivery vehicles for dermal and transdermal applications. *Archives of Dermatological Research,* 303**,** 607-621.

PRASHAR, D. & SHARMA, D. 2011. Cubosomes: a sustained drug delivery carrier. *Asian Journal of Research in Pharmaceutical Science,* 1**,** 59-62.

RATTANAPAK, T., BIRCHALL, J., YOUNG, K., ISHII, M., MEGLINSKI, I., RADES, T. & HOOK, S. 2013. Transcutaneous immunization using microneedles and cubosomes: Mechanistic investigations using Optical Coherence Tomography and Two-Photon Microscopy. *Journal of Controlled Release,* 172**,** 894-903.

RATTANAPAK, T., BIRCHALL, J. C., YOUNG, K., KUBO, A., FUJIMORI, S., ISHII, M. & HOOK, S. 2014. Dynamic visualization of dendritic cell-antigen interactions in the skin following transcutaneous immunization. *PLoS One,* 9**,** e89503.

REIMER, L. 2013. *Transmission electron microscopy: physics of image formation and microanalysis*, Springer.

RIDDICK, T. M. 1968. Control of colloid stability through zeta potential. *Blood,* 10.

RIZWAN, S. B., ASSMUS, D., BOEHNKE, A., HANLEY, T., BOYD, B. J., RADES, T. & HOOK, S. 2011. Preparation of phytantriol cubosomes by solvent precursor dilution for the delivery of protein vaccines. *Eur J Pharm Biopharm,* 79**,** 15-22.

SADHU, C., TING, H. J., LIPSKY, B., HENSLEY, K., GARCIA-MARTINEZ, L. F., SIMON, S. I. & STAUNTON, D. E. 2007. CD11c/CD18: novel ligands and a role in delayed-type hypersensitivity. *Journal of leukocyte biology,* 81**,** 1395-1403.

SCHWENDENER, R. A. 2014. Liposomes as vaccine delivery systems: a review of the recent advances. *Ther Adv Vaccines,* 2**,** 159-82.

SHORTMAN, K. & LIU, Y.-J. 2002. Mouse and human dendritic cell subtypes. *Nature Reviews Immunology,* 2**,** 151-161.

SO, P. T., DONG, C. Y., MASTERS, B. R. & BERLAND, K. M. 2000. Two-photon excitation fluorescence microscopy. *Annual review of biomedical engineering,* 2**,** 399-429.

VERMA, D. D., VERMA, S., BLUME, G. & FAHR, A. 2003. Particle size of liposomes influences dermal delivery of substances into skin. *Int J Pharm,* 258**,** 141-51.

WANG, P. M., CORNWELL, M., HILL, J. & PRAUSNITZ, M. R. 2006. Precise Microinjection into Skin Using Hollow Microneedles. *Journal of Investigative Dermatology,* 126**,** 1080-1087.

WATSON, D. S., ENDSLEY, A. N. & HUANG, L. 2012. Design considerations for liposomal vaccines: Influence of formulation parameters on antibody and cell-mediated immune responses to liposome associated antigens. *Vaccine,* 30**,** 2256-2272.

WEINER, N., WILLIAMS, N., BIRCH, G., RAMACHANDRAN, C., SHIPMAN JR, C. & FLYNN, G. 1989. Topical delivery of liposomally encapsulated interferon evaluated in a cutaneous herpes guinea pig model. *Antimicrobial Agents and Chemotherapy,* 33**,** 1217-1221.

WILLIAMS, A. C. & BARRY, B. W. 2012. Penetration enhancers. *Advanced Drug Delivery Reviews,* 64, Supplement**,** 128-137.

WILLIAMS, D. B. & CARTER, C. B. 1996. The Transmission Electron Microscope. *Transmission Electron Microscopy: A Textbook for Materials Science.* Boston, MA: Springer US.

WILLIAMS, R. M., ZIPFEL, W. R. & WEBB, W. W. 2005. Interpreting Second-Harmonic Generation Images of Collagen I Fibrils. *Biophysical Journal,* 88**,** 1377-1386.

Chapter 6: General Discussion

6.1 Brief Overview

The overarching aim of this Thesis was to improve the understanding of skin immune cell characteristics with a view to informing intradermal vaccination strategy. Three areas were studied to achieve this aim: dermal dendritic cells, epidermal Langerhans cells and the intradermal delivery of vaccines.

6.2 Dermal Dendritic Cells

Following their recognition as immune cells in the 1970s, Langerhans cells (LCs) garnered a reputation as the only dendritic cells (DCs) of the skin, being able to take up antigen in the epidermis before migrating to lymph nodes where they elicit an immune response (Romani et al., 2012, Stingl et al., 1978). The 1990s saw work that identified other dendritic cells resident within the skin- the dermal dendritic cells (dDCs) (Steinman, 1991, Banchereau and Steinman, 1998). Subsequent work identified the presence of multiple subsets of dDCs in normal and inflamed skin (Nestle et al., 1993, Haniffa et al., 2009, Jongbloed et al., 2010, Segura et al., 2012).

Whilst histological and 2PM techniques are useful in observing morphological behaviours of both LCs and dDCs, they are limited in the number of factors that can be studied concurrently, which makes identification of the dDC subsets difficult. This led to the adoption of an immune cell isolation method within this Thesis to allow the study of dDCs (and LCs) in a cell suspension. A range of methods have been used previously to obtain a suspension of immune cells from the skin (summarised in Section 3.1.2). The method which was utilised allowed rapid enzymatic separation of epidermis and dermis (McCully et al., 2012) and also allowed for the enrichment of DCs based on their motile nature (Nestle et al., 1993, Artyomov et al., 2015). A number of studies had utilised a further enrichment step with density centrifugation (Pena-Cruz et al., 2001), fluorescence-activated cell sorting (FACS) (Chu et al., 2012) or magnetic-activated cell sorting (MACS) (Segura et al., 2012) either after walkout (Goddard et al., 2004) or following lysis of the tissue (Haniffa et al., 2012). Whilst this would have provided a purer

DC population, it would no doubt involve the loss of cells so would be unsuitable for the small areas of excised human skin tissue that are often used for research e.g. from mastectomy surgeries. Thus, the majority of work in this Thesis was performed with dermal and epidermal walkout cells in the purities found directly after walkout. As dDCs do not reside in the epidermis and LCs did not make up a significant proportion of dermal walkout cells (Section 3.4.1), this allowed the comparison of the two populations of skin DCs in parallel. However, the differing characteristics of dDC subsets, which is one of the most disputed areas of current skin immunology, could not be studied unless cells were subsequently sorted (Section 4.4.6).

There is consensus that one subset of dDCs are the CD141+ dDCs, although the flow cytometric gating strategies used to arrive at this cell population are not consistent between groups (Chu et al., 2012, Artyomov et al., 2015, Haniffa et al., 2012). Some (Haniffa et al., 2012, Artyomov et al., 2015) exclude CD14+ dDCs before gating for CD141+ cells, whilst others gate overall dDCs for CD141+ cells (Chu et al., 2012). The work within this Thesis found that the vast majority of CD141+ cells amongst migratory dermal cells were also CD14+ (Section 3.4.1), in agreement with the latter gating method (Chu et al., 2012). The CD14-/CD141+ cells described were a much rarer cell population and have been best isolated via tissue digestion rather than walkout (Haniffa et al., 2012), which might explain the absence of a meaningful population in the results of this Thesis. Thus, tissue digestion should be utilised in the place of a walkout if this subset of dDCs are to be studied in future work.

Whilst most groups tend to agree there are two resident myeloid DC subsets in the dermis, the marker used to identify the second subset varies between groups. CD1a+ dDCs are sometimes used to indicate the second subset (Artyomov et al., 2015, Klechevsky et al., 2008b, Segura et al., 2012), though this is not an ideal marker as CD1a expression is low and variable in this subset. This issue is compounded by the presence of LCs, which have the highest CD1a expression in skin (Hunger et al., 2004, Klechevsky et al., 2008b) but are not dDCs. A separate strategy is to classify the remaining dDCs based on CD1c+ expression (Haniffa et al., 2012, Chu et al., 2012, Collin et al., 2013). CD1c+ dDCs also express CD11c (Chu et al., 2012), leading to the gating strategy used in this Thesis, with CD141+/CD11c+ dDCs representing CD141+ dDCs and CD141-/CD11c+ dDCs representing CD1c+ dDCs. A third subset which was negative for both CD141 and

CD11c was also found in migratory dermal cells. These cells have been identified in the blood as CD34+ dDC precursors (Haniffa et al., 2012), which may also be the case in skin where the cells have exited the vasculature but not fully developed into dDCs.

CD141+ dDCs are developmentally related to the rare blood CD141+ population, indicating that the blood DCs are able to migrate into the skin and take up residence there (Carpentier et al., 2016, Haniffa et al., 2012). These CD141+ blood DCs are potent cross-presenting cells which exclusively express the chemokine receptor XCR1 (Bachem et al., 2010). The CD141+ dDCs are potent cross-presenters of protein antigen including hepatitis B surface antigen (Haniffa et al., 2012), pre-proinsulin (Chu et al., 2012) and necrotic cell antigen (Jongbloed et al., 2010). The work in this Thesis with *ex vivo* human skin LCs and dDCs utilised whole inactivated influenza virus rather than soluble protein or peptide. It was found that walkout dDCs were able to cross-present the HLA A*0201-restricted influenza A virus-derived matrix protein (M1)-derived peptide (residues 58-66; GILGFVFTL) to ALF3 T-cell clones to a much greater extent than LCs from the same skin sample (Section 4.4.5). This was in agreement with results using GILGFVFTL-restricted T-cell clones with DCs incubated with live influenza virus (Ratzinger et al., 2004). It conflicted, however, with results obtained using DCs incubated with the full-length M1 protein which found that LCs were the better cross-presenting cells (Klechevsky et al., 2008b). A further study also infected skin walkout cells with live influenza virus and found that LCs were able to promote the greatest proliferative response in allogeneic CD8+ T-cells (van der Aar et al., 2011). The data utilising live virus is of less use as skin is not a major infection route for influenza and direct infection can lead to the presentation of *de novo* synthesised viral peptides on MHC-I molecules rather than true cross-presentation (van der Vlist et al., 2011). As the current influenza vaccines utilise inactivated virus, the work in this Thesis may provide a more accurate representation of the cells responsible for raising an adaptive immune response following intradermal immunisation. Thus, it can be concluded that targeting of the dermis, rather than epidermis, appears to be advantageous in producing an adaptive immune response against the M1 matrix peptide in influenza vaccine. Whether this is true for other influenza viral peptides will require further work to clarify.

Sorting of dermal walkout cells allowed for comparisons to be made between the dDC subsets. The high cell loss associated with cell sorting and the lower frequency

of the CD141+/CD11c+ and CD141-/CD11c- subsets meant that skin samples large enough to provide adequate starting populations of dDCs were limited and so experimental repeats were low. However, the results showed that whilst CD141+/CD11c+ dDCs were able to cross-present the influenza M1 peptide antigen as expected, the CD141-/CD11c+ dDCs were able to cross-present to a slightly greater extent. The lack of repeats meant that only tentative conclusions could be drawn and data suggested that the phenotypic markers used do not correspond with the function of dDCs. This is an issue that has been highlighted in the literature (Carpentier et al., 2016), where cell surface marker expression overlaps between multiple subsets. The cytokine receptor XCR1 has been identified as a marker unique to cross-presenting dDCs (Crozat et al., 2010) but neither reliable antibodies nor fluorescently conjugated ligand (XCL1 or XCL2) are commercially available and thus staining to identify these cells is challenging (Carpentier et al., 2016). The C-type lectin CLEC9A is also expressed on cross-presenting DCs (Schreibelt et al., 2012, Caminschi et al., 2008) and may be a useful marker for distinguishing dDC subsets. It may be the case that staining for one of these markers is required to reliably identify cross-presenting dDC subsets in the future. The lower level of cross-presentation by CD141-/CD11c- dDCs supports the theory that these are dDC precursor cells (Haniffa et al., 2012) which have not fully developed dDC characteristics and so do not participate meaningfully in creating an adaptive immune response.

The work in this Thesis investigated the cross-presentation of a single peptide derived from the complex influenza virus. An adaptive immune response against a virus involves the processing and presentation of multiple epitopes by APCs, with varying importance to counteracting the viral pathogen (Murphy et al., 2012). In the case of influenza, M1 matrix peptides alone are unlikely to elicit adequate immunity, otherwise their conserved nature between strains would allow cross-immunity to occur in patients immunised against any strain previously. Work has been done previously with a universal vaccine based on the M2 protein (De Filette et al., 2005, Huleatt et al., 2008), though this proved to have little clinical success. More recently, universal vaccines based on hemagglutinin envelope protein have shown more promise (Impagliazzo et al., 2015) in creating immune responses against the varying envelope proteins in seasonal influenza strains (e.g. H1N1, H5N2). Provided the necessary epitopes are identified and

the appropriate T-cell clones produced, the *ex vivo* skin cell model used in this Thesis could prove a useful tool for assessing the cross-presentation of antigen in novel intradermal vaccines prior to their assessment in animal models. It is also likely that data assessing classical antigen presentation on MHC-II molecules to CD4+ T-cells would be required to assess the humoral response to vaccination concurrently. The combined approach would allow assessment of both cellular and humoral arms of the adaptive immune response to be assessed in *ex vivo* human tissue prior to clinical work. Ultimately such a laboratory system could better predict the clinical response to candidate vaccines and thus promote more lean clinical trials.

The yield of walkout cells from *ex vivo* skin was proportional to the size of the skin sample, with larger skin samples providing a greater yield of dDCs and LCs. There appeared to be a weak correlation between the yield of DCs and age, with older skin samples producing a lower yield. The decrease in skin DCs in older patients agrees with previous literature (Grewe, 2001, Bhushan et al., 2002). However, the data was obtained retrospectively and did not control for sample size so requires further work to confirm. The skin samples were also not representative of the general population i.e. the skin was mostly from mastectomy surgeries and therefore most patients were elderly (mean age: 66 years) and all of them were Caucasian females. Obtaining skin from a single hospital also limited the genetic diversity, as patients were likely to be from the surrounding geographical area. This proved advantageous for cross-presentation experiments, as 6 of the 8 samples (75%) were found to be HLA-A2+ compared to the previously reported frequency of 49.6% amongst Caucasians (Ellis et al., 2000). The narrow diversity of age, gender and race must be taken into account when interpreting the results and drawing conclusions covering a wider population. For example, darker skin contains a comparable number of melanocytes but a much greater level of melanin than lighter skin (Tadokoro et al., 2005), which will affect UV penetration into the skin. This could affect skin DC characteristics as UV radiation has previously been shown to reduce the antigen presenting capabilities of LCs (Dittmar et al., 1999). Obtaining skin from other hospitals with a greater ethnic diversity would control for the effect of skin pigmentation. A better range of age and also gender could be obtained if skin were sourced from other surgical procedures e.g. abdominoplasty. A diversity of ethnicity, age and gender would allow the production of data which was more representative of

the global patient population, increasing its usefulness to the pharmaceutical industry, who distribute products internationally.

It had been reported than walkout dDCs from human skin possess a semi-mature phenotype following isolation that utilised a longer enzymatic incubation time and sorting via FACS (Chu et al., 2012). This is comparable to the dDCs that migrate at steady state from mouse skin to lymph nodes and possess tolerising rather than immunostimulatory capabilities (Kissenpfennig et al., 2005, Lutz and Schuler, 2002). Skin walkout DCs obtained using the shorter enzyme incubation time and without sorting (as described in Section 3.3.1) were assessed for their response to immunostimulatory substances such as LPS or poly(I:C) to determine if the reduced processing of cells allowed them to be isolated in an immature state. It found that it was possible to upregulate the maturation marker CD83 to some extent but that cells were already partially mature at the time of isolation, making the distinction between untreated cells and cells treated with TLR agonists difficult. Cytokine expression by the cells was also poor, even when the potent immunostimulator LPS was used. Thus, it was determined that the changes in the protocol did not lead to the isolation of immature DCs from the skin and the walkout cells that could be obtained would not be a useful tool for assessing the changes in maturation and cytokine expression as a result of vaccine antigen or adjuvants within this project. A tissue digestion protocol (Haniffa et al., 2009, Haniffa et al., 2012) may be advantageous as cells will not need to spontaneously migrate out of tissue and so will have less time to develop a semi-mature phenotype before use.

As well as viral vaccine antigen processing, it was possible to obtain data on the uptake and responses of skin DCs to an adjuvanted ovalbumin peptide vaccine using a mouse model. This data indicated that CD207+ dDCs were the most active antigen-internalising cells, in line with previously reported results using mouse skin-derived DCs (Rattanapak et al., 2014). It was not possible to distinguish lymph node-resident DCs from those which had migrated from the skin during the investigation. Thus, it could not be determined if antigen delivery to DCs occurred locally in the skin or via lymph vessels to lymph node-resident DCs which has been previously described (Li et al., 2014, Tozuka et al., 2016). Mouse CD207+ dDCs have been identified as the equivalent of the CD141+ skin dDCs in humans based on function (Chu et al., 2012, Bigley et al., 2015, Carpentier et al., 2016), which agrees with influenza virus data that indicates these cells are able to

uptake and process vaccine antigen rapidly. This provides further evidence for the dermal, rather than epidermal, targeting of vaccines.

6.3 Epidermal Langerhans Cells

The C-type lectin receptor Langerin (CD207) has made identification of LCs within the skin straightforward since its identification at the turn of the 21st century (Valladeau et al., 1999, Valladeau et al., 2000). LCs are also the lone DC population residing in the epidermis (Merad et al., 2008) and express higher levels of CD1a than dDCs (Stoitzner et al., 2010), making their phenotypic identification much more straightforward than that of dDC subsets. Our understanding of LCs role in skin immunity (both innate and adaptive), however, has been under constant revision (Romani et al., 2012).

One of the earliest properties of Langerhans cells to be identified was their ability to present antigen to naïve T-cells to elicit an adaptive immune response (Stingl et al., 1978). Their detection of foreign antigen in the skin leads to maturation and migration from the skin to lymph nodes (Cumberbatch et al., 2000, Johnston et al., 2000). In vivo, these LCs will be replaced to restore the normal complement within the epidermis by either mitotic LCs under normal turnover (Czernielewski and Demarchez, 1987, Kanitakis et al., 1993) or the recruitment of precursors from blood in cases of widespread depletion (Merad et al., 2002). *Ex vivo* human skin, which has been removed from the systemic circulation with carries LC precursors, can be used to study this depletion of LCs from the skin (Larsen et al., 1990). Tissue can be stained for CD207 to allow the specific visualisation of LCs (Valladeau et al., 1999). Using this model, the response of the LCs to vaccines (Li et al., 2014), infection by pathogens (Johnston et al., 2000), skin sensitising agents (Ratzinger et al., 2002) or UV exposure (Seite et al., 2003) can be examined.

Previously published work (Pearton et al., 2010b, Pearton et al., 2010c) in *ex vivo* human skin showed that LCs underwent morphological changes and their numbers decreased significantly following treatment with influenza vaccine. This work examined the response of LCs at 24 to 48 hours' post-exposure. In this Thesis the immediate response to influenza vaccine was evaluated at 2 and 4 hours but there was no

difference to the untreated samples. This suggests that LCs take some time to uptake antigen and migrate out of the epidermis. This may be influenced by the tightly packed nature of keratinocytes in the epidermis and the morphology of LCs at rest i.e. with dendrites extending in multiple directions between keratinocytes (Yu et al., 1994). Thus, even if a LC encounters antigen it must change its morphology and withdraw its dendrites to facilitate mobilisation. It has been previously reported that LCs are slower at migrating to the lymph nodes than dDCs (Kissenpfennig et al., 2005). Slow migration of LCs was also witnessed in those mouse models analysed using two-photon intravital microscopy (2PM), described in Section 5.4.7.1. An immune response to a pathogen can take up to 5 days to be raised and this does not preclude the involvement of LCs. The low level of LC motility will likely mean that vaccines need to be delivered over a large area of skin to ensure that a high number of LCs internalise the antigen, whereas dDCs were observed being able to migrate towards a single site of antigen delivery in the murine model.

LCs possess the cellular machinery required to cross-present antigen to naïve CD8+ T-cells (Artyomov et al., 2015) and have been shown to cross-present protein-derived (Klechevsky et al., 2008b) peptide antigens. These experiments have utilised LCs, obtained from skin, which have been conditioned with a cocktail of stimulatory substances (Artyomov et al., 2015, Klechevsky et al., 2008b) to mature the LCs prior to their use. Work with measles virus and skin LCs found that immature LCs neither cross-presented viral antigen nor became infected (van der Vlist et al., 2011). Inducing maturity in the LCs led to viral infection and presentation of antigen on MHC-I molecules independent of cross-presentation machinery. The work in this Thesis used LCs directly from walkout (i.e. no further maturation was induced) and found that LCs were able to cross-present to some extent but much less so than dDCs. It is possible that incubation with TLR-agonists or other inducers of LC maturation prior to adding the virus may have improved the cross-presentation, though this would not be representative of vaccination with inactivated virus, which does not include pre-treatment to activate skin LCs. Thus, the results obtained in this Thesis may be more representative of the *in vivo* response of skin cells to intradermal influenza vaccination, with LCs providing a lesser contribution to activation of CD8+ T-cells over the shorter time points observed in this Thesis.

The reduced peptide antigen uptake and reduced virus-derived cross-presenting abilities of LCs compared to dDCs may be explained by the growing opinion that LCs are not purely immunogenic cells, but can also act as tolerising cells (Romani et al., 2012, Steinman et al., 2003). LCs have been shown to lack TLR expression that senses bacterial PAMPs (van der Aar et al., 2007). This may prevent unnecessary immune responses to the presence of commensal bacteria at the epidermal surface. Recent genetic analysis has shown that LCs are derived from embryonic precursor cells, unlike dDCs which develop from bone marrow precursors (Carpentier et al., 2016), and so are in ontological terms closer to macrophages than dDCs (Ginhoux and Merad, 2010). Their functional gene expression, however, is more comparable to CD1c+ dDCs (Carpentier et al., 2016). This property of DCs, which are derived from distinct precursors but acquire functional similarities based on tissue conditioning, may explain the often conflicting results obtained when studying the immunogenic properties of LCs and dDCs.

It has been reported that LCs in culture lose their LC-like characteristics (Schuler and Steinman, 1985) and are less capable of presenting peptide antigen than freshly isolated LCs (Romani et al., 1989). This may explain to some extent the conflicting results seen in studies regarding the cross-presentational abilities of LCs. Studies using lymph node-derived DCs (which includes those that have migrated from skin) found that all DC subsets present could cross-present antigen (Segura et al., 2013). Thus, as Segura et al. (2013) concluded, cross-presentation of an antigen by a given DC subset is likely a function of the antigen type, the environment in which the DC encounters the antigen and the type of pathogen that the antigen is derived from. This must be taken into account with all work using skin cell models. The use of LCs that have migrated from skin suggests that they may already be at least partially matured. The lack of danger signals upon migration (as vaccine was added after the cells had migrated out of tissue), may mean that these cells are committed to a tolerogenic phenotype (Hawiger et al., 2001). Thus, future experiments may need to deliver antigen to LCs *in situ* in the epidermis or digest the epidermis using trypsin to ensure immature LCs encounter the vaccine as they would *in vivo*.

The role of DCs requires them to internalise viral pathogens without becoming directly infected. To allow this, they possess antiviral factors such as apolipoprotein B mRNA-editing enzyme catalytic polypeptide-like 3G (APOBEC3G), which counteracts

HIV-1 (Sheehy et al., 2002, Pion et al., 2006) and hepatitis B (Turelli et al., 2004) infection, or SAMHD1 which counteracts HIV-1 infection (Laguette et al., 2011). The work in this Thesis found that there was a significant increase in the infectability of LCs and dDCs after SAMHD1 knockdown. It was also noted that this increase in infectability was much more pronounced in the dDCs, confirming the work which had been performed in monocyte-derived models where LCs were found to be more resistant to HIV infection after SAMHD1 knockdown (Czubala et al., 2016). Colleagues used monocyte-derived models in further work to uncover the source of the difference in infectability post-SAMHD1 knockdown. This study concluded that a factor that operates at the point of viral reverse transcription and is independent of MX2 (another antiviral factor) was unique to LCs (Czubala et al., 2016).

Given that the mechanisms by which HIV infects a person and evades the immune system are still not fully characterised, this work represents a step towards a better understanding of the virus that will allow for better drug therapies or vaccines to be designed. Should the future work on monocyte models uncover a potential lead on the LC-specific antiviral factor, the *ex vivo* skin cell model will be well placed to carry out confirmatory studies. Skin-derived cells are particularly useful in studying HIV because the only animal models are primates and humanised mouse models (Hatziioannou and Evans, 2012), and human genital mucosal tissue is not readily available for research use (Dezzutti and Hladik, 2013). The animal models commonly used for genital mucosa such as porcine (Lorenzen et al., 2015) or guinea pig (Da Costa et al., 1997) are not directly infectable with HIV-1. Thus, *ex vivo* skin walkout cells represent a model that it representative of human cells and avoids the costs associated with using primate models. It is also possible that skin walkout cells could be used to study the infection pathways of other viral (Gebhardt et al., 2009), bacterial (Wu and Xu, 2014) or fungal (Trzaska et al., 2015) pathogens which directly infect skin or mucosal immune cells to try and elucidate infection pathways that can be targeted with novel drugs or vaccines. It is also possible that vaccine strategies such as anti-oncotic vaccines which utilise anti-tumour vaccines (Rolinski and Hus, 2010) might be able to utilise the cells e.g. in anti-melanoma vaccines (Banchereau et al., 2001, Carreno et al., 2015).

6.4 Intradermal Vaccine Delivery

The data presented within this Thesis provides insight into the cells that may be preferentially targeted within the skin to ensure successful adaptive immune response to influenza as an example of a disease where intradermal vaccination is used. This is of little use, however, without a means of delivering vaccine to the desired targets. Porcine skin is commonly used as a model for the physical barrier properties human skin (Kong and Bhargava, 2011), whilst murine models are used to study immune responses *in vivo* (Mestas and Hughes, 2004). Where available, *ex vivo* human skin provides an option for modelling both delivery of vaccines into skin and the response of localised skin-resident immune cells to the vaccine within a single model (Ng et al., 2009, Schmalfuß et al., 1997, Larsen et al., 1990).

The Mantoux technique, the most commonly used method for intradermal delivery of vaccines, is both complex and subject to high variability between healthcare professionals in both delivery depth and volume (Suh et al., 2014a). The skin is not well suited to receiving a large volume bolus dose of liquid due to the dimensions and properties of the tissue, with injections over 50µl tending to lead to leakage into the hypodermis (Diehl et al., 2001), which is not particularly immunogenic and can reduce immunisation success (Groswasser et al., 1997, Shaw et al., 1989). There is also injection pain associated with the needle used in the Mantoux technique, which reduces patient acceptability (Nir et al., 2003). This has led to the development of a number of alternative minimally invasive delivery strategies such as microneedle (Levin et al., 2015, Wang et al., 2006), jet injector (Williams et al., 2000, Soonawala et al., 2013) and tattoo gun (van den Berg et al., 2009, Verstrepen et al., 2008) delivery systems, all of which aim to improve the consistency of intradermal delivery. This Thesis focussed on microneedles as a delivery technology as they are a simple but flexible delivery platform which can be adapted to suit a range of delivery purposes and have the potential to eschew liquid formulations to avoid the need for cold-chain storage (Zehrung, 2009).

The methods of microneedle delivery that were used in this Thesis were not novel, with protein or peptide formulation being coated onto stainless steel microneedles and the formulation dried before insertion into the skin (Bariya et al., 2012, Gill and Prausnitz, 2007a). The fluorescently-conjugated ovalbumin protein and

fluorescent nanoparticle vaccine models were incorporated into a simple coating formulation which had been used in previous studies of delivery into human ex vivo skin (Pearton et al., 2010c). The model vaccine antigen allowed for straightforward visualisation of antigen on the microneedles, though storage stability studies would be required to determine whether the coating formulation also improved vaccine stability as has been shown for influenza virus vaccine-coated needles (Kim et al., 2010, Kim et al., 2011).

Coated microneedles were able to deliver formulation into the skin, as had been shown many times previously (Caucheteux et al., 2016, Chong et al., 2013, Gill and Prausnitz, 2007a, Pearton et al., 2010c). As previously described, coated microneedles deposited the coated formulation proximal to the microchannel they create in human skin (Gill and Prausnitz, 2007b). The use of an array of many microneedles can overcome the limited volume of material that can be coated onto a single needle, without affecting the overall needle shape (Gill and Prausnitz, 2007a). Considerations must be given to the length, density and sharpness of needles in an array to avoid the 'bed of nails' effect and ensure that skin penetration is successful (Cheung et al., 2014). The coating methods used within this Thesis were crude and the variability in coating was not quantified. There have, however, been investigations within the pharmaceutical industry which have shown reproducible coating of microneedle arrays with proteins such as human growth hormone (Ameri et al., 2014), parathyroid hormone (Daddona et al., 2011) and erythropoietin (Peters et al., 2012). The processes used within the pharmaceutical industry are automated and coat entire arrays concurrently, allowing the speed of production to greatly exceed the methods used within this Thesis. This is important to ensure dose reproducibility, and thus the safety and efficacy of vaccines, and acceptable device costs. These are crucial factors to those developing microneedle systems for clinical use and the regulation of these devices.

The vast majority of clinical research involving intradermal immunisation employs the commercially available intramuscular injection and compares its efficacy when delivered intradermally or via the conventional intramuscular route (Soonawala et al., 2013, Kenney et al., 2004). The use of formulations designed for intramuscular use in intradermal vaccination studies does not acknowledge the marked differences between the two tissues. It may be possible to improve existing formulations to suit

intradermal delivery, though the method of improvement will depend on the delivery method that is selected and the desired effects of the vaccine. For vaccines without adjuvant such as the seasonal influenza vaccine (Della Cioppa et al., 2014), it may be that a simple formulation coated onto microneedles would be adequate. On the other hand, a VLP vaccine such as Cervarix™ which contains 3-Odesacyl-4'-monophosphoryl lipid A as an adjuvant which activates TLR4 (Casella and Mitchell, 2008, Monie et al., 2008) may be more effective reformulated with a TLR3 agonist such as poly(I:C) to activate the antiviral immunity pathway in the skin based on the results in this Thesis. The results in this Thesis showed that influenza VLP vaccine without adjuvant was not cross-presented as much as inactivated virus, which is structurally identical but contains viral genetic material. This genetic material may well have acted as an adjuvant, activating skin DCs and increasing the cross-presentation of antigen. This highlights the importance of proper adjuvant usage in vaccines to ensure that immune cells recognise the antigen as representative of a pathogen threat and do not induce tolerance (Mutyambizi et al., 2009, Steinman et al., 2003).

The presentation of antigen in lymph nodes may be a result of APC transport of the antigen and/or transport of free peptide, that has avoided enzymatic degradation, in the skin via the lymph vessels (Reddy et al., 2007, Tozuka et al., 2016). Delivery to skin-resident cells, which can transport antigen to lymph nodes, was examined in separate stages within the Thesis. The delivery method that favoured LC exposure to vaccine appeared to be application of a cubosome formulation following microneedle pre-treatment. However this observation is based on the limited data obtained from the 2PM imaging of murine skin 48 hours after treatment. This method of vaccine delivery showed a greater reduction in LC density than an identical method using an aqueous formulation or the use of coated microneedles. Coated microneedles (Pearton et al., 2010c) and intradermal injection by the Mantoux technique (Pearton et al., 2010b) have been shown to deliver influenza vaccine to LCs and stimulate their migration out of the epidermis in *ex vivo* human skin. In both cases, however, there was no means of quantifying dDC activation concurrently so there is no means of comparing the relative activation of the two populations. The sessile nature of LCs means that antigen needs to be delivered locally to an LC to ensure its uptake. Thus, delivery methods that target the epidermis such as coated microneedles or application of a cubosome formulation

following microneedle pre-treatment may be favourable over the Mantoux injection technique, which deposits a liquid formulation in the dermal layer i.e. sub-epidermis. The more superficial microneedle based approaches are also able to target a greater surface area of the epidermis and thus a greater number of LCs.

Based on the data gathered in this Thesis, delivery to dDCs in skin may be advantageous in terms of the immune response generated. In the case of inactivated influenza virus vaccine, dDCs showed a much greater cross-presentation of vaccine antigen. This suggests a more robust CD8+ T-cell response to be generated, which is particularly important in influenza given the role of CD8+ T-cells in viral clearance from the lung (Helft et al., 2012). In this case localising delivery to the papillary dermis will be optimal as this is the most dDC-rich region of skin (Gerlini et al., 2001, Cerio et al., 1989, Chu et al., 2012). The increased mobility of dDCs also mean than delivery to an adequate number of dDCs to allow an adaptive immune response can be possible with delivery to a small area, as dDCs can migrate towards the vaccine delivery site to uptake antigen. If a vaccine should prove to be processed more effectively by a given dDC subset, affinity targeting by conjugation of an antibody to the antigen can be used to increase the specificity of delivery (Bonifaz et al., 2002) and improve the immune response of the immunised individual (Sancho et al., 2009, Idoyaga et al., 2011).

6.5 Future Work

The diverse nature of the work contained within this Thesis means that a broad range of further work is possible. The isolation of walkout dDCs and LCs from skin could form the basis of a study into the differing properties of skin immune cells in ageing skin. This could involve studying the varying frequencies of dDC subsets or the differing antigen presentational abilities of dDCs and LCs. The availability of abdominoplasty skin samples from younger patients would provide a comparator for the more elderly skin obtained via the average mastectomy surgery. This could prove informative as elderly patients tend to be poor responders to vaccination and so the elucidation of dDC/LC changes with age could help to inform vaccine design to improve immunisation in this population.

The work in this Thesis investigated the delivery of antigen into skin and its processing then presentation to T-cells separately. An interesting future study would be to deliver vaccine to *ex vivo* human skin using intradermal delivery technologies such as coated solid microneedle arrays, hollow microneedles and intradermal injection by hypodermic needle. The tissue could then be cultured to allow time for the vaccine to distribute within the skin. After this time, dDCs and LCs would be isolated from the skin and co-cultured with T-cell clones to allow quantification of antigen presentation. This would allow comparison of the effectiveness of the various delivery methods over and above the histological deposition studies in Chapters 2 and 5. This would also improve the representativeness of the model to vaccinating a patient compared to co-culturing isolated skin cells with vaccine, allowing the cells to encounter vaccine in their natural environment. This would also allow signalling from other skin cells such as keratinocytes to influence the immune response seen.

The finding that dDCs cross-present an influenza virus matrix peptide to a greater extent also provides a starting point for further work. The walkout skin cell model could be used in combination with other T-cell clones to provide complementary data on the presentation of antigen via MHC-II molecules or on the cross-presentation of other viral antigens. The fact that studies regarding the cross-presentational ability of skin immune cells often conflict one another highlights the fact that a greater body of data is required before the true properties of these cells can be fully understood.

Finally, work to improve the classification of dDCs into subsets based on functionality represents an important avenue of future work. The development of a reliable monoclonal antibody against XCR1 would allow for the co-localisation of this marker for cross presenting cells with other dDC markers such as CD11c and CD141 to determine which cells possessed this machinery. The conflicting results with skin-derived cells means that the effect of culture conditions on DC phenotype must also be considered as there may plasticity in DCs for conversion between the various subsets.

6.6 Concluding Remarks

The aim of this Thesis was to further the understanding of human skin immune cells in order to inform how best to deliver vaccines into the skin for effective immunisation. The objectives were met as follows:

i. Peptide, protein and nanoparticle-containing formulations were produced and coated successfully onto solid stainless steel microneedles. Two coating methods were used, one of which involved the deposition of formulation on the terminal portion of needles only whilst the other coated the entire length of the needle. Both of which were able to coat the tips of needles with a visually even coating of formulation.

ii. Following insertion of coated microneedles into *ex vivo* human skin, the formulation was deposited in the area proximal to the needle channel in the epidermis and upper dermis. The delivery of inactivated influenza virus from coated microneedles into *ex vivo* human skin did not elicit a change in LC density in the epidermis after 2 or 4 hours, suggesting migration of mature LCs occurs at some time point between 4 and 24 hours post-delivery of vaccine into skin.

iii. Walkout epidermal and dermal cells were obtained from live *ex vivo* human skin. Phenotyping of cells revealed on average epidermal walkout cells comprised 7.3% LCs, whilst dDCs were 34.1% of dermal walkout cells. LCs were found to be HLA-DR+/CD1a+/CD207+ by flow cytometric analysis. Total dDCs could be identified by size/granularity/HLA-DR+/CD45+ gating. The viability of LCs and dDCs was over 95% in the samples tested. Classification of dDC subsets was made on CD11c and CD141 expression, revealing 3 subsets: CD141+/CD11c+ (mean 17.3% of dDCs), CD141-/CD11c+ (mean 60.3% of dDCs) and CD141-/CD11c- (mean 21.6% of dDCs).

iv. Both walkout LCs and dDCs possessed a semi-mature phenotype following their isolation from *ex vivo* skin explants, meaning that treatment with either TLR3 agonist (poly(I:C)) or TLR4 agonist (LPS) were

unable to elicit a significant increase in cell maturation markers (CD83) or cytokine production (TNF-α or IL-12). Thus, the cells were deemed to be unsuitable to quantify the ability of vaccine candidates to activate LCs and dDCs.

v. LCs possess an antiviral factor which allows them to resist infection by HIV-1 to a greater extent than dDCs even after the knockdown of SAMHD1, confirming work performed using monocyte-derived dendritic cell models. Work is ongoing in monocyte-derived dendritic cell models to identify this factor.

vi. dDCs cross-present inactivated influenza virus-derived peptide to a much greater extent than LCs. Replacing inactivated virus with equivalent VLPs (which do not contain viral DNA or RNA) led to a marked reduction in cross-presentation. Both CD141+/CD11c+ and CD141-/CD11c+ dDC sorted subsets were able to cross present the virus-derived antigen, though further repeats are required to validate this result.

vii. Cubosomes were able to entrap protein or peptide vaccine and the colloidal formulations were physically stable for one month at room temperature. A cubosome formulation could be delivered into *ex vivo* human skin directly via hollow microneedles or applied to skin after pre-treatment with solid microneedles. The cubosomes could not be dry-coated reliably onto microneedles for delivery into skin. Work in a murine model showed that a topically-applied cubosome formulation could deliver vaccine to LCs (as determined by a decrease in LC density in the epidermis 48 hours after treatment). Coated microneedles enabled peptide delivery to dDCs, with CD207+ dDCs (considered the murine equivalent of CD141+ human dDCs) showing the greatest amount of internalised peptide in skin-draining lymph nodes, providing further evidence for the importance of these cells in intradermal vaccination.

6.7 Bibliography

ADEREM, A. & ULEVITCH, R. J. 2000. Toll-like receptors in the induction of the innate immune response. *Nature,* 406**,** 782-7.

AERTS-TOEGAERT, C., HEIRMAN, C., TUYAERTS, S., CORTHALS, J., AERTS, J. L., BONEHILL, A., THIELEMANS, K. & BRECKPOT, K. 2007. CD83 expression on dendritic cells and T cells: correlation with effective immune responses. *Eur J Immunol,* 37**,** 686-95.

AHMED, Z., KAWAMURA, T., SHIMADA, S. & PIGUET, V. 2015. The role of human dendritic cells in HIV-1 infection. *J Invest Dermatol,* 135**,** 1225-33.

AIKEN, C. 1997. Pseudotyping human immunodeficiency virus type 1 (HIV-1) by the glycoprotein of vesicular stomatitis virus targets HIV-1 entry to an endocytic pathway and suppresses both the requirement for Nef and the sensitivity to cyclosporin A. *J Virol,* 71**,** 5871-7.

ALBERT, M. L., SAUTER, B. & BHARDWAJ, N. 1998. Dendritic cells acquire antigen from apoptotic cells and induce class I-restricted CTLs. *Nature,* 392**,** 86-9.

ALBERTINI AÉ, A. V., BAQUERO, E., FERLIN, A. & GAUDIN, Y. 2012. Molecular and Cellular Aspects of Rhabdovirus Entry. *Viruses.*

ALDROVANDI, G. M., FEUER, G., GAO, L., JAMIESON, B., KRISTEVA, M., CHEN, I. S. & ZACK, J. A. 1993. The SCID-hu mouse as a model for HIV-1 infection. *Nature,* 363**,** 732-6.

ALEXANDER, M. Y. & AKHURST, R. J. 1995. Liposome-medicated gene transfer and expression via the skin. *Hum Mol Genet,* 4**,** 2279-85.

ALMGREN, M., EDWARDS, K. & KARLSSON, G. 2000. Cryo transmission electron microscopy of liposomes and related structures. *Colloid Surface A,* 174**,** 3-21.

AMADORI, A., ZAMARCHI, R., DE SILVESTRO, G., FORZA, G., CAVATTON, G., DANIELI, G. A., CLEMENTI, M. & CHIECO-BIANCHI, L. 1995. Genetic control of the CD4/CD8 T-cell ratio in humans. *Nat Med,* 1**,** 1279-83.

AMERI, M., KADKHODAYAN, M., NGUYEN, J., BRAVO, J. A., SU, R., CHAN, K., SAMIEE, A. & DADDONA, P. E. 2014. Human Growth Hormone Delivery with a Microneedle Transdermal System: Preclinical Formulation, Stability, Delivery and PK of Therapeutically Relevant Doses. *Pharmaceutics,* 6**,** 220-234.

ANDERSEN, M. H., SCHRAMA, D., THOR STRATEN, P. & BECKER, J. C. 2006. Cytotoxic T cells. *J Invest Dermatol,* 126**,** 32-41.

ANDREWS, S. N., JEONG, E. & PRAUSNITZ, M. R. 2013. Transdermal delivery of molecules is limited by full epidermis, not just stratum corneum. *Pharm Res,* 30**,** 1099-109.

ANGELOV, B., ANGELOVA, A., PAPAHADJOPOULOS-STERNBERG, B., HOFFMANN, S. V., NICOLAS, V. & LESIEUR, S. 2012. Protein-Containing PEGylated Cubosomic Particles: Freeze-Fracture Electron Microscopy and Synchrotron Radiation Circular Dichroism Study. *The Journal of Physical Chemistry B,* 116**,** 7676-7686.

ANTUNES, M. B. & COHEN, N. A. 2007. Mucociliary clearance- a critical upper airway host defense mechanism and methods of assessment. *Curr Opin Allergy Clin Immunol,* 7**,** 5-10.

ARNAIZ-VILLENA, A., BENMAMAR, D., ALVAREZ, M., DIAZ-CAMPOS, N., VARELA, P., GOMEZ-CASADO, E. & MARTINEZ-LASO, J. 1995. HLA allele and haplotype frequencies in Algerians. Relatedness to Spaniards and Basques. *Hum Immunol,* 43**,** 259-68.

ARTYOMOV, M. N., MUNK, A., GORVEL, L., KORENFELD, D., CELLA, M., TUNG, T. & KLECHEVSKY, E. 2015. Modular expression analysis reveals functional conservation between human Langerhans cells and mouse cross-priming dendritic cells. *J Exp Med,* 212**,** 743-57.

AUEWARAKUL, P., PAUNGCHAROEN, V., LOUISIRIROTCHANAKUL, S. & WASI, C. 2001. Application of HIV-1-green fluorescent protein (GFP) reporter viruses in neutralizing antibody assays. *Asian Pac J Allergy Immunol,* 19**,** 139-44.

AUNGST, B. J. 2012. Absorption Enhancers: Applications and Advances. *AAPS J,* 14**,** 10-18.

BACHEM, A., GUTTLER, S., HARTUNG, E., EBSTEIN, F., SCHAEFER, M., TANNERT, A., SALAMA, A., MOVASSAGHI, K., OPITZ, C., MAGES, H. W., HENN, V., KLOETZEL, P. M., GURKA, S. & KROCZEK, R. A. 2010. Superior antigen cross-presentation and XCR1 expression define human CD11c+CD141+ cells as homologues of mouse CD8+ dendritic cells. *J Exp Med,* 207**,** 1273-81.

BACHY, V., HERVOUET, C., BECKER, P. D., CHORRO, L., CARLIN, L. M., HERATH, S., PAPAGATSIAS, T., BARBAROUX, J. B., OH, S. J., BENLAHRECH, A., ATHANASOPOULOS, T., DICKSON, G., PATTERSON, S., KWON, S. Y., GEISSMANN, F. & KLAVINSKIS, L. S. 2013. Langerin negative dendritic cells promote potent CD8+ T-cell priming by skin delivery of live adenovirus vaccine microneedle arrays. *Proc Natl Acad Sci U S A,* 110**,** 3041-6.

BAKER, B. M., SCOTT, D. R., BLEVINS, S. J. & HAWSE, W. F. 2012. Structural and dynamic control of T-cell receptor specificity, cross-reactivity, and binding mechanism. *Immunol Rev,* 250**,** 10-31.

BANCHEREAU, J., PALUCKA, A. K., DHODAPKAR, M., BURKEHOLDER, S., TAQUET, N., ROLLAND, A., TAQUET, S., COQUERY, S., WITTKOWSKI, K. M., BHARDWAJ, N., PINEIRO, L., STEINMAN, R. & FAY, J. 2001. Immune and clinical responses in patients with metastatic melanoma to CD34(+) progenitor-derived dendritic cell vaccine. *Cancer Res,* 61**,** 6451-8.

BANCHEREAU, J. & STEINMAN, R. M. 1998. Dendritic cells and the control of immunity. *Nature,* 392**,** 245-252.

BARBERO, A. M. & FRASCH, H. F. 2006. Transcellular route of diffusion through stratum corneum: results from finite element models. *J Pharm Sci,* 95**,** 2186-94.

BARIYA, S. H., GOHEL, M. C., MEHTA, T. A. & SHARMA, O. P. 2012. Microneedles: an emerging transdermal drug delivery system. *J Pharm Pharmacol,* 64**,** 11-29.

BASHIR, S. J., CHEW, A. L., ANIGBOGU, A., DREHER, F. & MAIBACH, H. I. 2001. Physical and physiological effects of stratum corneum tape stripping. *Skin Res Technol,* 7**,** 40-8.

BAUMGARTH, N. & ROEDERER, M. 2000. A practical approach to multicolor flow cytometry for immunophenotyping. *J Immunol Methods,* 243**,** 77-97.

BEDOUI, S., WHITNEY, P. G., WAITHMAN, J., EIDSMO, L., WAKIM, L., CAMINSCHI, I., ALLAN, R. S., WOJTASIAK, M., SHORTMAN, K., CARBONE, F. R., BROOKS, A. G. & HEATH, W. R. 2009. Cross-presentation of viral and self antigens by skin-derived CD103+ dendritic cells. *Nat Immunol,* 10**,** 488-95.

BEI, D., MENG, J. & YOUAN, B. B. 2010. Engineering nanomedicines for improved melanoma therapy: progress and promises. *Nanomedicine,* 5**,** 1385-99.

BELKAID, Y. & ROUSE, B. T. 2005. Natural regulatory T cells in infectious disease. *Nat Immunol,* 6**,** 353-60.

BELTRAMI, E. M., WILLIAMS, I. T., SHAPIRO, C. N. & CHAMBERLAND, M. E. 2000. Risk and Management of Blood-Borne Infections in Health Care Workers. *Clin Microbiol Rev,* 13**,** 385-407.

BENDER, J., ERICSON, M. B., MERCLIN, N., IANI, V., ROSÉN, A., ENGSTRÖM, S. & MOAN, J. 2005. Lipid cubic phases for improved topical drug delivery in photodynamic therapy. *J Control Release,* 106**,** 350-360.

BENDER, J., SIMONSSON, C., SMEDH, M., ENGSTRÖM, S. & ERICSON, M. B. 2008. Lipid cubic phases in topical drug delivery: Visualization of skin distribution using two-photon microscopy. *J Control Release,* 129**,** 163-169.

BENNETT, C. L. 2015. Editorial: Faux amis: Langerin-expressing DC in humans and mice. *J Leukoc Biol.* United States.

BENSON, H. A. E. & NAMJOSHI, S. 2008. Proteins and Peptides: Strategies for Delivery to and Across the Skin. *J Pharm Sci,* 97**,** 3591-3610.

BERGER, C. L., VASQUEZ, J. G., SHOFNER, J., MARIWALLA, K. & EDELSON, R. L. 2006. Langerhans cells: Mediators of immunity and tolerance. *Int J Biochem Cell Biol,* 38**,** 1632-1636.

BERGES, B. K., WHEAT, W. H., PALMER, B. E., CONNICK, E. & AKKINA, R. 2006. HIV-1 infection and CD4 T cell depletion in the humanized Rag2(-/-)γc(-/-)(RAG-hu) mouse model. *Retrovirology,* 3**,** 76-76.

BERGMANN-LEITNER, E. S. & LEITNER, W. W. 2015. Vaccination Using Gene-Gun Technology. *Methods Mol Biol,* 1325**,** 289-302.

BERNE, B. J. & PECORA, R. 1976. *Dynamic light scattering: with applications to chemistry, biology, and physics*, Courier Corporation.

BERTON, A., GODEAU, G., EMONARD, H., BABA, K., BELLON, P., HORNEBECK, W. & BELLON, G. 2000. Analysis of the ex vivo specificity of human gelatinases A and B towards skin collagen and elastic fibers by computerized morphometry. *Matrix Biol,* 19**,** 139-148.

BEUTLER, B. 2000. TLR4: central component of the sole mammalian LPS sensor. *Curr Opin Immunol,* 12**,** 20-26.

BHAUMIK, S. 2012. Polio eradication: Current status and challenges. *J Family Med Prim Care,* 1**,** 84-85.

BHUSHAN, M., CUMBERBATCH, M., DEARMAN, R. J., ANDREW, S. M., KIMBER, I. & GRIFFITHS, C. E. 2002. Tumour necrosis factor-alpha-induced migration of human Langerhans cells: the influence of ageing. *Br J Dermatol,* 146**,** 32-40.

BIANCHI, M. E. 2007. DAMPs, PAMPs and alarmins: all we need to know about danger. *J Leukoc Biol,* 81**,** 1-5.

BIGLEY, V., MCGOVERN, N., MILNE, P., DICKINSON, R., PAGAN, S., COOKSON, S., HANIFFA, M. & COLLIN, M. 2015. Langerin-expressing dendritic cells in human tissues are related to CD1c+ dendritic cells and distinct from Langerhans cells and CD141high XCR1+ dendritic cells. *J Leukoc Biol,* 97**,** 627-34.

BILL, R. M. 2015. Recombinant protein subunit vaccine synthesis in microbes: a role for yeast? *Journal of Pharmacy and Pharmacology,* 67**,** 319-328.

BJORKLUND, S., ENGBLOM, J., THURESSON, K. & SPARR, E. 2010. A water gradient can be used to regulate drug transport across skin. *J Control Release,* 143**,** 191-200.

BONIFAZ, L., BONNYAY, D., MAHNKE, K., RIVERA, M., NUSSENZWEIG, M. C. & STEINMAN, R. M. 2002. Efficient targeting of protein antigen to the dendritic cell receptor DEC-205 in the steady state leads to antigen presentation on major histocompatibility complex class I products and peripheral CD8+ T cell tolerance. *J Exp Med,* 196**,** 1627-38.

BONIFAZ, L. C., BONNYAY, D. P., CHARALAMBOUS, A., DARGUSTE, D. I., FUJII, S., SOARES, H., BRIMNES, M. K., MOLTEDO, B., MORAN, T. M. & STEINMAN, R. M. 2004. In vivo targeting of antigens to maturing dendritic cells via the DEC-205 receptor improves T cell vaccination. *J Exp Med,* 199**,** 815-24.

BOS, J. D., HAGENAARS, C., DAS, P. K., KRIEG, S. R., VOORN, W. J. & KAPSENBERG, M. L. 1989. Predominance of "memory" T cells (CD4+, CDw29+) over "naive" T cells (CD4+, CD45R+) in both normal and diseased human skin. *Arch Dermatol Res,* 281**,** 24-30.

BRENNAN, P. J., BRIGL, M. & BRENNER, M. B. 2013. Invariant natural killer T cells: an innate activation scheme linked to diverse effector functions. *Nat Rev Immunol,* 13**,** 101-117.

BRENNER, M. & HEARING, V. J. 2008. The Protective Role of Melanin Against UV Damage in Human Skin. *Photochem Photobiol,* 84**,** 539-549.

BRIGGAMAN, R. A., DALLDORF, F. G. & WHEELER, C. E., JR. 1971. Formation and origin of basal lamina and anchoring fibrils in adult human skin. *J Cell Biol,* 51**,** 384-95.

BROERE, F., APASOV, S. G., SITKOVSKY, M. V. & VAN EDEN, W. 2011. A2 T cell subsets and T cell-mediated immunity. *In:* NIJKAMP, F. P. & PARNHAM, J. M. (eds.) *Principles of Immunopharmacology: 3rd revised and extended edition.* Basel: Birkhäuser Basel.

BRONAUGH, R. L., STEWART, R. F. & CONGDON, E. R. 1982. Methods for in vitro percutaneous absorption studies II. Animal models for human skin. *Toxicol Appl Pharmacol,* 62**,** 481-488.

BROWN, M. B., MARTIN, G. P., JONES, S. A. & AKOMEAH, F. K. 2006. Dermal and transdermal drug delivery systems: current and future prospects. *Drug Deliv,* 13**,** 175-87.

BRUCKNER, M., DICKEL, D., SINGER, E. & LEGLER, D. F. 2012. Converse regulation of CCR7-driven human dendritic cell migration by prostaglandin E(2) and liver X receptor activation. *Eur J Immunol,* 42**,** 2949-58.

BU, M., TANG, J., WEI, Y., SUN, Y., WANG, X., WU, L. & LIU, H. 2015. Enhanced bioavailability of nerve growth factor with phytantriol lipid-based crystalline nanoparticles in cochlea. *Int J Nanomedicine,* 10**,** 6879-89.

BUCHWALOW, I., SAMOILOVA, V., BOECKER, W. & TIEMANN, M. 2011. Non-specific binding of antibodies in immunohistochemistry: fallacies and facts. *Sci Rep,* 1**,** 28.

BURGDORF, S., KAUTZ, A., BOHNERT, V., KNOLLE, P. A. & KURTS, C. 2007. Distinct pathways of antigen uptake and intracellular routing in CD4 and CD8 T cell activation. *Science,* 316**,** 612-6.

CALABRO, K., CURTIS, A., GALARNEAU, J.-R., KRUCKER, T. & BIGIO, I. J. 2011. Gender variations in the optical properties of skin in murine animal models. *Journal of Biomedical Optics,* 16**,** 011008-011008-8.

CAMINSCHI, I., PROIETTO, A. I., AHMET, F., KITSOULIS, S., SHIN TEH, J., LO, J. C. Y., RIZZITELLI, A., WU, L., VREMEC, D., VAN DOMMELEN, S. L. H., CAMPBELL, I. K., MARASKOVSKY, E., BRALEY, H., DAVEY, G. M., MOTTRAM, P., VAN DE VELDE, N., JENSEN, K., LEW, A. M., WRIGHT, M. D., HEATH, W. R., SHORTMAN, K. & LAHOUD, M. H. 2008. The dendritic cell subtype-restricted C-type lectin Clec9A is a target for vaccine enhancement. *Blood,* 112**,** 3264-3273.

CAMPAGNOLA, P. J., WEI, M.-D., LEWIS, A. & LOEW, L. M. 1999. High-Resolution Nonlinear Optical Imaging of Live Cells by Second Harmonic Generation. *Biophys J,* 77**,** 3341-3349.

CAMPANELLI, R., PALERMO, B., GARBELLI, S., MANTOVANI, S., LUCCHI, P., NECKER, A., LANTELME, E. & GIACHINO, C. 2002. Human CD8 co-receptor is strictly involved in MHC-peptide tetramer-TCR binding and T cell activation. *Int Immunol,* 14**,** 39-44.

CARPENTIER, S., VU MANH, T.-P., CHELBI, R., HENRI, S., MALISSEN, B., HANIFFA, M., GINHOUX, F. & DALOD, M. 2016. Comparative genomics analysis of mononuclear phagocyte subsets confirms homology between lymphoid tissue-resident and dermal XCR1+ DCs in mouse and human and distinguishes them from Langerhans cells. *J Immunol Methods,* 432**,** 35-49.

CARRENO, B. M., MAGRINI, V., BECKER-HAPAK, M., KAABINEJADIAN, S., HUNDAL, J., PETTI, A. A., LY, A., LIE, W. R., HILDEBRAND, W. H., MARDIS, E. R. & LINETTE, G. P. 2015. Cancer immunotherapy. A dendritic cell vaccine increases the breadth and diversity of melanoma neoantigen-specific T cells. *Science,* 348**,** 803-8.

CASELLA, C. R. & MITCHELL, T. C. 2008. Putting endotoxin to work for us: Monophosphoryl lipid A as a safe and effective vaccine adjuvant. *Cell Mol Life Sci,* 65**,** 3231-3240.

CAUCHETEUX, S. M., MITCHELL, J. P., IVORY, M. O., HIROSUE, S., HAKOBYAN, S., DOLTON, G., LADELL, K., MINERS, K., PRICE, D. A., KAN-MITCHELL, J., SEWELL, A. K., NESTLE, F., MORIS, A., KAROO, R. O., BIRCHALL, J. C., SWARTZ, M. A., HUBBEL, J. A., BLANCHET, F. P. & PIGUET, V. 2016. Polypropylene Sulfide Nanoparticle p24 Vaccine Promotes Dendritic Cell-Mediated Specific Immune Responses against HIV-1. *J Invest Dermatol,* 136**,** 1172-81.

CERIO, R., GRIFFITHS, C. E., COOPER, K. D., NICKOLOFF, B. J. & HEADINGTON, J. T. 1989. Characterization of factor XIIIa positive dermal dendritic cells in normal and inflamed skin. *Br J Dermatol,* 121**,** 421-31.

CEVC, G. 1996. Transfersomes, Liposomes and Other Lipid Suspensions on the Skin: Permeation Enhancement, Vesicle Penetration, and Transdermal Drug Delivery. 13**,** 257-388.

CHALLIER, J., BRUNIQUEL, D., SEWELL, A. K. & LAUGEL, B. 2013. Adenosine and cAMP signalling skew human dendritic cell differentiation towards a tolerogenic phenotype with defective CD8(+) T-cell priming capacity. *Immunology,* 138**,** 402-10.

CHATTOPADHYAY, P. K., PRICE, D. A., HARPER, T. F., BETTS, M. R., YU, J., GOSTICK, E., PERFETTO, S. P., GOEPFERT, P., KOUP, R. A., DE ROSA, S. C., BRUCHEZ, M. P. & ROEDERER, M. 2006. Quantum dot semiconductor nanocrystals for immunophenotyping by polychromatic flow cytometry. *Nat Med,* 12**,** 972-7.

CHEMAXON. 2016. *Chemicalize.org* [Online]. Available: http://www.chemicalize.org/structure/#!mol=Alexa+Fluor+555Available: http://www.chemicalize.org/structure/#!mol=S%3DC%3DN%2Fc5cc1c(C(%3DO)OC13c4ccc(O)cc4Oc2cc(O)ccc23)cc5 [Accessed 21st March 2016].

CHEN, R., LOWE, L., WILSON, J. D., CROWTHER, E., TZEGGAI, K., BISHOP, J. E. & VARRO, R. 1999. Simultaneous Quantification of Six Human Cytokines in a Single Sample Using Microparticle-based Flow Cytometric Technology. *Clin Chem,* 45**,** 1693-1694.

CHEN, T., LANGER, R. & WEAVER, J. C. 1998. Skin electroporation causes molecular transport across the stratum corneum through localized transport regions. *J Investig Dermatol Symp Proc,* 3**,** 159-65.

CHEN, X., KIM, P., FARINELLI, B., DOUKAS, A., YUN, S. H., GELFAND, J. A., ANDERSON, R. R. & WU, M. X. 2010. A novel laser vaccine adjuvant increases the motility of antigen presenting cells. *PLoS One,* 5**,** e13776.

CHEUNG, K., HAN, T. & DAS, D. B. 2014. Effect of Force of Microneedle Insertion on the Permeability of Insulin in Skin. *J Diabetes Sci Technol,* 8**,** 444-452.

CHONG, R. H., GONZALEZ-GONZALEZ, E., LARA, M. F., SPEAKER, T. J., CONTAG, C. H., KASPAR, R. L., COULMAN, S. A., HARGEST, R. & BIRCHALL, J. C. 2013. Gene silencing following siRNA delivery to skin via coated steel microneedles: In vitro and in vivo proof-of-concept. *J Control Release,* 166**,** 211-9.

CHU, C. C., ALI, N., KARAGIANNIS, P., DI MEGLIO, P., SKOWERA, A., NAPOLITANO, L., BARINAGA, G., GRYS, K., SHARIF-PAGHALEH, E., KARAGIANNIS, S. N., PEAKMAN, M., LOMBARDI, G. & NESTLE, F. O. 2012. Resident CD141 (BDCA3)+ dendritic cells in human skin produce IL-10 and induce regulatory T cells that suppress skin inflammation. *J Exp Med,* 209**,** 935-45.

CHU, L. Y., YE, L., DONG, K., COMPANS, R. W., YANG, C. & PRAUSNITZ, M. R. 2016. Enhanced Stability of Inactivated Influenza Vaccine Encapsulated in Dissolving Microneedle Patches. *Pharm Res,* 33**,** 868-78.

CLARK, R. A. 2010. Skin resident T cells: the ups and downs of on site immunity. *J Invest Dermatol,* 130**,** 362-370.

CLARK, R. A., CHONG, B. F., MIRCHANDANI, N., YAMANAKA, K., MURPHY, G. F., DOWGIERT, R. K. & KUPPER, T. S. 2006. A novel method for the isolation of skin resident T cells from normal and diseased human skin. *J Invest Dermatol,* 126**,** 1059-70.

CLEMENT, M., LADELL, K., EKERUCHE-MAKINDE, J., MILES, J. J., EDWARDS, E. S., DOLTON, G., WILLIAMS, T., SCHAUENBURG, A. J., COLE, D. K., LAUDER, S. N., GALLIMORE, A. M., GODKIN, A. J., BURROWS, S. R., PRICE, D. A., SEWELL, A. K. & WOOLDRIDGE, L. 2011. Anti-CD8 antibodies can trigger CD8+ T cell effector function in the absence of TCR engagement and improve peptide-MHCI tetramer staining. *J Immunol,* 187**,** 654-63.

CLINT, J. H. 1998. Surfactants: applications in plastics. *In:* PRITCHARD, G. (ed.) *Plastics Additives: An A-Z reference.* Dordrecht: Springer Netherlands.

CLOGSTON, J. & CAFFREY, M. 2005. Controlling release from the lipidic cubic phase. Amino acids, peptides, proteins and nucleic acids. *J Control Release,* 107**,** 97-111.

CODY, C. L., BARAFF, L. J., CHERRY, J. D., MARCY, S. M. & MANCLARK, C. R. 1981. Nature and rates of adverse reactions associated with DTP and DT immunizations in infants and children. *Pediatrics,* 68**,** 650-60.

COFFMAN, R. L., SHER, A. & SEDER, R. A. 2010. Vaccine Adjuvants: Putting Innate Immunity to Work. *Immunity,* 33**,** 492-503.

COLLIN, M., MCGOVERN, N. & HANIFFA, M. 2013. Human dendritic cell subsets. *Immunology,* 140**,** 22-30.

COULMAN, S. A., ANSTEY, A., GATELEY, C., MORRISSEY, A., MCLOUGHLIN, P., ALLENDER, C. & BIRCHALL, J. C. 2009. Microneedle mediated delivery of nanoparticles into human skin. *Int J Pharm,* 366**,** 190-200.

CROZAT, K., GUITON, R., CONTRERAS, V., FEUILLET, V., DUTERTRE, C. A., VENTRE, E., VU MANH, T. P., BARANEK, T., STORSET, A. K., MARVEL, J., BOUDINOT, P., HOSMALIN, A., SCHWARTZ-CORNIL, I. & DALOD, M. 2010. The XC chemokine receptor 1 is a conserved selective marker of mammalian cells homologous to mouse CD8alpha+ dendritic cells. *J Exp Med,* 207**,** 1283-92.

CUMBERBATCH, M., DEARMAN, R. J., GRIFFITHS, C. E. & KIMBER, I. 2000. Langerhans cell migration. *Clin Exp Dermatol,* 25**,** 413-8.

CZERNIELEWSKI, J. M. & DEMARCHEZ, M. 1987. Further evidence for the self-reproducing capacity of Langerhans cells in human skin. *J Invest Dermatol,* 88**,** 17-20.

CZUBALA, M. A., FINSTERBUSCH, K., IVORY, M. O., MITCHELL, J. P., AHMED, Z., SHIMAUCHI, T., KAROO, R. O., COULMAN, S. A., GATELEY, C., BIRCHALL, J. C., BLANCHET, F. P. & PIGUET, V. 2016. TGFbeta Induces a SAMHD1-independent Post-Entry Restriction to HIV-1 Infection of Human Epithelial Langerhans Cells. *J Invest Dermatol*.

DA COSTA, X. J., BOURNE, N., STANBERRY, L. R. & KNIPE, D. M. 1997. Construction and characterization of a replication-defective herpes simplex virus 2 ICP8 mutant strain and its use in immunization studies in a guinea pig model of genital disease. *Virology,* 232**,** 1-12.

DA COSTA, X. J., BROCKMAN, M. A., ALICOT, E., MA, M., FISCHER, M. B., ZHOU, X., KNIPE, D. M. & CARROLL, M. C. 1999. Humoral response to herpes simplex virus is complement-dependent. *Proc Natl Acad Sci U S A,* 96**,** 12708-12.

DADDONA, P. E., MATRIANO, J. A., MANDEMA, J. & MAA, Y. F. 2011. Parathyroid hormone (1-34)-coated microneedle patch system: clinical pharmacokinetics and pharmacodynamics for treatment of osteoporosis. *Pharm Res,* 28**,** 159-65.

DANSO, M. O., BERKERS, T., MIEREMET, A., HAUSIL, F. & BOUWSTRA, J. A. 2015. An ex vivo human skin model for studying skin barrier repair. *Exp Dermatol,* 24**,** 48-54.

DAVEY, G. M., WOJTASIAK, M., PROIETTO, A. I., CARBONE, F. R., HEATH, W. R. & BEDOUI, S. 2010. Cutting edge: priming of CD8 T cell immunity to herpes simplex virus type 1 requires cognate TLR3 expression in vivo. *J Immunol,* 184**,** 2243-6.

DAVIS, M. M., BONIFACE, J. J., REICH, Z., LYONS, D., HAMPL, J., ARDEN, B. & CHIEN, Y. 1998. Ligand recognition by alpha beta T cell receptors. *Annu Rev Immunol,* 16**,** 523-44.

DE FILETTE, M., MIN JOU, W., BIRKETT, A., LYONS, K., SCHULTZ, B., TONKYRO, A., RESCH, S. & FIERS, W. 2005. Universal influenza A vaccine: Optimization of M2-based constructs. *Virology,* 337**,** 149-161.

DE JONG, M. A., DE WITTE, L. & GEIJTENBEEK, T. B. 2010. Isolation of immature primary Langerhans cells from human epidermal skin. *Methods Mol Biol,* 595**,** 55-65.

DE WITTE, L., NABATOV, A., PION, M., FLUITSMA, D., DE JONG, M. A., DE GRUIJL, T., PIGUET, V., VAN KOOYK, Y. & GEIJTENBEEK, T. B. 2007. Langerin is a natural barrier to HIV-1 transmission by Langerhans cells. *Nat Med,* 13**,** 367-71.

DEARMAN, R. J., BHUSHAN, M., CUMBERBATCH, M., KIMBER, I. & GRIFFITHS, C. E. 2004. Measurement of cytokine expression and Langerhans cell migration in human skin following suction blister formation. *Exp Dermatol,* 13**,** 452-60.

DELLA CIOPPA, G., NICOLAY, U., LINDERT, K., LEROUX-ROELS, G., CLEMENT, F., CASTELLINO, F., GALLI, C., GROTH, N., LEVIN, Y. & DEL GIUDICE, G. 2014. A dose-ranging study in older adults to compare the safety and immunogenicity profiles of MF59(R)-adjuvanted and non-adjuvanted seasonal influenza vaccines following intradermal and intramuscular administration. *Hum Vaccin Immunother,* 10**,** 1701-10.

DEMPSEY, P. W., VAIDYA, S. A. & CHENG, G. 2003. The art of war: Innate and adaptive immune responses. *Cell Mol Life Sci,* 60**,** 2604-21.

DEMURTAS, D., GUICHARD, P., MARTIEL, I., MEZZENGA, R., HÉBERT, C. & SAGALOWICZ, L. 2015. Direct visualization of dispersed lipid bicontinuous cubic phases by cryo-electron tomography. *Nat Commun,* 6**,** 8915.

DENK, W., PISTON, D. W. & WEBB, W. W. 1995. Two-Photon Molecular Excitation in Laser-Scanning Microscopy. *In:* PAWLEY, J. B. (ed.) *Handbook of Biological Confocal Microscopy.* Boston, MA: Springer US.

DENK, W., STRICKLER, J. H. & WEBB, W. W. 1990. Two-photon laser scanning fluorescence microscopy. *Science,* 248**,** 73-76.

DESAI, P., PATLOLLA, R. R. & SINGH, M. 2010. Interaction of nanoparticles and cell-penetrating peptides with skin for transdermal drug delivery. *Mol Membr Biol,* 27**,** 247-59.

DEZZUTTI, C. S. & HLADIK, F. 2013. Use of Human Mucosal Tissue to Study HIV-1 Pathogenesis and Evaluate HIV-1 Prevention Modalities. *Curr HIV/AIDS Rep,* 10**,** 12-20.

DIEHL, K. H., HULL, R., MORTON, D., PFISTER, R., RABEMAMPIANINA, Y., SMITH, D., VIDAL, J. M. & VORSTENBOSCH, C. V. D. 2001. A good practice guide to the administration of substances and removal of blood, including routes and volumes. *J Appl Toxicol,* 21**,** 15-23.

DITTMAR, H. C., WEISS, J. M., TERMEER, C. C., DENFELD, R. W., WANNER, M. B., SKOV, L., BARKER, J. N., SCHOPF, E., BAADSGAARD, O. & SIMON, J. C. 1999. In vivo UVA-1 and UVB irradiation differentially perturbs the antigen-presenting function of human epidermal Langerhans cells. *J Invest Dermatol,* 112**,** 322-5.

DOLTON, G., TUNGATT, K., LLOYD, A., BIANCHI, V., THEAKER, S. M., TRIMBY, A., HOLLAND, C. J., DONIA, M., GODKIN, A. J., COLE, D. K., THOR STRATEN, P., PEAKMAN, M., SVANE, I. M. & SEWELL, A. K. 2015. More tricks with tetramers: a practical guide to staining T cells with peptide–MHC multimers. *Immunology,* 146**,** 11-22.

DONNELLY, R. F., MOFFATT, K., ALKILANI, A. Z., VICENTE-PEREZ, E. M., BARRY, J., MCCRUDDEN, M. T. & WOOLFSON, A. D. 2014. Hydrogel-forming microneedle arrays can be effectively inserted in skin by self-application: a pilot study centred on pharmacist intervention and a patient information leaflet. *Pharm Res,* 31**,** 1989-99.

DUCLOS, P. & BENTSI-ENCHILL, A. 1993. Current thoughts on the risks and benefits of immunisation. *Drug Saf,* 8**,** 404-13.

DUDZIAK, D., KAMPHORST, A. O., HEIDKAMP, G. F., BUCHHOLZ, V. R., TRUMPFHELLER, C., YAMAZAKI, S., CHEONG, C., LIU, K., LEE, H.-W. & PARK, C. G. 2007. Differential antigen processing by dendritic cell subsets in vivo. *Science,* 315**,** 107-111.

DUNKELBERGER, J. R. & SONG, W. C. 2010. Complement and its role in innate and adaptive immune responses. *Cell Res,* 20**,** 34-50.

DURAES, F. V., CARVALHO, N. B., MELO, T. T., OLIVEIRA, S. C. & FONSECA, C. T. 2009. IL-12 and TNF-alpha production by dendritic cells stimulated with Schistosoma mansoni schistosomula tegument is TLR4- and MyD88-dependent. *Immunol Lett,* 125**,** 72-7.

DUTERTRE, C. A., WANG, L. F. & GINHOUX, F. 2014. Aligning bona fide dendritic cell populations across species. *Cell Immunol,* 291**,** 3-10.

ECKERT, R. L. & RORKE, E. A. 1989. Molecular biology of keratinocyte differentiation. *Environ Health Persp,* 80**,** 109-116.

EIDSMO, L., ALLAN, R., CAMINSCHI, I., VAN ROOIJEN, N., HEATH, W. R. & CARBONE, F. R. 2009. Differential migration of epidermal and dermal dendritic cells during skin infection. *J Immunol,* 182**,** 3165-72.

EL-SAHRIGY, S. A., MOHAMED, N. A., TALKHAN, H. A. & RAHMAN, A. M. 2015. Comparison between magnetic activated cell sorted monocytes and monocyte adherence techniques for in vitro generation of immature dendritic cells: an Egyptian trial. *Cent Eur J Immunol,* 40**,** 18-24.

ELIAS, P. M. 2005. Stratum corneum defensive functions: an integrated view. *J Invest Dermatol,* 125**,** 183-200.

ELIAS, P. M. 2007. The skin barrier as an innate immune element. *Sem Immunopath,* 29**,** 3-14.

ELLIS, J. M., HENSON, V., SLACK, R., NG, J., HARTZMAN, R. J. & KATOVICH HURLEY, C. 2000. Frequencies of HLA-A2 alleles in five U.S. population groups: Predominance of A∗02011 and identification of HLA-A∗0231. *Hum Immunol,* 61**,** 334-340.

ENGELHARD, V. H. 1994. Structure of peptides associated with class I and class II MHC molecules. *Annu Rev Immunol,* 12**,** 181-207.

ENGERING, A. J., CELLA, M., FLUITSMA, D. M., HOEFSMIT, E. C., LANZAVECCHIA, A. & PIETERS, J. 1997. Mannose receptor mediated antigen uptake and presentation in human dendritic cells. *Adv Exp Med Biol,* 417**,** 183-7.

ERICKSON, H. P. 2009. Size and shape of protein molecules at the nanometer level determined by sedimentation, gel filtration, and electron microscopy. *Biol Proced Online,* 11**,** 32-51.

ESPOSITO, E., CORTESI, R., DRECHSLER, M., PACCAMICCIO, L., MARIANI, P., CONTADO, C., STELLIN, E., MENEGATTI, E., BONINA, F. & PUGLIA, C. 2005.

Cubosome dispersions as delivery systems for percutaneous administration of indomethacin. *Pharm Res,* 22**,** 2163-73.

FAN, H., LIN, Q., MORRISSEY, G. R. & KHAVARI, P. A. 1999. Immunization via hair follicles by topical application of naked DNA to normal skin. *Nat Biotechnol,* 17**,** 870-2.

FINKELSHTEIN, D., WERMAN, A., NOVICK, D., BARAK, S. & RUBINSTEIN, M. 2013. LDL receptor and its family members serve as the cellular receptors for vesicular stomatitis virus. *Proc Natl Acad Sci U S A,* 110**,** 7306-11.

FISCHER, A. H., JACOBSON, K. A., ROSE, J. & ZELLER, R. 2008. Hematoxylin and eosin staining of tissue and cell sections. *CSH Protoc,* 2008**,** pdb.prot4986.

FLEISHER, D., NIEMIEC, S. M., OH, C. K., HU, Z., RAMACHANDRAN, C. & WEINER, N. 1995. Topical delivery of growth hormone releasing peptide using liposomal systems: an in vitro study using hairless mouse skin. *Life Sci,* 57**,** 1293-7.

FLUHR, J. W., MAO-QIANG, M., BROWN, B. E., WERTZ, P. W., CRUMRINE, D., SUNDBERG, J. P., FEINGOLD, K. R. & ELIAS, P. M. 2003. Glycerol regulates stratum corneum hydration in sebaceous gland deficient (asebia) mice. *J Invest Dermatol,* 120**,** 728-37.

FORE, J. 2006. A review of skin and the effects of aging on skin structure and function. *Ostomy Wound Manage,* 52**,** 24-35; quiz 36-7.

FORSTER, R., DAVALOS-MISSLITZ, A. C. & ROT, A. 2008. CCR7 and its ligands: balancing immunity and tolerance. *Nat Rev Immunol,* 8**,** 362-71.

FORTHAL, D. N. 2014. Functions of Antibodies. *Microbiol Spectrum,* 2**,** 1-17.

FOSTER, B., PRUSSIN, C., LIU, F., WHITMIRE, J. K. & WHITTON, J. L. 2007. Detection of intracellular cytokines by flow cytometry. *Curr Protoc Immunol,* Chapter 6**,** Unit 6.24.

FOX, J. P., ELVEBACK, L., SCOTT, W., GATEWOOD, L. & ACKERMAN, E. 1971. Herd Immunity: Basic Concept and Relevance to Public Health and Immunization Practices. *American Journal of Epidemiology,* 94**,** 179-189.

FRASER, S. J., ROSE, R., HATTARKI, M. K., HARTLEY, P. G., DOLEZAL, O., DAWSON, R. M., SEPAROVIC, F. & POLYZOS, A. 2011. Preparation and biological evaluation of self-assembled cubic phases for the polyvalent inhibition of cholera toxin. *Soft Matter,* 7**,** 6125-6134.

FUKUSHIMA, S., KISHIMOTO, S., HORAI, S., MIYAWAKI, K., KAMIYABU, S., KAMATA, Y., YAMAOKA, Y. & TAKEUCHI, Y. 2001. Transdermal drug delivery by

electroporation applied on the stratum corneum of rat using stamp-type electrode and frog-type electrode in vitro. *Biol Pharm Bull,* 24**,** 1027-31.

FURUYA, Y., REGNER, M., LOBIGS, M., KOSKINEN, A., MULLBACHER, A. & ALSHARIFI, M. 2010. Effect of inactivation method on the cross-protective immunity induced by whole 'killed' influenza A viruses and commercial vaccine preparations. *J Gen Virol,* 91**,** 1450-60.

GALINSKI, M., SRA, K., HAYNES, J., II & NASPINSKI, J. 2015. Live Attenuated Viral Vaccines. *In:* NUNNALLY, B. K., TURULA, V. E. & SITRIN, R. D. (eds.) *Vaccine Analysis: Strategies, Principles, and Control.* Springer Berlin Heidelberg.

GANGLOFF, S. C., HIJIYA, N., HAZIOT, A. & GOYERT, S. M. 1999. Lipopolysaccharide structure influences the macrophage response via CD14-independent and CD14-dependent pathways. *Clin Infect Dis,* 28**,** 491-6.

GANGULY, D., HAAK, S., SISIRAK, V. & REIZIS, B. 2013. The role of dendritic cells in autoimmunity. *Nat Rev Immunol,* 13**,** 566-77.

GARG, G. & SARAF, S. 2007. Cubosomes: an overview. *Biol Pharm Bull,* 30**,** 350-3.

GEBHARDT, T., WAKIM, L. M., EIDSMO, L., READING, P. C., HEATH, W. R. & CARBONE, F. R. 2009. Memory T cells in nonlymphoid tissue that provide enhanced local immunity during infection with herpes simplex virus. *Nat Immunol,* 10**,** 524-530.

GEHERIN, S. A., FINTUSHEL, S. R., LEE, M. H., WILSON, R. P., PATEL, R. T., ALT, C., YOUNG, A. J., HAY, J. B. & DEBES, G. F. 2012. The skin, a novel niche for recirculating B cells. *J Immunol,* 188**,** 6027-35.

GEISSMANN, F., PROST, C., MONNET, J.-P., DY, M., BROUSSE, N. & HERMINE, O. 1998. Transforming Growth Factor β1, in the Presence of Granulocyte/Macrophage Colony-stimulating Factor and Interleukin 4, Induces Differentiation of Human Peripheral Blood Monocytes into Dendritic Langerhans Cells. *J Exp Med,* 187**,** 961-966.

GERLINI, G., HEFTI, H. P., KLEINHANS, M., NICKOLOFF, B. J., BURG, G. & NESTLE, F. O. 2001. Cd1d is expressed on dermal dendritic cells and monocyte-derived dendritic cells. *J Invest Dermatol,* 117**,** 576-82.

GILL, H. S., DENSON, D. D., BURRIS, B. A. & PRAUSNITZ, M. R. 2008. Effect of microneedle design on pain in human volunteers. *Clin J Pain,* 24**,** 585-94.

GILL, H. S. & PRAUSNITZ, M. R. 2007a. Coated microneedles for transdermal delivery. *J Control Release,* 117**,** 227-37.

GILL, H. S. & PRAUSNITZ, M. R. 2007b. Coating Formulations for Microneedles. *Pharm Res,* 24**,** 1369-1380.

GILL, H. S., SODERHOLM, J., PRAUSNITZ, M. R. & SALLBERG, M. 2010. Cutaneous vaccination using microneedles coated with hepatitis C DNA vaccine. *Gene Ther,* 17**,** 811-4.

GINHOUX, F. & MERAD, M. 2010. Ontogeny and homeostasis of Langerhans cells. *Immunol Cell Biol,* 88**,** 387-392.

GODDARD, S., YOUSTER, J., MORGAN, E. & ADAMS, D. H. 2004. Interleukin-10 secretion differentiates dendritic cells from human liver and skin. *Am J Pathol,* 164**,** 511-9.

GOODMAN, S. & CHECK, E. 2002. The great primate debate. *Nature.* England.

GORDON, S., YOUNG, K., WILSON, R., RIZWAN, S., KEMP, R., RADES, T. & HOOK, S. 2012. Chitosan hydrogels containing liposomes and cubosomes as particulate sustained release vaccine delivery systems. *J Liposome Res,* 22**,** 193-204.

GOUJON, C., RIVIERE, L., JARROSSON-WUILLEME, L., BERNAUD, J., RIGAL, D., DARLIX, J. L. & CIMARELLI, A. 2007. SIVSM/HIV-2 Vpx proteins promote retroviral escape from a proteasome-dependent restriction pathway present in human dendritic cells. *Retrovirology,* 4**,** 2.

GOUWS, E., WHITE, P. J., STOVER, J. & BROWN, T. 2006. Short term estimates of adult HIV incidence by mode of transmission: Kenya and Thailand as examples. *Sex Transm Infect,* 82 Suppl 3**,** iii51-55.

GREENSPAN, P., MAYER, E. P. & FOWLER, S. D. 1985. Nile red: a selective fluorescent stain for intracellular lipid droplets. *J Cell Biol,* 100**,** 965-73.

GREWE, M. 2001. Chronological ageing and photoageing of dendritic cells. *Clin Exp Dermatol,* 26**,** 608-12.

GROSWASSER, J., KAHN, A., BOUCHE, B., HANQUINET, S., PERLMUTER, N. & HESSEL, L. 1997. Needle length and injection technique for efficient intramuscular vaccine delivery in infants and children evaluated through an ultrasonographic determination of subcutaneous and muscle layer thickness. *Pediatrics,* 100**,** 400-3.

GROVES, R. B., COULMAN, S. A., BIRCHALL, J. C. & EVANS, S. L. 2012. Quantifying the mechanical properties of human skin to optimise future microneedle device design. *Comput Methods Biomech Biomed Engin,* 15**,** 73-82.

GUERMONPREZ, P., VALLADEAU, J., ZITVOGEL, L., THERY, C. & AMIGORENA, S. 2002. Antigen presentation and T cell stimulation by dendritic cells. *Annu Rev Immunol,* 20**,** 621-67.

GUIRONNET, G., DEZUTTER-DAMBUYANT, C., VINCENT, C., BECHETOILLE, N., SCHMITT, D. & PEGUET-NAVARRO, J. 2002. Antagonistic effects of IL-4 and TGF-beta1 on Langerhans cell-related antigen expression by human monocytes. *J Leukoc Biol,* 71**,** 845-53.

HACKSTEIN, H. & THOMSON, A. W. 2004. Dendritic cells: emerging pharmacological targets of immunosuppressive drugs. *Nat Rev Immunol,* 4**,** 24-34.

HALEY, P. J. 2003. Species differences in the structure and function of the immune system. *Toxicology,* 188**,** 49-71.

HANIFFA, M., GINHOUX, F., WANG, X. N., BIGLEY, V., ABEL, M., DIMMICK, I., BULLOCK, S., GRISOTTO, M., BOOTH, T., TAUB, P., HILKENS, C., MERAD, M. & COLLIN, M. 2009. Differential rates of replacement of human dermal dendritic cells and macrophages during hematopoietic stem cell transplantation. *J Exp Med,* 206**,** 371-85.

HANIFFA, M., SHIN, A., BIGLEY, V., MCGOVERN, N., TEO, P., SEE, P., WASAN, P. S., WANG, X. N., MALINARICH, F., MALLERET, B., LARBI, A., TAN, P., ZHAO, H., POIDINGER, M., PAGAN, S., COOKSON, S., DICKINSON, R., DIMMICK, I., JARRETT, R. F., RENIA, L., TAM, J., SONG, C., CONNOLLY, J., CHAN, J. K., GEHRING, A., BERTOLETTI, A., COLLIN, M. & GINHOUX, F. 2012. Human tissues contain CD141hi cross-presenting dendritic cells with functional homology to mouse CD103+ nonlymphoid dendritic cells. *Immunity,* 37**,** 60-73.

HANLEY, K. A. 2011. The double-edged sword: How evolution can make or break a live-attenuated virus vaccine. *Evolution,* 4**,** 635-643.

HANNOUN, C. 2013. The evolving history of influenza viruses and influenza vaccines. *Expert Rev Vaccines,* 12**,** 1085-94.

HANSEN, L. S., COGGLE, J. E., WELLS, J. & CHARLES, M. W. 1984. The influence of the hair cycle on the thickness of mouse skin. *Anat Rec,* 210**,** 569-73.

HAO, W. L. & LEE, Y. K. 2004. Microflora of the gastrointestinal tract: a review. *Methods Mol Biol,* 268**,** 491-502.

HARMAN, A. N., BYE, C. R., NASR, N., SANDGREN, K. J., KIM, M., MERCIER, S. K., BOTTING, R. A., LEWIN, S. R., CUNNINGHAM, A. L. & CAMERON, P. U. 2013. Identification of lineage relationships and novel markers of blood and skin human dendritic cells. *J Immunol,* 190**,** 66-79.

HATZIIOANNOU, T. & EVANS, D. T. 2012. Animal models for HIV/AIDS research. *Nat Rev Microbiol,* 10**,** 852-67.

HAWIGER, D., INABA, K., DORSETT, Y., GUO, M., MAHNKE, K., RIVERA, M., RAVETCH, J. V., STEINMAN, R. M. & NUSSENZWEIG, M. C. 2001. Dendritic cells induce peripheral T cell unresponsiveness under steady state conditions in vivo. *J Exp Med,* 194**,** 769-779.

HEATH, W. R. & CARBONE, F. R. 2001. Cross-presentation, dendritic cells, tolerance and immunity. *Annu Rev Immunol,* 19**,** 47-64.

HELFT, J., MANICASSAMY, B., GUERMONPREZ, P., HASHIMOTO, D., SILVIN, A., AGUDO, J., BROWN, B. D., SCHMOLKE, M., MILLER, J. C., LEBOEUF, M., MURPHY, K. M., GARCIA-SASTRE, A. & MERAD, M. 2012. Cross-presenting CD103+ dendritic cells are protected from influenza virus infection. *J Clin Invest,* 122**,** 4037-47.

HELMCHEN, F. & DENK, W. 2005. Deep tissue two-photon microscopy. *Nat Methods,* 2**,** 932-40.

HENRI, S., POULIN, L. F., TAMOUTOUNOUR, S., ARDOUIN, L., GUILLIAMS, M., DE BOVIS, B., DEVILARD, E., VIRET, C., AZUKIZAWA, H., KISSENPFENNIG, A. & MALISSEN, B. 2010. CD207⁺ CD103⁺ dermal dendritic cells cross-present keratinocyte-derived antigens irrespective of the presence of Langerhans cells. *The Journal of Experimental Medicine,* 207**,** 189.

HENTZER, B. & KOBAYASI, T. 1978. Enzymatic liberation of viable cells of human skin. *Acta Derm Venereol,* 58**,** 197-202.

HERZENBERG, L. A., PARKS, D., SAHAF, B., PEREZ, O. & ROEDERER, M. 2002. The history and future of the fluorescence activated cell sorter and flow cytometry: a view from Stanford. *Clin Chem,* 48**,** 1819-27.

HICKLING, J. K., JONES, K. R., FRIEDE, M., ZEHRUNG, D., CHEN, D. & KRISTENSEN, D. 2011. Intradermal delivery of vaccines: potential benefits and current challenges. *Bulletin of the World Health Organization,* 89**,** 221-226.

HIROBE, S., AZUKIZAWA, H., HANAFUSA, T., MATSUO, K., QUAN, Y.-S., KAMIYAMA, F., KATAYAMA, I., OKADA, N. & NAKAGAWA, S. 2015. Clinical study and stability assessment of a novel transcutaneous influenza vaccination using a dissolving microneedle patch. *Biomaterials,* 57**,** 50-58.

HOBOT, J. A. & NEWMAN, G. R. 1996. Immunomicroscopy: resin techniques and on-section labelling with immunocolloidal gold or immunoperoxidase--planning a protocol. *Scanning Microsc,* 10**,** 121-43; discussion 143-5.

HOEFFEL, G., WANG, Y., GRETER, M., SEE, P., TEO, P., MALLERET, B., LEBOEUF, M., LOW, D., OLLER, G., ALMEIDA, F., CHOY, S. H. Y., GRISOTTO, M., RENIA, L., CONWAY, S. J., STANLEY, E. R., CHAN, J. K. Y., NG, L. G., SAMOKHVALOV, I.

M., MERAD, M. & GINHOUX, F. 2012. Adult Langerhans cells derive predominantly from embryonic fetal liver monocytes with a minor contribution of yolk sac–derived macrophages. *J Exp Med,* 209**,** 1167-1181.

HOGAN, N. C., TABERNER, A. J., JONES, L. A. & HUNTER, I. W. 2015. Needle-free delivery of macromolecules through the skin using controllable jet injectors. *Expert Opin Drug Deliv,* 12**,** 1637-48.

HOLBROOK, K. A., BYERS, P. H. & PINNELL, S. R. 1982. The structure and function of dermal connective tissue in normal individuals and patients with inherited connective tissue disorders. *Scan Electron Microsc***,** 1731-44.

HOLTMEIER, W. & KABELITZ, D. 2005. gammadelta T cells link innate and adaptive immune responses. *Chem Immunol Allergy,* 86**,** 151-83.

HONEYWELL-NGUYEN, P. L. & BOUWSTRA, J. A. 2003. The in vitro transport of pergolide from surfactant-based elastic vesicles through human skin: a suggested mechanism of action. *J Control Release,* 86**,** 145-56.

HORNEF, M. W., WICK, M. J., RHEN, M. & NORMARK, S. 2002. Bacterial strategies for overcoming host innate and adaptive immune responses. *Nat Immunol,* 3**,** 1033-40.

HRECKA, K., HAO, C., GIERSZEWSKA, M., SWANSON, S. K., KESIK-BRODACKA, M., SRIVASTAVA, S., FLORENS, L., WASHBURN, M. P. & SKOWRONSKI, J. 2011. Vpx relieves inhibition of HIV-1 infection of macrophages mediated by the SAMHD1 protein. *Nature,* 474**,** 658-61.

HUA, S. 2014. Comparison of in vitro dialysis release methods of loperamide-encapsulated liposomal gel for topical drug delivery. *Int J Nanomedicine,* 9**,** 735-44.

HUA, S. 2015. Lipid-based nano-delivery systems for skin delivery of drugs and bioactives. *Front Pharmacol,* 6**,** 219.

HUBO, M., TRINSCHEK, B., KRYCZANOWSKY, F., TÜTTENBERG, A., STEINBRINK, K. & JONULEIT, H. 2013. Costimulatory molecules on immunogenic versus tolerogenic human dendritic cells. *Front Immunol,* 4.

HULEATT, J. W., NAKAAR, V., DESAI, P., HUANG, Y., HEWITT, D., JACOBS, A., TANG, J., MCDONALD, W., SONG, L., EVANS, R. K., UMLAUF, S., TUSSEY, L. & POWELL, T. J. 2008. Potent immunogenicity and efficacy of a universal influenza vaccine candidate comprising a recombinant fusion protein linking influenza M2e to the TLR5 ligand flagellin. *Vaccine,* 26**,** 201-214.

HUNGER, R. E., SIELING, P. A., OCHOA, M. T., SUGAYA, M., BURDICK, A. E., REA, T. H., BRENNAN, P. J., BELISLE, J. T., BLAUVELT, A., PORCELLI, S. A. & MODLIN,

R. L. 2004. Langerhans cells utilize CD1a and langerin to efficiently present nonpeptide antigens to T cells. *J Clin Invest,* 113**,** 701-708.

HUNTER, R. J. 2013. *Zeta potential in colloid science: principles and applications*, Academic press.

IAC. 2015. *How to Administer Intramuscular and Subcutaneous Vaccine Injections* [Online]. Minnesota: Centers for Disease Control and Prevention. Available: http://www.immunize.org/catg.d/p2020.pdf [Accessed 30 June 2016].

ICHINOHE, T., WATANABE, I., ITO, S., FUJII, H., MORIYAMA, M., TAMURA, S., TAKAHASHI, H., SAWA, H., CHIBA, J., KURATA, T., SATA, T. & HASEGAWA, H. 2005. Synthetic double-stranded RNA poly(I:C) combined with mucosal vaccine protects against influenza virus infection. *J Virol,* 79**,** 2910-9.

IDOYAGA, J., LUBKIN, A., FIORESE, C., LAHOUD, M. H., CAMINSCHI, I., HUANG, Y., RODRIGUEZ, A., CLAUSEN, B. E., PARK, C. G., TRUMPFHELLER, C. & STEINMAN, R. M. 2011. Comparable T helper 1 (Th1) and CD8 T-cell immunity by targeting HIV gag p24 to CD8 dendritic cells within antibodies to Langerin, DEC205, and Clec9A. *Proc Natl Acad Sci U S A,* 108**,** 2384-2389.

IMPAGLIAZZO, A., MILDER, F., KUIPERS, H., WAGNER, M. V., ZHU, X., HOFFMAN, R. M. B., VAN MEERSBERGEN, R., HUIZINGH, J., WANNINGEN, P., VERSPUIJ, J., DE MAN, M., DING, Z., APETRI, A., KÜKRER, B., SNEEKES-VRIESE, E., TOMKIEWICZ, D., LAURSEN, N. S., LEE, P. S., ZAKRZEWSKA, A., DEKKING, L., TOLBOOM, J., TETTERO, L., VAN MEERTEN, S., YU, W., KOUDSTAAL, W., GOUDSMIT, J., WARD, A. B., MEIJBERG, W., WILSON, I. A. & RADOŠEVIĆ, K. 2015. A stable trimeric influenza hemagglutinin stem as a broadly protective immunogen. *Science,* 349**,** 1301-1306.

INABA, K., TURLEY, S., YAMAIDE, F., IYODA, T., MAHNKE, K., INABA, M., PACK, M., SUBKLEWE, M., SAUTER, B., SHEFF, D., ALBERT, M., BHARDWAJ, N., MELLMAN, I. & STEINMAN, R. M. 1998. Efficient presentation of phagocytosed cellular fragments on the major histocompatibility complex class II products of dendritic cells. *J Exp Med,* 188**,** 2163-73.

ISAAC, M. & HOLVEY, C. 2012. Transdermal patches: the emerging mode of drug delivery system in psychiatry. *Ther Adv Psychopharmacol,* 2**,** 255-263.

ITA, K. 2015. Transdermal Delivery of Drugs with Microneedles-Potential and Challenges. *Pharmaceutics,* 7**,** 90-105.

ITO, T., GORMAN, O. T., KAWAOKA, Y., BEAN, W. J. & WEBSTER, R. G. 1991. Evolutionary analysis of the influenza A virus M gene with comparison of the M1 and M2 proteins. *J Virol,* 65**,** 5491-5498.

JACQUES, S. L., MCAULIFFE, D. J., BLANK, I. H. & PARRISH, J. A. 1987. Controlled removal of human stratum corneum by pulsed laser. *J Invest Dermatol,* 88**,** 88-93.

JANEWAY, C. A., JR. 1991. The co-receptor function of CD4. *Semin Immunol,* 3**,** 153-60.

JENSEN, E. C. 2012. Types of imaging, Part 2: an overview of fluorescence microscopy. *Anat Rec (Hoboken),* 295**,** 1621-7.

JI, X., TANG, C., ZHAO, Q., WANG, W. & XIONG, Y. 2014. Structural basis of cellular dNTP regulation by SAMHD1. *Proc Natl Acad Sci U S A,* 111**,** E4305-14.

JIANG, X., CLARK, R. A., LIU, L., WAGERS, A. J., FUHLBRIGGE, R. C. & KUPPER, T. S. 2012. Skin infection generates non-migratory memory CD8+ TRM cells providing global skin immunity. *Nature,* 483**,** 227-231.

JIN, J.-F., ZHU, L.-L., CHEN, M., XU, H.-M., WANG, H.-F., FENG, X.-Q., ZHU, X.-P. & ZHOU, Q. 2015. The optimal choice of medication administration route regarding intravenous, intramuscular, and subcutaneous injection. *Patient Prefer Adherence,* 9**,** 923-942.

JOFFRE, O. P., SEGURA, E., SAVINA, A. & AMIGORENA, S. 2012. Cross-presentation by dendritic cells. *Nat Rev Immunol,* 12**,** 557-569.

JOHNSTON, L. J., HALLIDAY, G. M. & KING, N. J. 2000. Langerhans cells migrate to local lymph nodes following cutaneous infection with an arbovirus. *J Invest Dermatol,* 114**,** 560-8.

JOHNSTON, M. I. & FAUCI, A. S. 2008. An HIV vaccine--challenges and prospects. *N Engl J Med,* 359**,** 888-90.

JOLLES, S. 2002. Paul Langerhans. *J Clin Pathol,* 55**,** 243-243.

JONES, P. S., ELIAS, J. M. & SCHECTER, N. 1986. An Improved Method for Embedding Retina for Cryosectioning. *J Histotechnol,* 9**,** 181-182.

JONGBLOED, S. L., KASSIANOS, A. J., MCDONALD, K. J., CLARK, G. J., JU, X., ANGEL, C. E., CHEN, C. J., DUNBAR, P. R., WADLEY, R. B., JEET, V., VULINK, A. J., HART, D. N. & RADFORD, K. J. 2010. Human CD141+ (BDCA-3)+ dendritic cells (DCs) represent a unique myeloid DC subset that cross-presents necrotic cell antigens. *J Exp Med,* 207**,** 1247-60.

KAECH, S. M., WHERRY, E. J. & AHMED, R. 2002. Effector and memory T-cell differentiation: implications for vaccine development. *Nat Rev Immunol,* 2**,** 251-262.

KAGAWA, Y., MAEDA, S., MORI, M. & ISHII, M. 2012. Intravital imaging of cancer cell dynamics. *Nihon Geka Gakkai Zasshi,* 113**,** 171-6.

KALIA, Y. N., ALBERTI, I., SEKKAT, N., CURDY, C., NAIK, A. & GUY, R. H. 2000. Normalization of Stratum Corneum Barrier Function and Transepidermal Water Loss In Vivo. *Pharm Res,* 17**,** 1148-1150.

KALISH, R. S., WOOD, J. A. & LAPORTE, A. 1994. Processing of urushiol (poison ivy) hapten by both endogenous and exogenous pathways for presentation to T cells in vitro. *J Clin Invest,* 93**,** 2039-2047.

KANG, S.-M., YOO, D.-G., LIPATOV, A. S., SONG, J.-M., DAVIS, C. T., QUAN, F.-S., CHEN, L.-M., DONIS, R. O. & COMPANS, R. W. 2009. Induction of Long-Term Protective Immune Responses by Influenza H5N1 Virus-Like Particles. *PLoS ONE,* 4**,** e4667.

KANITAKIS, J. 2002. Anatomy, histology and immunohistochemistry of normal human skin. *Eur J Dermatol,* 12**,** 390-9; quiz 400-1.

KANITAKIS, J., HOYO, E., PERRIN, C. & SCHMITT, D. 1993. Electron-microscopic observation of a human epidermal Langerhans cell in mitosis. *J Dermatol,* 20**,** 35-9.

KARAMI, Z. & HAMIDI, M. 2015. Cubosomes: remarkable drug delivery potential. *Drug Discov Today,* 21**,** 789-801.

KARANDE, P., ARORA, A., PHAM, T. K., STEVENS, D., WOJICKI, A. & MITRAGOTRI, S. 2009. Transcutaneous immunization using common chemicals. *J Control Release,* 138**,** 134-40.

KARANDE, P., JAIN, A. & MITRAGOTRI, S. 2004. Discovery of transdermal penetration enhancers by high-throughput screening. *Nat Biotechnol,* 22**,** 192-7.

KAZI, K. M., MANDAL, A. S., BISWAS, N., GUHA, A., CHATTERJEE, S., BEHERA, M. & KUOTSU, K. 2010. Niosome: A future of targeted drug delivery systems. *J Adv Pharm Technol Res,* 1**,** 374-380.

KEL, J. M., GIRARD-MADOUX, M. J., REIZIS, B. & CLAUSEN, B. E. 2010. TGF-beta is required to maintain the pool of immature Langerhans cells in the epidermis. *J Immunol,* 185**,** 3248-55.

KENNEY, R. T., FRECH, S. A., MUENZ, L. R., VILLAR, C. P. & GLENN, G. M. 2004. Dose sparing with intradermal injection of influenza vaccine. *N Engl J Med,* 351**,** 2295-301.

KHAN, M., DHANWANI, R., RAO, P. V. & PARIDA, M. 2012. Subunit vaccine formulations based on recombinant envelope proteins of Chikungunya

virus elicit balanced Th1/Th2 response and virus-neutralizing antibodies in mice. *Virus Res,* 167**,** 236-46.

KIM, S., SHETTY, S., PRICE, D. & BHANSALI, S. 2006. Skin penetration of silicon dioxide microneedle arrays. *Conf Proc IEEE Eng Med Biol Soc,* 1**,** 4088-91.

KIM, Y.-C., PARK, J.-H. & PRAUSNITZ, M. R. 2012a. Microneedles for drug and vaccine delivery. *Advanced drug delivery reviews,* 64**,** 1547-1568.

KIM, Y.-C., PARK, J.-H. & PRAUSNITZ, M. R. 2012b. Microneedles for drug and vaccine delivery. *Adv Drug Deliver Rev,* 64**,** 1547-1568.

KIM, Y.-C. & PRAUSNITZ, M. R. 2011. Enabling skin vaccination using new delivery technologies. *Drug Deliv Transl Res,* 1**,** 7-12.

KIM, Y.-C., QUAN, F.-S., COMPANS, R. W., KANG, S.-M. & PRAUSNITZ, M. R. 2011. Stability Kinetics of Influenza Vaccine Coated onto Microneedles During Drying and Storage. *Pharm Res,* 28**,** 135-144.

KIM, Y. C., QUAN, F. S., COMPANS, R. W., KANG, S. M. & PRAUSNITZ, M. R. 2010. Formulation and coating of microneedles with inactivated influenza virus to improve vaccine stability and immunogenicity. *J Control Release,* 142**,** 187-95.

KING, M. A. 2000. Detection of dead cells and measurement of cell killing by flow cytometry. *J Immunol Methods,* 243**,** 155-166.

KISSENPFENNIG, A., HENRI, S., DUBOIS, B., LAPLACE-BUILHE, C., PERRIN, P., ROMANI, N., TRIPP, C. H., DOUILLARD, P., LESERMAN, L., KAISERLIAN, D., SAELAND, S., DAVOUST, J. & MALISSEN, B. 2005. Dynamics and function of Langerhans cells in vivo: dermal dendritic cells colonize lymph node areas distinct from slower migrating Langerhans cells. *Immunity,* 22**,** 643-54.

KLECHEVSKY, E., MORITA, R., LIU, M., CAO, Y., COQUERY, S., THOMPSON-SNIPES, L., BRIERE, F., CHAUSSABEL, D., ZURAWSKI, G., PALUCKA, A. K., REITER, Y., BANCHEREAU, J. & UENO, H. 2008a. Functional specializations of human epidermal Langerhans cells and CD14+ dermal dendritic cells. *Immunity,* 29**,** 497-510.

KLECHEVSKY, E., MORITA, R., LIU, M., CAO, Y., COQUERY, S., THOMPSON-SNIPES, L. A., BRIERE, F., CHAUSSABEL, D., ZURAWSKI, G., PALUCKA, A. K., REITER, Y., BANCHEREAU, J. & UENO, H. 2008b. Functional Specializations of Human Epidermal Langerhans Cells and CD14(+) Dermal Dendritic Cells. *Immunity,* 29**,** 497-510.

KLIGMAN, A. M. & CHRISTOPHERS, E. 1963. PREPARATION OF ISOLATED SHEETS OF HUMAN STRATUM CORNEUM. *Arch Dermatol,* 88**,** 702-5.

KOJARUNCHITT, T., HOOK, S., RIZWAN, S., RADES, T. & BALDURSDOTTIR, S. 2011. Development and characterisation of modified poloxamer 407 thermoresponsive depot systems containing cubosomes. *Int J Pharm,* 408**,** 20-26.

KOK, P. W., KENYA, P. R. & ENSERING, H. 1983. Measles immunization with further attenuated heat-stable measles vaccine using five different methods of administration. *Trans R Soc Trop Med Hyg,* 77**,** 171-6.

KONG, R. & BHARGAVA, R. 2011. Characterization of porcine skin as a model for human skin studies using infrared spectroscopic imaging. *Analyst,* 136**,** 2359-66.

KORETZKY, G. A., PICUS, J., THOMAS, M. L. & WEISS, A. 1990. Tyrosine phosphatase CD45 is essential for coupling T-cell antigen receptor to the phosphatidyl inositol pathway. *Nature,* 346**,** 66-8.

KOUIAVSKAIA, D., MIROCHNITCHENKO, O., DRAGUNSKY, E., KOCHBA, E., LEVIN, Y., TROY, S. & CHUMAKOV, K. 2015. Intradermal inactivated poliovirus vaccine: a preclinical dose-finding study. *J Infect Dis,* 211**,** 1447-50.

KOWADA, T., KIKUTA, J., KUBO, A., ISHII, M., MAEDA, H., MIZUKAMI, S. & KIKUCHI, K. 2011. In vivo fluorescence imaging of bone-resorbing osteoclasts. *J Am Chem Soc,* 133**,** 17772-6.

KUMAR, H., KAWAI, T. & AKIRA, S. 2011. Pathogen recognition by the innate immune system. *Int Rev Immunol,* 30**,** 16-34.

KUROSAKI, T., KOMETANI, K. & ISE, W. 2015. Memory B cells. *Nat Rev Immunol,* 15**,** 149-159.

LADDY, D. J., YAN, J., KHAN, A. S., ANDERSEN, H., COHN, A., GREENHOUSE, J., LEWIS, M., MANISCHEWITZ, J., KING, L. R., GOLDING, H., DRAGHIA-AKLI, R. & WEINER, D. B. 2009. Electroporation of synthetic DNA antigens offers protection in nonhuman primates challenged with highly pathogenic avian influenza virus. *J Virol,* 83**,** 4624-30.

LAGUETTE, N., SOBHIAN, B., CASARTELLI, N., RINGEARD, M., CHABLE-BESSIA, C., SEGERAL, E., YATIM, A., EMILIANI, S., SCHWARTZ, O. & BENKIRANE, M. 2011. SAMHD1 is the dendritic- and myeloid-cell-specific HIV-1 restriction factor counteracted by Vpx. *Nature,* 474**,** 654-7.

LALVANI, A., BROOKES, R., HAMBLETON, S., BRITTON, W. J., HILL, A. V. & MCMICHAEL, A. J. 1997. Rapid effector function in CD8+ memory T cells. *J Exp Med,* 186**,** 859-65.

LARSEN, C. P., STEINMAN, R. M., WITMER-PACK, M., HANKINS, D. F., MORRIS, P. J. & AUSTYN, J. M. 1990. Migration and maturation of Langerhans cells in skin transplants and explants. *J Exp Med,* 172**,** 1483-93.

LAUTERBACH, H., BATHKE, B., GILLES, S., TRAIDL-HOFFMANN, C., LUBER, C. A., FEJER, G., FREUDENBERG, M. A., DAVEY, G. M., VREMEC, D., KALLIES, A., WU, L., SHORTMAN, K., CHAPLIN, P., SUTER, M., O'KEEFFE, M. & HOCHREIN, H. 2010. Mouse CD8alpha+ DCs and human BDCA3+ DCs are major producers of IFN-lambda in response to poly IC. *J Exp Med,* 207**,** 2703-17.

LE GOFFIC, R., POTHLICHET, J., VITOUR, D., FUJITA, T., MEURS, E., CHIGNARD, M. & SI-TAHAR, M. 2007. Cutting Edge: Influenza A virus activates TLR3-dependent inflammatory and RIG-I-dependent antiviral responses in human lung epithelial cells. *J Immunol,* 178**,** 3368-72.

LECHLER, T. & FUCHS, E. 2005. Asymmetric cell divisions promote stratification and differentiation of mammalian skin. *Nature,* 437**,** 275-280.

LEE, H.-K., DUNZENDORFER, S., SOLDAU, K. & TOBIAS, P. S. 2006. Double-Stranded RNA-Mediated TLR3 Activation Is Enhanced by CD14. *Immunity,* 24**,** 153-163.

LEE, H. K., ZAMORA, M., LINEHAN, M. M., IIJIMA, N., GONZALEZ, D., HABERMAN, A. & IWASAKI, A. 2009. Differential roles of migratory and resident DCs in T cell priming after mucosal or skin HSV-1 infection. *J Exp Med,* 206**,** 359-70.

LEE, J. W., PARK, J.-H. & PRAUSNITZ, M. R. 2008. Dissolving microneedles for transdermal drug delivery. *Biomaterials,* 29**,** 2113-2124.

LEE, W. R., SHEN, S. C., PAI, M. H., YANG, H. H., YUAN, C. Y. & FANG, J. Y. 2010. Fractional laser as a tool to enhance the skin permeation of 5-aminolevulinic acid with minimal skin disruption: a comparison with conventional erbium:YAG laser. *J Control Release,* 145**,** 124-33.

LEENAARS, M. & HENDRIKSEN, C. F. 1998. Influence of Route of Injection on Efficacy and Side Effects of Immunisation. *Altex,* 15**,** 87.

LEON, B., LOPEZ-BRAVO, M. & ARDAVIN, C. 2005. Monocyte-derived dendritic cells. *Semin Immunol,* 17**,** 313-8.

LEVIN, A., BURGESS, C., GARRISON, L. P., JR., BAUCH, C., BABIGUMIRA, J., SIMONS, E. & DABBAGH, A. 2011. Global eradication of measles: an epidemiologic and economic evaluation. *J Infect Dis,* 204 Suppl 1**,** S98-106.

LEVIN, Y., KOCHBA, E., HUNG, I. & KENNEY, R. 2015. Intradermal vaccination using the novel microneedle device MicronJet600: Past, present, and future. *Hum Vaccin Immunother,* 11**,** 991-7.

LEVIN, Y., KOCHBA, E. & KENNEY, R. 2014. Clinical evaluation of a novel microneedle device for intradermal delivery of an influenza vaccine: are all delivery methods the same? *Vaccine,* 32**,** 4249-52.

LEVINE, M. M. 2003. Can needle-free administration of vaccines become the norm in global immunization? *Nat Med,* 9**,** 99-103.

LI, D., MULLER, M. B., GILJE, S., KANER, R. B. & WALLACE, G. G. 2008. Processable aqueous dispersions of graphene nanosheets. *Nat Nano,* 3**,** 101-105.

LI, N., PENG, L. H., CHEN, X., ZHANG, T. Y., SHAO, G. F., LIANG, W. Q. & GAO, J. Q. 2014. Antigen-loaded nanocarriers enhance the migration of stimulated Langerhans cells to draining lymph nodes and induce effective transcutaneous immunization. *Nanomedicine,* 10**,** 215-23.

LI, N., ZHANG, W. & CAO, X. 2000. Identification of human homologue of mouse IFN-gamma induced protein from human dendritic cells. *Immunol Lett,* 74**,** 221-4.

LIARD, C., MUNIER, S., JOULIN-GIET, A., BONDUELLE, O., HADAM, S., DUFFY, D., VOGT, A., VERRIER, B. & COMBADIERE, B. 2012. Intradermal immunization triggers epidermal Langerhans cell mobilization required for CD8 T-cell immune responses. *J Invest Dermatol,* 132**,** 615-25.

LICHTMAN, J. W. & CONCHELLO, J.-A. 2005. Fluorescence microscopy. *Nat Methods,* 2**,** 910-919.

LINDBACK, S., BROSTROM, C., KARLSSON, A. & GAINES, H. 1994. Does symptomatic primary HIV-1 infection accelerate progression to CDC stage IV disease, CD4 count below 200× 106/l, AIDS, and death from AIDS? *BMJ,* 309**,** 1535-1537.

LINDQUIST, R. L., SHAKHAR, G., DUDZIAK, D., WARDEMANN, H., EISENREICH, T., DUSTIN, M. L. & NUSSENZWEIG, M. C. 2004. Visualizing dendritic cell networks in vivo. *Nat Immunol,* 5**,** 1243-1250.

LOPES, L. B., LOPES, J. L. C., OLIVEIRA, D. C. R., THOMAZINI, J. A., GARCIA, M. T. J., FANTINI, M. C. A., COLLETT, J. H. & BENTLEY, M. V. L. B. 2006. Liquid crystalline phases of monoolein and water for topical delivery of cyclosporin A: Characterization and study of in vitro and in vivo delivery. *Eur J Pharm Biopharm,* 63**,** 146-155.

LOPES, L. B., SPERETTA, F. F. & BENTLEY, M. V. 2007. Enhancement of skin penetration of vitamin K using monoolein-based liquid crystalline systems. *Eur J Pharm Sci,* 32**,** 209-15.

LORENZEN, E., FOLLMANN, F., JUNGERSEN, G. & AGERHOLM, J. S. 2015. A review of the human vs. porcine female genital tract and associated immune

system in the perspective of using minipigs as a model of human genital Chlamydia infection. *Vet Res,* 46**,** 116.

LU, Y.-C., YEH, W.-C. & OHASHI, P. S. 2008. LPS/TLR4 signal transduction pathway. *Cytokine,* 42**,** 145-151.

LUKAS, M., STOSSEL, H., HEFEL, L., IMAMURA, S., FRITSCH, P., SEPP, N. T., SCHULER, G. & ROMANI, N. 1996. Human cutaneous dendritic cells migrate through dermal lymphatic vessels in a skin organ culture model. *J Invest Dermatol,* 106**,** 1293-9.

LUNDBERG, K., ALBREKT, A. S., NELISSEN, I., SANTEGOETS, S., DE GRUIJL, T. D., GIBBS, S. & LINDSTEDT, M. 2013. Transcriptional profiling of human dendritic cell populations and models--unique profiles of in vitro dendritic cells and implications on functionality and applicability. *PLoS One,* 8**,** e52875.

LUTZ, M. B. & SCHULER, G. 2002. Immature, semi-mature and fully mature dendritic cells: which signals induce tolerance or immunity? *Trends Immunol,* 23**,** 445-449.

MAECKER, H. T. & TROTTER, J. 2006. Flow cytometry controls, instrument setup, and the determination of positivity. *Cytometry A,* 69**,** 1037-42.

MAKHATADZE, N. J., FRANCO, M. T. & LAYRISSE, Z. 1997. HLA class I and class II allele and haplotype distribution in the Venezuelan population. *Hum Immunol,* 55**,** 53-8.

MAKSIMOVIC, S., NAKATANI, M., BABA, Y., NELSON, A. M., MARSHALL, K. L., WELLNITZ, S. A., FIROZI, P., WOO, S.-H., RANADE, S., PATAPOUTIAN, A. & LUMPKIN, E. A. 2014. Epidermal Merkel cells are mechanosensory cells that tune mammalian touch receptors. *Nature,* 509**,** 617-621.

MALISSEN, B., TAMOUTOUNOUR, S. & HENRI, S. 2014. The origins and functions of dendritic cells and macrophages in the skin. *Nat Rev Immunol,* 14**,** 417-28.

MALVERN INSTRUMENTS 2011. Dynamic Light Scattering: Common Terms Defined. *In:* LTD., M. I. (ed.). Worcestershire, UK.

MANDZY, N., GRULKE, E. & DRUFFEL, T. 2005. Breakage of TiO2 agglomerates in electrostatically stabilized aqueous dispersions. *Powder Technol,* 160**,** 121-126.

MARIOTTI, S. & NISINI, R. 2009. Generation of human T cell clones. *Methods Mol Biol,* 514**,** 65-93.

MARTIN, N. H. 1969. The immunoglobulins: a review. *J Clin Pathol,* 22**,** 117-131.

MATTHIS, J. & REIJONEN, H. 2013. Production of Primary Human CD4+ T Cell Lines and Clones. *Methods Mol Biol,* 960**,** 545-555.

MAYER, A., LEE, S., LENDLEIN, A., JUNG, F. & HIEBL, B. 2011. Efficacy of CD14(+) blood monocytes/macrophages isolation: positive versus negative MACS protocol. *Clin Hemorheol Microcirc,* 48**,** 57-63.

MCALLISTER, L., ANDERSON, J., WERTH, K., CHO, I., COPELAND, K., LE CAM BOUVERET, N., PLANT, D., MENDELMAN, P. M. & COBB, D. K. 2014. Needle-free jet injection for administration of influenza vaccine: a randomised non-inferiority trial. *Lancet,* 384**,** 674-81.

MCCULLY, M. L., LADELL, K., HAKOBYAN, S., MANSEL, R. E., PRICE, D. A. & MOSER, B. 2012. Epidermis instructs skin homing receptor expression in human T cells. *Blood,* 120**,** 4591-8.

MCGOVERN, N., SCHLITZER, A., GUNAWAN, M., JARDINE, L., SHIN, A., POYNER, E., GREEN, K., DICKINSON, R., WANG, X.-N., LOW, D., BEST, K., COVINS, S., MILNE, P., PAGAN, S., ALJEFRI, K., WINDEBANK, M., SAAVEDRA, DIEGO M., LARBI, A., WASAN, PAVANDIP S., DUAN, K., POIDINGER, M., BIGLEY, V., GINHOUX, F., COLLIN, M. & HANIFFA, M. 2014. Human Dermal CD14(+) Cells Are a Transient Population of Monocyte-Derived Macrophages. *Immunity,* 41**,** 465-477.

MCGRATH, M. G., VRDOLJAK, A., O'MAHONY, C., OLIVEIRA, J. C., MOORE, A. C. & CREAN, A. M. 2011. Determination of parameters for successful spray coating of silicon microneedle arrays. *Int J Pharm,* 415**,** 140-149.

MEDZHITOV, R. 2001. Toll-like receptors and innate immunity. *Nat Rev Immunol,* 1**,** 135-45.

MEDZHITOV, R. 2008. Origin and physiological roles of inflammation. *Nature,* 454**,** 428-435.

MEDZHITOV, R. & JANEWAY, C. 2000. Innate Immunity. *N Engl J Med,* 343**,** 338-344.

MELBY, E. C. & ALTMAN, N. H. 1974. *Handbook of Laboratory Animal Science. Volume 2*, CRC Press Inc.

MERAD, M., GINHOUX, F. & COLLIN, M. 2008. Origin, homeostasis and function of Langerhans cells and other langerin-expressing dendritic cells. *Nat Rev Immunol,* 8**,** 935-947.

MERAD, M., MANZ, M. G., KARSUNKY, H., WAGERS, A., PETERS, W., CHARO, I., WEISSMAN, I. L., CYSTER, J. G. & ENGLEMAN, E. G. 2002. Langerhans cells renew in the skin throughout life under steady-state conditions. *Nat Immunol,* 3**,** 1135-41.

MERAD, M., SATHE, P., HELFT, J., MILLER, J. & MORTHA, A. 2013. The Dendritic Cell Lineage: Ontogeny and Function of Dendritic Cells and Their Subsets in the Steady State and the Inflamed Setting. *Annu Rev Immunol,* 31**,** 10.1146/annurev-immunol-020711-074950.

MESTAS, J. & HUGHES, C. C. 2004. Of mice and not men: differences between mouse and human immunology. *J Immunol,* 172**,** 2731-8.

MILLER, C. J. & SHATTOCK, R. J. 2003. Target cells in vaginal HIV transmission. *Microbes Infect,* 5**,** 59-67.

MILSTONE, L. M. 2004. Epidermal desquamation. *J Dermatol Sci,* 36**,** 131-40.

MITTAL, A., RABER, A. S., SCHAEFER, U. F., WEISSMANN, S., EBENSEN, T., SCHULZE, K., GUZMAN, C. A., LEHR, C. M. & HANSEN, S. 2013. Non-invasive delivery of nanoparticles to hair follicles: a perspective for transcutaneous immunization. *Vaccine,* 31**,** 3442-51.

MITTAL, A., SCHULZE, K., EBENSEN, T., WEISSMANN, S., HANSEN, S., LEHR, C. M. & GUZMAN, C. A. 2015. Efficient nanoparticle-mediated needle-free transcutaneous vaccination via hair follicles requires adjuvantation. *Nanomedicine,* 11**,** 147-54.

MOBERG, C. L. 2011. An appreciation of Ralph Marvin Steinman (1943–2011). *J Exp Med,* 208**,** 2337-2342.

MOGA, K. A., BICKFORD, L. R., GEIL, R. D., DUNN, S. S., PANDYA, A. A., WANG, Y., FAIN, J. H., ARCHULETA, C. F., O'NEILL, A. T. & DESIMONE, J. M. 2013. Rapidly-dissolvable microneedle patches via a highly scalable and reproducible soft lithography approach. *Adv Mater,* 25**,** 5060-6.

MOHAMMED, J., BEURA, L. K., BOBR, A., ASTRY, B., CHICOINE, B., KASHEM, S. W., WELTY, N. E., IGYARTO, B. Z., WIJEYESINGHE, S., THOMPSON, E. A., MATTE, C., BARTHOLIN, L., KAPLAN, A., SHEPPARD, D., BRIDGES, A. G., SHLOMCHIK, W. D., MASOPUST, D. & KAPLAN, D. H. 2016. Stromal cells control the epithelial residence of DCs and memory T cells by regulated activation of TGF-beta. *Nat Immunol,* 17**,** 414-21.

MOHLER, W., MILLARD, A. C. & CAMPAGNOLA, P. J. 2003. Second harmonic generation imaging of endogenous structural proteins. *Methods,* 29**,** 97-109.

MOLLAH, S. A., DOBRIN, J. S., FEDER, R. E., TSE, S.-W., MATOS, I. G., CHEONG, C., STEINMAN, R. M. & ANANDASABAPATHY, N. Flt3L Dependence Helps Define an Uncharacterized Subset of Murine Cutaneous Dendritic Cells. *Journal of Investigative Dermatology,* 134**,** 1265-1275.

MONIE, A., HUNG, C.-F., RODEN, R. & WU, T. C. 2008. Cervarix™: a vaccine for the prevention of HPV 16, 18-associated cervical cancer. *Biologics,* 2**,** 107-113.

MORGAN, A. J. & PARKER, S. 2007. Translational Mini-Review Series on Vaccines: The Edward Jenner Museum and the history of vaccination. *Clinical and Experimental Immunology,* 147**,** 389-394.

MURPHY, D. B. & DAVIDSON, M. W. 2012. Fundamentals of Light Microscopy. *Fundamentals of Light Microscopy and Electronic Imaging.* John Wiley & Sons, Inc.

MURPHY, K., TRAVERS, P., WALPORT, M. & JANEWAY, C. 2012. *Janeway's Immunobiology (8th ed.),* New York, Garland Science.

MUTYAMBIZI, K., BERGER, C. L. & EDELSON, R. L. 2009. The balance between immunity and tolerance: the role of Langerhans cells. *Cell Mol Life Sci,* 66**,** 831-40.

NEGRE, D., MANGEOT, P. E., DUISIT, G., BLANCHARD, S., VIDALAIN, P. O., LEISSNER, P., WINTER, A. J., RABOURDIN-COMBE, C., MEHTALI, M., MOULLIER, P., DARLIX, J. L. & COSSET, F. L. 2000. Characterization of novel safe lentiviral vectors derived from simian immunodeficiency virus (SIVmac251) that efficiently transduce mature human dendritic cells. *Gene Ther,* 7**,** 1613-23.

NEIRYNCK, S., DEROO, T., SAELENS, X., VANLANDSCHOOT, P., JOU, W. M. & FIERS, W. 1999. A universal influenza A vaccine based on the extracellular domain of the M2 protein. *Nat Med,* 5**,** 1157-63.

NELSON, J. S., MCCULLOUGH, J. L., GLENN, T. C., WRIGHT, W. H., LIAW, L. H. & JACQUES, S. L. 1991. Mid-infrared laser ablation of stratum corneum enhances in vitro percutaneous transport of drugs. *J Invest Dermatol,* 97**,** 874-9.

NESTLE, F. O., ZHENG, X. G., THOMPSON, C. B., TURKA, L. A. & NICKOLOFF, B. J. 1993. Characterization of dermal dendritic cells obtained from normal human skin reveals phenotypic and functionally distinctive subsets. *J Immunol,* 151**,** 6535-45.

NETZLAFF, F., SCHAEFER, U. F., LEHR, C. M., MEIERS, P., STAHL, J., KIETZMANN, M. & NIEDORF, F. 2006. Comparison of bovine udder skin with human and porcine skin in percutaneous permeation experiments. *Altern Lab Anim,* 34**,** 499-513.

NG, K. W., PEARTON, M., COULMAN, S., ANSTEY, A., GATELEY, C., MORRISSEY, A., ALLENDER, C. & BIRCHALL, J. 2009. Development of an ex vivo human skin model for intradermal vaccination: tissue viability and Langerhans cell behaviour. *Vaccine,* 27**,** 5948-5955.

NG, W. C., LONDRIGAN, S. L., NASR, N., CUNNINGHAM, A. L., TURVILLE, S., BROOKS, A. G. & READING, P. C. 2016. The C-type Lectin Langerin Functions as a Receptor for Attachment and Infectious Entry of Influenza A Virus. *J Virol,* 90**,** 206-21.

NGUYEN, V. A., EBNER, S., FURHAPTER, C., ROMANI, N., KOLLE, D., FRITSCH, P. & SEPP, N. 2002. Adhesion of dendritic cells derived from CD34+ progenitors to resting human dermal microvascular endothelial cells is down-regulated upon maturation and partially depends on CD11a-CD18, CD11b-CD18 and CD36. *Eur J Immunol,* 32**,** 3638-50.

NI, K. & O'NEILL, H. C. 1997. The role of dendritic cells in T cell activation. *Immunol Cell Biol,* 75**,** 223-30.

NIR, Y., PAZ, A., SABO, E. & POTASMAN, I. 2003. Fear of injections in young adults: prevalence and associations. *Am J Trop Med Hyg,* 68**,** 341-4.

NOMURA, T., KABASHIMA, K. & MIYACHI, Y. 2014. The panoply of αβT cells in the skin. *J Derm Sci,* 76**,** 3-9.

NORLÉN, L. 2006. Stratum corneum keratin structure, function and formation – a comprehensive review. *Int J Cosmetic Sci,* 28**,** 397-425.

NORMAN, J. J., CHOI, S. O., TONG, N. T., AIYAR, A. R., PATEL, S. R., PRAUSNITZ, M. R. & ALLEN, M. G. 2013. Hollow microneedles for intradermal injection fabricated by sacrificial micromolding and selective electrodeposition. *Biomed Microdevices,* 15**,** 203-10.

NORMAN, J. J., GUPTA, J., PATEL, S. R., PARK, S., JARRAHIAN, C., ZEHRUNG, D. & PRAUSNITZ, M. R. 2014. Reliability and accuracy of intradermal injection by Mantoux technique, hypodermic needle adapter, and hollow microneedle in pigs. *Drug Deliv Transl Res,* 4**,** 126-30.

NORRIS, P. J., SUMAROKA, M., BRANDER, C., MOFFETT, H. F., BOSWELL, S. L., NGUYEN, T., SYKULEV, Y., WALKER, B. D. & ROSENBERG, E. S. 2001. Multiple Effector Functions Mediated by Human Immunodeficiency Virus-Specific CD4(+) T-Cell Clones. *J Virol,* 75**,** 9771-9779.

OCHSENBEIN, A. F. & ZINKERNAGEL, R. M. 2000. Natural antibodies and complement link innate and acquired immunity. *Immunol Today,* 21**,** 624-30.

OH, J. Z., KURCHE, J. S., BURCHILL, M. A. & KEDL, R. M. 2011. TLR7 enables cross-presentation by multiple dendritic cell subsets through a type I IFN-dependent pathway. *Blood,* 118**,** 3028-3038.

PAN, X., HAN, K., PENG, X., YANG, Z., QIN, L., ZHU, C., HUANG, X., SHI, X., DIAN, L., LU, M. & WU, C. 2013. Nanostructured cubosomes as advanced drug delivery system. *Curr Pharm Des,* 19**,** 6290-7.

PARKER, V. 1984. Jet gun or syringe? A trial of alternative methods of BCG vaccination. *Public Health,* 98**,** 315-20.

PARTHASARATHI, G., NYFORT-HANSEN, K. & NAHATA, M. C. 2004. *A text book of clinical pharmacy practice : essential concepts and skills,* Hyderabad ; Great Britain, Orient Longman Ltd.

PASPARAKIS, M., HAASE, I. & NESTLE, F. O. 2014. Mechanisms regulating skin immunity and inflammation. *Nat Rev Immunol,* 14**,** 289-301.

PATTERSON, G. H. & PISTON, D. W. 2000. Photobleaching in Two-Photon Excitation Microscopy. *Biophys J,* 78**,** 2159-2162.

PAULS, E., BALLANA, E. & ESTÉ, J. A. 2013. Nucleotide embargo by SAMHD1: A strategy to block retroviral infection. *Antiviral Res,* 97**,** 180-182.

PEARTON, M., ALLENDER, C., BRAIN, K., ANSTEY, A., GATELEY, C., WILKE, N., MORRISSEY, A. & BIRCHALL, J. 2008. Gene Delivery to the Epidermal Cells of Human Skin Explants Using Microfabricated Microneedles and Hydrogel Formulations. *Pharm Res,* 25**,** 407-416.

PEARTON, M., KANG, S.-M., SONG, J.-M., ANSTEY, A. V., IVORY, M., COMPANS, R. W. & BIRCHALL, J. C. 2010a. Changes in Human Langerhans Cells Following Intradermal Injection of Influenza Virus-Like Particle Vaccines. *PLoS ONE,* 5**,** e12410.

PEARTON, M., KANG, S.-M., SONG, J.-M., ANSTEY, A. V., IVORY, M. O., COMPANS, R. W. & BIRCHALL, J. C. 2010b. Changes in Human Langerhans Cells Following Intradermal Injection of Influenza Virus-Like Particle Vaccines. *PLoS ONE,* 5**,** e12410.

PEARTON, M., KANG, S.-M., SONG, J.-M., KIM, Y.-C., QUAN, F.-S., ANSTEY, A., IVORY, M., PRAUSNITZ, M. R., COMPANS, R. W. & BIRCHALL, J. C. 2010c. Influenza Virus-Like Particles coated onto microneedles can elicit stimulatory effects on Langerhans cells in human skin. *Vaccine,* 28**,** 6104-6113.

PEARTON, M., PIRRI, D., KANG, S.-M., COMPANS, R. W. & BIRCHALL, J. C. 2013. Host responses in human skin after conventional intradermal injection or microneedle administration of virus-like-particle influenza vaccine. *Adv Healthc Mater,* 2**,** 1401-1410.

PEARTON, M., SALLER, V., COULMAN, S. A., GATELEY, C., ANSTEY, A. V., ZARNITSYN, V. & BIRCHALL, J. C. 2012. Microneedle delivery of plasmid DNA to living

human skin: Formulation coating, skin insertion and gene expression. *J Control Release,* 160**,** 561-9.

PEGG, D. E. 1987. Mechanisms of freezing damage. *Symp Soc Exp Biol,* 41**,** 363-78.

PEISER, M., WANNER, R. & KOLDE, G. 2004. Human epidermal Langerhans cells differ from monocyte-derived Langerhans cells in CD80 expression and in secretion of IL-12 after CD40 cross-linking. *J Leukoc Biol,* 76**,** 616-22.

PENA-CRUZ, V., ITO, S., OUKKA, M., YONEDA, K., DASCHER, C. C., VON LICHTENBERG, F. & SUGITA, M. 2001. Extraction of human Langerhans cells: a method for isolation of epidermis-resident dendritic cells. *J Immunol Methods,* 255**,** 83-91.

PENG, X., ZHOU, Y., HAN, K., QIN, L., DIAN, L., LI, G., PAN, X. & WU, C. 2015. Characterization of cubosomes as a targeted and sustained transdermal delivery system for capsaicin. *Drug Des Devel Ther,* 9**,** 4209-18.

PERRIN, L., KAISER, L. & YERLY, S. 2003. Travel and the spread of HIV-1 genetic variants. *Lancet Infect Dis,* 3**,** 22-7.

PETERS, E. E., AMERI, M., WANG, X., MAA, Y. F. & DADDONA, P. E. 2012. Erythropoietin-coated ZP-microneedle transdermal system: preclinical formulation, stability, and delivery. *Pharm Res,* 29**,** 1618-26.

PIEMONTI, L., MONTI, P., SIRONI, M., FRATICELLI, P., LEONE, B. E., DAL CIN, E., ALLAVENA, P. & DI CARLO, V. 2000. Vitamin D3 affects differentiation, maturation, and function of human monocyte-derived dendritic cells. *J Immunol,* 164**,** 4443-51.

PIERRE, M. B. R. & DOS SANTOS MIRANDA COSTA, I. 2011. Liposomal systems as drug delivery vehicles for dermal and transdermal applications. *Arch Dermatol Res,* 303**,** 607-621.

PIGUET, V., CAUCHETEUX, S. M., IANNETTA, M. & HOSMALIN, A. 2014. Altered antigen-presenting cells during HIV-1 infection. *Curr Opin HIV AIDS,* 9**,** 478-84.

PION, M., GRANELLI-PIPERNO, A., MANGEAT, B., STALDER, R., CORREA, R., STEINMAN, R. M. & PIGUET, V. 2006. APOBEC3G/3F mediates intrinsic resistance of monocyte-derived dendritic cells to HIV-1 infection. *J Exp Med,* 203**,** 2887-93.

POLLARD, V. W. & MALIM, M. H. 1998. The HIV-1 Rev protein. *Annu Rev Microbiol,* 52**,** 491-532.

POULIN, L. F., SALIO, M., GRIESSINGER, E., ANJOS-AFONSO, F., CRACIUN, L., CHEN, J. L., KELLER, A. M., JOFFRE, O., ZELENAY, S., NYE, E., LE MOINE, A., FAURE,

F., DONCKIER, V., SANCHO, D., CERUNDOLO, V., BONNET, D. & REIS E SOUSA, C. 2010. Characterization of human DNGR-1+ BDCA3+ leukocytes as putative equivalents of mouse CD8alpha+ dendritic cells. *J Exp Med,* 207**,** 1261-71.

PRASHAR, D. & SHARMA, D. 2011. Cubosomes: a sustained drug delivery carrier. *Asian J Res Pharm Sci,* 1**,** 59-62.

PRAUSNITZ, M. R. 2004. Microneedles for transdermal drug delivery. *Adv Drug Deliver Rev,* 56**,** 581-587.

PRAUSNITZ, M. R. & LANGER, R. 2008. Transdermal drug delivery. *Nat Biotechnol,* 26**,** 1261-1268.

QUAH, B. J. C. & PARISH, C. R. 2010. The Use of Carboxyfluorescein Diacetate Succinimidyl Ester (CFSE) to Monitor Lymphocyte Proliferation. *J Vis Exp***,** 2259.

QUAN, F. S., KIM, Y., LEE, S., YI, H., KANG, S. M., BOZJA, J., MOORE, M. L. & COMPANS, R. W. 2011. Viruslike particle vaccine induces protection against respiratory syncytial virus infection in mice. *J Infect Dis,* 204**,** 987-95.

QUIROZ, E., MORENO, N., PERALTA, P. H. & TESH, R. B. 1988. A human case of encephalitis associated with vesicular stomatitis virus (Indiana serotype) infection. *Am J Trop Med Hyg,* 39**,** 312-4.

RAJEWSKY, K. & VON BOEHMER, H. 2008. Lymphocyte development. Overview. *Curr Opin Immunol,* 20**,** 127-130.

RANI, Z. & HUSSAIN, I. 2003. Immunofluorescence in immunobullous diseases. *J Pakistan Assoc Dermatol,* 13**,** 76-88.

RATTANAPAK, T., BIRCHALL, J., YOUNG, K., ISHII, M., MEGLINSKI, I., RADES, T. & HOOK, S. 2013. Transcutaneous immunization using microneedles and cubosomes: Mechanistic investigations using Optical Coherence Tomography and Two-Photon Microscopy. *J Control Release,* 172**,** 894-903.

RATTANAPAK, T., BIRCHALL, J. C., YOUNG, K., KUBO, A., FUJIMORI, S., ISHII, M. & HOOK, S. 2014. Dynamic visualization of dendritic cell-antigen interactions in the skin following transcutaneous immunization. *PLoS One,* 9**,** e89503.

RATZINGER, G., BAGGERS, J., DE COS, M. A., YUAN, J., DAO, T., REAGAN, J. L., MUNZ, C., HELLER, G. & YOUNG, J. W. 2004. Mature human Langerhans cells derived from CD34+ hematopoietic progenitors stimulate greater cytolytic T lymphocyte activity in the absence of bioactive IL-12p70, by either single peptide presentation or cross-priming, than do dermal-interstitial or monocyte-derived dendritic cells. *J Immunol,* 173**,** 2780-91.

RATZINGER, G., STOITZNER, P., EBNER, S., LUTZ, M. B., LAYTON, G. T., RAINER, C., SENIOR, R. M., SHIPLEY, J. M., FRITSCH, P., SCHULER, G. & ROMANI, N. 2002. Matrix metalloproteinases 9 and 2 are necessary for the migration of Langerhans cells and dermal dendritic cells from human and murine skin. *J Immunol,* 168**,** 4361-71.

RAVENSCROFT, N., COSTANTINO, P., TALAGA, P., RODRIGUEZ, R. & EGAN, W. 2015. Glycoconjugate Vaccines. *In:* NUNNALLY, B. K., TURULA, V. E. & SITRIN, R. D. (eds.) *Vaccine Analysis: Strategies, Principles, and Control.* Springer Berlin Heidelberg.

REDDY, S. T., VAN DER VLIES, A. J., SIMEONI, E., ANGELI, V., RANDOLPH, G. J., O'NEIL, C. P., LEE, L. K., SWARTZ, M. A. & HUBBELL, J. A. 2007. Exploiting lymphatic transport and complement activation in nanoparticle vaccines. *Nat Biotech,* 25**,** 1159-1164.

REIMER, L. 2013. *Transmission electron microscopy: physics of image formation and microanalysis*, Springer.

REIMER, T., BRCIC, M., SCHWEIZER, M. & JUNGI, T. W. 2008. poly(I:C) and LPS induce distinct IRF3 and NF-kappaB signaling during type-I IFN and TNF responses in human macrophages. *J Leukoc Biol,* 83**,** 1249-57.

REIS E SOUSA, C. 2004. Activation of dendritic cells: translating innate into adaptive immunity. *Curr Opin Immunol,* 16**,** 21-25.

REPNIK, U., KNEZEVIC, M. & JERAS, M. 2003. Simple and cost-effective isolation of monocytes from buffy coats. *J Immunol Methods,* 278**,** 283-92.

REYGROBELLET, C., VIALA-DANTEN, M., MEUNIER, J., WEBER, F. & NGUYEN, V. H. 2010. Perception and acceptance of intradermal influenza vaccination: Patient reported outcomes from phase 3 clinical trials. *Hum Vaccin,* 6**,** 336-45.

RIDDICK, T. M. 1968. Control of colloid stability through zeta potential. *Blood,* 10.

RIZWAN, S. B., ASSMUS, D., BOEHNKE, A., HANLEY, T., BOYD, B. J., RADES, T. & HOOK, S. 2011. Preparation of phytantriol cubosomes by solvent precursor dilution for the delivery of protein vaccines. *Eur J Pharm Biopharm,* 79**,** 15-22.

RIZZA, P., SANTINI, S. M., LOGOZZI, M. A., LAPENTA, C., SESTILI, P., GHERARDI, G., LANDE, R., SPADA, M., PARLATO, S., BELARDELLI, F. & FAIS, S. 1996. T-cell dysfunctions in hu-PBL-SCID mice infected with human immunodeficiency virus (HIV) shortly after reconstitution: in vivo effects of HIV on highly activated human immune cells. *J Virol,* 70**,** 7958-64.

ROEDERER, M. 2002. Compensation in flow cytometry. *Curr Protoc Cytom,* Chapter 1, Unit 1.14.

ROLINSKI, J. & HUS, I. 2010. Dendritic-Cell Tumor Vaccines. *Transplant Proc,* 42, 3306-3308.

ROMANI, N., BRUNNER, P. M. & STINGL, G. 2012. Changing Views of the Role of Langerhans Cells. *J Invest Dermatol,* 132, 872-881.

ROMANI, N., CLAUSEN, B. E. & STOITZNER, P. 2010. Langerhans cells and more: langerin-expressing dendritic cell subsets in the skin. *Immunol Rev,* 234, 120-141.

ROMANI, N., KOIDE, S., CROWLEY, M., WITMER-PACK, M., LIVINGSTONE, A. M., FATHMAN, C. G., INABA, K. & STEINMAN, R. M. 1989. Presentation of exogenous protein antigens by dendritic cells to T cell clones. Intact protein is presented best by immature, epidermal Langerhans cells. *J Exp Med,* 169, 1169-78.

ROMANOVSKY, A. A. 2014. Skin temperature: its role in thermoregulation. *Acta Physiol,* 210, 498-507.

RUEDL, C., STORNI, T., LECHNER, F., BACHI, T. & BACHMANN, M. F. 2002. Cross-presentation of virus-like particles by skin-derived CD8(-) dendritic cells: a dispensable role for TAP. *Eur J Immunol,* 32, 818-25.

RUSSELL-JONES, G. J. 2000. Oral vaccine delivery. *J Control Release,* 65, 49-54.

SADHU, C., TING, H. J., LIPSKY, B., HENSLEY, K., GARCIA-MARTINEZ, L. F., SIMON, S. I. & STAUNTON, D. E. 2007. CD11c/CD18: novel ligands and a role in delayed-type hypersensitivity. *J Leukoc Biol,* 81, 1395-1403.

SALLUSTO, F., CELLA, M., DANIELI, C. & LANZAVECCHIA, A. 1995. Dendritic cells use macropinocytosis and the mannose receptor to concentrate macromolecules in the major histocompatibility complex class II compartment: downregulation by cytokines and bacterial products. *J Exp Med,* 182, 389-400.

SALLUSTO, F. & LANZAVECCHIA, A. 1994. Efficient presentation of soluble antigen by cultured human dendritic cells is maintained by granulocyte/macrophage colony-stimulating factor plus interleukin 4 and downregulated by tumor necrosis factor alpha. *J Exp Med,* 179, 1109-18.

SALMON, P., KINDLER, V., DUCREY, O., CHAPUIS, B., ZUBLER, R. H. & TRONO, D. 2000a. High-level transgene expression in human hematopoietic progenitors and differentiated blood lineages after transduction with improved lentiviral vectors. *Blood,* 96, 3392-8.

SALMON, P., OBERHOLZER, J., OCCHIODORO, T., MOREL, P., LOU, J. & TRONO, D. 2000b. Reversible immortalization of human primary cells by lentivector-mediated transfer of specific genes. *Mol Ther,* 2**,** 404-14.

SAMJI, T. 2009. Influenza A: Understanding the Viral Life Cycle. *Yale J Biol Med,* 82**,** 153-159.

SANCHO, D., JOFFRE, O. P., KELLER, A. M., ROGERS, N. C., MARTINEZ, D., HERNANZ-FALCON, P., ROSEWELL, I. & SOUSA, C. R. E. 2009. Identification of a dendritic cell receptor that couples sensing of necrosis to immunity. *Nature,* 458**,** 899-903.

SANDERS, B., KOLDIJK, M. & SCHUITEMAKER, H. 2015. Inactivated Viral Vaccines. *In:* NUNNALLY, B. K., TURULA, V. E. & SITRIN, R. D. (eds.) *Vaccine Analysis: Strategies, Principles, and Control.* Springer Berlin Heidelberg.

SANDERS, D. A. 2002. No false start for novel pseudotyped vectors. *Curr Opin Biotechnol,* 13**,** 437-442.

SANGIULIANO, B., PEREZ, N. M., MOREIRA, D. F. & BELIZARIO, J. E. 2014. Cell death-associated molecular-pattern molecules: inflammatory signaling and control. *Mediators Inflamm,* 2014**,** 821043.

SANTAMBROGIO, L., SATO, A. K., CARVEN, G. J., BELYANSKAYA, S. L., STROMINGER, J. L. & STERN, L. J. 1999. Extracellular antigen processing and presentation by immature dendritic cells. *Proc Natl Acad Sci U S A,* 96**,** 15056-15061.

SATPATHY, A. T., KC, W., ALBRING, J. C., EDELSON, B. T., KRETZER, N. M., BHATTACHARYA, D., MURPHY, T. L. & MURPHY, K. M. 2012. Zbtb46 expression distinguishes classical dendritic cells and their committed progenitors from other immune lineages. *J Exp Med,* 209**,** 1135-52.

SCHMALFUß, U., NEUBERT, R. & WOHLRAB, W. 1997. Modification of drug penetration into human skin using microemulsions. *J Control Release,* 46**,** 279-285.

SCHMITZ, B., RADBRUCH, A., KUMMEL, T., WICKENHAUSER, C., KORB, H., HANSMANN, M. L., THIELE, J. & FISCHER, R. 1994. Magnetic activated cell sorting (MACS)--a new immunomagnetic method for megakaryocytic cell isolation: comparison of different separation techniques. *Eur J Haematol,* 52**,** 267-75.

SCHRAMM, J. & MITRAGOTRI, S. 2002. Transdermal drug delivery by jet injectors: energetics of jet formation and penetration. *Pharm Res,* 19**,** 1673-9.

SCHRAMM-BAXTER, J., KATRENCIK, J. & MITRAGOTRI, S. 2004. Jet injection into polyacrylamide gels: investigation of jet injection mechanics. *J Biomech,* 37**,** 1181-8.

SCHREIBELT, G., KLINKENBERG, L. J., CRUZ, L. J., TACKEN, P. J., TEL, J., KREUTZ, M., ADEMA, G. J., BROWN, G. D., FIGDOR, C. G. & DE VRIES, I. J. 2012. The C-type lectin receptor CLEC9A mediates antigen uptake and (cross-)presentation by human blood BDCA3+ myeloid dendritic cells. *Blood,* 119**,** 2284-92.

SCHROEDER, H. W. & CAVACINI, L. 2010. Structure and Function of Immunoglobulins. *J Allergy Clin Immun,* 125**,** S41-S52.

SCHULER, G. & STEINMAN, R. M. 1985. Murine epidermal Langerhans cells mature into potent immunostimulatory dendritic cells in vitro. *J Exp Med,* 161**,** 526-46.

SCHULZ, O., DIEBOLD, S. S., CHEN, M., NASLUND, T. I., NOLTE, M. A., ALEXOPOULOU, L., AZUMA, Y. T., FLAVELL, R. A., LILJESTROM, P. & REIS E SOUSA, C. 2005. Toll-like receptor 3 promotes cross-priming to virus-infected cells. *Nature,* 433**,** 887-92.

SCHWANKE, U., NABEREIT, A. & MOOG, R. 2006. Isolation of monocytes from whole blood-derived buffy coats by continuous counter-flow elutriation. *J Clin Apher,* 21**,** 153-7.

SCHWENDENER, R. A. 2014. Liposomes as vaccine delivery systems: a review of the recent advances. *Ther Adv Vaccines,* 2**,** 159-82.

SEGURA, E., DURAND, M. & AMIGORENA, S. 2013. Similar antigen cross-presentation capacity and phagocytic functions in all freshly isolated human lymphoid organ-resident dendritic cells. *J Exp Med,* 210**,** 1035-47.

SEGURA, E., VALLADEAU-GUILEMOND, J., DONNADIEU, M. H., SASTRE-GARAU, X., SOUMELIS, V. & AMIGORENA, S. 2012. Characterization of resident and migratory dendritic cells in human lymph nodes. *J Exp Med,* 209**,** 653-60.

SEITE, S., ZUCCHI, H., MOYAL, D., TISON, S., COMPAN, D., CHRISTIAENS, F., GUENICHE, A. & FOURTANIER, A. 2003. Alterations in human epidermal Langerhans cells by ultraviolet radiation: quantitative and morphological study. *Br J Dermatol,* 148**,** 291-9.

SHAPIRO, H. M. 2005. *Practical Flow Cytometry*, John Wiley & Sons.

SHAW, F. E., JR., GUESS, H. A., ROETS, J. M., MOHR, F. E., COLEMAN, P. J., MANDEL, E. J., ROEHM, R. R., JR., TALLEY, W. S. & HADLER, S. C. 1989. Effect of anatomic injection site, age and smoking on the immune response to hepatitis B vaccination. *Vaccine,* 7**,** 425-30.

SHEEHY, A. M., GADDIS, N. C., CHOI, J. D. & MALIM, M. H. 2002. Isolation of a human gene that inhibits HIV-1 infection and is suppressed by the viral Vif protein. *Nature,* 418**,** 646-50.

SHKLOVSKAYA, E., O'SULLIVAN, B. J., NG, L. G., ROEDIGER, B., THOMAS, R., WENINGER, W. & FAZEKAS DE ST GROTH, B. 2011. Langerhans cells are precommitted to immune tolerance induction. *Proc Natl Acad Sci U S A,* 108**,** 18049-54.

SHORTMAN, K. & LIU, Y.-J. 2002. Mouse and human dendritic cell subtypes. *Nat Rev Immunol,* 2**,** 151-161.

SHORTMAN, K. & NAIK, S. H. 2007. Steady-state and inflammatory dendritic-cell development. *Nat Rev Immunol,* 7**,** 19-30.

SIEGRIST, C.-A. 2013. 2 - Vaccine immunology. *In:* OFFIT, S. A. P. A. O. A. (ed.) *Vaccines (Sixth Edition).* London: W.B. Saunders.

SIMS, S., WILLBERG, C. & KLENERMAN, P. 2010. MHC-peptide tetramers for the analysis of antigen-specific T cells. *Expert Rev Vaccines,* 9**,** 765-74.

SITRIN, R., ZHAO, Q., POTTER, C., CARRAGHER, B. & WASHABAUGH, M. 2015. Recombinant Virus-like Particle Protein Vaccines. *In:* NUNNALLY, B. K., TURULA, V. E. & SITRIN, R. D. (eds.) *Vaccine Analysis: Strategies, Principles, and Control.* Springer Berlin Heidelberg.

SKOUNTZOU, I., QUAN, F. S., JACOB, J., COMPANS, R. W. & KANG, S. M. 2006. Transcutaneous immunization with inactivated influenza virus induces protective immune responses. *Vaccine,* 24**,** 6110-9.

SO, P. T., DONG, C. Y., MASTERS, B. R. & BERLAND, K. M. 2000. Two-photon excitation fluorescence microscopy. *Annu Rev Biomed Eng,* 2**,** 399-429.

SOONAWALA, D., VERDIJK, P., WIJMENGA-MONSUUR, A. J., BOOG, C. J., KOEDAM, P., VISSER, L. G. & ROTS, N. Y. 2013. Intradermal fractional booster dose of inactivated poliomyelitis vaccine with a jet injector in healthy adults. *Vaccine,* 31**,** 3688-3694.

SRIVASTAVA, I. K. & LIU, M. A. 2003. Gene vaccines. *Ann Intern Med,* 138**,** 550-9.

STEIMER, K. S. & HAIGWOOD, N. L. 1991. Importance of conformation on the neutralizing antibody response to HIV-1 gp120. *Biotechnol Ther,* 2**,** 63-89.

STEINMAN, R. M. 1991. The dendritic cell system and its role in immunogenicity. *Annu Rev Immunol,* 9**,** 271-96.

STEINMAN, R. M., HAWIGER, D. & NUSSENZWEIG, M. C. 2003. Tolerogenic dendritic cells. *Annu Rev Immunol,* 21**,** 685-711.

STENN, K. S., LINK, R., MOELLMANN, G., MADRI, J. & KUKLINSKA, E. 1989. Dispase, a neutral protease from Bacillus polymyxa, is a powerful fibronectinase and type IV collagenase. *J Invest Dermatol,* 93**,** 287-90.

STERN, A. M. & MARKEL, H. 2005. The history of vaccines and immunization: familiar patterns, new challenges. *Health Aff,* 24**,** 611-21.

STINGL, G., KATZ, S. I., CLEMENT, L., GREEN, I. & SHEVACH, E. M. 1978. Immunologic functions of Ia-bearing epidermal Langerhans cells. *J Immunol,* 121**,** 2005-13.

STOITZNER, P. 2010. The Langerhans cell controversy: are they immunostimulatory or immunoregulatory cells of the skin immune system[quest]. *Immunol Cell Biol,* 88**,** 348-350.

STOITZNER, P., HOLZMANN, S., MCLELLAN, A. D., IVARSSON, L., STOSSEL, H., KAPP, M., KAMMERER, U., DOUILLARD, P., KAMPGEN, E., KOCH, F., SAELAND, S. & ROMANI, N. 2003. Visualization and characterization of migratory Langerhans cells in murine skin and lymph nodes by antibodies against Langerin/CD207. *J Invest Dermatol,* 120**,** 266-74.

STOITZNER, P., ROMANI, N., MCLELLAN, A. D., TRIPP, C. H. & EBNER, S. 2010. Isolation of skin dendritic cells from mouse and man. *Methods Mol Biol,* 595**,** 235-48.

STOITZNER, P., TRIPP, C. H., EBERHART, A., PRICE, K. M., JUNG, J. Y., BURSCH, L., RONCHESE, F. & ROMANI, N. 2006. Langerhans cells cross-present antigen derived from skin. *Proc Natl Acad Sci U S A,* 103**,** 7783-8.

SUH, H., SHIN, J. & KIM, Y.-C. 2014a. Microneedle patches for vaccine delivery. *Clin Exp Vaccine Res,* 3**,** 42-49.

SUH, H., SHIN, J. & KIM, Y.-C. 2014b. Microneedle patches for vaccine delivery. *Clinical and Experimental Vaccine Research,* 3**,** 42-49.

SULLIVAN, S. P., KOUTSONANOS, D. G., DEL PILAR MARTIN, M., LEE, J. W., ZARNITSYN, V., CHOI, S.-O., MURTHY, N., COMPANS, R. W., SKOUNTZOU, I. & PRAUSNITZ, M. R. 2010. Dissolving polymer microneedle patches for influenza vaccination. *Nat Med,* 16**,** 915-920.

SUPERTI, F., SEGANTI, L., RUGGERI, F. M., TINARI, A., DONELLI, G. & ORSI, N. 1987. Entry pathway of vesicular stomatitis virus into different host cells. *J Gen Virol,* 68 (Pt 2)**,** 387-99.

SWARBRICK, J., LEE, G. & BROM, J. 1982. Drug Permeation through Human Skin: I. Effects of Storage Conditions of Skin. *J Invest Dermatol,* 78**,** 63-66.

TADOKORO, T., YAMAGUCHI, Y., BATZER, J., COELHO, S. G., ZMUDZKA, B. Z., MILLER, S. A., WOLBER, R., BEER, J. Z. & HEARING, V. J. 2005. Mechanisms of Skin Tanning in Different Racial/Ethnic Groups in Response to Ultraviolet Radiation. *J Invest Dermatol,* 124**,** 1326-1332.

TAKEUCHI, O. & AKIRA, S. 2010. Pattern recognition receptors and inflammation. *Cell,* 140**,** 805-20.

TAMOUTOUNOUR, S., GUILLIAMS, M., MONTANANA SANCHIS, F., LIU, H., TERHORST, D., MALOSSE, C., POLLET, E., ARDOUIN, L., LUCHE, H., SANCHEZ, C., DALOD, M., MALISSEN, B. & HENRI, S. 2013. Origins and functional specialization of macrophages and of conventional and monocyte-derived dendritic cells in mouse skin. *Immunity,* 39**,** 925-38.

TAUBENBERGER, J. K. & KASH, J. C. 2010. Influenza Virus Evolution, Host Adaptation and Pandemic Formation. *Cell Host Microbe,* 7**,** 440-451.

TAUBENBERGER, J. K. & MORENS, D. M. 2008. The Pathology of Influenza Virus Infections. *Annu Rev Pathol,* 3**,** 499-522.

THEOHARIDES, T. C., ALYSANDRATOS, K.-D., ANGELIDOU, A., DELIVANIS, D.-A., SISMANOPOULOS, N., ZHANG, B., ASADI, S., VASIADI, M., WENG, Z., MINIATI, A. & KALOGEROMITROS, D. 2012. Mast cells and inflammation. *BBA-Mol Basis Dis,* 1822**,** 21-33.

THOMAS, A. A., VRIJSEN, R. & BOEYE, A. 1986. Relationship between poliovirus neutralization and aggregation. *J Virol,* 59**,** 479-85.

TIWARI, T. S. P. & WHARTON, M. 2013. 12 - Diphtheria toxoid. *In:* OFFIT, S. A. P. A. O. A. (ed.) *Vaccines (Sixth Edition).* London: W.B. Saunders.

TORRISI, B. M., ZARNITSYN, V., PRAUSNITZ, M. R., ANSTEY, A., GATELEY, C., BIRCHALL, J. C. & COULMAN, S. A. 2013. Pocketed microneedles for rapid delivery of a liquid-state botulinum toxin A formulation into human skin. *J Control Release,* 165**,** 146-52.

TOUITOU, E. 2002. Drug delivery across the skin. *Expert Opin Biol Ther,* 2**,** 723-33.

TOZUKA, M., OKA, T., JOUNAI, N., EGAWA, G., ISHII, K. J., KABASHIMA, K. & TAKESHITA, F. 2016. Efficient antigen delivery to the draining lymph nodes is a key component in the immunogenic pathway of the intradermal vaccine. *J Derm Sci,* 82**,** 38-45.

TRZASKA, W. J., CORREIA, J. N., VILLEGAS, M. T., MAY, R. C. & VOELZ, K. 2015. pH Manipulation as a Novel Strategy for Treating Mucormycosis. *Antimicrob Agents Chemother,* 59**,** 6968-6974.

TURELLI, P., MANGEAT, B., JOST, S., VIANIN, S. & TRONO, D. 2004. Inhibition of Hepatitis B Virus Replication by APOBEC3G. *Science,* 303**,** 1829-1829.

TURLEY, S. J., INABA, K., GARRETT, W. S., EBERSOLD, M., UNTERNAEHRER, J., STEINMAN, R. M. & MELLMAN, I. 2000. Transport of peptide-MHC class II complexes in developing dendritic cells. *Science,* 288**,** 522-7.

UNANUE, E. R. 1984. Antigen-presenting function of the macrophage. *Annu Rev Immunol,* 2**,** 395-428.

VALLADEAU, J., DUVERT-FRANCES, V., PIN, J.-J., DEZUTTER-DAMBUYANT, C., VINCENT, C., MASSACRIER, C., VINCENT, J., YONEDA, K., BANCHEREAU, J., CAUX, C., DAVOUST, J. & SAELAND, S. 1999. The monoclonal antibody DCGM4 recognizes Langerin, a protein specific of Langerhans cells, and is rapidly internalized from the cell surface. *Eur J Immunol,* 29**,** 2695-2704.

VALLADEAU, J., RAVEL, O., DEZUTTER-DAMBUYANT, C., MOORE, K., KLEIJMEER, M., LIU, Y., DUVERT-FRANCES, V., VINCENT, C., SCHMITT, D., DAVOUST, J., CAUX, C., LEBECQUE, S. & SAELAND, S. 2000. Langerin, a Novel C-Type Lectin Specific to Langerhans Cells, Is an Endocytic Receptor that Induces the Formation of Birbeck Granules. *Immunity,* 12**,** 71-81.

VAN DAMME, P., OOSTERHUIS-KAFEJA, F., VAN DER WIELEN, M., ALMAGOR, Y., SHARON, O. & LEVIN, Y. 2009. Safety and efficacy of a novel microneedle device for dose sparing intradermal influenza vaccination in healthy adults. *Vaccine,* 27**,** 454-9.

VAN DEN BERG, J. H., NUJIEN, B., BEIJNEN, J. H., VINCENT, A., VAN TINTEREN, H., KLUGE, J., WOERDEMAN, L. A., HENNINK, W. E., STORM, G., SCHUMACHER, T. N. & HAANEN, J. B. 2009. Optimization of intradermal vaccination by DNA tattooing in human skin. *Hum Gene Ther,* 20**,** 181-9.

VAN DER AAR, A. M., DE GROOT, R., SANCHEZ-HERNANDEZ, M., TAANMAN, E. W., VAN LIER, R. A., TEUNISSEN, M. B., DE JONG, E. C. & KAPSENBERG, M. L. 2011. Cutting edge: virus selectively primes human langerhans cells for CD70 expression promoting CD8+ T cell responses. *J Immunol,* 187**,** 3488-92.

VAN DER AAR, A. M., PICAVET, D. I., MULLER, F. J., DE BOER, L., VAN CAPEL, T. M., ZAAT, S. A., BOS, J. D., JANSSEN, H., GEORGE, T. C., KAPSENBERG, M. L., VAN HAM, S. M., TEUNISSEN, M. B. & DE JONG, E. C. 2013. Langerhans cells favor skin flora tolerance through limited presentation of bacterial antigens and induction of regulatory T cells. *J Invest Dermatol,* 133**,** 1240-9.

VAN DER AAR, A. M., SYLVA-STEENLAND, R. M., BOS, J. D., KAPSENBERG, M. L., DE JONG, E. C. & TEUNISSEN, M. B. 2007. Loss of TLR2, TLR4, and TLR5 on Langerhans cells abolishes bacterial recognition. *J Immunol,* 178**,** 1986-90.

VAN DER VLIST, M., DE WITTE, L., DE VRIES, R. D., LITJENS, M., DE JONG, M. A., FLUITSMA, D., DE SWART, R. L. & GEIJTENBEEK, T. B. 2011. Human Langerhans cells capture measles virus through Langerin and present viral antigens to CD4(+) T cells but are incapable of cross-presentation. *Eur J Immunol,* 41**,** 2619-31.

VAN DER WORP, H. B., HOWELLS, D. W., SENA, E. S., PORRITT, M. J., REWELL, S., O'COLLINS, V. & MACLEOD, M. R. 2010. Can animal models of disease reliably inform human studies? *PLoS Med,* 7**,** e1000245.

VANDERMEULEN, G., DAUGIMONT, L., RICHIARDI, H., VANDERHAEGHEN, M. L., LECOUTURIER, N., UCAKAR, B. & PREAT, V. 2009. Effect of tape stripping and adjuvants on immune response after intradermal DNA electroporation. *Pharm Res,* 26**,** 1745-51.

VANDESANDE, F. 1979. A critical review of immunocytochemical methods for light microscopy. *J Neurosci Methods,* 1**,** 3-23.

VERMA, D. D., VERMA, S., BLUME, G. & FAHR, A. 2003. Particle size of liposomes influences dermal delivery of substances into skin. *Int J Pharm,* 258**,** 141-51.

VERSTREPEN, B. E., BINS, A. D., ROLLIER, C. S., MOOIJ, P., KOOPMAN, G., SHEPPARD, N. C., SATTENTAU, Q., WAGNER, R., WOLF, H., SCHUMACHER, T. N. M., HEENEY, J. L. & HAANEN, J. B. A. G. 2008. Improved HIV-1 specific T-cell responses by short-interval DNA tattooing as compared to intramuscular immunization in non-human primates. *Vaccine,* 26**,** 3346-3351.

WANG, P. M., CORNWELL, M., HILL, J. & PRAUSNITZ, M. R. 2006. Precise Microinjection into Skin Using Hollow Microneedles. *J Invest Dermatol,* 126**,** 1080-1087.

WANG, X., UTO, T., AKAGI, T., AKASHI, M. & BABA, M. 2008. Poly(gamma-glutamic acid) nanoparticles as an efficient antigen delivery and adjuvant system: potential for an AIDS vaccine. *J Med Virol,* 80**,** 11-9.

WANG, Y., HAMMES, F., DE ROY, K., VERSTRAETE, W. & BOON, N. 2010. Past, present and future applications of flow cytometry in aquatic microbiology. *Trends Biotechnol,* 28**,** 416-24.

WATANABE, R., GEHAD, A., YANG, C., SCOTT, L. L., TEAGUE, J. E., SCHLAPBACH, C., ELCO, C. P., HUANG, V., MATOS, T. R., KUPPER, T. S. & CLARK, R. A. 2015. Human skin is protected by four functionally and phenotypically discrete populations of resident and recirculating memory T cells. *Sci Transl Med,* 7**,** 279ra39.

WATSON, D. S., ENDSLEY, A. N. & HUANG, L. 2012. Design considerations for liposomal vaccines: Influence of formulation parameters on antibody and cell-mediated immune responses to liposome associated antigens. *Vaccine,* 30**,** 2256-2272.

WEILAND, O., AHLEN, G., DIEPOLDER, H., JUNG, M. C., LEVANDER, S., FONS, M., MATHIESEN, I., SARDESAI, N. Y., VAHLNE, A., FRELIN, L. & SALLBERG, M. 2013. Therapeutic DNA vaccination using in vivo electroporation followed by standard of care therapy in patients with genotype 1 chronic hepatitis C. *Mol Ther,* 21**,** 1796-805.

WEINER, N., WILLIAMS, N., BIRCH, G., RAMACHANDRAN, C., SHIPMAN JR, C. & FLYNN, G. 1989. Topical delivery of liposomally encapsulated interferon evaluated in a cutaneous herpes guinea pig model. *Annu Rev Biomed Eng,* 33**,** 1217-1221.

WEINTRAUB, A. 2003. Immunology of bacterial polysaccharide antigens. *Carbohydr Res,* 338**,** 2539-47.

WHO 2010. Rabies vaccines: WHO position paper. *Weekly Epidemiol Rec,* 32**,** 309-320.

WHO. 2012a. *Fact Sheet No. 360: HIV/AIDS* [Online]. Geneva: World Health Organisation. Available: http://www.who.int/mediacentre/factsheets/fs360/en/ [Accessed 28 April 2016].

WHO. 2012b. *Module 2- Types of Vaccine and Adverse Reactions* [Online]. Available: http://vaccine-safety-training.org/route-of-administration.html [Accessed July 11th 2016].

WHO. 2014. *Influenza (Seasonal)* [Online]. Switzerland. Available: http://www.who.int/mediacentre/factsheets/fs211/en/ [Accessed July 9th 2016].

WILEN, C. B., TILTON, J. C. & DOMS, R. W. 2012. HIV: cell binding and entry. *Cold Spring Harb Perspect Med,* 2.

WILLIAMS, A. C. & BARRY, B. W. 2012. Penetration enhancers. *Adv Drug Deliv Rev,* 64, Supplement**,** 128-137.

WILLIAMS, D. B. & CARTER, C. B. 1996. The Transmission Electron Microscope. *Transmission Electron Microscopy: A Textbook for Materials Science.* Boston, MA: Springer US.

WILLIAMS, J., FOX-LEYVA, L., CHRISTENSEN, C., FISHER, D., SCHLICTING, E., SNOWBALL, M., NEGUS, S., MAYERS, J., KOLLER, R. & STOUT, R. 2000. Hepatitis A vaccine administration: comparison between jet-injector and needle injection. *Vaccine,* 18**,** 1939-1943.

WILLIAMS, R. M., ZIPFEL, W. R. & WEBB, W. W. 2005. Interpreting Second-Harmonic Generation Images of Collagen I Fibrils. *Biophys J,* 88**,** 1377-1386.

WINSOR, L. 1994. Section 4 Tissue and section preparation. *Laboratory Histopathology. A complete reference.* First ed. New York: Churchill Livingstone.

WITTING, N., SVENSSON, P., GOTTRUP, H., ARENDT-NIELSEN, L. & JENSEN, T. S. 2000. Intramuscular and intradermal injection of capsaicin: a comparison of local and referred pain. *Pain,* 84**,** 407-412.

WOLLENBERG, A., MOMMAAS, M., OPPEL, T., SCHOTTDORF, E. M., GUNTHER, S. & MODERER, M. 2002. Expression and function of the mannose receptor CD206 on epidermal dendritic cells in inflammatory skin diseases. *J Invest Dermatol,* 118**,** 327-34.

WOOF, J. M. & RUSSELL, M. W. 2011. Structure and function relationships in IgA. *Mucosal Immunol,* 4**,** 590-7.

WRAITH, D. C., GOLDMAN, M. & LAMBERT, P. H. 2003. Vaccination and autoimmune disease: what is the evidence? *Lancet,* 362**,** 1659-66.

WU, S. J., GROUARD-VOGEL, G., SUN, W., MASCOLA, J. R., BRACHTEL, E., PUTVATANA, R., LOUDER, M. K., FILGUEIRA, L., MAROVICH, M. A., WONG, H. K., BLAUVELT, A., MURPHY, G. S., ROBB, M. L., INNES, B. L., BIRX, D. L., HAYES, C. G. & FRANKEL, S. S. 2000. Human skin Langerhans cells are targets of dengue virus infection. *Nat Med,* 6**,** 816-20.

WU, X. & XU, F. 2014. Dendritic cells during Staphylococcus aureus infection: subsets and roles. *J Transl Med,* 12**,** 358.

WÖLFL, M. & GREENBERG, P. D. 2014. Antigen-specific activation and cytokine-facilitated expansion of naive, human CD8+ T cells. *Nat Protocols,* 9**,** 950-966.

XU, W., JONG HONG, S., JIA, S., ZHAO, Y., GALIANO, R. D. & MUSTOE, T. A. 2012. Application of a partial-thickness human ex vivo skin culture model in cutaneous wound healing study. *Lab Invest,* 92**,** 584-99.

YAMAMOTO, A., SERIZAWA, S., ITO, M. & SATO, Y. 1991. Stratum corneum lipid abnormalities in atopic dermatitis. *Arch Dermatol Res,* 283**,** 219-223.

YOSHIDA, A., NAGATA, T., UCHIJIMA, M., HIGASHI, T. & KOIDE, Y. 2000. Advantage of gene gun-mediated over intramuscular inoculation of plasmid DNA vaccine in reproducible induction of specific immune responses. *Vaccine,* 18**,** 1725-9.

YOSHIDA, K., KUBO, A., FUJITA, H., YOKOUCHI, M., ISHII, K., KAWASAKI, H., NOMURA, T., SHIMIZU, H., KOUYAMA, K., EBIHARA, T., NAGAO, K. & AMAGAI, M. 2014. Distinct behavior of human Langerhans cells and

inflammatory dendritic epidermal cells at tight junctions in patients with atopic dermatitis. *J Allergy Clin Immunol,* 134**,** 856-864.

YU, R. C., ABRAMS, D. C., ALAIBAC, M. & CHU, A. C. 1994. Morphological and quantitative analyses of normal epidermal Langerhans cells using confocal scanning laser microscopy. *Br J Dermatol,* 131**,** 843-8.

ZEHRUNG, D. 2009. Intradermal Delivery of Vaccines: A review of the literature and the potential for development for use in low- and middle income countries. *In:* KRISTENSEN, D. (ed.). Program for Appropriate Technology in Health (PATH).

ZELLER, R. 2001. Fixation, Embedding, and Sectioning of Tissues, Embryos, and Single Cells. *Current Protocols in Molecular Biology.* John Wiley & Sons, Inc.

ZHAO, Y. L., MURTHY, S. N., MANJILI, M. H., GUAN, L. J., SEN, A. & HUI, S. W. 2006. Induction of cytotoxic T-lymphocytes by electroporation-enhanced needle-free skin immunization. *Vaccine,* 24**,** 1282-90.

ZUCKERMAN, J. N. 2000. The importance of injecting vaccines into muscle : Different patients need different needle sizes. *BMJ,* 321**,** 1237-1238.

ZUFFEREY, R., NAGY, D., MANDEL, R. J., NALDINI, L. & TRONO, D. 1997. Multiply attenuated lentiviral vector achieves efficient gene delivery in vivo. *Nat Biotechnol,* 15**,** 871-5.